

# Dynamical Symmetry Breaking in the Gauged Nambu–Jona-Lasinio Model

Manuel Reenders

Ph.D. Thesis  
University of Groningen  
26 March 1999

*To the people of Ukraine*

Supervisor

Prof. Dr. M. Winnink

Co-supervisor

Dr. V. P. Gusynin

Referees

Prof. Dr. T. C. Dorlas

Prof. Dr. V. A. Miransky

Prof. Dr. M. R. Pennington

ISBN 90-367-1042-1

Rijksuniversiteit Groningen

Dynamical Symmetry Breaking in  
the Gauged Nambu–Jona-Lasinio Model

Proefschrift

ter verkrijging van het doctoraat in de  
Wiskunde en Natuurwetenschappen  
aan de Rijksuniversiteit Groningen

op gezag van de  
Rector Magnificus, Dr. D. F. J. Bosscher,  
in het openbaar te verdedigen op  
vrijdag 26 maart 1999  
om 14.15 uur

door

Klaas Hommo Immanuel Reenders

geboren op 8 april 1970  
te Groningen

Promotor  
Prof. Dr. M. Winnink

Referent  
Dr. V. P. Gusynin

# Contents

<b>Introduction and summary</b>	<b>1</b>
List of short-hand notations . . . . .	10
<b>1 Phase transitions and quantum field theory</b>	<b>11</b>
1.1 Review of the path-integral formalism . . . . .	11
1.2 Continuous phase transitions . . . . .	14
1.2.1 The scaling hypothesis . . . . .	16
1.2.2 The scaling hypothesis for the equation of state . . . . .	17
1.2.3 The scaling hypothesis for the free energy . . . . .	18
1.2.4 The scaling hypothesis for the two-point correlation functions	19
1.3 Wilson's renormalization group . . . . .	21
1.3.1 Step 1. Regularization and coarse graining . . . . .	22
1.3.2 Step 2. The origin of singular behavior and anomalous scaling	26
1.3.3 Step 3. Renormalization and fine-tuning . . . . .	31
1.4 The Goldstone mechanism . . . . .	35
1.4.1 Chiral symmetry . . . . .	36
1.5 The gauged Nambu–Jona-Lasinio model . . . . .	38
1.6 The auxiliary field method . . . . .	39
<b>2 SDEs of the GNJL model</b>	<b>41</b>
2.1 The generating functional . . . . .	41
2.1.1 Condensates . . . . .	44
2.1.2 The SDE for the photon propagator . . . . .	44
2.1.3 The SDE for the fermion propagator . . . . .	45
2.1.4 SDEs for the scalar and pseudoscalar propagators . . . . .	46
2.1.5 SDEs of the vertices . . . . .	47
2.2 Ward–Takahashi identities . . . . .	51
2.2.1 Vector Ward-Takahashi identities . . . . .	51
2.2.2 Chiral Ward–Takahashi identities . . . . .	52
2.2.3 The axial vector vertex and PCAC . . . . .	53
2.3 Particles . . . . .	58

2.3.1	The Wick rotation . . . . .	60
<b>3</b>	<b>Dynamical chiral symmetry breaking</b>	<b>61</b>
3.1	The quenched ladder approximation . . . . .	62
3.2	The Gap equation . . . . .	63
3.2.1	The linearized approximation . . . . .	64
3.3	The equation of state . . . . .	66
3.4	Scaling laws in the chiral limit . . . . .	68
3.5	The critical exponents and scaling . . . . .	70
3.6	The conformal phase transition . . . . .	74
3.7	RG equations and fine-tuning . . . . .	78
3.7.1	RG flow in the broken phase . . . . .	79
3.7.2	RG flow in the symmetric phase . . . . .	80
3.8	Lattice simulations of strong coupling QED . . . . .	81
3.9	Beyond the ladder approximation . . . . .	83
<b>4</b>	<b>Scalar composites in the symmetric phase</b>	<b>85</b>
4.1	Introduction . . . . .	85
4.2	Scalar vertex in quenched-ladder approximation . . . . .	87
4.3	Analytic structure of the scalar propagator . . . . .	96
4.3.1	The pure NJL limit . . . . .	97
4.3.2	Asymptotic behavior of the $\sigma$ boson vacuum polarization . . . . .	97
4.3.3	The $\sigma$ boson at critical gauge coupling . . . . .	98
4.3.4	Analytic continuation across the critical curve . . . . .	99
4.4	Comparison with earlier work . . . . .	99
4.5	Light scalar resonances near criticality . . . . .	101
4.6	Again: the conformal phase transition . . . . .	103
4.7	Renormalization and the scaling hypothesis . . . . .	105
4.8	Summary of results . . . . .	108
<b>5</b>	<b>On the existence of ultra-violet fixed points</b>	<b>111</b>
5.1	Beyond the quenched approximation . . . . .	111
5.2	Beyond the mean field approach . . . . .	115
5.3	The $1/N$ expansion . . . . .	117
5.4	Regularization and the fermion wave function . . . . .	119
5.5	Scalars, pseudoscalars, and charge screening . . . . .	120
5.6	The vacuum polarization in the $1/N$ expansion . . . . .	122
5.7	Analysis of the Johnson–Willey–Baker functions . . . . .	126
5.8	UV fixed points . . . . .	132
5.8.1	Close to the NJL point . . . . .	137
5.9	Discussion . . . . .	138
<b>A</b>	<b>GNJL model with <math>U(N)</math> symmetry</b>	<b>143</b>

<b>Contents</b>	<b>vii</b>
<b>B Green functions, propagators, and proper vertices</b>	<b>145</b>
B.1 Green functions of the GNJL model . . . . .	145
B.2 Connected Green functions . . . . .	146
B.3 Fourier transforms . . . . .	147
B.4 The Bethe–Salpeter scattering kernel . . . . .	148
<b>C Feynman rules</b>	<b>151</b>
<b>D Analysis of the Chebyshev expansion</b>	<b>155</b>
<b>E Two-loop vacuum polarization</b>	<b>163</b>
E.1 Two-loop vacuum polarization . . . . .	163
E.2 Scalar and pseudoscalar contributions . . . . .	167
E.3 Perturbative four-fermionic contributions . . . . .	169
<b>F A derivation of the JWB equation</b>	<b>173</b>
<b>References</b>	<b>179</b>
<b>Samenvatting</b>	<b>187</b>
<b>Acknowledgements</b>	<b>191</b>



# Introduction and summary

In this thesis we perform an analytic study of the gauged Nambu–Jona–Lasinio (GNJL) model. The GNJL model is a “toy-model” of dynamical chiral symmetry breaking (D $\chi$ SB). The famous Nambu–Jona–Lasinio (NJL) model [1] is one of the first models exhibiting D $\chi$ SB in relativistic quantum field theory and was inspired by models of superconductivity.

D $\chi$ SB is based on the phenomenon that strongly attractive interactions between massless fermions give rise to the formation of fermion–anti-fermion bound states and generation of a fermion mass. In this way dynamical symmetry breaking is a special case of spontaneous symmetry breaking where a symmetry of a particular model is broken by the appearance of a vacuum expectation value (VEV) of a composite operator (*e.g.*  $\langle\bar{\psi}\psi\rangle$ ) instead of the VEV of a fundamental field (*e.g.* the VEV of the Higgs field in the standard model). If the broken symmetry is continuous, such as the chiral symmetry, dynamical symmetry breaking gives rise to the Goldstone mechanism, *e.g.* see Refs. [2, 3].

Probably the most well-known realization of D $\chi$ SB and the Goldstone mechanism is provided by the low-energy dynamics of hadrons. Even long before the formulation of QCD (the microscopic theory of the strong interactions) the NJL model formed a basis for the phenomenological description of the chiral dynamics of hadrons.

Chiral symmetry is a symmetry of models with massless fermions. In such models “left-handed” spinors and “right-handed” spinors<sup>1</sup> do not interact and consequently their corresponding quantum numbers are conserved. To be more precise, chiral symmetry is the invariance of a model under independent unitary transformations of left-handed and right-handed spinors, for example  $U_L \times U_R$ .

Whenever a mass term is added to the Lagrangian of the model an interaction between left-handed and right-handed spinors is introduced, giving fermions a mass, and the chiral symmetry is lost. This is called explicit chiral symmetry breaking. However, in the case of strong interactions between the fermions it is possible that a mass is generated dynamically and a chiral condensate,  $\langle\bar{\psi}\psi\rangle$ , is formed.

---

<sup>1</sup>Left-handedness, respectively right-handedness, refers to the helicity properties of the fermions.

The chiral condensate is the “order parameter” of chiral symmetry breaking and plays a quite similar role as the total magnetization in models of magnets in statistical mechanics. In this context, the presence of an explicit mass parameter is analogous to the presence of an external magnetic field in *e.g.* certain Ising models.

Due to the existence of chiral (axial) Ward–Takahashi identities the generation of a fermion mass (*i.e.* the appearance of a gap in the fermion spectrum) coincides with the appearance of spinless bound states. This, then, is the dynamical realization of the Goldstone mechanism.

Suppose that the space of fermion mass operators is spanned by the “orthogonal” operators  $\bar{\psi}\psi$  and  $\bar{\psi}i\gamma_5\psi$ . Then we choose the chiral symmetry breaking (the long range ordering) to be in the direction of  $\bar{\psi}\psi$ . The massless bound states or Nambu–Goldstone (NG) bosons are given by correlations “transverse” to the direction of ordering. These states are called the pseudoscalar composites or the  $\pi$  bosons. The massive spinless scalar bound states (*i.e.* the “Higgs” bosons) describe correlations “longitudinal” to the direction of ordering and are referred to as the scalar composites or the  $\sigma$  bosons.

Moreover, in analogy with statistical mechanics, the generated mass  $m_\sigma$  of the  $\sigma$  should be considered as the inverse of the correlation length, *i.e.*  $m_\sigma \sim 1/\xi$ . The correlation length describes the spatial extent of fluctuations of a physical quantity (*e.g.* see Refs. [4, 5, 6]). In quantum field theories (QFTs) the correlation length describes the range of forces (interactions). Of course a well-known example is given by QED. The Coulomb interaction has “infinite” range, which is reflected by the fact that the photon, the carrier of the electromagnetic interaction, is massless. The range of the electroweak force is given in terms the masses of the  $W$  and  $Z$  gauge bosons,  $\xi \sim 1/M_W$ , respectively  $\xi \sim 1/M_Z$ .

The equation for the fermion mass is called the gap equation and describes the self-interaction (self-energy) of the fermion fields. The gap equation is a non-linear eigenvalue equation. For values of the coupling constants above some critical coupling the gap equation has a nonzero solution for the fermion mass even in the absence of an explicit external mass. This solution leads to a nonvanishing chiral condensate and consequently the chiral symmetry is broken. For values of the coupling below the critical value the gap equation only has the trivial solution with zero fermion mass and the chiral symmetry is unbroken. Exactly at the critical coupling the fermion mass is zero and the condensate vanishes; the gap equation describes a continuous phase transition. This is reflected by the non-analyticity of the gap equation in the coupling constant which causes the change of phase. The chiral condensate continuously changes from zero in the symmetric phase to nonzero values in the broken phase. As was pointed out by Yang and Lee [7] this non-analyticity is characteristic for phase transitions and can only occur in systems describing an infinite number of degrees of freedom.<sup>2</sup>

The realization of D $\chi$ SB is inherently nonperturbative and typically requires

---

<sup>2</sup>Relativistic quantum field theories are systems with an infinite number of degrees of freedom.

that coupling constants describing the “fundamental” interactions between fermions are of order one.

In the NJL model dynamical chiral symmetry breaking was realized by strong attractive four-fermion interactions (think of  $(\bar{\psi}\psi)^2$ ) which were incorporated in a mean-field approach known as the Hartree–Fock approximation. In mean-field approximations the composite operators such as  $\bar{\psi}\psi$  are replaced by their VEVs ( $\bar{\psi}\psi \rightarrow \langle \bar{\psi}\psi \rangle$ ) and fluctuations about that value are ignored. However the NJL model turned out to be “in the language of the sixties” a nonrenormalizable model. It has a limited range of applicability because of the explicit dependence on the ultra-violet cutoff  $\Lambda$ .<sup>3</sup>

It was realized by the Kiev group in Refs. [8, 9] that QED in the quenched-ladder approximation also exhibits dynamical chiral symmetry breaking for values of the bare gauge coupling  $\alpha_0 > \alpha_c \sim 1$ , where  $\alpha_0 = e_0^2/4\pi$ . This was argued to be intimately connected with the “fall into the center” phenomenon. By considering the Dirac equation describing a light fermion in a static Coulomb potential, it was shown that, when the Coulomb attraction dominates the centrifugal barrier for  $\alpha_0 \geq \alpha_c$ , the system “collapses” (*i.e.* a drastic rearrangement of the ground state (vacuum) occurs). Later it was pointed out in Refs. [10, 11] that the critical coupling  $\alpha_c$  above which the chiral symmetry is broken should be considered as an ultra-violet (UV) fixed point.

An important step was performed by Bardeen, Leung, and Love in Refs. [12, 13]. These authors realized that, in quenched-ladder QED, four-fermion interactions have a so-called scaling dimension 4 instead of 6 at the critical gauge coupling  $\alpha_0 = \alpha_c$ . Consequently these operators mix with the gauge interaction which also has dimension 4 in four space-time dimensions; this means that QED is not a closed theory at the chiral phase transition. The scaling dimension of an operator is important since it determines the possible range of the interaction which the operator describes. Their model is referred to as the gauged Nambu–Jona-Lasinio (GNJL) model.

The origin and physical significance of scaling dimensions is undoubtedly best explained by the renormalization-group methods of Wilson [14, 15]. Wilson stressed the importance of defining a low-energy effective action or microscopic action from which a generating functional can be constructed. The Wilsonian effective action is an action describing local interactions defined at some microscopic length scale  $a \sim 1/\Lambda$ . The interactions between the degrees of freedom corresponding to distances shorter than  $1/\Lambda$  are not defined and such dynamics are “effectively” described by the coupling constants of the microscopic action. In this way the high energy frequencies of the fields with  $E \geq \Lambda$  are “coarse grained” or “integrated out” into the coupling constants and the coupling constants implicitly depend on the cutoff  $\Lambda$ .

The interesting question is what type of macroscopic physics characterized by

---

<sup>3</sup>The cutoff is required to render the theory finite.

an “infra-red (IR)” energy scale  $E$  with  $E \ll \Lambda$  can be realized from the microscopic action. The transformation of the microscopic action to the macroscopic action is governed by the renormalization-group (RG) transformation of the coupling constants of the model. If a macroscopic model can be derived from a microscopic model in such a way that the macroscopic dynamics can be formulated independently of the scale  $\Lambda$  and only depend on the coupling constants of the microscopic model, the microscopic model is said to be renormalizable.

Wilson pointed out that such a macroscopic theory can only be formulated if the RG transformation exhibits UV fixed points. UV fixed points are “singular” points<sup>4</sup> of the RG transformation at which the model becomes scale (*i.e.* conformal) invariant. Wilson pointed out that natural candidates for UV fixed points are critical points governing a continuous phase transition. Since, at a continuous phase transition, the correlation length  $\xi$  is infinite, the model is scale invariant and the dynamics is extremely sensitive to external perturbations.

A mathematical formulation of the RG transformation and UV fixed points for QED was already given by Gell-Mann and Low in Ref. [16]. But the physical significance of such fixed points and the interpretation of infinities appearing in Feynman diagrams were not fully understood in the fifties and sixties.

The most crucial observation of Wilson is that in the RG transformation, *i.e.* the “coarse graining” process, new types of local interactions are generated and that the new interactions can be classified as either irrelevant or relevant interactions. In this way the RG transformation is a nontrivial improvement of the coarse graining methods of Kadanoff [17]. By definition, the effect of an irrelevant interaction<sup>5</sup> of a microscopic action is suppressed by positive powers of  $E/\Lambda$  in the macroscopic action. This is closely related to the Appelquist–Carazzone decoupling theorem [18]. Hence only relevant interactions are important in determining what kind of macroscopic dynamics emerges from microscopic models. The effect of irrelevant interactions can always be absorbed by adapting the coupling constants of relevant and marginal interactions. Marginal interactions are in between irrelevant and relevant and are considered the most interesting ones; in four dimensions they comprise the gauge interactions.

In analogy with statistical mechanics, the continuous chiral phase transition can be classified in terms of critical exponents which describe the scaling of various macroscopic quantities (*e.g.* the chiral condensate, correlation length, effective potential, chiral susceptibility) close to or at the critical point. It is considered a strong indication of the existence of a nontrivial continuum limit ( $\Lambda \rightarrow \infty$ ), if so-called hyperscaling relations between these various critical exponents are satisfied. The RG of Wilson provides the framework for explanation and computation of the critical exponents and makes an intimate connection between critical phenomena (in particular continuous phase transitions) in statistical mechanics and the renormalization

---

<sup>4</sup> UV fixed points are specific roots of the  $\beta$  functions.

<sup>5</sup> Irrelevant interactions are also referred to as nonrenormalizable.

and existence of the continuum limit in quantum field theories.

Especially, close to a phase transition, the RG methods of Wilson show that it is not possible, a priori (without solving the equations of motion), to determine which interactions are relevant or irrelevant; particular interactions can acquire anomalous dimensions and interactions which are irrelevant in a certain region of coupling constant space might become relevant in another region.

The coupling constants which govern the chiral phase transition are similar to the inverse of the temperature in models of statistical mechanics.

Perturbatively the four-fermion interaction is irrelevant, which is supposedly due to the fact that the four-fermion coupling constant has negative dimension (in mass units). However, as was shown by Bardeen, Love, and Leung [12, 13] the solutions to the gap equation in the GNJL model suggest that the four-fermion interactions acquire a large anomalous dimension. The anomalous dimension  $\gamma_m$  of the mass operator  $\bar{\psi}\psi$  equals one ( $\gamma_m = 1$ ) at  $\alpha_0 = \alpha_c$ .

The GNJL model literally is the gauged version of the NJL model. It is based on induced chiral invariant and gauge invariant four-fermion interactions. The gauge group can be either a  $U(1)$  gauge symmetry or some non-Abelian gauge symmetry. In case of GNJL model there are two attractive interactions: an attractive four-fermion interaction and a gauge interaction (with gauge coupling  $\alpha_0$ ). In this thesis we will consider the GNJL model with  $U(1)$  gauge symmetry, in that case the GNJL model is a generalization of quantum electrodynamics (QED). The microscopic Lagrangian for a single fermion flavor reads

$$\mathcal{L} = -\frac{1}{4}F_{\mu\nu}^2 + \bar{\psi}(i\gamma^\mu D_\mu - m_0)\psi + \frac{G_0}{2}[(\bar{\psi}\psi)^2 + (\bar{\psi}i\gamma_5\psi)^2], \quad (1)$$

where  $D_\mu = \partial_\mu - ie_0A_\mu$ , and where  $G_0$  is the positive four-fermion coupling. The Lagrangian is determined by the following three dimensionless coupling constants:

$$\mu_0 = m_0/\Lambda, \quad \alpha_0 = e_0^2/4\pi, \quad g_0 = G_0\Lambda^2/4\pi^2, \quad (2)$$

where  $\Lambda$  is the ultraviolet cutoff. The GNJL model can be conveniently analyzed in terms of so called auxiliary fields ( $\sigma = -G_0\bar{\psi}\psi$  and  $\pi = -G_0\bar{\psi}i\gamma_5\psi$ ) describing scalar and pseudoscalar degrees of freedom. In such a formulation, the four-fermion interactions are described by the interactions of the auxiliary fields with the fermion fields. Then the connected two-point Green function of the  $\pi$  field describes the NG-boson and the connected two-point Green function of the  $\sigma$  field describes the “Higgs” boson.

In the quenched-ladder (quenched-planar) approximation the chiral phase structure was computed in Refs. [19, 20]. There is a critical curve in the coupling constant plane  $(\alpha_0, g_0)$  which separates a chiral symmetric phase from a phase in which the chiral symmetry is dynamically broken.

In Ref. [21] the anomalous dimension  $\gamma_m$  along the critical curve was computed (in the broken phase) and it was found that  $1 \leq \gamma_m \leq 2$ , where  $\gamma_m = 1$  at  $\alpha_0 = \alpha_c$  and  $\gamma_m = 2$  at  $\alpha_0 = 0$ .

The particle spectrum consists of pseudoscalar ( $\pi$ ) and scalar ( $\sigma$ ) bound states which become relevant degrees of freedom (their masses are light) in the vicinity of the critical curve. In the D $\chi$ SB phase there is a massless pseudoscalar (NG-boson) and a massive scalar. Since the phase transition is second order along the critical curve there are scalar and pseudoscalar resonances on the symmetric side of the curve whose masses also vanish as the critical curve is approached [22]. The phase transition at NJL point ( $\alpha_0 = 0$ ) is believed to be of the mean field type (up to logarithmic corrections) and to correspond to that of a trivial theory, *e.g.* see Ref. [3].

In the intermediate region ( $0 < \alpha_0 < \alpha_c$ ), the phase transition is quite similar to the pure NJL case except that the critical exponents satisfy nonmean-field hyperscaling relations which supports the view that the quenched approximation has a nontrivial continuum limit [23, 24].

At, what is referred to as the QED point,  $\alpha_0 = \alpha_c$ , the phase transition is rather special and is characterized by a scaling law with an essential singularity (instead of a power law) for the fermion dynamical mass. There is an abrupt change in the particle spectrum when the phase boundary is crossed. This peculiar phase transition has properties similar to the Berezinsky-Kosterlitz-Thouless phase transition [25, 26] and is referred to as the conformal phase transition (CPT) [27]. The crucial point is that the symmetry is broken by marginal operators instead of by relevant operators.

Whereas from the “perturbative” point of view the correlation length of a four-fermion interaction is typically the inverse of the cutoff  $\xi \sim 1/\Lambda$ , close to a critical point in the GNJL model we find that

$$\xi \sim 1/m_\sigma, \quad m_\sigma = (\Delta g_0)^\nu, \quad (3)$$

where  $\Delta g_0 = |g_0 - g_c|$  measures the distance of  $g_0$  to critical point  $g_c$  and  $\nu$  is a (positive) critical exponent. Thus, when  $\Delta g_0 \rightarrow 0$ , the correlation length goes to infinity. This is interpreted as a dimensional transmutation of the four-fermion operator  $(\bar{\psi}\psi)^2$  which has a canonical dimension of 6 to a nonperturbatively induced dynamical dimension  $d_{\text{dyn}} \leq 4$  (hence relevant (marginal)) at the critical point:

$$\dim(\bar{\psi}\psi)^2 = 6 - 2\gamma_m \leq 4, \quad \dim(\bar{\psi}\psi) = 3 - \gamma_m. \quad (4)$$

The factorization property  $\dim(\bar{\psi}\psi)^2 = 2\dim(\bar{\psi}\psi)$  is implicit in the quenched-ladder approximation and is crucial for the nonperturbative renormalizability of the GNJL model [23]; it leads to the requirement that the critical exponent  $\gamma$  of the so-called chiral susceptibility equals one,  $\gamma = 1$ .

The interest in the GNJL has been stimulated by its importance for constructing new scenarios of dynamical realization of electroweak symmetry breaking. Examples are strong extended technicolor models (*e.g.* see Refs. [28, 29, 30, 21]) and the top-quark condensate model (*e.g.* see Refs. [31, 32, 33]). It was argued in Refs. [34, 35, 36, 37] that large anomalous dimensions could solve the problem of

flavor changing neutral currents in technicolor and extended technicolor models. For a general introduction into these models and their predecessors we refer to the book by Miransky [3].

Since these models are based on strong interactions, giving rise to the appearance of a large anomalous dimension for the mass operator  $\bar{\psi}\psi$ , these models are inherently nonperturbative. The origin of the four-fermion interactions is assumed to be given by physics at or above some high energy scale  $\Lambda$ . Two natural candidates for the high energy scale or ultra-violet cutoff  $\Lambda$  are the scale of grand unified theories (GUTs), *i.e.*  $\Lambda \sim 10^{15} - 10^{16}$  GeV, and the Planck scale  $\Lambda \sim 10^{19}$  GeV. The relevant physics at these scales should somehow be given by GUTs, supersymmetric field theories, supergravity, string theory, or perhaps  $M$ -theory. However, the main point is that as long as the model is close to criticality the low-energy effective dynamics is rather insensitive to the details of the interactions at  $\Lambda$ . This is known as universality. For instance the exchange of a heavy gauge boson with a mass of the order of the cutoff  $\Lambda$  could induce such a local four-fermion interacting for energies  $E \leq \Lambda$ .

The GNJL model in the quenched approximation has been studied extensively on the lattice (in so-called noncompact formulation, *e.g.* see Ref. [38]), by means of nonperturbative renormalization group (NPRG) methods, and with Schwinger–Dyson (SD) techniques. In the quenched approximation fermion-loops are omitted, and consequently the gauge coupling  $\alpha_0$  does not run. In addition to the quenched approximation, the SDEs are studied by taking the gauge interaction in the ladder or planar approximation; this means that crossed photon graphs and vertex corrections are omitted.

A very useful and popular method is the computation of the low-energy effective action for the composite fields which is obtained after integrating out the fermion and photon fields in the generating functional. Such methods are capable of computing macroscopic quantities such as the effective Yukawa coupling,  $\lambda_Y$ , the mass of the  $\sigma$  boson,  $m_\sigma$ , and the “pion” decay constant,  $f_\pi$ .

The comparison of the lattice simulations and NPRG methods show that qualitatively the ladder approximation is reliable, and rather small quantitative differences arise because of the neglect of vertex corrections and crossed photon exchange diagrams. The advantage however of the quenched-ladder SD formalism with respect to the numerical methods is that results can be obtained analytically.

The first three chapters of this thesis cover most of the important achievements and results on dynamical chiral symmetry breaking in the GNJL model and QED, which we feel are necessary to understand the results of chapters 4 and 5.

In chapter 1 we review the path-integral formalism for the generating functional and the Schwinger–Dyson equation (SDE). We briefly discuss the basic features governing phase transitions and critical phenomena in statistical mechanics and discuss the RG of Wilson, the Goldstone mechanism, and the auxiliary field method for the GNJL model. In chapter 2 we derive both the Schwinger–Dyson equations

and the so-called partial conserved axial currents (PCAC). Chapter 3 is devoted to the gap equation, scaling laws, the critical curve etcetera. Moreover in chapter 3 we compare the SD quenched-ladder approach with other nonperturbative techniques. The results and conclusions of this thesis are the following.

In chapter 4: in quenched-ladder approximation, treating the four-fermion interaction in the mean-field setting, we have computed analytically the scalar Yukawa vertex in specific kinematical regimes. The Yukawa vertex describes the interaction between fermions and the composite states, *i.e.* the spinless  $\sigma$  and  $\pi$  bosons. By making use of Chebyshev expansions we are able to derive asymptotic expressions for the Yukawa vertex as functions of the in-going momentum of the fermions and out-going momentum of the  $\sigma$  boson. This allows us to derive an analytic expression for the scalar propagator (the  $\sigma$  boson propagator), which is valid along the entire critical curve.

Our results are in agreement with previous work of Appelquist *et al.* [22], and related work [39], who used a resummation technique which applies only for relatively small values of  $\alpha_0$ . Near the critical gauge coupling  $\alpha_0 = \alpha_c$  the light resonances in the symmetric phase disappear from the particle spectrum, and the scaling law with an essential singularity, which is characteristic for the CPT of Miransky and Yamawaki ([27]), is recovered by analytic continuation of the  $\sigma$  boson propagator across the critical curve. The results of chapter 4 were published in Ref. [40].

In chapter 5 we study the “unquenched” GNJL model<sup>6</sup> and reinvestigate the screening of the gauge coupling  $\alpha_0$  by computing the vacuum polarization. We consider the GNJL model with global  $U_L(N) \times U_R(N)$  chiral symmetry, where  $N$  is the number of fermion flavors.<sup>7</sup> The interesting question is whether the GNJL model exhibits ultra-violet fixed points or the gauge coupling  $\alpha_0$ ,

$$\beta_\alpha(\alpha_0) = 0, \quad \beta'_\alpha(\alpha_0) < 0, \quad \beta_\alpha(\alpha_0) \equiv \Lambda \frac{d\alpha_0}{d\Lambda}. \quad (5)$$

The function  $\beta_\alpha$  describes the renormalization group flow of  $\alpha_0$ . If such an UV fixed point exists the model has a nontrivial (interacting) continuum limit.

Many works on QED conclude, following Landau and Pomeranchuk [42], that QED is trivial (non-interacting) in four dimensions; the continuum limit describes a free-field theory (there is no root of the  $\beta$  function satisfying Eq. (5)). This is a result of the total screening of the gauge coupling by virtual fermion pairs (fermion loops) from the vacuum. However we think that the main ingredient for settling the charge screening problem is missing, namely the contribution of the composite  $\sigma$  and  $\pi$  bosons and their effective interactions with fermions.

The observation that hyperscaling relations are satisfied ([23, 24]) clearly indicates that the correlations corresponding to the four-fermion interactions are not of

---

<sup>6</sup>That means we turn back on fermion loops.

<sup>7</sup>The global  $U_L(N) \times U_R(N)$  chiral symmetry comprises the largest set of relevant chiral invariant four-fermion operators (*e.g.* see Ref. [41]).

the mean-field type. According to Landau's mean-field theory only specific mean-field exponents can describe the scaling near the critical point. Therefore any deviation from the mean-field exponents signals the inconsistency of the mean-field approach and suggests that fluctuations of the composite  $\sigma$  and  $\pi$  fields about their mean value cannot be ignored.

We argue that in case of the GNJL model close to the chiral phase transition the virtual fermion loops causing charge screening are suppressed due to the appearance of attractive relevant four-fermion interactions, where we recall that the four-fermion interactions are represented by the exchange of  $\sigma$  and  $\pi$  bosons. The standard picture of the QED-vacuum as a medium of virtual electric dipoles formed by virtual fermion-anti-fermion pairs breaks down due to the strong self-interactions of the fermions. Moreover the problem is flavor dependent; the larger the number of fermion flavors, the more the charge is screened. On the other hand with  $N$  fermion flavors there are  $2N^2$  chiral invariant four-fermion interactions. Thus increase of  $N$  increases the role of four-fermion interactions. The four-fermion interactions induce a nontrivial Yukawa interaction, this is also referred to as the nondecoupling of the composites, see Ref. [43]. The spinless composites states are relevant degrees of freedom for a large range of momenta  $m_\sigma \leq p \leq \Lambda$ .

We incorporate the  $\sigma$  and  $\pi$  exchanges using the skeleton expansion [44] for the irreducible Bethe-Salpeter kernel and the  $1/N$  expansion of 't Hooft [45]. The skeleton expansion is formulated in terms of "fully dressed" vertices and propagators for which we substitute the asymptotic expressions for the scalar Yukawa vertex and  $\sigma$  boson propagator derived in chapter 4. The basic idea of the  $1/N$  expansion is that for  $N$  large only the planar (*i.e.* ladder) exchanges of  $\sigma$  and  $\pi$  bosons are dominant. Then by making use of a resummation technique of Johnson *et al.* [46] we can compute the  $\beta$  function of the gauge coupling  $\alpha_0$  defined by Eq. (5) and search for ultra-violet fixed points. We find that UV fixed points exist for values of  $N$  above a critical value  $N_c \approx 54$ . The largest UV fixed point is  $\alpha_0 \approx 0.14$ .

Assuming that our results are qualitatively correct, we have realized, in an inherently nonperturbative manner<sup>8</sup>, a nontrivial (*i.e.* interacting) continuum limit for a nonasymptotically free gauge field theory in four dimensions. This means that the low-energy dynamics characterized by an energy scale  $E$  ( $E \ll \Lambda$ ) can be formulated independent of the ultra-violet cutoff  $\Lambda$  by tuning the bare couplings to their critical values. Thus the trade-off is that bare couplings have to be fine-tuned to their critical values (the UV fixed points).

This fine-tuning, which is also known in the literature as the gauge hierarchy problem ( $m_\sigma \ll \Lambda$ ), is not (yet) explained by the model itself. Studies of dynamical symmetry breaking in supersymmetric models provide a promising solution, *e.g.* see Ref. [47]. The crucial question is; why is the system close to criticality? An interesting resolution is that of self-organizing criticality, see Ref. [48].

The realization of such a nontrivial theory requires a large number of fermion

---

<sup>8</sup>Perturbatively the GNJL model is a trivial theory.

flavors  $N > N_c \approx 54$  and the fine-tuning of the four-fermion coupling  $g_0$  and gauge coupling  $\alpha_0$  to their UV fixed points. Clearly our claims should be verified in the future by quantitatively more reliable techniques such as lattice simulations and nonperturbative renormalization group methods. Especially we believe that the determination of the critical value  $N_c$  is rather sensitive to the various approximations used, hence  $N_c$  is a so-called nonuniversal quantity.

## List of short-hand notations

BS	Bethe–Salpeter
CJT	Cornwall–Jackiw–Tomboulis
CP	Charge Parity
CPT	Conformal Phase Transition
D $\chi$ SB	Dynamical Chiral Symmetry Breaking
EOS	Equation of State
ETC	Extended technicolour
GNJL	Gauged Nambu–Jona–Lasinio
GUT	Grand Unified Theory
IR	Infra-red
JWB	Johnson–Willey–Baker
NG	Nambu–Goldstone
NJL	Nambu–Jona–Lasinio
NPRG	Nonperturbative Renormalization Group
QCD	Quantum Chromodynamics
QED	Quantum Electrodynamics
QFT	Quantum Field Theory
PCAC	Partial Conserved Axial Currents
PCDC	Partial Conserved Dilaton Currents
RG	Renormalization Group
SDE	Schwinger–Dyson Equation
UV	Ultra-violet
VEV	Vacuum Expectation Value
WTI	Ward–Takahashi Identity

# Chapter 1

## Phase transitions and quantum field theory

This chapter provides the basic framework of this thesis. After introducing the path-integral formalism for relativistic quantum field theory, we discuss the feature of critical phenomena (such as continuous phase transitions) and scaling in statistical mechanics. We review the renormalization group methods of Wilson and the Goldstone mechanism. This chapter is concluded with the introduction of the GNJL model and the auxiliary field method.

### 1.1 Review of the path-integral formalism

Relativistic quantum field theory (QFT) is governed by expectation values of operator-valued fields on Minkowski space-time. The field at each space-time point is referred to as a degree of freedom, thus any particular finite region of space-time deals with an infinite number of degrees of freedom. The “vacuum” expectation values are particular expectation values of the fields. These so-called Green functions (“or correlation functions”) describe the behavior of elementary particles. The interactions are given by an action  $S$ , and the dynamics is derived from a generating functional  $Z$ . From this generating functional the entire (infinite) set of Green functions can be constructed. The generating functional is analogous to the partition function or Gibbs integral in statistical mechanics. The generating functional is given as a functional path-integral over all field configurations weighted by the “classical” action times  $i/\hbar$ , henceforth we will use units in which  $\hbar = 1$ . This so-called path-integral formalism was introduced by Feynman [49, 50] for quantum mechanics and quantum field theory.

In what follows only one scalar field is considered for simplicity. The generating functional  $Z$  as the function of some arbitrary “external” source  $J(x)$  can be written

as

$$Z[K, J] = N \int \mathcal{D}\phi \exp\{iS[K, \phi, J]\}, \quad (1.1)$$

where  $N$  is some normalization constant such that  $Z[K, J = 0] = 1$ , and where the action (or weight)  $S[K, \phi, J]$  is the sum of some particular fundamental action  $S_f$ , and the source action  $S_J$  describing the coupling to the arbitrary source  $J$ :

$$S[K, \phi, J] = S_f[K, \phi] + S_J[J, \phi]. \quad (1.2)$$

The source action,  $S_J$ , is of the form

$$S_J[J, \phi] \sim \int d^d x J(x) \phi(x), \quad (1.3)$$

in  $d$  dimensions. We consider actions of local operators  $O_i$  of  $\phi$ :

$$S_f[K, \phi] = \int d^d x \sum_i K_i O_i [\phi(x)], \quad (1.4)$$

where an example of a local (Euclidean) operator  $O$  is

$$O[\phi(x)] = -\phi(x) \Delta \phi(x), \quad (1.5)$$

with  $\Delta$  the Laplacian. The generating functional  $Z$  is a functional of the external sources  $J(x)$  and couplings  $K$ ;  $Z$  is by construction analytic in the sources  $J$ , see Refs. [51, 6], and Eq. (1.7). Green functions are defined as time-ordered vacuum expectation values (VEV) of a specific number of fields, *e.g.*,

$$\begin{aligned} iG^{(n)}(x_1, x_2, \dots, x_n) &\equiv \langle 0 | T(\phi(x_1)\phi(x_2)\dots\phi(x_n)) | 0 \rangle \\ &= \frac{\delta}{i\delta J(x_n)} \dots \frac{\delta}{i\delta J(x_2)} \frac{\delta}{i\delta J(x_1)} Z[K, J] \Big|_{J=0}, \end{aligned} \quad (1.6)$$

*i.e.* the generating functional generates VEVs of time-ordered products of fields. Hence the Green functions can be constructed by functionally differentiating  $Z$  with respect to sources. Since the generating functional is analytic in  $J(x)$ , the generating functional can be expressed as a Taylor series in sources,

$$Z[K, J] = \sum_{n=0}^{\infty} \frac{i^n}{n!} \int d^d x_1 \dots d^d x_n iG^{(n)}(x_1, \dots, x_n) J(x_1) \dots J(x_n), \quad (1.7)$$

where the Green function depend implicitly on the couplings  $K$ . However, although the above construction of functional integration might appear to be rather straightforward and intuitive, this is deceptive. It is a highly nontrivial mathematical

problem how to define the functional integration measure,  $\mathcal{D}\phi$ , and functional integration properly. In Ref. [52] the problem of functional integration is addressed, and a new perspective on functional integration is presented. The idea of de Mirleau is to define such functional integration just as one would define integration, *i.e.*, as a solution of a differential equation, with appropriate boundary conditions.

For a fixed Euclidean action  $S$ , consider the following linear functional

$$\langle f \rangle \equiv N \int \mathcal{D}\phi f \exp\{-S[\phi]\}, \quad (1.8)$$

where  $f$  and  $S$  belong to the same algebra, and  $N$  is a number. The functional integration is defined by the following properties:

1. The Schwinger–Dyson equation (SDE):  $\langle (\delta S)f \rangle - \langle \delta f \rangle = 0$ ,
2. Positivity:  $f \geq 0 \implies \langle f \rangle \geq 0$ ,
3. Normalization:  $\langle 1 \rangle = N \int \mathcal{D}\phi \exp\{-S[\phi]\}$ ,

where the  $\delta$  represent derivatives (mutually commuting (bosons) or anti-commuting (fermions)) of the particular functional space or algebra, (*e.g.*  $\delta \sim \delta/\delta\phi(x)$ ). The normalization condition 3 is straightforward for finite dimensional integration, but is not always applicable to the infinite dimensional case. We refer to [52] for an extensive discussion of this point. The Schwinger–Dyson equation (SDE) was independently formulated by Dyson [53] and Schwinger [54].

Let us consider the Euclidean version of generating functional  $Z$  of Eq. (1.1) which is defined as

$$Z[K, J] \equiv \langle \exp\{-\int d^d x J(x)\phi(x)\} \rangle_{S_f}, \quad (1.9)$$

$$\langle f[\phi] \rangle_{S_f} \equiv N \int \mathcal{D}\phi f[\phi] \exp\{-S_f[K, \phi, J]\}. \quad (1.10)$$

Then, the SDE for  $Z$  can be written as

$$\left\{ \frac{\delta S_f [K, \phi]}{\delta \phi(x)} \bigg|_{\phi(x)=\delta/\delta J(x)} + J(x) \right\} Z [K, J] = 0. \quad (1.11)$$

Such an equation was in fact formulated already by Feynman in Ref. [49]. The SDE for any Green function corresponding to this particular model (1.9) can be obtained by first differentiating Eq. (1.11) with respect to appropriate combinations of sources ( $J(x)$ ,  $J(y)$ ,  $\dots$ ) and then putting all sources equal to zero.

From the generating functional one can construct the following functional (in Euclidean formulation):

$$\begin{aligned} W[K, J] &\equiv \log Z[K, J] \\ &= \sum_{n=1}^{\infty} \frac{1}{n!} \int d^d x_1 \cdots d^d x_n G_C^{(n)}(x_1, \dots, x_n) J(x_1) \cdots J(x_n), \end{aligned} \quad (1.12)$$

which is the generating functional for connected Green functions,  $G_C^{(n)}$ , *i.e.* Green functions which satisfy the cluster property, see Ref. [6]<sup>1</sup>. The functional  $W$  is now convex in the couplings  $K$ , and analytic in the sources  $J$ ;  $W$  is extensive, *i.e.* proportional to the total volume, and is analogous to the free energy in statistical mechanics.

The Green functions given by Eq. (1.7) and the connected Green functions of Eq. (1.12) are not defined on the entire space-time manifold, because of the existence of so called short distance singularities, *e.g.* the limit

$$\lim_{x_1 \rightarrow x_2} iG^{(n)}(x_1, x_2, x_3, \dots, x_n) \quad (1.13)$$

is ill defined. Regularization (*e.g.* Pauli–Villars), which we will discuss in section 1.3, permits a setting for the treatment of Eq. (1.13).

## 1.2 Continuous phase transitions

Phase transitions can occur in systems containing an infinite number of degrees of freedom exhibiting nonanalytic behavior (*e.g.* in certain VEVs) in one (or more) of its parameters such as the temperature. A model in statistical mechanics, *e.g.* the Ising model, is given in terms of a partition function

$$Z_\Omega [K] \equiv \text{Tr} \exp\{-\beta H_\Omega\}, \quad (1.14)$$

where  $\beta \equiv 1/k_B T$  ( $k_B$  is Boltzman’s constant). The partition function is defined over a finite region  $\Omega$  with a volume  $V(\Omega) \sim L^d$ , surface  $S(\Omega) \sim L^{d-1}$ , and with  $N(\Omega)$  degrees of freedom, where  $L$  is characteristic length scale, and  $d$  the dimension of the system. The Hamiltonian for the system is written as

$$\beta H_\Omega = \sum_i^n K_i O_i [S], \quad (1.15)$$

where  $K = (K_1, K_2, \dots, K_n) \sim (T, h, \dots)$  (with  $T$  the temperature,  $h$  the external magnetic field etc.) are coupling constants and the (local) operators  $O$  are functionals of the dynamical degrees of freedom, which in case of the Ising model are spins  $S_j$  ( $1 \leq j \leq N(\Omega) \sim (L/a)^d$ ) on lattice sites with a lattice spacing  $a$ . The lattice spacing  $a$  is then referred to as the microscopic length scale, since interactions on a scale smaller than  $a$  are not defined. The trace,  $\text{Tr}$ , in Eq. (1.14) represents the sum over all possible configurations of spins, and is analogous to the functional integration in Eq. (1.1).

The free energy is defined by

$$F_\Omega [K] = -k_B T \log Z_\Omega [K]. \quad (1.16)$$

---

<sup>1</sup>In short, the cluster property states that the vacuum expectation value of a product of local operators factorizes when their space-like separations become large [2].

Assuming that the thermodynamic limit,

$$V(\Omega), S(\Omega), N(\Omega) \longrightarrow \infty, \quad N(\Omega)/V(\Omega) = \text{constant}, \quad (1.17)$$

for the free energy exists, we can define the bulk free energy density  $f_b$  (the free energy per lattice site):

$$f_b[K] = \lim_{N(\Omega) \rightarrow \infty} \frac{F_\Omega[K]}{N(\Omega)}. \quad (1.18)$$

The so-called extensive thermodynamic behavior is now described by  $f_b[K]$ , and its derivatives with respect to coupling parameters such as the temperature  $T$  or external magnetic field  $h$ . An example of a macroscopic quantity is the magnetization  $M$ ,

$$M \equiv \frac{\partial f_b[K]}{\partial h} \propto \langle S \rangle. \quad (1.19)$$

The bulk free energy  $f_b$  is a convex function of the coupling parameters.

A phase of a system is defined by regions of analyticity of  $f_b[K]$ . Possible non-analyticities of  $f_b[K]$  occur at points, lines or hyperplanes in parameter space. We define  $D_S$  as the dimension of a particular non-analyticity region of  $f_b[K]$ . Suppose that  $f_b[K]$  is given in terms of  $D$  coupling constants. If the dimension  $D$  of the space of coupling constants, and the dimension  $D_S$  of the non-analyticity is such that the co-dimension

$$C = D - D_S = 1, \quad (1.20)$$

then this non-analyticity is referred to as a phase-boundary. Thus, a phase boundary is defined by non-analyticities of  $f_b[K]$  which separate phases. Whenever, by changing the coupling constants  $K$ , the phase boundary is crossed, the model is said to undergo a phase transition.

The bulk free energy  $f_b[K]$ , because it is convex, is continuous everywhere. Phase transitions are classified into first order, respectively, continuous phase transitions depending on whether the first derivatives of  $f_b$  with respect to  $K$  are continuous or not.

1. We speak of a first order phase transition, if one (or more) of the first derivatives  $\partial f_b / \partial K_i$  of the bulk free energy is discontinuous at the phase boundary (critical point). It means that an order parameter changes discontinuously across the phase boundary.
2. We speak of a continuous phase transition, if all first derivatives of the bulk free energy are continuous at the phase boundary, meaning that an order parameter changes continuously across the phase boundary. The non-analyticity of the phase boundary is reflected by discontinuities of certain higher order (than one) derivatives of the order parameter at the phase boundary.

In case of the Ising model the order parameter is the magnetization  $M$ , which in absence of an external magnetic field is zero for temperatures  $T \geq T_c$ , and  $M$  is nonzero for  $T < T_c$  (long range order), where  $T_c$  is the critical temperature. Although (for specific Ising models) the magnetization  $M$  changes continuously from zero ( $T \geq T_c$ ) to nonzero values for  $T < T_c$  (thus the phase transition is continuous, since  $M$  is a first derivative of  $f_b$ ), the magnetization  $M$  as function of  $T$  is nonanalytic at  $T = T_c$ , *i.e.* the left and right derivatives of  $M$  with respect to  $T$  differ at  $T = T_c$ .

For quantum field theories the analogue of the free energy is the generating functional  $W$  (*e.g.* Eq. (1.12)) of connected Green functions. The above classification of phase transitions applies to QFTs too. An order parameter can usually be given in terms of a first derivative of  $W$ , and we speak of a continuous phase transition whenever the order parameter changes continuously across the phase boundary. The phase boundary is then characterized by the non-analyticities of  $W$  in certain couplings.

An important quantity in the study of continuous phase transitions is the correlation length. The correlation length  $\xi$  is the characteristic length scale of fluctuations of a physical quantity such as the local magnetization  $S_i$  around its average  $\langle S_i \rangle$ . Let us consider the “connected” two-point correlation function defined by

$$G_C(\vec{r}_i - \vec{r}_j) = \langle S_i S_j \rangle - \langle S_i \rangle \langle S_j \rangle, \quad (1.21)$$

which can be obtained by differentiating the free energy with respect to external fields (or sources). The correlation function  $G_C$  describes local fluctuations parallel to the long range ordering in the system, and the properties of  $G_C$  are:

$$\begin{aligned} G_C(\vec{r}) &\sim \frac{e^{-r/\xi}}{r^{(d-1)/2}\xi^{(d-3)/2}}, \quad r \equiv |\vec{r}| \gg \xi, \\ G_C(\vec{r}) &\sim \frac{1}{r^{d-2+\eta}}, \quad r \equiv |\vec{r}| \ll \xi, \end{aligned} \quad (1.22)$$

where  $\xi$  is called the correlation length, and  $\eta$  is the anomalous dimension.

### 1.2.1 The scaling hypothesis

A very useful mathematical tool in the study of continuous phase transitions and critical phenomena is provided by the existence of scaling laws. For a system close to a critical point separating different phases, a set of critical exponents is introduced to describe both the scaling of thermodynamic quantities, such as a the magnetization  $M$ , specific heat, etc., as well as local ordering, correlations, and fluctuations given in terms of correlation functions and a correlation length  $\xi$ .

The scaling laws are motivated by assuming that the only relevant length scale near criticality is the correlation length  $\xi$ . The renormalization group (RG) methods of Kadanoff and Wilson, which will be discussed later on, show that this assumption

is incorrect. Apart from the correlation length another length scale is crucial for understanding critical phenomena, namely the microscopic length scale, *e.g.* the lattice spacing  $a$ .

There is a threefold way of considering the phenomenon of scaling, namely, the scaling form for the so-called equation of state (EOS), the scaling form for the singular part of the free energy, and the scaling form for the correlation function.

### 1.2.2 The scaling hypothesis for the equation of state

The “equation of state” for an order parameter (which characterizes a certain phase of the system) can be obtained by differentiating the free energy of the system with respect to some external local source or external field, to which the order parameter is coupled. In the context of magnetic systems, the EOS of a magnet is written as

$$h = f_e(M, T), \quad (1.23)$$

where  $h$  is the external magnetic field,  $M$  the spontaneous magnetization, and  $T$  the temperature ( $f_e$  follows from the thermodynamics of some microscopic model). It is implicitly assumed that there is some microscopic model, *e.g.* an Ising model with spins  $S_i$  on a lattice (with lattice spacing  $a$ ), producing the function  $f_e$  of Eq. (1.23) relating the macroscopic quantities  $M$ ,  $T$  and  $h$  in the thermodynamic limit. The magnet undergoes a phase transition at  $T = T_c$ , where for temperatures  $T < T_c$  the system exhibits long range order, *i.e.* the spins degrees of freedom become highly correlated and align to form a nonzero magnetization  $M$ , even in absence of an external magnetic field  $h = 0$ . For temperatures  $T > T_c$  thermal fluctuations dominate the free-energy and spins are randomly oriented giving a zero magnetization  $M = 0$  at  $h = 0$ . This is a typical example of a continuous phase transition in a thermodynamic system; the order parameter  $M$  changes continuously from zero for  $T \geq T_c$  to nonzero values at temperatures  $T < T_c$ , in the limit  $h \rightarrow +0$ .

Based on experimental results, Widom [55] discovered that the EOS can be written as a function of a single variable near a critical point  $T = T_c$ :

$$h = M^\delta \mathcal{F}_e \left( t M^{-1/\beta} \right), \quad (1.24)$$

where  $t = T - T_c$  is the temperature relative to the critical point. Thus Eq. (1.24) is a relation between the scaled variables  $hM^{-\delta}$  and  $tM^{-1/\beta}$ . The function  $\mathcal{F}_e$  is regular at  $t = 0$ , thus we can write

$$h = \mathcal{F}_e(0) M^\delta + \mathcal{F}'_{e\pm}(0) t M^{\delta-1/\beta}, \quad (t = T - T_c) \quad (1.25)$$

where the minus sign in  $\mathcal{F}'_{e\pm}$  corresponds to  $t = T - T_c < 0$ , and the plus sign to  $t > 0$ . This notation is used to reflect the fact that the function  $\mathcal{F}_e$  though continuous is not analytic at  $t = 0$  ( $T = T_c$ ). The critical exponent  $\delta$  follows from Eq. (1.25) at  $t = 0$ :

$$M \sim h^{1/\delta}, \quad t = 0. \quad (1.26)$$

The critical exponent  $\beta$  follows from Eq. (1.25) at zero external field  $h = 0$ :

$$M \sim t^\beta, \quad h = 0. \quad (1.27)$$

The critical exponent  $\gamma$  describes the scaling of the magnetic susceptibility  $\chi$ , which is defined as

$$\chi \equiv \left. \frac{\partial M}{\partial h} \right|_{h=0}, \quad (1.28)$$

close to the critical point:

$$\chi \sim t^{-\gamma}. \quad (h = 0) \quad (1.29)$$

Differentiating Eq. (1.25) with respect to  $h$  and putting  $h = 0$  yields the scaling relation

$$\gamma = \beta(\delta - 1). \quad (1.30)$$

Thus the critical exponent  $\gamma$  is not really a new critical exponent.

### 1.2.3 The scaling hypothesis for the free energy

The scaling laws for the “singular part”  $f_s$  of the free energy  $f_b$  is written as

$$f_s(t, h) = t^{2-\alpha} \mathcal{F}_f(ht^{-\Delta}), \quad (1.31)$$

near criticality, where  $\mathcal{F}_f$  is regular at  $h = 0$ . The critical exponent  $\alpha$  is related to the specific heat. The magnetization  $M$  is obtained by differentiation of  $f_s$  with respect to the external field  $h$ :

$$M \equiv -\frac{1}{k_B T} \frac{\partial f_s}{\partial h} \sim t^{2-\alpha-\Delta} \mathcal{F}'_f(ht^{-\Delta}). \quad (1.32)$$

Since the scaling of  $M$  near criticality is given by the exponent  $\beta$  Eq. (1.27), we find the scaling law

$$\beta = 2 - \alpha - \Delta. \quad (1.33)$$

Subsequently the magnetic susceptibility  $\chi$ , Eq. (1.28), follows from one more differentiation of  $f_s$  with respect to  $h$ :

$$\chi \sim t^{2-\alpha-2\Delta} \mathcal{F}''_f(ht^{-\Delta}). \quad (1.34)$$

Close to criticality  $\chi$  should tend towards  $t^{-\gamma}$  as  $h \rightarrow 0$ , see Eq. (1.29). Hence we find another scaling law

$$2 - \alpha - 2\Delta = -\gamma. \quad (1.35)$$

After eliminating  $\Delta$  in Eqs. (1.33) and (1.35) we obtain the Rushbrooke scaling law

$$\alpha + 2\beta + \gamma = 2. \quad (1.36)$$

### 1.2.4 The scaling hypothesis for the two-point correlation functions

The connected two-point correlation function  $G_C$  longitudinal (*i.e.* parallel) to the direction of ordering is defined in Eq. (1.22). The scaling hypothesis for the two-point correlation function reads

$$G_C(r, t, h) = \frac{1}{r^{d-2+\eta}} \mathcal{F}_G(rt^\nu, ht^{-\Delta}), \quad (1.37)$$

which, in momentum space, after a Fourier transformation, has the following form at zero external field  $h = 0$

$$\hat{G}_C(p, t) \sim \int d^d r e^{ipr} G_C(r, t, 0) = \frac{1}{p^{2-\eta}} \hat{\mathcal{F}}_G(t^\nu/p). \quad (1.38)$$

In analogy with Eq. (1.22), the quantity

$$\xi \sim t^{-\nu}, \quad h = 0, \quad (1.39)$$

is defined as the correlation length. One can derive that the magnetic susceptibility should be proportional to the (longitudinal) two-point correlation function in momentum space

$$\hat{G}_C(p = 0, t) \sim \chi, \quad (1.40)$$

thus  $p \ll t^\nu$ . Then the limit

$$\lim_{p \rightarrow 0} \frac{1}{p^{2-\eta}} \hat{\mathcal{F}}_G(t^\nu/p) \sim t^{-\gamma}, \quad (1.41)$$

gives the scaling law

$$\gamma = \nu(2 - \eta). \quad (1.42)$$

The Josephson scaling law follows from the requirement that the singular part of the free energy  $f_s$  is independent of microscopic length scales in the limit  $t \rightarrow 0$  and at zero external field  $h = 0$ , thus the only length scale is then given by the correlation length  $\xi \sim t^{-\nu}$ , thus

$$f_s(t, 0) \sim \xi^{-d} \sim t^{\nu d} \sim t^{2-\alpha}, \quad (1.43)$$

where the last step follows from the definition of the critical exponent  $\alpha$  in Eq. (1.31) Hence

$$d\nu = 2 - \alpha. \quad (1.44)$$

Since it involves the dimension  $d$  of the system explicitly, Eq. (1.44) is referred to as a hyperscaling law.

The six critical exponents  $\alpha$ ,  $\beta$ ,  $\gamma$ ,  $\delta$ ,  $\eta$  and  $\nu$  are related by the four (hyper)-scaling laws (1.30), (1.36), (1.42), and (1.44), thus only two of the critical exponents are independent.

The critical exponents are referred to as universal quantities; they don't depend much on microscopic details of the underlying theory describing macroscopic quantities. Universality means that the critical exponents are determined by only a few global features of system; the symmetries of the Hamiltonian or action, the dimensionality, and whether or not the forces are short-ranged.

The above mentioned scaling hypothesis for the EOS, the singular part of the free energy and the correlation function, were for a long time predominantly experimentally motivated, and only Landau theory or mean field theory was capable of computing explicitly critical exponents. However in Landau's mean field theory, only one set of critical exponents could be accounted for. These are referred to as mean field exponents:

$$\begin{aligned} \alpha &= 0, & \beta &= 1/2, & \gamma &= 1, \\ \delta &= 3, & \eta &= 0, & \nu &= 1/2, \end{aligned} \quad (1.45)$$

and the hyperscaling laws are only satisfied at the critical dimension  $d = 4$ . Any other set of critical exponents satisfying the hyperscaling laws would certainly be inconsistent with mean field theory. But it is known experimentally that certain ferromagnetic systems could be consistently described by critical exponents satisfying hyperscaling laws, which were clearly incompatible with the mean field exponents.

The problem of mean field theory is that it is based on the assumption that the only relevant length scale near criticality is the correlation length  $\xi$ . This appears to be wrong. In order to account for nonmean field critical exponents, and anomalous scaling laws (*i.e.* the critical exponent  $\eta \neq 0$ ), the microscopic length scale  $a \sim 1/\Lambda$  plays a crucial role in the dimensional analysis<sup>2</sup> even when the correlation length is much larger than the microscopic scale or lattice spacing  $a$ .

Kadanoff [17] presented an intuitive picture by “coarse graining” degrees of freedom, and invented block spin transformations, in which a particular set of spin degrees of freedom is described by a single spin degrees of freedom. His crucial assumption is that the Hamiltonian for the new coarse grained degrees of freedom is of the same form as the Hamiltonian for the original degrees of freedom, except that the couplings constants of the Hamiltonian now run as functions of a “new” larger microscopic length scale corresponding to the coarse grained degrees of freedom. Kadanoff's block spin transformations, and the concept of running coupling constants provided a clear motivation for the scaling hypothesis of Widom *et al.* However Kadanoff's method could neither give rise to the critical exponents nor

---

<sup>2</sup> Dimensional analysis, in this context, means the analysis of scale transformations.

the so-called non-universal quantities, such as  $\mathcal{F}_e(0)$  and  $\mathcal{F}'_e(0)$  of Eq. (1.25). The flaw in Kadanoff's picture is the assumption that the coarse grained Hamiltonian is of the same form as the original Hamiltonian; he assumed that if the fundamental Hamiltonian described only nearest neighbour spin-interactions, the coarse grained Hamiltonian would also have only nearest neighbour spin interactions. This assumption is in general not valid. Wilson refined the concept of block spin transformation and coarse graining, and his theory "the renormalization group" (RG) provides a constructive method to derive the coarse grained Hamiltonian, which he realized was not necessarily of the same form as the fundamental Hamiltonian. In coarse graining degrees of freedom new types of interactions can appear, and need therefore to be taken into account. In this way, Wilson's RG methods are capable of explicitly computing the critical exponents, and non-universal quantities. In the next section, we will discuss the RG of Wilson in the context of quantum field theory.

### 1.3 Wilson's renormalization group

This section is an introduction to the essential concepts of the renormalization group methods of K.G. Wilson, Refs. [14, 15]. Large parts of this section are derived and compiled from the following references. Excellent reviews on the principles of Wilson's RG in statistical mechanics are given in Refs. [4, 15], and for quantum field theories, in Refs. [3, 6, 56, 5], see also [18]. For literature on the fundamental axioms of Euclidean and Minkowskian quantum field theory, and functional integration techniques we refer to Ref. [51], and for a modern view of functional integration see Ref. [52].

Wilson elaborated and completed Kadanoff's argument, and his RG method provides the constructive framework in which to understand critical phenomena, universality and renormalization. Wilson's RG allows for explicit computation of the relationship between coupling constants at different length scales, at least approximately. The basic meaning of a RG transformation is the redefinition or the change (running) of the coupling constants under a change of scale, and a rescaling of the fields, and to allow for the possibility that new local operators are generated during the RG transformation.

We will present the renormalization group (RG) in three steps. The first step is a concrete realization of the coarse-graining transformations, and in the language of QFT it means that we have to construct a low-energy effective action or regulated action defining a particular generating functional from which the RG transformations can be derived (in principle). The second step is the identification of the origin of critical phenomena and singular behavior with the existence of fixed points of the RG transformations. Also we discuss the concept of relevant, marginal, and irrelevant interactions (operators), and the flow of coupling constants close to a particular fixed point. Finally, in step three we discuss renormalization, and the

continuum limit of QFTs.

### 1.3.1 Step 1. Regularization and coarse graining

Let us consider the following generating functional described by some “fundamental” action  $S_f$  in  $d$  dimensional Euclidean space time, which is obtained after a standard Wick rotation [57]

$$Z [K, J] = N \int \mathcal{D}\phi \exp\{-S_f [K, \phi] - S_J [J, \phi]\}, \quad (1.46)$$

$$S_f [K, \phi] = \int d^d x \sum_{i=1}^{n_f} K_i O_i [\phi(x)], \quad (1.47)$$

where the  $K = (K_1, K_2, \dots, K_{n_f})$  are a set of  $n_f$  coupling constants (some of which have a dimension), and where the  $O_i$  are some local operators of the elementary fields  $\phi = (\phi_1, \phi_2, \dots, \phi_a)$ , thus

$$\mathcal{D}\phi = \prod_{i=1}^a \mathcal{D}\phi_i. \quad (1.48)$$

In the Euclidean formulation, we suppose that the  $O_i$  are positive operators, and that the couplings  $K_i$  take only nonnegative values, so that the action is positive and the generating functional “well-defined”, see also the discussion in section 1.1 and [52]. The source action  $S_J$  is of the form Eq. (1.3).

The initial step in Wilson’s approach is to introduce a cutoff  $\Lambda$  in the action. A convenient way to do that is by using the generalized Pauli–Villars regularization (see Ref. [58, 6] and *e.g.* [59] and references therein). We define the “regularized action”,

$$S_\Lambda^{reg} [K, \phi] = N_{pv}(\Lambda) \int \mathcal{D}\phi_{pv} \exp\{-S_\Lambda^{pv} [K, \phi, \phi_{pv}]\}, \quad (1.49)$$

where the fields  $\phi_{pv}$  are a set of Pauli–Villars fields. An example of such an action  $S_\Lambda^{pv}$  for scalar field theory is

$$\begin{aligned} S_\Lambda^{pv} [K, \phi, \phi_{pv}] = & \int d^d x \left[ \frac{1}{2} \phi(-\Delta + m^2) \phi - \frac{1}{2} \phi_{pv}(-\Delta + \Lambda^2) \phi_{pv} \right. \\ & \left. + V(\phi + \phi_{pv}) \right], \end{aligned} \quad (1.50)$$

where the initial action  $S_f$  was

$$S_f [K, \phi] = \int d^d x \left[ \frac{1}{2} \phi(-\Delta + m^2) \phi + V(\phi) \right]. \quad (1.51)$$

The mass  $m$  and the potential  $V$  are defined in terms of the coupling constants  $K$ , and yet unspecified local operators.

The basic principle of Pauli–Villars regularization methods is that any internal propagator of  $\phi$  is replaced after the regularization by the sum of the  $\phi$  and  $\phi_{pv}$  propagators:

$$\frac{1}{p^2 + m^2} \longrightarrow \frac{1}{p^2 + m^2} - \frac{1}{p^2 + \Lambda^2}. \quad (1.52)$$

For modes of  $\phi$  corresponding to energies  $p^2 \ll \Lambda^2$  the propagator is of the form

$$\frac{1}{p^2 + m^2} - \frac{1}{\Lambda^2} + \frac{1}{\Lambda^2} \mathcal{O}(p^2/\Lambda^2), \quad (1.53)$$

whereas for modes of  $\phi$  corresponding to energies  $p^2 \gg \Lambda^2$  the propagator vanishes as fast as  $\Lambda^2/p^4$  making Feynman diagrams finite. In the continuum limit  $\Lambda \rightarrow \infty$  the original propagator is recovered. The Pauli–Villars field  $\phi_{pv}$  does not correspond to a “physical” particle, since the action cannot be based on a Hermitian Hamiltonian, see Chapt. 7 of Zinn–Justin [6].

In the abstract example given above, we introduced only a single Pauli–Villars field; in general more Pauli–Villars fields are needed to render all Feynman diagrams finite. The Pauli–Villars regularization seems to work very well for Abelian gauge theories describing the interaction between fermions such as QED, since it is possible to regularize in a gauge invariant manner keeping the Lorentz covariance. Moreover the Pauli–Villars regularization is supposed to work also nonperturbatively. A problem turns up when considering symmetries of an initial action  $S_f$ . After regularization it might be the case that a continuous symmetry of the initial action is lost in the regularization process by the appearance of operators, which violate that particular symmetry. Such a violation of the symmetry is called an anomaly. An example in fermionic gauge field theories is the well-known Adler–Bell–Jackiw  $U(1)$ -axial anomaly, Refs. [60, 61], see also section 2.2.

Let us consider the regularized action Eq. (1.49) in more detail. The functional integral over Pauli–Villars field  $\phi_{pv}$  introduces a smearing of interactions at modes of  $\phi$  with energy scale  $E \sim \Lambda$ . Due to such smearing effects the action  $S_\Lambda^{reg}$  is nonlocal in the fields  $\phi$ . Suppose we split the fields  $\phi$  into high- and low-energy parts:

$$\phi = \phi_h + \phi_l, \quad (1.54)$$

where the energy  $E = |p| > \Lambda$  for  $\phi_h$  and  $E \leq \Lambda$  for  $\phi_l$ . Then, since the Pauli–Villars construction is such that the high energy modes  $\phi_h$  are canceled by the Pauli–Villars fields, the action is independent of  $\phi_h$ . The remaining fields  $\phi_l$  are of energy  $E < \Lambda$ , and the action  $S_\Lambda^{reg}$  is approximately local in low energy modes with  $E \ll \Lambda$ . The idea is that the nonlocal action  $S_\Lambda^{reg}$  can be expanded in terms

of local operators  $O_i$ :

$$S_{\Lambda}^{reg} [K, \phi] = S_{\Lambda}^{eff} [\kappa(\Lambda), \phi_l] = \int d^d x \sum_{i=1}^{\infty} \kappa_i(\Lambda) \Lambda^{d-d_i^c} O_i [\phi_l(x)], \quad (1.55)$$

where we have introduced the dimensionless running coupling constants

$$\kappa(\Lambda) = (\kappa_1(\Lambda), \kappa_2(\Lambda), \dots, \kappa_{\infty}(\Lambda)), \quad (1.56)$$

and new local interactions  $O_i [\phi_l(x)]$ ,  $i = n_f, \dots, \infty$ . Since the action is dimensionless,  $d_i^c$  is the canonical dimension (in units of mass) of the operator  $O_i$ ,

$$\dim [O_i] = d_i^c. \quad (1.57)$$

Now that we have an action spanned by a space of an infinite number of couplings and operators  $O_i$ , the question arises: how can this be useful?

The crucial observation is that operators and corresponding coupling constants can be classified as relevant or irrelevant. It will turn out that it is sufficient to consider only the (in practice) finite set of operators  $O_i$  ( $1 < i \leq n$ ) and corresponding coupling constants, which are relevant with respect to a particular fixed point, (see later discussion in this section), so we write

$$S_{\Lambda}^{eff} [\kappa(\Lambda), \phi_l] \approx \int d^d x \left\{ \sum_{i=1}^n \kappa_i(\Lambda) \Lambda^{d-d_i^c} O_i [\phi_l(x)] + \text{irrelevant} \right\}, \quad (1.58)$$

and the property of the “irrelevant” part describing the irrelevant operators and couplings is that it gives rise to corrections to Green functions in terms of positive powers of  $E/\Lambda$ , and the “irrelevant” part becomes negligible for  $E$  sufficiently smaller than  $\Lambda$  ( $E \ll \Lambda$ ).

The apparent straightforward decomposition of  $\phi$ ’s into  $\phi_l$  and  $\phi_h$ , Eq. (1.54), is in practice nontrivial and rather technical. The functional space of fields  $\phi$  is chosen such that the  $\phi(x)$  have Fourier transforms:

$$\phi(x) \sim \int d^d p e^{ipx} \hat{\phi}(p). \quad (1.59)$$

Then think of  $\phi_l$  in terms of Fourier modes  $\hat{\phi}(p)$  with  $E = |p| \leq \Lambda$ , and  $\phi_h$  as modes  $\hat{\phi}(p)$  with  $E = |p| > \Lambda$ :

$$\phi_l \sim \int_{|p| \leq \Lambda} d^d p e^{ipx} \hat{\phi}(p), \quad \phi_h \sim \int_{|p| > \Lambda} d^d p e^{ipx} \hat{\phi}(p). \quad (1.60)$$

In this way, the measure  $N(\Lambda) \int \mathcal{D}\phi_l$  introduces a momentum cutoff  $\Lambda$  in the SDEs for the momentum space Green functions. For technicalities involved in the “projection” leading to Eq. (1.54), and the cutoff  $\Lambda$ , we refer to [51] (Chap. 8).

If we compare this local “low-energy effective” action  $S_{\Lambda}^{eff}$ , Eq. (1.58), with the fundamental or initial action  $S_f$  of (1.47), we see that new coupling constants  $\kappa_i(\Lambda)$  and new operators  $O_i$  with  $n \geq i > n_f$  have been introduced, and that the couplings are now defined as functions of  $\Lambda$ . In principle the couplings  $\kappa_i(\Lambda)\Lambda^{d-d_i^c}$  can and will differ from the initial coupling constants  $K_i$  ( $i = 1, \dots, n_f$ ) of  $S_f$ . These new couplings or new interactions are a results of the nonlocality of the regularized action  $S_{\Lambda}^{reg}$ .

The fundamental notion introduced by Wilson is that, through coarse graining the degrees of freedom, new local operators appear with corresponding couplings constants, and the coupling constants “run” as a function of the cutoff  $\Lambda$  (the cutoff is analogous to the microscopic length scale in lattice models  $a \sim 1/\Lambda$ ). The high energy modes  $\phi_h$  are integrated out thereby introducing new interactions and running coupling constants.

From the local low energy effective action  $S_{\Lambda}^{eff}$ , Eq. (1.55), we construct a generating functional

$$Z_{\Lambda}[\kappa(\Lambda), J_{\Lambda}] \equiv N(\Lambda) \int \mathcal{D}\phi_l \exp\{-S_{\Lambda}^{eff}[\kappa(\Lambda), \phi_l] - S_J[J_{\Lambda}, \phi_l]\}, \quad (1.61)$$

where the external sources  $J_{\Lambda}$  are introduced to generate the low-energy Green functions ( $E \ll \Lambda$ ). The sources  $J_{\Lambda}$  explicitly depend on  $\Lambda$ , and in momentum space we suppose that the sources  $J_{\Lambda}(p)$  vanish for momenta  $p > \Lambda$ . We only probe physics at a scale  $E < \Lambda$ . The generating functional  $Z_{\Lambda}$  should be defined via the implementation of the SD scheme as discussed in section 1.1, with a normalization  $N(\Lambda)$  so that  $Z_{\Lambda}[\kappa(\Lambda), J_{\Lambda} = 0] = 1$ .

We can repeat the above coarse graining and consider now an effective action at a cutoff  $\Lambda' < \Lambda$ . Split the fields  $\phi_l$  into:

$$\phi_l = \phi_{l'} + \phi_{h'}, \quad (1.62)$$

where the energy  $E$  is  $\Lambda > E > \Lambda'$  for  $\phi_{h'}$  and  $E \leq \Lambda'$  for  $\phi_{l'}$ . Then we define a coarse grained local effective action at scale  $\Lambda'$  as follows:

$$N(\Lambda') \exp\{-S_{\Lambda'}^{eff}[\kappa(\Lambda'), \phi_{l'}]\} = N(\Lambda) \int \mathcal{D}\phi_{h'} \exp\{-S_{\Lambda}^{eff}[\kappa(\Lambda), \phi_l]\}, \quad (1.63)$$

where

$$S_{\Lambda'}^{eff}[\kappa(\Lambda'), \phi_{l'}] \approx \int d^d x \sum_{i=1}^n \kappa_i(\Lambda') \Lambda'^{d-d_i^c} O_i[\phi_{l'}(x)]. \quad (1.64)$$

In principle the right-hand side of Eq. (1.63) corresponds to a nonlocal action for energy scales scales  $E \sim \Lambda'$ , however again we assume it is well approximated for energies  $E < \Lambda'$  by the local action  $S_{\Lambda'}^{eff}$ . Furthermore, by definition, the coarse

grained effective action  $S_{\Lambda'}^{eff}$  should yield the same generating functional, thus we have the identity

$$Z_{\Lambda'} [\kappa(\Lambda'), J_{\Lambda'}] = Z_{\Lambda} [\kappa(\Lambda), J_{\Lambda}], \quad (1.65)$$

since

$$N(\Lambda') \int \mathcal{D}\phi_{l'} \exp\{-S_{\Lambda'}^{eff} [\kappa(\Lambda'), \phi_{l'}]\} = N(\Lambda) \int \mathcal{D}\phi_l \exp\{-S_{\Lambda}^{eff} [\kappa(\Lambda), \phi_l]\}. \quad (1.66)$$

Hence the generating functional  $Z_{\Lambda}$  is independent of  $\Lambda$ , *i.e.*

$$\Lambda \frac{dZ_{\Lambda}}{d\Lambda} = 0. \quad (1.67)$$

The identities (1.65) and (1.67) define a RG transformation  $\mathcal{R}$  in the space of coupling constants (thus in the space of actions) mapping couplings  $\kappa(\Lambda)$  to couplings  $\kappa(\Lambda')$ :

$$\kappa(\Lambda') = \mathcal{R} [\Lambda'/\Lambda, \kappa(\Lambda)]. \quad (1.68)$$

The RG transformation  $\mathcal{R}$  can be derived from the generating functional  $Z_{\Lambda}$  given in terms of an low energy effective action  $S_{\Lambda}^{eff}$ . Since  $Z_{\Lambda}$  is defined via the SDE, positivity, and normalization (section 1.1), the solutions (or approximate solutions) of SDEs for the Green function of  $\phi_l$  ultimately provide us with the RG transformation  $\mathcal{R}$ . In what follows we discuss the properties of  $\mathcal{R}$ .

### 1.3.2 Step 2. The origin of singular behavior and anomalous scaling

The RG transformation  $\mathcal{R}$  maps couplings  $\kappa(\Lambda)$  to  $\kappa(\Lambda')$ ,

$$\kappa(\Lambda') = \mathcal{R} [\Lambda'/\Lambda, \kappa(\Lambda)], \quad \Lambda' \leq \Lambda \leq 1, \quad (1.69)$$

where the cutoff's  $\Lambda'$  and  $\Lambda$  have been redefined as dimensionless quantities related to the unit energy scale. The transformation  $\mathcal{R}$  for different  $\Lambda \leq 1$  form a semi-group. Two successive transformations with  $\Lambda_1$  and  $\Lambda_2$  should be equivalent to a combined scale change of  $\Lambda_1 \Lambda_2$ :

$$\kappa(\Lambda_0) = \mathcal{R} [1, \kappa(\Lambda_0)], \quad \Lambda_0 \leq 1, \quad (1.70)$$

$$\kappa(\Lambda_1) = \mathcal{R} [\Lambda_1/\Lambda_0, \kappa(\Lambda_0)], \quad \Lambda_1 \leq \Lambda_0, \quad (1.71)$$

$$\begin{aligned} \kappa(\Lambda_1 \Lambda_2) &= \mathcal{R} [\Lambda_2, \kappa(\Lambda_1)] \\ &= \mathcal{R} [\Lambda_2, \mathcal{R} [\Lambda_1/\Lambda_0, \kappa(\Lambda_0)]], \quad \Lambda_2 \leq 1, \end{aligned} \quad (1.72)$$

and thus (taking  $\Lambda_0 = 1$ )

$$\mathcal{R} [\Lambda_1 \Lambda_2, \kappa_0] = \mathcal{R} [\Lambda_2, \mathcal{R} [\Lambda_1, \kappa_0]], \quad \kappa_0 \equiv \kappa(1). \quad (1.73)$$

By construction the  $\mathcal{R}$  satisfies the above group properties, where we recall that the transformation  $\mathcal{R}$  follows from Eq. (1.65).

The differential form of the RGE can be obtained by taking  $\Lambda_2 = (1 - \epsilon)$  in Eq. (1.72) and taking the limit  $\epsilon \rightarrow +0$ :

$$\Lambda_1 \frac{d\kappa_i(\Lambda_1)}{d\Lambda_1} = \left. \frac{\partial \mathcal{R}_i [\Lambda_2, \kappa(\Lambda_1)]}{\partial \Lambda_2} \right|_{\Lambda_2=1} \equiv \beta_i(\kappa(\Lambda_1)), \quad (1.74)$$

where the  $\beta_i$  function is defined with respect to the particular coupling  $\kappa_i$  of the set of couplings  $\kappa = (\kappa_1, \kappa_2, \dots)$ . The differential RG equation (1.74) follows from the differential identity, Eq. (1.67), for the generating functional.

A crucial step, in understanding anomalous scaling behavior and critical phenomena, is the recognition of the importance of fixed points of the RG transformation. A fixed point of the RG transformation is a point  $\kappa_c$  in coupling constant space satisfying

$$\kappa_c = \mathcal{R} [\sigma, \kappa_c] \implies \beta(\kappa_c) = 0, \quad (1.75)$$

for any  $\sigma < 1$ . A fixed point is a property of the transformation  $\mathcal{R}$ , that, in general, corresponds to nonanalytic behavior, hence it can only appear in a system with infinitely many degrees of freedom [7]. Fixed points are not necessarily isolated points. It is possible to have lines or hypersurfaces of fixed points, in fact in a large part of this thesis we consider a critical line or curve. Moreover, a RG transformation can have several isolated fixed points.

The fixed points are either classified as critical fixed points, or as Gaussian fixed points. In the context of quantum field theory, we refer to a critical fixed point or an ultraviolet (UV) fixed point, if the continuum limit (*i.e.* taking the cutoff  $\Lambda \rightarrow \infty$ ) corresponds to an interacting theory, in which a macroscopic quantity such as a correlation length  $\xi \sim 1/m$  (where  $m$  is a mass) can be defined. An UV fixed point of a  $\beta$  function of coupling  $\kappa_i$  is a point  $\kappa_c$  with the properties:

$$\beta(\kappa_c) = 0, \quad \left. \frac{\partial \beta_i(\kappa)}{\partial \kappa_i} \right|_{\kappa=\kappa_c} < 0. \quad (1.76)$$

We speak of a trivial or Gaussian fixed point if in the continuum limit the interactions between fields (and thus particles) vanish, and the theory reduces effectively to a free field or Gaussian theory. In general a Gaussian fixed point can be classified as being an IR fixed point, *i.e.*,

$$\beta(\kappa_c) = 0, \quad \left. \frac{\partial \beta_i(\kappa)}{\partial \kappa_i} \right|_{\kappa=\kappa_c} \geq 0. \quad (1.77)$$

Thus close to a trivial or Gaussian fixed point (corresponding to noninteracting theories), a macroscopic quantity such as a correlation length is not defined (there are

no correlations at all). An UV fixed point corresponds to interacting theories, and a correlation length  $\xi$  can be defined; right at the critical fixed point the correlation length diverges  $\xi = \infty$  ( $m = 0$ ), see section 1.3.3.

The critical fixed points will describe singular critical behavior, such as phase transitions, and can correspond to phase boundaries, separating two distinct phases of a model (whether or not a phase boundary exists depends on the so-called co-dimensions of the fixed point (see Ref. [4]).) Thus knowledge of the location of and nature of fixed points of a RG transformation enables the phase diagram to be determined, and vice versa. We will show now that the critical exponents follow from the RG transformation in the neighbourhood of a critical fixed point.

Let us consider the RG transformation close to a critical point  $\kappa_c$ ,

$$\kappa_i(\Lambda) = \kappa_{ci} + \delta\kappa_i(\Lambda), \quad (1.78)$$

since

$$\begin{aligned} \kappa_n(\Lambda') &= \mathcal{R}_n[\Lambda'/\Lambda, \kappa(\Lambda)] \\ &= \kappa_{cn} + \sum_m \delta\kappa_m(\Lambda) \frac{\partial \mathcal{R}_n[\Lambda'/\Lambda, \kappa]}{\partial \kappa_m} \Big|_{\kappa=\kappa_c} + \mathcal{O}((\delta\kappa)^2) \\ &\approx \kappa_{cn} + \delta\kappa_n(\Lambda'), \quad \Lambda' < \Lambda. \end{aligned} \quad (1.79)$$

Hence<sup>3</sup>

$$\delta\kappa_n(\Lambda') = M_{nm}(\Lambda'/\Lambda) \delta\kappa_m(\Lambda), \quad (1.80)$$

where the matrix  $M$  is defined as

$$M_{nm}(\Lambda'/\Lambda) \equiv \frac{\partial \mathcal{R}_n[\Lambda'/\Lambda, \kappa]}{\partial \kappa_m} \Big|_{\kappa=\kappa_c}. \quad (1.81)$$

The semi-group property of Eq. (1.73) implies that

$$M_{nl}(\Lambda''/\Lambda') M_{lm}(\Lambda'/\Lambda) = M_{nm}(\Lambda''/\Lambda). \quad (1.82)$$

The equation (1.80) is called the linearized RG transformation in the vicinity of the fixed point. The matrix  $M$  is real, but in general not symmetric. However, we assume that  $M$  is diagonalizable, with real eigenvalues. Therefore, for simplicity, we assume that for a particular set of couplings  $\tilde{\kappa}$  the matrix  $\tilde{M}$  is diagonal:

$$\tilde{M}_{nm}(\Lambda'/\Lambda) = \lambda^{(n)}(\Lambda'/\Lambda) \delta_{mn}, \quad (1.83)$$

so that

$$\delta\tilde{\kappa}_n(\sigma\Lambda) = \lambda^{(n)}(\sigma) \delta\tilde{\kappa}(\Lambda), \quad \sigma = \Lambda'/\Lambda. \quad (1.84)$$

---

<sup>3</sup>Using the Einstein summation convention.

With Eq. (1.83) this implies that

$$\lambda^{(n)}(\Lambda''/\Lambda')\lambda^{(n)}(\Lambda'/\Lambda) = \lambda^{(n)}(\Lambda''/\Lambda). \quad (1.85)$$

Thus, the solution to the eigenvalue  $\lambda^{(n)}$  is

$$\lambda^{(n)}(\sigma) = \sigma^{\eta_n}, \quad (1.86)$$

where the exponent  $\eta_n$  is independent of  $\sigma$ , in general the exponent is a function of the critical point, *i.e.*  $\eta_n \rightarrow \eta_n(\kappa_c)$ . Now we can distinguish three cases, since  $\sigma < 1$ :

- (1)  $\lambda^{(n)}(\sigma) > 1$ , *i.e.*  $\eta_n < 0$ , which corresponds to an eigenvalue of a “relevant” coupling  $\tilde{\kappa}_n$ .
- (2)  $\lambda^{(n)}(\sigma) = 1$ , *i.e.*  $\eta_n = 0$ , which corresponds to an eigenvalue of a “marginal” coupling  $\tilde{\kappa}_n$ .
- (3)  $\lambda^{(n)}(\sigma) < 1$ , *i.e.*  $\eta_n > 0$ , which corresponds to an eigenvalue of an “irrelevant” coupling  $\tilde{\kappa}_n$ .

The marginal eigenvalues usually correspond to logarithmic corrections to scaling. Eq. (1.84) implies then that for a relevant coupling  $\delta\tilde{\kappa}(\sigma\Lambda)$  increases as  $\sigma$  decreases; for a marginal coupling  $\delta\tilde{\kappa}(\sigma\Lambda)$  stays fixed (up to logarithmic corrections); and for an irrelevant coupling  $\delta\tilde{\kappa}(\sigma\Lambda)$  shrinks. Thus the irrelevant couplings flow towards the fixed point for  $\sigma \ll 1$ , whereas the relevant couplings flow from the fixed point. The terms relevant, marginal, and irrelevant couplings (eigenvalues) are always defined with respect to a particular fixed point.

So we have seen that from the RG transformation  $\mathcal{R}$  we obtain the fixed points  $\kappa_c$ , the RG flows near a particular fixed point can be decomposed into relevant, marginal, and irrelevant couplings, and from the eigenvalues  $\lambda^{(n)}$  close to the fixed point we can derive the “critical exponents”  $\eta_n$ . The critical exponents  $\eta_n$ , for many practical explicit cases, can be shown to be related to the critical exponents defined in section 1.2. Thus the RG transformation  $\mathcal{R}$  enables us to calculate the critical points and critical exponents. In a mean field approach the exponents have rational values, whereas in general they can have irrational values. In a case where critical exponents differ from the canonical (*i.e.* mean field) values we speak of anomalous scalings, or anomalous dimensions. The dynamics (which determine  $\mathcal{R}$ ) of the system under consideration are such that fluctuations around some mean-value of operators cannot be neglected.

Let us discuss some examples. Close to a fixed point, it follows straightforwardly from Eq. (1.84) that the  $\beta$  function for a coupling  $\kappa_n$  of a set of couplings  $\kappa(\Lambda)$ <sup>4</sup>, can be written as

$$\beta_n(\kappa) \equiv \Lambda \frac{d\kappa_n}{d\Lambda} \approx \eta_n(\kappa_c) \delta\kappa_n + \mathcal{O}((\delta\kappa)^2), \quad \delta\kappa_n = \kappa_n - \kappa_{cn}, \quad (1.87)$$

---

<sup>4</sup>For which the matrix  $M$  (Eq. (1.81)) is diagonal.

where  $\eta_n(\kappa_c) < 0$  implies that  $\kappa_n$  is a relevant coupling, and  $\eta_n(\kappa_c) > 0$  implies that  $\kappa_n$  is irrelevant. Now differentiating  $\beta_n$  with respect to  $\kappa_n$ ,

$$\left. \frac{\partial \beta_n(\kappa)}{\partial \kappa_n} \right|_{\kappa=\kappa_c} \approx \eta_n, \quad (1.88)$$

leads, with Eqs. (1.76) and (1.77), to the conclusion that  $\kappa_c$  is an UV fixed point for a relevant coupling, and  $\kappa_c$  is an IR fixed point in case of an irrelevant coupling.

More complicated are in general the marginal couplings. Consider the following RG of a single marginal coupling  $\kappa$ :

$$\kappa(\Lambda') = \mathcal{R}[\Lambda'/\Lambda, \kappa(\Lambda)], \quad (1.89)$$

$$\mathcal{R}[\Lambda'/\Lambda, \kappa(\Lambda)] = \frac{\kappa(\Lambda)}{1 + \kappa(\Lambda)(\kappa_c - \kappa(\Lambda)) \log \Lambda/\Lambda'}. \quad (1.90)$$

Then, when  $\kappa(\Lambda)$  is “fine-tuned” sufficiently close to  $\kappa_c$  so that we can write

$$\delta\kappa(\Lambda') = (1 + \kappa(\Lambda)^2 \log \Lambda/\Lambda') \delta\kappa(\Lambda), \quad (1.91)$$

clearly the eigenvalue of this equation is not of the form Eq. (1.86) due to the logarithmic correction, which is typical for marginal couplings. The  $\beta$  function can be obtained from Eq. (1.74) and (1.90), and reads

$$\beta(\kappa) = \kappa^2(\kappa_c - \kappa). \quad (1.92)$$

Thus the  $\beta$  function has two fixed points,  $\kappa = 0$ , respectively,  $\kappa = \kappa_c$ . According to the definitions given by Eqs. (1.76) and (1.77)  $\kappa = \kappa_c$  is an UV fixed point, and  $\kappa = 0$  an IR fixed point.

In practical applications of the RG method to quantum field theories, it turns out that the actual computation of critical fixed points is highly complicated, even more so when more than one coupling is relevant or marginal, therefore it is sometimes useful to address the problem in the following manner. Consider a model with two coupling constants  $\kappa_1$  and  $\kappa_2$ , then the fixed point  $\kappa_c = (\kappa_{c1}, \kappa_{c2})$  is a solution of

$$\beta_1(\kappa_1, \kappa_2) = 0, \quad (1.93)$$

$$\beta_2(\kappa_1, \kappa_2) = 0. \quad (1.94)$$

Suppose we first solve  $\beta_1$  for  $\kappa_1$ , and we assume that the solution can be expressed in terms of a function  $f$  with the property

$$\kappa_1 = f(\kappa_2) \rightarrow \beta_1(f(\kappa_2), \kappa_2) = 0. \quad (1.95)$$

Then  $\kappa_{c2}$ , provided that it exists, follows from the solution(s) of

$$\beta_2(f(\kappa_2), \kappa_2) = 0, \quad (1.96)$$

and  $\kappa_{c1} = f(\kappa_{c2})$ . The above sketched method is particularly useful when the function  $\beta_1$  has a much simpler structure than the function  $\beta_2$ , *i.e.* the function  $f$  is rather easy to determine from Eq. (1.93).

### 1.3.3 Step 3. Renormalization and fine-tuning

The renormalization of a QFT can be considered as the RG transformation of a set of so-called bare couplings  $\kappa(\Lambda)$  defined at an UV cutoff  $\Lambda$  to a set of couplings  $\kappa(\mu)$ , where  $\mu \ll \Lambda$  is some energy scale related to the resolution of an experimental apparatus (think of particle accelerators). Thus the couplings  $\kappa(\mu)$  are assumed to be related to experimentally measurable quantities (of course only interacting particles are measurable). Then if the limit

$$\kappa(\mu) = \lim_{\Lambda \rightarrow \infty} \mathcal{R}[\mu/\Lambda, \kappa(\Lambda)], \quad (1.97)$$

(with  $\mu$  fixed) exists and can be arranged in such a way that the set of couplings  $\kappa(\mu)$  describe an interacting theory<sup>5</sup>, then this particular QFT is said to have a nontrivial continuum limit. That is, the set of couplings  $\kappa(\mu)$  (“macroscopic quantities”) obtained from experiments are independent of any microscopic length scale  $1/\Lambda$ . When a nontrivial continuum limit does not exist, it does not necessarily imply that the corresponding QFT is useless, such a model can still be used as a low energy effective field theory for physics corresponding to energies  $E \leq \Lambda$ , where the cutoff  $\Lambda$  now has physical implications. For gauge theories, the Ward-Takahashi identities (or Slavnov–Taylor identities for non-Abelian gauge theories) reflecting the local gauge symmetry are crucial for a non-trivial continuum limit to exist.

The “arrangement” of the continuum limit, as mentioned previously depends on the so-called fine-tuning of relevant and marginal interactions. In order that the couplings  $\kappa(\mu)$  coincide with *e.g.* experimental values, one has to choose particular values for the relevant and marginal “bare” couplings  $\kappa(\Lambda)$  which lie in the neighbourhood of a critical fixed point. This is referred to as fine-tuning.

Now that we have a method to identify couplings  $\kappa$  and, consequently, the corresponding operators  $O$  as relevant, marginal and irrelevant, the question arises: why are irrelevant interactions irrelevant? The answer is: irrelevant interactions or couplings do not have to be fine-tuned, and their effect can completely be absorbed by suitable modifications of the fine-tuning of relevant and marginal couplings. As a result, the effect of irrelevant interactions in the infrared region is suppressed by factors  $(\mu/\Lambda)^{\eta_i}$  with  $\eta_i > 0$ . From Eqs. (1.84) and (1.86), and assuming  $\kappa_i(\Lambda)$  is sufficiently close to  $\kappa_{ci}$  we obtain that

$$\beta_i(\kappa) \approx \eta_i(\kappa_i - \kappa_{ci}) \implies \kappa_i(\mu) \approx \kappa_{ci} + (\mu/\Lambda)^{\eta_i} (\kappa_i(\Lambda) - \kappa_{ci}). \quad (1.98)$$

Thus, if  $\eta_i > 0$  (*i.e.*  $\kappa_i$  is irrelevant) the value of  $\kappa_i(\mu)$  is insensitive to the bare value  $\kappa_i(\Lambda)$  for  $\mu \ll \Lambda$ , and  $\kappa_i(\mu)$  approaches the IR fixed point  $\kappa_{ci}$ ; the effect of  $\kappa_i(\Lambda)$  is suppressed by a factor  $(\mu/\Lambda)^{\eta_i}$ . This also means that the IR fixed point of an irrelevant coupling is determined in terms of the relevant and marginal couplings.

However, if  $\eta_i < 0$  (*i.e.*  $\kappa_i$  is relevant) the second term on the right-hand side of Eq. (1.98) dominates, for  $\mu \ll \Lambda$ , and the only way to get a small value for  $\kappa(\mu)$

---

<sup>5</sup>At least one  $\kappa_i$  of the set of couplings  $\kappa(\mu)$  should have a non-Gaussian value.

in the infrared is to fine-tune  $\kappa_i(\Lambda)$  precisely to the UV fixed point  $\kappa_{ci}$ . Marginal couplings ( $\eta_i = 0$ ), because they usually are described by logarithmic scaling, are less restricted in the fine-tuning process.

The relevant and marginal couplings with UV fixed points correspond to interacting theories, and a correlation length  $\xi = 1/m$  can be defined; right at the critical fixed point the correlation length diverges  $\xi = \infty$  (thus zero mass  $m = 0$ ). Usually the correlation length can be identified with a physical observable, and in order to get a finite nonzero value for  $m$ , this requires fine-tuning of bare couplings. Suppose we have a model with one coupling  $\kappa$  describing interactions, then

$$\Lambda \frac{d\kappa}{d\Lambda} = \beta(\kappa) \implies \log \Lambda/m = \int_{\kappa(m)}^{\kappa(\Lambda)} \frac{d\kappa}{\beta(\kappa)}, \quad m = 1/\xi. \quad (1.99)$$

Thus, keeping the correlation length  $\xi = 1/m$  fixed, in the continuum limit  $\Lambda \rightarrow \infty$  the integral on the left-hand side diverges to  $+\infty$ . Hence, in order that the right-hand side diverges too,  $\kappa(\Lambda)$  has to be fine-tuned to  $\kappa_c$  for an UV fixed point (provided that  $\beta$  has a first order zero (or higher) at  $\kappa_c$ ).

In order to pin-point whether a coupling is irrelevant or not, the critical exponent  $\eta_i$  is usually written as

$$\eta_i = d_i^c - d - \gamma_i, \quad (1.100)$$

where  $d_i^c$  is the canonical dimension defined in Eq. (1.57),  $d$  dimension of the space-time manifold, and  $\gamma_i$  defined as the anomalous dimension of the corresponding operator  $O_i$ . The existence of an anomalous dimension is a result of (non-trivial) dynamics near a critical point, and therefore the quantity

$$d_i^{dyn} \equiv d_i^c - \gamma_i \quad (1.101)$$

is called the “dynamical” dimension of the operator  $O_i$ . By neglecting the effect of dynamics, thus neglecting  $\gamma_i$ ,  $\eta_i$  is determined by the canonical dimension  $d_i^c$  of the operator  $O_i$  (this is referred to as naive dimensional analysis). By so comparing the effective actions (1.55) and (1.64), we expect the couplings  $\kappa$  to have the scaling relations

$$\kappa(\Lambda') \sim \kappa(\Lambda) (\Lambda/\Lambda')^{d-d^c} \implies \beta(\kappa(\Lambda)) = (d^c - d)\kappa(\Lambda). \quad (1.102)$$

In this context, operators with  $d^c > d$  are labeled naively irrelevant, and the anomalous dimension  $\gamma$ , Eq. (1.100), can turn naively irrelevant operators into relevant (or marginal) ones, and vice versa.

Since the generating functional is functional integral of the field degrees of freedom, we can rescale the fundamental fields  $\phi = (\phi_1, \phi_2, \dots)$ . This is equivalent to a redefinition of couplings and sources, see Zinn-Justin Chapt. 8 [6]. The couplings which correspond to a rescaling of the fundamental degrees of freedom (*i.e.*

the fields) are called  $Z$  factors, and the remaining couplings  $g$  are “physical” coupling constants. For instance, suppose for a theory with two fundamental fields  $\phi = (\phi_1, \phi_2)$ , the action  $S_{\Lambda}^{eff}$  Eq. (1.55) contains a term  $\propto \kappa_i O_i[\phi_1, \phi_2]$ , then we define:

$$g_i(\Lambda) Z_{\phi_1}^{n/2}(\Lambda, g(\Lambda)) Z_{\phi_2}^{m/2}(\Lambda, g(\Lambda)) \equiv \kappa_i(\Lambda), \quad (1.103)$$

where the operator  $O_i$  contains  $n$  powers of  $\phi_1$ , and  $m$  powers of  $\phi_2$ , and where  $g = (g_1, g_2, \dots)$  is the set of “physical” coupling constants. With such a redefinition of coupling constants, the connected Green functions now implicitly depend on couplings  $g$  only. Renormalizability is now the statement that a connected Green function<sup>6</sup>

$$\begin{aligned} G_C^{(n,m)}[x_1, \dots, x_n, y_1, \dots, y_m, \Lambda, g(\Lambda)] \\ \sim \langle 0 | T(\phi_{1l}(x_1) \cdots \phi_{1l}(x_n) \phi_{2l}(y_1) \cdots \phi_{2l}(y_m)) | 0 \rangle_{connected}, \end{aligned} \quad (1.104)$$

satisfies the identity

$$\begin{aligned} Z_{\phi_1}^{n/2}(\Lambda', g') Z_{\phi_2}^{m/2}(\Lambda', g') G_C^{(n,m)}[x_1, \dots, x_n, y_1, \dots, y_m, \Lambda', g'] \\ = Z_{\phi_1}^{n/2}(\Lambda, g) Z_{\phi_2}^{m/2}(\Lambda, g) G_C^{(n,m)}[x_1, \dots, x_n, y_1, \dots, y_m, \Lambda, g], \end{aligned} \quad (1.105)$$

where  $g' = g(\Lambda')$ , and  $g = g(\Lambda)$ . Thus

$$0 = \Lambda \frac{d}{d\Lambda} \left\{ Z_{\phi_1}^{n/2}(\Lambda, g) Z_{\phi_2}^{m/2}(\Lambda, g) G_C^{(n,m)}[x_1, \dots, x_n, y_1, \dots, y_m, \Lambda, g] \right\}. \quad (1.106)$$

The identities Eq.(1.105) and (1.106) follow in theory from the RG invariance of the generating functional, Eq. (1.65), and the SDE (1.11). They are supposedly exact<sup>7</sup>, if the generating functional is spanned by the entire (infinite) set of operators  $O_i$ . However, the RG method tells us we only need to take into account the relevant and marginal operators, and then the identity is an approximate one, with corrections of the irrelevant type (e.g.  $(E/\Lambda)^n$ ,  $n \geq 0$ , and  $E \ll \Lambda$  in momentum space). As an example consider a connected two-point Green function (see Eq. (1.12)):

$$\begin{aligned} G_C^{(2)}(x, y) &= G_C^{(2)}[x, y, \Lambda, g] \sim \frac{\delta^2 \log Z_{\Lambda}[Z_{\phi}, g, J_{\Lambda}]}{\delta J_{\Lambda}(y) \delta J_{\Lambda}(x)} \\ &\sim \int_{p \leq \Lambda} d^4 p e^{-ip(x-y)} G_C^{(2)}[p, \Lambda, g], \end{aligned} \quad (1.107)$$

where  $G_C^{(2)}[p, \Lambda, g]$  is the Fourier transform of  $G_C^{(2)}[x, y, \Lambda, g]$ .

<sup>6</sup>We introduce the notation  $\langle \rangle_{connected}$  for connected time-ordered vacuum expectation values.

<sup>7</sup>Though a proof of the identities Eq.(1.105) and (1.106) is highly nontrivial, and cannot be given for most practical applications of QFT beyond perturbation theory.

Analogous to Eq. (1.105), we have the identity

$$Z_\phi(\Lambda', g') G_C^{(2)}[p, \Lambda', g'] = Z_\phi(\Lambda, g) G_C^{(2)}[p, \Lambda, g], \quad p \leq \Lambda' < \Lambda. \quad (1.108)$$

Thus

$$0 = \Lambda \frac{d}{d\Lambda} \left\{ Z_\phi(\Lambda, g) G_C^{(2)}[p, \Lambda, g] \right\} \implies \quad (1.109)$$

$$0 = \left[ \eta(g) + \sum_i \beta_i(g) \frac{\partial}{\partial g_i(\Lambda)} + \Lambda \frac{\partial}{\partial \Lambda} \right] G_C^{(2)}[p, \Lambda, g], \quad (1.110)$$

where we have defined

$$\beta_i(g) \equiv \Lambda \frac{dg_i}{d\Lambda}, \quad \eta(g) Z_\phi \equiv \Lambda \frac{dZ_\phi}{d\Lambda}. \quad (1.111)$$

Equation (1.110) is an example of a Callan–Symanzik equation, see Ref. [62, 63]. If we consider the asymptotic behavior, or short distance behavior, *i.e.*

$$\xi^{-1} \ll p \ll \Lambda, \quad (1.112)$$

of the connected two-point function  $G_C^{(2)}$ :

$$G_C^{(2)}[p, \Lambda, g] \approx \frac{1}{\Lambda^2} \left( \frac{\Lambda}{p} \right)^{2-\eta(g)} \left[ 1 + a \left( \frac{m}{p} \right)^{2-\eta} + b \left( \frac{p}{\Lambda} \right)^{\sigma_1} + \dots \right], \quad (1.113)$$

where  $a, b$ , are nonuniversal constants, the exponent  $\sigma_1$  is positive ( $\sigma_1 > 0$ ), and  $m = 1/\xi$ . Then such an asymptotic behavior approximately satisfies the Callan–Symanzik Eq. (1.110) (*i.e.* up to corrections of the irrelevant type) provided the physical couplings are close to their critical values, *i.e.*  $\beta_i(g) \approx 0$ .

Naive dimensional analysis implies that  $Z_\phi$  is of the marginal type,  $\eta = 0$ , hence  $\eta$  is referred to as twice the anomalous dimension of the field  $\phi$ , or in fact the anomalous dimension of the kinetic term. The above derivation of the Callan–Symanzik equation for a two-point Green function can straightforwardly be generalized for arbitrary  $n$ -point Green functions.

In the context of renormalizability, we conclude this section by mentioning some properties of gauge theories. As mentioned previously, gauge symmetries are continuous local symmetries of the classical action, and give rise to Ward–Takahashi identities. These so-called WTIs follow in principle from the SDEs, and are crucial in determining whether or not a nontrivial continuum limit exists.

A problem connected with the gauge symmetry is the gauge fixing procedure. The problem occurs in the functional integration, where the integration of paths, which are mutually connected by gauge transformations, and hence have the same functional weight, give rise to uncontrollable infinities. To control these infinities, one has to gauge fix the generating functional. The BRST formalism, see for an introduction Ref. [64], takes care of this gauge fixing mechanism, and for QED (and thus the GNJL model) it is similar to the Gupta–Bleuler formalism.

## 1.4 The Goldstone mechanism

The Goldstone theorem was first suggested by Goldstone [65] and later proved by Goldstone, Salam, and Weinberg [66]. Many textbooks on QFT discuss the Goldstone mechanism extensively; we refer to Refs. [3, 2]. The first example of the Goldstone mechanism in relativistic particle physics is given by the Nambu–Jona-Lasinio model, [1], where the chiral symmetry is spontaneously broken.

Spontaneous symmetry breaking is the phenomenon that an invariance of the action of a model (*i.e.* a symmetry on the dynamical level) is not an invariance of its vacuum. If the broken symmetry is a continuous one, it gives rise to the Goldstone mechanism.

In classical field theory, a continuous symmetry described by a Lie group  $G$  of an action implies, according to Noether’s theorem, the existence of conserved local currents  $j_\mu^a(x)$

$$\partial^\mu j_\mu^a(x) = 0, \quad (1.114)$$

with  $a = 1, 2, \dots, n$ , where  $n$  is the number of the group generators. Then the space integrals of the time component of the currents  $j_a^\mu$  define conserved charges  $Q^a$  corresponding to continuous symmetry (by implementation of the Stokes theorem neglecting surface terms):

$$Q^a \equiv \int d^3x j_0^a(x) \quad \longrightarrow \quad \frac{d}{dt} Q^a(t) = 0. \quad (1.115)$$

The charges  $Q^a$  can be considered as the generators of the Lie group  $G$ , *i.e.* the action or Lagrangian is invariant under unitary transformations of the fundamental field  $\phi$

$$U(\theta) \in G, \quad \phi \rightarrow \phi' = U^\dagger(\theta)\phi U(\theta), \quad U(\theta) = \exp\{i\theta^a Q^a\}. \quad (1.116)$$

The infinitesimal transformations  $\theta^a \ll 1$  of operators  $O_i$  of fields  $\phi$  are generated by  $Q_a$ :

$$\delta O_i[\phi] = -i\theta^a \{Q^a, O_i[\phi]\}, \quad (1.117)$$

where  $\{, \}$  is the Poisson bracket. In quantum field theory the Poisson bracket is replaced by a commutator if  $Q$  is a bosonic operator or by an anti-commutator if  $Q$  is fermionic.

In a quantum field model with a conserved current operator  $j_\mu^a(x)$ , spontaneous symmetry breaking is now characterized by the condition that there exist an operator  $O_i$  for which

$$\langle 0 | \delta O_i[\phi] | 0 \rangle \neq 0, \quad (1.118)$$

thus at least one of the charges  $Q^a$  of Eq. (1.117) does not annihilate the vacuum; the vacuum is not invariant under the continuous symmetry transformation. If the operator  $O_i[\phi]$  breaking the invariance of the vacuum is a composite operator, instead of being a single field, we speak of a dynamically broken symmetry.

The Goldstone theorem states the following. Consider a Lorentz and translational invariant local field theory, with conserved currents  $j_\mu^a$  relating to a Lie group  $G$ . Assume that this symmetry is spontaneously broken so that Eq. (1.118) holds. Then there are massless particles (The Nambu–Goldstone (NG) bosons) with the same quantum numbers as the operators  $O_i[\phi]$ , which couple both to the currents  $j_\mu^a$  and operators  $O_i[\phi]$ . The NG–bosons are indeed bosons if the  $O_i[\phi]$  is a bosonic operator, however in general this need not be the case.

The degeneracy of the vacuum in a theory with a spontaneously broken symmetry is connected with existence of a phase transition in the model, hence vacuum degeneracy can only occur in systems with infinitely many degrees of freedom.

In the framework of SDEs a particular continuous symmetry gives rise to so-called Green–Ward–Takahashi or Ward–Takahashi identities, and the existence of a massless particle follows from the low-energy limits ( $p \rightarrow 0$ ) of corresponding Ward–Takahashi identities. These low-energy relations are very useful when a symmetry is not completely exact, but explicitly broken by a small external field (think of the external field  $h$  in magnetic systems, or a bare particle mass  $m_0$  in case of chiral symmetry). If the spontaneous symmetry breaking mechanism is much stronger than the explicit symmetry breaking, then one can derive, in case of chiral symmetries (see next section), the partial-conserved-axial-current (PCAC) relations.

Let us discuss now the specific case of dynamical chiral symmetry breaking.

#### 1.4.1 Chiral symmetry

Chiral symmetry is a special continuous symmetry of massless fermions. In nature, most fermions that we know of do have masses (even neutrinos are not (anymore) believed to be completely massless), hence the chiral symmetry is a broken symmetry. Consider the following Lagrangian in 4 dimensions,

$$\mathcal{L} = \bar{\psi}(x)\hat{D}\psi(x), \quad (1.119)$$

where  $\hat{D} = \gamma^\mu D_\mu$  is a covariant derivative supposedly containing gauge interactions. Then, the Lagrangian is invariant under the chiral transformations

$$\psi \rightarrow \psi' = e^{i\theta\gamma_5}\psi, \quad \bar{\psi} \rightarrow \bar{\psi}' = \bar{\psi} e^{i\theta\gamma_5}, \quad (1.120)$$

where  $\theta$  is some arbitrary parameter, and the  $\gamma_5$  matrix is defined as

$$\gamma_5 = i\gamma^0\gamma^1\gamma^2\gamma^3 = \gamma_5^\dagger, \quad \{\gamma^\mu, \gamma_5\} = 0, \quad \gamma_5^2 = 1. \quad (1.121)$$

The chiral symmetry implies that the Lagrangian can be written in terms of “left-handed”, and “right-handed” spinors,

$$\psi_L = \left( \frac{1 + \gamma_5}{2} \right) \psi, \quad \psi_R = \left( \frac{1 - \gamma_5}{2} \right) \psi, \quad (1.122)$$

so that

$$\mathcal{L} = \bar{\psi}_L \hat{D} \psi_L + \bar{\psi}_R \hat{D} \psi_R. \quad (1.123)$$

A mass term  $m_0 \bar{\psi} \psi$  is not invariant under the chiral transformations, and the Lagrangian with mass term would read

$$\mathcal{L} = \bar{\psi}_L \hat{D} \psi_L + \bar{\psi}_R \hat{D} \psi_R - m_0 \bar{\psi}_L \psi_R - m_0 \bar{\psi}_R \psi_L. \quad (1.124)$$

Thus a mass term mixes the left-handed and right-handed spinors. The chiral symmetry gives rise to a conserved axial current:

$$j^{5\mu} = \bar{\psi} \gamma^5 \gamma^\mu \psi, \quad \partial_\mu j^{5\mu} = 0. \quad (1.125)$$

With a bare mass term, the chiral symmetry is explicitly broken and the current is not conserved

$$\partial_\mu j^{5\mu} = m_0 \bar{\psi} i \gamma^5 \psi. \quad (1.126)$$

The current  $j^{5\mu}$  defines a charge  $Q^5$  as the generator of the chiral symmetry.

In the framework of spontaneous symmetry breaking given by Eq. (1.118), let us consider a composite pseudoscalar operator  $O[\bar{\psi}, \psi] = \bar{\psi}(x) i \gamma_5 \psi(x)$ . Under the infinitesimal chiral transformations (1.120) (*i.e.*  $\theta \ll 1$ ), the operator transforms as

$$\delta(\bar{\psi} i \gamma_5 \psi) = -2\theta \bar{\psi} \psi. \quad (1.127)$$

If now, in absence of bare masses in the Lagrangian (1.119),

$$\langle 0 | \delta(\bar{\psi} i \gamma_5 \psi) | 0 \rangle \neq 0 \implies \langle 0 | \bar{\psi} \psi | 0 \rangle \neq 0, \quad (1.128)$$

we conclude that the chiral symmetry is dynamically broken (*i.e.* spontaneously broken by a composite operator). The Goldstone theorem implies the existence of a massless pseudoscalar particle (a pion).

By using the chiral symmetry, we can always rotate in such a way that the spontaneous symmetry breaking or “long range order” is in the same direction (in the space spanned by the operators  $\bar{\psi} \psi$  and  $\bar{\psi} i \gamma_5 \psi$ ) as the explicit symmetry breaking caused by a bare mass term  $m_0 \bar{\psi} \psi$  term, *i.e.*

$$\langle 0 | \bar{\psi} i \gamma_5 \psi | 0 \rangle = 0, \quad \langle 0 | \bar{\psi} \psi | 0 \rangle \neq 0. \quad (1.129)$$

Thus the “long-range order” is in the direction of the bare mass operator  $\bar{\psi}\psi$ . Then correlations

$$\langle 0 | T(\bar{\psi}\psi(x)\bar{\psi}\psi(0)) | 0 \rangle_{connected} \quad (1.130)$$

of the operator  $\bar{\psi}\psi$  are referred to as longitudinal, and correlations

$$\langle 0 | T(\bar{\psi}i\gamma_5\psi(x)\bar{\psi}i\gamma_5\psi(0)) | 0 \rangle_{connected} \quad (1.131)$$

of the operator  $\bar{\psi}i\gamma_5\psi$  are transverse to  $\bar{\psi}\psi$ . The massless NG–boson is described by the correlations transverse to the direction of ordering. It means that it costs a small amount of energy to change the direction of ordering in the transverse direction.

## 1.5 The gauged Nambu–Jona-Lasinio model

Let us introduce the gauged Nambu–Jona-Lasinio (GNJL) model. The GNJL model is the gauged version of the first model describing dynamical breaking of chiral symmetry in particles physics, *i.e.* the Nambu–Jona-Lasinio model [1]. If the gauge symmetry is  $U(1)$ , the GNJL model can also be consider as QED with additional four-fermion interactions. Bardeen, Leung, and Love proposed to study the GNJL model in Refs. [12, 13]. They argued that, due to the appearance of large anomalous dimension for the four-fermion operators, the formally irrelevant operators become marginal at the critical gauge coupling  $\alpha_0 = \alpha_c$  of QED.

The interest in the GNJL model has been stimulated by its importance for constructing extended technicolour models (ETC) and top-quark condensate models. For an extensive introduction to such models see [3].

The gauged NJL model is described by the Lagrangian

$$\mathcal{L}_1 = \bar{\psi}(i\gamma^\mu D_\mu - m_0)\psi - \frac{1}{4}F_{\mu\nu}F^{\mu\nu} + \frac{G_0}{2} [(\bar{\psi}\psi)^2 + (\bar{\psi}i\gamma_5\psi)^2], \quad (1.132)$$

where  $D_\mu = \partial_\mu + ie_0 A_\mu$  is the covariant derivative, and where  $G_0$  is the dimensionful coupling constant<sup>8</sup> of the chirally invariant four-fermion interaction. Since the canonical dimension of fermion fields is  $3/2$ , the dimension of  $G_0$  is negative in terms of energy units,

$$\dim(G_0) = -2. \quad (1.133)$$

In other words, the canonical dimension  $d^c$ , Eq. (1.57), of the local operator  $(\bar{\psi}\psi)^2$  is six, and naively it corresponds to an irrelevant operator. In the absence of a fermion mass term  $m_0$  which breaks the chiral symmetry explicitly, the Lagrangian (1.132) possesses a  $U(1)$  gauge symmetry and a global  $U_L(1) \times U_R(1)$  chiral symmetry. It is straightforward to extend and consider the GNJL model describing  $N$

---

<sup>8</sup> $G_0$  is commonly referred to as the Fermi coupling constant.

fermion flavors with a  $U_L(N) \times U_R(N)$  (or  $U_V(N) \times U_A(N)$ ) chiral symmetry. The Lagrangian of the GNJL model with  $N$  fermion flavors is described in appendix A, and the SDEs of this model will be given in chapter 2. In chapter 5 the large  $N$  limit of the GNJL model will be analyzed.

## 1.6 The auxiliary field method

The four-fermion interaction of (1.132) is quartic in the fermion fields, which is rather inconvenient for the description of the quantum field model in terms of Feynman graphs and Schwinger-Dyson equations. The quartic terms give rise to two-loop SDEs for even the two-point Green functions such as the fermion propagator. The problem can be circumvented elegantly by introducing auxiliary chiral fields  $\sigma$  and  $\pi$ , which are (real) spinless scalar fields. We can rewrite the Lagrangian Eq. (1.132) as follows

$$\mathcal{L}_2 = \bar{\psi}i\gamma^\mu D_\mu\psi - \frac{1}{4}F_{\mu\nu}F^{\mu\nu} - \bar{\psi}(\sigma + i\gamma_5\pi)\psi - \frac{1}{2G_0}[(\sigma - m_0)^2 + \pi^2]. \quad (1.134)$$

The Euler-Lagrange equations for the auxiliary fields  $\sigma, \pi$  are

$$\sigma = m_0 - G_0\bar{\psi}\psi, \quad \pi = -G_0\bar{\psi}i\gamma_5\psi, \quad (1.135)$$

which ensure the equivalence of the Lagrangians  $\mathcal{L}_1$  and  $\mathcal{L}_2$  on-shell. The Lagrangian  $\mathcal{L}_2$  is now only quadratic in the fermion fields. The constraints (1.135) represent the fact that the auxiliary fields  $\sigma$  and  $\pi$  describe the scalar and pseudoscalar fermion-anti-fermion degrees of freedom given by the composite operators  $\bar{\psi}\psi$  and  $\bar{\psi}i\gamma_5\psi$ .

In terms of the path integral formalism the equivalence of the Lagrangians (1.132) and (1.134) emerges from the following equality for the generating functional  $Z$ :

$$\begin{aligned} Z &= N \int \mathcal{D}\psi \mathcal{D}\bar{\psi} \mathcal{D}A \exp \left[ i \int d^4x \mathcal{L}_1(\psi, \bar{\psi}, A) \right] \\ &= N' \int \mathcal{D}\psi \mathcal{D}\bar{\psi} \mathcal{D}A \mathcal{D}\sigma \mathcal{D}\pi \exp \left[ i \int d^4x \mathcal{L}_2(\psi, \bar{\psi}, A, \sigma, \pi) \right], \end{aligned} \quad (1.136)$$

where  $N$  and  $N'$  are some normalization constants, and it is implicitly understood that the integration measure of the gauge field  $A$  includes factors connected with the gauge fixing. The equality in Eq. (1.136) is the so-called Hubbard-Stratonovich trick or the auxiliary field method, reintroduced into quantum field theory by Gross and Neveu [67].

The model described by  $\mathcal{L}_2$  is invariant under the combined chiral transformations Eq. (1.120), and

$$\begin{pmatrix} \sigma \\ \pi \end{pmatrix} \rightarrow \begin{pmatrix} \sigma' \\ \pi' \end{pmatrix} = \begin{pmatrix} \cos 2\theta & \sin 2\theta \\ -\sin 2\theta & \cos 2\theta \end{pmatrix} \begin{pmatrix} \sigma \\ \pi \end{pmatrix}, \quad (1.137)$$

for the auxiliary or composite fields. If  $m_0 = 0$ , the chiral symmetry gives rise to the conserved axial current  $j^{5\mu}$ :

$$j^{5\mu} = \bar{\psi} \gamma^5 \gamma^\mu \psi, \quad \partial_\mu j^{5\mu} = 0. \quad (1.138)$$

with a bare mass the chiral symmetry is explicitly broken as given by Eq. (1.126).

After performing a regularization of the generating functional, Eq. (1.136), and introducing the ultra-violet cutoff  $\Lambda$ , we have three “physical” bare running coupling constants,  $m_0$ ,  $g_0$ ,  $\alpha_0$ :

$$m_0 \equiv m(\Lambda), \quad g_0 = G_0 \Lambda^2 / 4\pi^2 \equiv g(\Lambda), \quad \alpha_0 = e_0^2 / 4\pi \equiv \alpha(\Lambda), \quad (1.139)$$

and four  $Z$  factors or renormalization constants  $Z_2$ ,  $Z_3$ ,  $Z_\sigma$ , and  $Z_\pi$ :

$$Z_2^{1/2}(\Lambda'/\Lambda) \psi_{(\Lambda')}(x) = \psi(x), \quad Z_3^{1/2}(\Lambda'/\Lambda) A_{(\Lambda')}^\mu(x) = A^\mu(x), \quad (1.140)$$

$$Z_\sigma(\Lambda'/\Lambda) \sigma_{(\Lambda')}(x) = \sigma(x), \quad Z_\pi(\Lambda'/\Lambda) \pi_{(\Lambda')}(x) = \pi(x), \quad (1.141)$$

where  $\Lambda'/\Lambda \leq 1$ , and the fields  $\psi$ ,  $A^\mu$ ,  $\pi$ ,  $\sigma$  are the bare fields defined at the UV cutoff  $\Lambda$ , *e.g.* compare with  $\phi_l$  of Eq. (1.54), and the fields  $\psi_{(\Lambda')}$  are “renormalized fields” defined at the scale  $\Lambda'$ , *e.g.* compare with  $\phi_{l'}$  of Eq. (1.62).

## Chapter 2

# SDEs of the GNJL model

In this chapter we introduce the Schwinger–Dyson (SDE) equations, and the Ward identities for the GNJL model. In section 2.1 after introducing the generating functional, we present a derivation of SDEs for the Green functions in momentum space. In section 2.2 we review the vector and axial Ward identities, and derive the SDE for the axial-vector vertex. In addition the partial conserved axial current (PCAC) relation are discussed briefly. Finally some basic properties of particles, resonances and tachyons are mentioned in section 2.3.

### 2.1 The generating functional

Suppose that we have some fundamental action  $S_f$  analogous to Eq. (1.47) (*e.g* the action of QED) for which the Wilsonian effective action (1.58) given at some cutoff  $\Lambda$  is the GNJL model. We assume that the GNJL model action can be hypothetically obtained from  $S_f$  after a suitable Pauli–Villars regularization as described in subsection 1.3.1. Thus we write in Minkowski space

$$S_{\Lambda}^{eff} [\kappa(\Lambda), \phi_l] = \int d^4x [\mathcal{L}_{GNJL} + \mathcal{L}_{GF}], \quad (2.1)$$

where we omit the infinite sum of irrelevant interactions. The GNJL model Lagrangian  $\mathcal{L}_{GNJL}$  describes the local interactions of the fields, and for the GNJL model with  $N$  fermion flavors we have

$$\begin{aligned} \mathcal{L}_{GNJL} = & -\frac{1}{4}F_{\mu\nu}F^{\mu\nu} + \sum_{i=1}^N \bar{\psi}_i i\gamma^\mu D_\mu \psi_i - \sum_{i,j=1}^N \sum_{\alpha=0}^{N^2-1} \bar{\psi}_i \tau_{ij}^\alpha (\sigma^\alpha + i\gamma_5 \pi^\alpha) \psi_j \\ & - \frac{1}{2G_0} \sum_{\alpha=0}^{N^2-1} [(\sigma^\alpha)^2 + (\pi^\alpha)^2) - 2c^\alpha \sigma^\alpha], \end{aligned} \quad (2.2)$$

where  $\tau^\alpha$  are the generators of  $U(N)$ ,  $c^\alpha = \text{Tr}[M\tau^\alpha]$ , and  $M_{ij} = m^{(i)}\delta_{ij}$  is the diagonal mass matrix, see also appendix A. The term  $\mathcal{L}_{\text{GF}}$  in Eq. (2.1) represents the gauge fixing part of the Lagrangian. An additional condition is needed, the Gupta–Bleuler gauge fixing. We use a standard covariant gauge fixing with a constant gauge parameter  $\xi$ , *i.e.*

$$\mathcal{L}_{\text{GF}} = -1/2\xi(\partial_\mu A^\mu)^2. \quad (2.3)$$

In case of the GNJL model the coupling constants and fields are

$$\kappa(\Lambda) = (m_0, g_0, \alpha_0, \xi, Z_2, Z_3, Z_\sigma, Z_\pi), \quad (2.4)$$

$$\phi_l = (A, \bar{\psi}, \psi, \sigma, \pi), \quad (2.5)$$

The set of bare coupling constants (except  $\xi$ ) and renormalization constants are given by Eqs. (1.139)–(1.141), and the set of fields  $\phi_l$  are the “low” energy modes analogous to  $\phi_l$  of Eqs. (1.54) and (1.60).

From Eq. (2.1) we construct the generating functional analogous to Eq. (1.61),

$$Z[\mathbf{J}] = N(\Lambda) \int \mathcal{D}\phi_l \exp \left\{ iS_\Lambda^{\text{eff}} [\kappa(\Lambda), \phi_l] + iS_J[\mathbf{J}, \phi_l] \right\}, \quad (2.6)$$

where the dependence of  $Z$  on the cutoff  $\Lambda$  and the couplings  $\kappa(\Lambda)$  is taken implicitly. The functional “measure” is defined as

$$\mathcal{D}\phi_l \equiv \mathcal{D}A \mathcal{D}\bar{\psi} \mathcal{D}\psi \mathcal{D}\sigma \mathcal{D}\pi. \quad (2.7)$$

We implicitly take the product of measures over all flavor, Dirac, and Lorentz indices of the fields. The “source” action  $S_J$  is given by

$$S_J[\mathbf{J}, \phi_l] = \int d^4x \left[ J_\mu A^\mu + \sum_{i=1}^N [\bar{\eta}_i \psi_i + \bar{\psi}_i \eta_i] + \sum_{\alpha=0}^{N^2-1} [J_\sigma^\alpha \sigma^\alpha + J_\pi^\alpha \pi^\alpha] \right], \quad (2.8)$$

where

$$\mathbf{J} = (J, \eta, \bar{\eta}, J_\sigma, J_\pi). \quad (2.9)$$

The sources  $\mathbf{J}$  are defined in a similar manner as the sources  $J_\Lambda$  of Eq. (1.61). The source action defines the response of the system to arbitrary perturbations for which the sources form a suitable basis.  $J$ ,  $\eta$  and  $\bar{\eta}$  are the usual sources of QED, and  $J_\sigma$  and  $J_\pi$  are the sources which couple to the auxiliary fields,  $\sigma$  and  $\pi$ .

As was discussed in section 1.1, the starting point to derive the Schwinger-Dyson equations (SDE) is the following formal identity for the generating functional (2.6):

$$\int \mathcal{D}\phi_l \exp \left\{ iS_\Lambda^{\text{eff}} + iS_J \right\} \frac{\delta}{\delta \phi_l(x)} (S_\Lambda^{\text{eff}} + S_J) = 0, \quad (2.10)$$

where  $\phi_l$  is either one of the five fields of the model  $\phi_l = A, \psi, \bar{\psi}, \sigma, \pi$ . From Eq. (2.10) the SDE for the propagators and vertices in momentum space can be obtained.

Taking into account that the fields  $\bar{\psi}, \psi$  and the sources  $\eta$  and  $\bar{\eta}$  are Grassman variables, we obtain five functional differential equations for the generating functional  $Z$ . The functional derivates in Eq. (2.10) follow from Eqs. (2.2), (2.3), and (2.8). If we then replace the functional integrand by differentiations with respect to source terms the equation (2.10) is equivalent to the following set of functional differential equations:

$$0 = \left\{ \left[ \partial_\lambda \partial^\lambda g^{\mu\nu} - \frac{(\xi - 1)}{\xi} \partial^\mu \partial^\nu \right] \frac{\delta}{i\delta J^\nu(x)} - e_0 \gamma_{ba}^\mu \frac{\delta}{i\delta \bar{\eta}_{ai}(x)} \frac{\delta}{i\delta \eta_{bi}(x)} + J^\mu(x) \right\} Z[\mathbf{J}], \quad (2.11)$$

$$0 = \left\{ (i\hat{\partial})_{be} \frac{\delta}{i\delta \eta_{bj}(x)} + e_0 \gamma_{be}^\mu \frac{\delta}{i\delta J^\mu(x)} \frac{\delta}{i\delta \eta_{bj}(x)} + \tau_{ij}^\alpha \left[ \frac{\delta}{i\delta J_\sigma^\alpha(x)} + i\gamma_5 \frac{\delta}{i\delta J_\pi^\alpha(x)} \right]_{be} \frac{\delta}{i\delta \eta_{bi}(x)} + \bar{\eta}_{ej}(x) \right\} Z[\mathbf{J}], \quad (2.12)$$

$$0 = \left\{ (i\hat{\partial})_{ea} \frac{\delta}{i\delta \bar{\eta}_{ai}(x)} - e_0 \gamma_{ea}^\mu \frac{\delta}{i\delta J^\mu(x)} \frac{\delta}{i\delta \bar{\eta}_{ai}(x)} - \tau_{ij}^\alpha \frac{\delta}{i\delta \bar{\eta}_{aj}(x)} \left[ \frac{\delta}{i\delta J_\sigma^\alpha(x)} + i\gamma_5 \frac{\delta}{i\delta J_\pi^\alpha(x)} \right]_{ea} + \eta_{ei}(x) \right\} Z[\mathbf{J}], \quad (2.13)$$

$$0 = \left\{ -\frac{1}{G_0} \frac{\delta}{i\delta J_\sigma^\alpha(x)} - \tau_{ij}^\alpha \mathbf{1}_{cd} \frac{\delta}{i\delta \bar{\eta}_{dj}(x)} \frac{\delta}{i\delta \eta_{ci}(x)} + \frac{c^\alpha}{G_0} + J_\sigma^\alpha(x) \right\} Z[\mathbf{J}], \quad (2.14)$$

$$0 = \left\{ -\frac{1}{G_0} \frac{\delta}{i\delta J_\pi^\alpha(x)} - \tau_{ij}^\alpha i\gamma_5 \mathbf{1}_{cd} \frac{\delta}{i\delta \bar{\eta}_{dj}(x)} \frac{\delta}{i\delta \eta_{ci}(x)} + J_\pi^\alpha(x) \right\} Z[\mathbf{J}]. \quad (2.15)$$

We use the standard summation convention, *i.e.* a respective sum over double indices (flavor, Lorentz, Dirac indices).

SDEs for time-order vacuum expectation values can be obtained by differentiating the above expression with respect to various source terms. The above set of five functional differential equations determine the entire structure of our model and should be considered as the equations of motion.

As was pointed out in subsection 1.3.1, the low energy modes  $\phi_l$  of Eq. (2.5) give rise to a momentum cutoff  $\Lambda$  in the Fourier transforms of these modes, see Eq. (1.60). Consequently the cutoff  $\Lambda$  enters the expressions for the momentum space Green functions. Therefore we introduce the notation

$$\int_\Lambda d^4p = \int_{|p| \leq \Lambda} d^4p. \quad (2.16)$$

This is referred to as the “hard” cutoff regularization.

### 2.1.1 Condensates

Condensates are described as nonzero vacuum expectation values of local operators at a single space time point, *e.g.*  $\langle 0|\phi(x)|0\rangle$ . Because of the translational invariance of the vacuum, a condensate is independent of the space-time point  $x$ ,  $\langle\phi(x)\rangle = \langle\phi(0)\rangle$ .

Most condensates are zero, for instance the vacuum expectation value of a single vector field  $A_\mu$  will be zero due to charge conjugation. The SDEs for the chiral condensates can be derived from SDE (2.14) by putting the sources to zero. The chiral symmetry is used in such a way that all pseudoscalar condensates are zero,

$$\langle 0|\pi^\alpha|0\rangle = 0. \quad (2.17)$$

For the scalar condensates we then find

$$\langle 0|\sigma^\alpha|0\rangle = c^\alpha + G_0 \sum_{i=1}^N \tau_{ii}^\alpha \text{Tr} [iS^{(i)}(0)], \quad (2.18)$$

where  $iS^{(i)}(0)$  the fermion propagator in coordinate space and  $\text{Tr} [iS^{(i)}(0)]$  is the fermionic chiral condensate of a specific flavor  $i$

$$-\langle 0|\bar{\psi}_i\psi_i|0\rangle \equiv \text{Tr} [iS^{(i)}(0)] = \int_\Lambda \frac{d^4k}{(2\pi)^4} \text{Tr} [iS^{(i)}(k)]. \quad (2.19)$$

One should note that when the bare masses of the fermions are identical (the  $N$  fermions are degenerate) the mass matrix  $M$  is proportional to the identity matrix and all condensates vanish except  $\langle 0|\sigma^0|0\rangle$ .

### 2.1.2 The SDE for the photon propagator

The SDE for the gauge boson, the photon, is derived from Eq. (2.11) by differentiating with respect to  $J_\mu(y)$ , and in momentum space reads

$$-iD^{\mu\nu-1}(q) = -i \left[ -q^2 g^{\mu\nu} + \frac{(\xi-1)}{\xi} q^\mu q^\nu \right] - i\Pi^{\mu\nu}(q), \quad (2.20)$$

where  $\Pi_{\mu\nu}(q)$  is the vacuum polarization defined as

$$\begin{aligned} i\Pi^{\mu\nu}(q) &\equiv (-1) \sum_{i=1}^N \int_\Lambda \frac{d^4k}{(2\pi)^4} \\ &\times \text{Tr} [(-ie_0)\gamma^\mu iS^{(i)}(k)(-ie_0)\Gamma^{(i)\nu}(k, k-q)iS^{(i)}(k-q)]. \end{aligned} \quad (2.21)$$

The vector Ward-Takahashi, which will be introduced in the next section, ensures that the vacuum polarization tensor is transverse,  $q_\mu \Pi^{\mu\nu}(q) = 0$ , hence we write

$$\Pi^{\mu\nu}(q) = (-q^2 g^{\mu\nu} + q^\mu q^\nu) \Pi(q^2), \quad (2.22)$$

in terms of the vacuum polarization  $\Pi(p^2)$ . The SDE for the photon propagator is depicted in Fig. 2.1. For the “Feynman rules” we refer to appendix C.

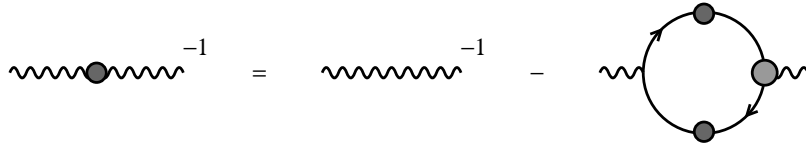


Figure 2.1: The SDE for the photon propagator.

### 2.1.3 The SDE for the fermion propagator

The SDE for the fermion propagator (see definition in appendix B, Eq. (B.21)) in momentum space follows from Eq. (2.13) by differentiating with respect to  $\eta_{bj}(y)$  and setting sources to zero.<sup>1</sup> After Fourier transforming the SDE in coordinate space to momentum space, we obtain the SDE for the fermion propagator

$$\begin{aligned} -iS^{(i)-1}(p) &= -i(\hat{p} - m^{(i)}) - (-i\mathbf{1})G_0 \int_{\Lambda} \frac{d^4 k}{(2\pi)^4} \text{Tr} [iS^{(i)}(k)] \\ &\quad - \int_{\Lambda} \frac{d^4 k}{(2\pi)^4} (-ie_0)\gamma^\mu iS^{(i)}(k)(-ie_0)\Gamma^{(i)\nu}(k, p)iD_{\nu\mu}(k - p) \\ &\quad - \sum_{j=1}^N \sum_{\beta=0}^{N^2-1} \int_{\Lambda} \frac{d^4 k}{(2\pi)^4} (-i\mathbf{1})\tau_{ij}^\beta iS^{(j)}(k)(-i)\Gamma_{Sji}^\beta(k, p)i\Delta_S^{(\beta)}(k - p) \\ &\quad - \sum_{j=1}^N \sum_{\beta=0}^{N^2-1} \int_{\Lambda} \frac{d^4 k}{(2\pi)^4} (\gamma_5)\tau_{ij}^\beta iS^{(j)}(k)(-i)\Gamma_{Pji}^\beta(k, p)i\Delta_P^{(\beta)}(k - p), \end{aligned} \quad (2.23)$$

where Dirac indices have been omitted. In the derivation of the above equation we have used Eqs. (2.17) and (2.18) and the Fierz identity (see for instance [3] and appendix A).

The general structure of the fermion propagator of flavor  $(f)$  is

$$S^{(f)-1}(p) = \frac{\hat{p} - \Sigma_{(f)}(p^2)}{\mathcal{Z}_{(f)}(p^2)}, \quad (2.24)$$

---

<sup>1</sup>Or, equivalently, from Eq. (2.12) by differentiation with respect to  $\bar{\eta}$

since we have rotated all parts proportional to  $i\gamma_5$  to zero. The scalar function  $\mathcal{Z}$  is called the fermion wave function, and  $\Sigma$  the fermion mass function.<sup>2</sup> The SDE for the fermion propagator is depicted in Fig. 2.2.

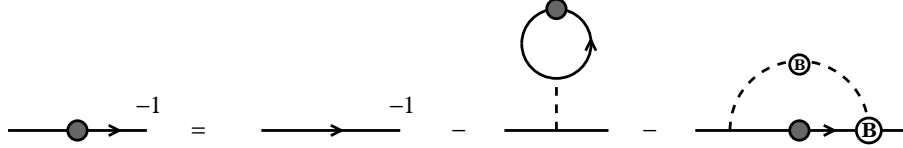


Figure 2.2: The SDE for the fermion propagator.

#### 2.1.4 SDEs for the scalar and pseudoscalar propagators

SDEs for the scalar and pseudoscalar follow from Eqs.(2.14) and (2.15) by differentiating with respect to appropriate sources. Inverting the equations subsequently to momentum space by using the definitions given in appendix B, we find the following SDEs. The SDE for the scalar propagator is

$$-i\Delta_S^{(\alpha)-1}(q) = (-iG_0)^{-1} - i\Pi_S^{(\alpha)}(q^2), \quad (2.25)$$

where the scalar vacuum polarization is defined as

$$\begin{aligned} i\Pi_S^{(\alpha)}(q^2) &\equiv (-1) \sum_{i=1}^N \sum_{j=1}^N \int_{\Lambda} \frac{d^4 k}{(2\pi)^4} \\ &\times \text{Tr} \left[ (-i\mathbf{1}) \tau_{ij}^{\alpha} iS^{(j)}(k) (-i) \Gamma_{Sji}^{\alpha}(k, k-q) iS^{(i)}(k-q) \right], \end{aligned} \quad (2.26)$$

where the factor (-1) is a consequence of the fermion loop.

The SDE for the pseudoscalar propagator is

$$-i\Delta_P^{(\alpha)-1}(q) = (-iG_0)^{-1} - i\Pi_P^{(\alpha)}(q^2). \quad (2.27)$$

The pseudoscalar vacuum polarization is defined as

$$\begin{aligned} i\Pi_P^{(\alpha)}(q^2) &\equiv (-1) \sum_{i=1}^N \sum_{j=1}^N \int_{\Lambda} \frac{d^4 k}{(2\pi)^4} \\ &\times \text{Tr} \left[ (\gamma_5) \tau_{ij}^{\alpha} iS^{(j)}(k) (-i) \Gamma_{Pji}^{\alpha}(k, k-q) iS^{(i)}(k-q) \right]. \end{aligned} \quad (2.28)$$

These SDEs for scalar respectively pseudoscalar propagator ar depicted in Fig. 2.3 and Fig. 2.4.

---

<sup>2</sup>Another decomposition is quite common, namely  $S^{-1}(p) = \hat{p}A(p^2) - B(p^2)$ .

$$\text{---} \circledcirc \text{---}^{-1} = \text{---} \text{---}^{-1} - \text{---} \circlearrowleft \text{---}$$

Figure 2.3: The SDE for the scalar propagator.

$$\text{---} \circledcirc \text{---}^{-1} = \text{---} \text{---}^{-1} - \text{---} \circlearrowleft \text{---}$$

Figure 2.4: The SDE for the pseudoscalar propagator.

### 2.1.5 SDEs of the vertices

In this subsection the SDEs of the proper vertices of the GNJL model are introduced. Important in the derivation of the SDE is the four-point function  $K^{(0)}$ . In appendix B we define the 1-boson irreducible four-point function  $K^{(1)}$  in Eq. (B.29) and the 2-fermion 1-boson irreducible Bethe–Salpeter kernel  $K^{(2)}$  in Eq. (B.28).

**The photon-fermion vertex:** The SDE for the photon-fermion vertex is obtained from Eq. (2.11) by differentiation with respect to  $\eta$  and  $\bar{\eta}$ , and transforming the equation to momentum space.<sup>3</sup> Using the definition of  $K^{(2)}$  and the SDE for the photon propagator, Eq. (2.20), we obtain

$$\begin{aligned} (-ie_0)\Gamma_{ab}^{(i)\mu}(k+q, k) &= (-ie_0)\gamma_{ab}^\mu + \sum_{f=1}^N \int_\Lambda \frac{d^4 k_1}{(2\pi)^4} \\ &\times \left[ iS^{(f)}(k_1+q)(-ie_0)\Gamma^{(f)\mu}(k_1+q, k_1)iS^{(f)}(k_1) \right]_{dc} \\ &\times (-ie_0^2)K_{cd,ab}^{(2)}(k_1, k_1+q, k+q), \end{aligned} \quad (2.29)$$

where we have used that for  $i \neq j$ ,

$$0 = \sum_{f=1}^N \int \frac{d^4 k_1}{(2\pi)^4} \left[ (-ie_0)\gamma_\mu iS^{(f)}(k_1)iS^{(f)}(k_1+q) \right]_{dc}$$

<sup>3</sup>An alternative way is to differentiate Eq. (2.12) with respect to  $\bar{\eta}$  and  $J_\mu$ . In this way the SDE for the vertex is given in term of the two-photon two-fermion scattering kernel or compton kernel, see Ref. [68].

$$\times (-ie_0^2) K_{cd,ab}^{(1)}(k_1, k_1 + q, k + q). \quad (2.30)$$

The SDE for the photon-fermion vertex is depicted in Fig. 2.5.

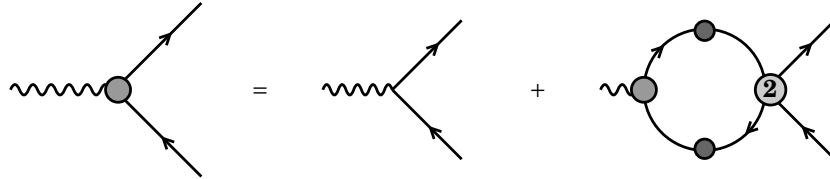


Figure 2.5: The SDE for the photon-fermion vertex.

The photon-fermion vertex has a rich tensor structure; it is both a spinor matrix and a four-vector, and therefore it can be decomposed into 12 spin-vector amplitudes and 12 coefficients. The photon fermion vertex is written as a sum of a longitudinal and transverse part

$$\Gamma^\mu(k, p) = \Gamma_L^\mu(k, p) + \Gamma_T^\mu(k, p), \quad (2.31)$$

where the longitudinal part satisfies a Ward–Takahashi identity

$$q_\mu \Gamma_L^\mu(k + q, k) = S^{-1}(k + q) - S^{-1}(k). \quad (2.32)$$

This vector-Ward–Takahashi (which will be reviewed in the next section) fixes four of the coefficients constituting the longitudinal part. The eight remaining amplitudes are referred to as transverse, since they vanish after projection with in-going photon momentum

$$q_\mu \Gamma_T^\mu(k + q, k) = 0. \quad (2.33)$$

The transverse part is written as a product of eight Ball–Chiu tensors [69],  $T_i^\mu$ , and eight scalar coefficient functions,  $\tau_i((k + q)^2, k^2, q^2)$ ,

$$\Gamma_T^\mu(k + q, k) = \sum_{i=1}^8 T_i^\mu(k + q, k) \tau_i(k + q, k), \quad (2.34)$$

where we write for notational convenience the scalar functions as  $\tau_i(k + q, k) \equiv \tau_i((k + q)^2, k^2, q^2)$ . A modification of the  $T_4^\mu$  was proposed in [70]. The tensors are listed below

$$\begin{aligned} T_1^\mu(k + q, k) &= k^\mu q^2 - q^\mu (k \cdot q), \\ T_2^\mu(k + q, k) &= (2\hat{k} + \hat{q}) T_1^\mu(k + q, k), \\ T_3^\mu(k + q, k) &= q^2 \gamma^\mu - q^\mu \hat{q}, \end{aligned}$$

$$\begin{aligned}
T_4^\mu(k+q, k) &= q^2 \left[ \gamma^\mu (2\hat{k} + \hat{q}) - 2k^\mu - q^\mu \right] + 2q^\mu \sigma_{\nu\rho} k^\nu q^\rho, \\
T_5^\mu(k+q, k) &= \sigma^{\mu\rho} q_\rho, \\
T_6^\mu(k+q, k) &= \gamma^\mu ((k+q)^2 - k^2) - (2k^\mu + q^\mu) \hat{q}, \\
T_7^\mu(k+q, k) &= \frac{(k+q)^2 - k^2}{2} \left[ \gamma^\mu (2\hat{k} + \hat{q}) - 2k^\mu - q^\mu \right] \\
&\quad + (2k^\mu + q^\mu) \sigma_{\nu\rho} k^\nu q^\rho, \\
T_8^\mu(k+q, k) &= -\gamma^\mu \sigma_{\nu\rho} k^\nu q^\rho + k^\mu \hat{q} - q^\mu \hat{k},
\end{aligned} \tag{2.35}$$

where

$$\sigma^{\mu\nu} = \frac{1}{2} [\gamma^\mu, \gamma^\nu]. \tag{2.36}$$

In the Feynman gauge,  $\xi = 1$ , the transverse scalar functions,  $\tau_i$  have been computed to one-loop order by Ball and Chiu in [69], the extension to a general covariant gauge  $\xi$  was done by Kizilersü *et al.* [70].

A general constraint on the eight  $\tau_i$ 's comes from  $C$ -parity transformations. The full vertex must transform under charge conjugation  $C$  in the same way as the bare vertex, so that

$$C\Gamma_\mu(k, p)C^{-1} = -\Gamma_\mu^T(-p, -k). \tag{2.37}$$

Thus Eq. (2.37) together with

$$C\gamma_\mu C^{-1} = -\gamma_\mu^T \tag{2.38}$$

gives, using Eqs. (2.34) and (2.35),

$$\begin{aligned}
\tau_i(k^2, p^2, q^2) &= \tau_i(p^2, k^2, q^2), \quad \text{for } i = 1, 2, 3, 4, 5, 7, 8, \\
\tau_6(k^2, p^2, q^2) &= -\tau_6(p^2, k^2, q^2).
\end{aligned} \tag{2.39}$$

**The scalar and pseudoscalar vertex:** The SDE for scalar vertex is obtained from Eq. (2.14) by differentiation with respect to  $\eta$  and  $\bar{\eta}$ , and Fourier transforming the equation to momentum space. Using the definition of  $K^{(2)}$  and the SDE for the scalar propagator, Eq. (2.25), we find

$$\begin{aligned}
(-i)\Gamma_{S_{ij}^{ab}}^\alpha(k+q, k) &= (-i\mathbf{1})_{ab} \tau_{ij}^\alpha + \sum_{k=1}^N \sum_{l=1}^N \int_\Lambda \frac{d^4 k_1}{(2\pi)^4} \\
&\times \left[ iS^{(k)}(k_1 + q) (-i)\Gamma_{Sk_l}^\alpha(k_1 + q, k_1) iS^{(l)}(k_1) \right]_{dc} \\
&\times (-ie_0^2) K_{lk, ij}^{(2)}(k_1, k_1 + q, k + q),
\end{aligned} \tag{2.40}$$

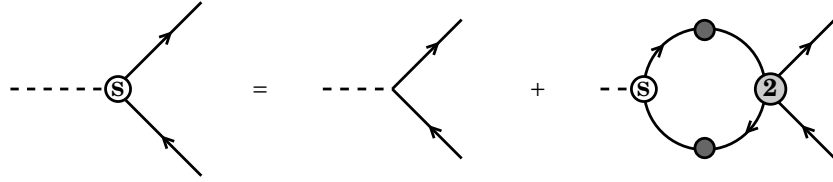


Figure 2.6: The SDE for the scalar vertex.

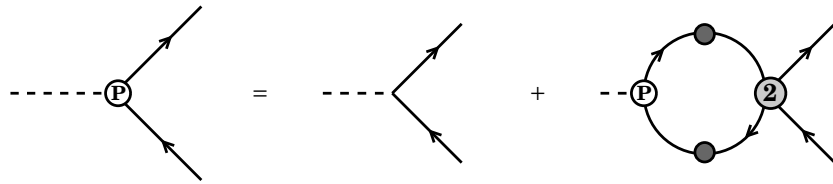


Figure 2.7: The SDE for the pseudoscalar vertex.

and in a similar manner the SDE for the pseudoscalar vertex is obtained,

$$\begin{aligned}
 (-i)\Gamma_{P_{ij}^{ab}}^{\alpha}(k+q, k) &= (\gamma_5)_{ab}\tau_{ij}^{\alpha} + \sum_{k=1}^N \sum_{l=1}^N \int_{\Lambda} \frac{d^4 k_1}{(2\pi)^4} \\
 &\times \left[ iS^{(k)}(k_1+q)(-i)\Gamma_{Pkl}^{\alpha}(k_1+q, k_1)iS^{(l)}(k_1) \right]_{dc} \\
 &\times (-ie_0^2)K_{cd,ab}^{(2)}(k_1, k_1+q, k+q). \tag{2.41}
 \end{aligned}$$

These SDEs are depicted in Fig. 2.6 and Fig. 2.7.

If we consider for simplicity one fermion flavor, then, in momentum space, the scalar and pseudoscalar vertices can be decomposed over four spinor structures<sup>4</sup> with scalar functions in the following way

$$\begin{aligned}
 \Gamma_S(k+q, k) &= F_1^{(s)}(k+q, k) + (\hat{q}\hat{k} - \hat{k}\hat{q})F_2^{(s)}(k+q, k) \\
 &+ (\hat{k} + \hat{q})F_3^{(s)}(k+q, k) + \hat{k}F_4^{(s)}(k+q, k), \tag{2.42}
 \end{aligned}$$

$$\begin{aligned}
 \Gamma_P(k+q, k) &= (i\gamma_5) \left[ F_1^{(p)}(k+q, k) + (\hat{q}\hat{k} - \hat{k}\hat{q})F_2^{(p)}(k+q, k) \right. \\
 &\left. + (\hat{k} + \hat{q})F_3^{(p)}(k+q, k) + \hat{k}F_4^{(p)}(k+q, k) \right], \tag{2.43}
 \end{aligned}$$

where the scalar functions  $F_i^{(s)}$  and  $F_i^{(p)}$  depends on the squares of the Minkowski momenta,  $(k+q)^2, k^2, q^2$ , i.e.,  $F(k+q, k) \equiv F((k+q)^2, k^2, q^2)$ .

<sup>4</sup>This follows from Lorentz covariance.

Now  $C$  invariance

$$C\Gamma_S(k, p)C^{-1} = \Gamma_S^T(-p, -k), \quad C\Gamma_P(k, p)C^{-1} = \Gamma_P^T(-p, -k). \quad (2.44)$$

implies that the functions  $F_1^{(s)}$ ,  $F_1^{(p)}$ , and  $F_2^{(s)}$  and  $F_2^{(p)}$  are symmetric under interchange of fermion momenta

$$F_i^{(s)}(k^2, p^2, q^2) = F_i^{(s)}(p^2, k^2, q^2), \quad F_i^{(p)}(k^2, p^2, q^2) = F_i^{(p)}(p^2, k^2, q^2), \quad (2.45)$$

with  $i = 1, 2$ .

## 2.2 Ward–Takahashi identities

In this section we review the vector and chiral Ward–Takahashi identities (WTIs), which reflect the gauge invariance and the chiral symmetry of the GNJL model. WTIs represent the symmetry structure of the model in terms of relations between Green functions.

The WTIs follow from the SDEs Eq. (2.11)–Eq. (2.15) provided the model is properly regularized.<sup>5</sup> But usually the Ward identities are derived in a more heuristic way by performing a change of the functional integration variable in the generating functional. It is then assumed that local unitary transformations leave the path-integral measure invariant. The invariance of the measure under unitary axial and vector symmetry transformations gives rise to the vector WTIs and chiral WTIs.

### 2.2.1 Vector Ward-Takahashi identities

In Abelian gauge field theories the  $U(1)$  WTI corresponding to the local symmetry plays an essential role in the renormalizability of the model. The WTIs constrain the independent scalings of the model and are crucial for renormalizability.

The  $U(1)$  part of the vector symmetry is local, and we assume that the functional measure  $\mathcal{D}\phi_l$  of Eq. (2.7) is invariant under local  $U_V(1)$  transformations. This statement gives a functional differential equation for the generating functional consistent with the SDEs as mentioned previously. Hence we get for  $U_V(1)$  transformations the following functional differential equation:

$$0 = \left\{ \frac{1}{\xi} \partial_\nu \partial^\nu \partial_\mu \frac{\delta}{i\delta J_\mu} + \partial_\mu J^\mu + e_0 i \bar{\eta}_{bj} \frac{\delta}{i\delta \bar{\eta}_{bj}} - e_0 i \eta_{ai} \frac{\delta}{i\delta \eta_{ai}} \right\}_x Z[\mathbf{J}], \quad (2.46)$$

---

<sup>5</sup>This is similar to the derivation of Noether currents from Euler–Lagrange equations in classical field theory. Contrary to what sometimes is believed, WTIs are not additional constraints imposed on the Green functions other than already imposed by the SDEs.

from which the Ward–Takahashi identities for Green functions can be generated. The above expression is to be evaluated at space-time point  $x$ . Differentiation of Eq. (2.46) with respect to  $J_\nu$  gives the well-known identity for photon propagator

$$q_\mu D^{\mu\nu}(q) = -\xi \frac{q^\nu}{q^2}. \quad (2.47)$$

This condition for the photon propagator implies that the vacuum polarization defined in Eq. (2.21) is transverse

$$q_\mu \Pi^{\mu\nu}(q) = 0. \quad (2.48)$$

Hence we can write the photon propagator as

$$D_{\mu\nu}(q) = -\frac{1}{q^2} \left( g_{\mu\nu} - \frac{q_\mu q_\nu}{q^2} \right) \frac{1}{1 + \Pi(q^2)} - \xi \frac{q_\mu q_\nu}{q^4}, \quad (2.49)$$

where  $\Pi(q^2)$  is the vacuum polarization defined in Eq. (2.22).

Differentiating Eq. (2.46) with respect to  $\eta$  and  $\bar{\eta}$  and Fourier transforming the equation to momentum space yields the WTI for the photon-fermion vertex,

$$(k - p)_\mu \Gamma^{(i)\mu}(k, p) = S^{(i)-1}(k) - S^{(i)-1}(p). \quad (2.50)$$

This identity relates the longitudinal part, Eq (2.31), of the vertex to the fermion propagator.

**Other vector symmetries:** For the sake of completeness we also mention here the  $SU_V(N)$  WTI. This WTI follows from  $SU_V(N)$  symmetry of the GNJL model with  $N$  fermion flavors, see appendix A, and the functional differential equation reads

$$\begin{aligned} 0 &= \left\{ -\partial_\mu (i\gamma^\mu)_{ba} \tau_{ji}^\alpha \frac{\delta^2}{i\delta\bar{\eta}_{ai} i\delta\eta_{bj}} + \tau_{ji}^\alpha \left[ \bar{\eta}_{bj} \frac{\delta}{i\delta\bar{\eta}_{bi}} - \eta_{ai} \frac{\delta}{i\delta\eta_{aj}} \right] \right. \\ &+ \left. \frac{f^{\alpha\beta\gamma} c^\gamma}{G_0} \frac{\delta}{i\delta J_\sigma^\beta} + f^{\alpha\beta\gamma} J_\sigma^\gamma \frac{\delta}{i\delta J_\pi^\beta} + f^{\alpha\beta\gamma} J_\pi^\gamma \frac{\delta}{i\delta J_\sigma^\beta} \right\}_x Z[\mathbf{J}]. \end{aligned} \quad (2.51)$$

## 2.2.2 Chiral Ward–Takahashi identities

Of great importance for the study of dynamical chiral symmetry breaking are the chiral WTIs. These identities are similar to the vector WTIs, and can be derived accordingly. The functional differential equation which generates chiral WTIs is

$$\begin{aligned} 0 &= \left\{ \delta_{\alpha 0} A + \partial_\mu (\gamma^\mu \gamma_5)_{ba} \tau_{ji}^\alpha \frac{\delta^2}{i\delta\bar{\eta}_{ai} i\delta\eta_{bj}} + (i\gamma_5)_{ba} \tau_{ji}^\alpha \left[ \bar{\eta}_{bj} \frac{\delta}{i\delta\bar{\eta}_{ai}} + \eta_{ai} \frac{\delta}{i\delta\eta_{bj}} \right] \right. \\ &+ \left. \frac{g^{\alpha\beta\gamma} c^\gamma}{G_0} \frac{\delta}{i\delta J_\pi^\beta} + g^{\alpha\beta\gamma} J_\sigma^\gamma \frac{\delta}{i\delta J_\pi^\beta} - g^{\alpha\beta\gamma} J_\pi^\gamma \frac{\delta}{i\delta J_\sigma^\beta} \right\}_x Z[\mathbf{J}], \end{aligned} \quad (2.52)$$

where  $\alpha = 0, \dots, N^2 - 1$ . The first term on the right-hand side,  $A$ , is the anomaly operator which is only present in the  $U_A(1)$  Ward identity ( $\alpha = 0$ ), it is the well known Adler–Bell–Jackiw axial-anomaly [60, 61] and can be derived from Eqs. (2.12), (2.13), once these equations are properly regularized by Pauli–Villars fields. The naive assumption is that the functional measure is invariant under local unitary transformations, however it was shown by Fujikawa [71, 72] that this is not the case, proper regularization of the functional measure shows that the under  $U_A(1)$  transformations

$$\psi(x) \rightarrow \psi'(x) = e^{i\theta(x)\gamma_5} \psi(x), \quad (2.53)$$

$$\bar{\psi}(x) \rightarrow \bar{\psi}'(x) = \bar{\psi}(x) e^{i\theta(x)\gamma_5}, \quad (2.54)$$

the measure (2.7) transforms as

$$\mathcal{D}\phi_l \rightarrow \mathcal{D}\phi_l \exp \left[ -2i \int d^d x \theta(x) A(x) \right], \quad (2.55)$$

where  $A$  is the defined as the anomaly. It was shown by Hams [73] that when the generating functional is regularized with Pauli–Villars fields, the SDEs do indeed generate the anomaly.

In four dimensions, the anomaly term is of the form:

$$A(x) \sim \frac{\alpha_0}{4\pi} \epsilon^{\mu\nu\rho\sigma} F_{\mu\nu} F_{\rho\sigma}, \quad (2.56)$$

where  $F$  is the field strength tensor and  $\epsilon$  the totally antisymmetric Levi–Civita tensor. The anomaly terms represents the explicit breakdown of  $U_A(1)$  symmetry due to quantum corrections.

In this thesis we completely neglect the role of the axial-anomaly, since at the moment it is not clear how to implement it properly in nonperturbative studies of chiral symmetry breaking. Secondly the dynamical breakdown of the  $U_A(1)$  symmetry, with neglect of anomaly, serves as a very useful model for the breakdown of the more (complicated) involved  $SU_A(N)$  symmetries, which are free of anomalies.

### 2.2.3 The axial vector vertex and PCAC

In this subsection some interesting relations following from the chiral WTI (2.52) are reviewed. From Eq. (2.52) we can derive the identity for the axial-vector vertex. For simplicity the case with a single fermion flavor case ( $N = 1$ ) is considered with the neglect of the ABJ-anomaly and the axial-vector vertex is defined as

$$\begin{aligned} [iS(k)(-i)\Gamma_5^\mu(k, p)iS(p)]_{ab} &\equiv \int d^4x d^4y e^{ikx - ipy} \\ &\times \langle 0 | T(\bar{\psi}(0)(-i\gamma^\mu\gamma_5)\psi(0)\psi_a(x)\bar{\psi}_b(y)) | 0 \rangle \end{aligned}$$

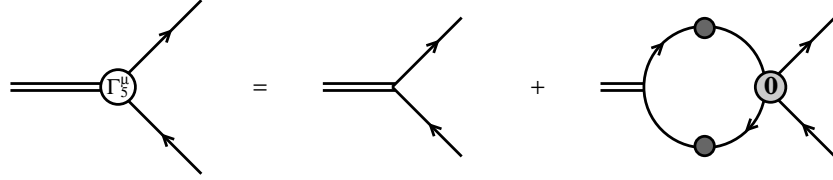


Figure 2.8: The SDE for the axial-vector vertex.

$$= \int d^4x d^4y e^{ikx - ipy} (-i\gamma^\mu \gamma_5)_{dc} iD_{cd,ab}^{(4)}(0,0,x,y). \quad (2.57)$$

and the axial vertex as

$$\begin{aligned} [iS(k)(-i)\Gamma_5(k,p)iS(p)]_{ab} &\equiv \int d^4x d^4y e^{ikx - ipy} \\ &\times \langle 0 | T(\bar{\psi}(0)\gamma_5\psi(0)\psi_a(x)\bar{\psi}_b(y)) | 0 \rangle \\ &= \int d^4x d^4y e^{ikx - ipy} (\gamma_5)_{dc} iD_{cd,ab}^{(4)}(0,0,x,y). \end{aligned} \quad (2.58)$$

Using the definitions given in appendix B the following SDE for the axial-vector vertex can be derived:

$$\begin{aligned} (-i)\Gamma_{5ab}^\mu(k+q,k) &= (-i\gamma^\mu \gamma_5)_{ab} + \int_\Lambda \frac{d^4k_1}{(2\pi)^4} [iS(k_1+q)(-i\gamma^\mu \gamma_5)iS(k_1)]_{dc} \\ &\times (-ie_0^2)K_{cd,ab}^{(0)}(k_1, k_1+q, k+q), \end{aligned} \quad (2.59)$$

which is depicted in Fig. 2.8, with the Feynman rules given in appendix C. The SDE for the axial vertex is

$$\begin{aligned} (-i)\Gamma_{5ab}(k+q,k) &= (\gamma_5)_{ab} + \int_\Lambda \frac{d^4k_1}{(2\pi)^4} [iS(k_1+q)(\gamma_5)iS(k_1)]_{dc} \\ &\times (-ie_0^2)K_{cd,ab}^{(0)}(k_1, k_1+q, k+q). \end{aligned} \quad (2.60)$$

The combination of the previous equation with the SDE for the pseudoscalar vertex Eq. (2.41) yields the following relation between the pseudoscalar vertex and axial vertex<sup>6</sup>:

$$(-i)\Gamma_5(k+q,k) = (-iG_0)^{-1}i\Delta_P(q)(-i)\Gamma_P(k+q,k). \quad (2.61)$$

<sup>6</sup>Rewrite Eq. (2.41) in terms of the scattering kernel  $K^{(0)}$ .

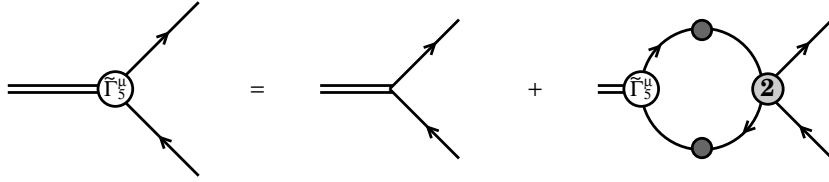


Figure 2.9: The SDE for the regular axial-vector vertex.

From this relation it is clear that when the pseudoscalar propagator  $i\Delta_P$  describes a particle with a physical mass pole at  $q^2 = m_\pi^2$ , the axial vertex  $\Gamma_5$  also has a pole at  $q^2 = m_\pi^2$ .

If we now differentiate Eq. (2.52) with respect to  $\bar{\eta}(y)$  and  $\eta(z)$  and transform the equation to momentum space we find the chiral WTI for the axial-vector vertex:

$$\begin{aligned} (k-p)_\mu \Gamma_5^\mu(k, p) &= S^{-1}(k)(\gamma_5) + (\gamma_5)S^{-1}(p) \\ &\quad - 2im_0(-iG_0)^{-1}i\Delta_P(k-p)\Gamma_P(k, p) \\ &= S^{-1}(k)(\gamma_5) + (\gamma_5)S^{-1}(p) - 2im_0\Gamma_5(k, p). \end{aligned} \quad (2.62)$$

Hence the axial-vector vertex is related to the fermion propagator and the pseudoscalar vertex via the chiral WTI. Also we can show that the axial-vector vertex contains a pole at the physical mass of the pseudoscalar by rewriting the SDE (2.59). Using the definitions of the kernels  $K^{(1)}$  and  $K^{(2)}$ , Eqs. (B.29) and (B.28), we obtain from Eq. (2.59)

$$\begin{aligned} (-i)\tilde{\Gamma}_{5ab}^\mu(k+q, k) &= (-i\gamma^\mu\gamma_5)_{ab} + \int_\Lambda \frac{d^4k_1}{(2\pi)^4} \\ &\quad \times \left[ iS(k_1+q)(-i)\tilde{\Gamma}_5^\mu(k+q, k)iS(k_1) \right]_{dc} \\ &\quad \times (-ie_0^2)K_{cd,ab}^{(2)}(k_1, k_1+q, k+q), \end{aligned} \quad (2.63)$$

see Fig. 2.9. Since the Bethe–Salpeter kernel  $K^{(2)}$  is defined to contains no four-fermion poles, *i.e.*, all scalar and pseudoscalars have been subtracted in Eq. (B.29), this “regular” axial-vertex  $\tilde{\Gamma}_5^\mu$  now contains no poles at scalar or pseudoscalar masses and is defined as

$$(-i)\tilde{\Gamma}_{5ab}^\mu(p+q, p) = (-i)\Gamma_{5ab}^\mu(p+q, p) - \Pi_5^\mu(q)i\Delta_P(q)(-i)\Gamma_P(p+q, p), \quad (2.64)$$

where the pseudovector polarization  $\Pi_5^\mu$  is

$$\begin{aligned} \Pi_5^\mu(q) &\equiv (-1) \int_\Lambda \frac{d^4k}{(2\pi)^4} \text{Tr} [(-i)\Gamma_P(k, k+q)iS(k+q)(-i\gamma^\mu\gamma_5)iS(k)] \\ &= \int_\Lambda \frac{d^4k}{(2\pi)^4} \text{Tr} [(-i\gamma^\mu\gamma_5)iS(k+q)(-i)\Gamma_P(k+q, k)iS(k)] \\ &= q^\mu \Pi_5(q^2), \end{aligned} \quad (2.65)$$

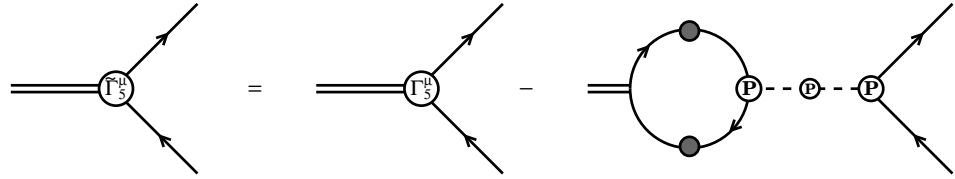


Figure 2.10: Definition of the regular axial-vector vertex.

since the expression can only be proportional to  $q^\mu$  times a scalar function  $\Pi_5$  of  $q^2$ . The change of sign results from reversing the fermion-loop or in fact from reversing direction of  $q$ . The definition of  $(-i)\tilde{\Gamma}_5^\mu$  is depicted in Fig. 2.10. The last term on the right-hand side of (2.64) contains a pole at the pseudoscalar mass and is subtracted. The residue of the pole is thus directly related to the pseudoscalar vertex and the pseudovector polarization (2.65).

A chiral WTI exists for this pseudovector polarization which can be obtained directly from (2.52) by differentiation with respect to source  $J_\pi(y)$  of  $\pi$  and a transformation to momentum space. The chiral WTI reads

$$q_\mu \Pi_5^\mu(q) = q^2 \Pi_5(q^2) = \frac{2m_0}{G_0} + 2\langle\sigma\rangle \Delta_P^{-1}(q). \quad (2.66)$$

Since the pseudovector polarization contains no ‘‘pseudoscalar’’ pole it will be finite at  $q^2 = 0$ . Hence at  $q^2 = 0$  we have

$$\Delta_P(q^2 = 0) = -\frac{G_0\langle\sigma\rangle}{m_0}. \quad (2.67)$$

Using now the fact that

$$\lim_{q \rightarrow 0} q_\mu \tilde{\Gamma}_5^\mu(p + q, p) = 0, \quad (2.68)$$

since possible mass pole terms have been subtracted, and using the chiral WTI (2.62), we obtain a relation between the pseudoscalar vertex at zero boson momentum and the fermion mass function,

$$\Gamma_P(p, p) = (i\gamma_5) \frac{\Sigma(p^2)}{\langle\sigma\rangle}, \quad (2.69)$$

with  $\Sigma$  defined in Eq. (2.24). In the above derivation it was assumed that the fermion wave function is one,  $\mathcal{Z}(p^2) = 1$ <sup>7</sup>.

---

<sup>7</sup>This assumption is believed to be reliable for the quenched-ladder approximation in the Landau gauge,  $\xi = 0$

The identities (2.67) and (2.69) are usually mentioned, in the literature, together with the zero boson momentum expressions for the scalar propagator and scalar vertex

$$\Delta_S(q^2 = 0) = -G_0 \frac{\partial \langle \sigma \rangle}{\partial m_0}, \quad (2.70)$$

$$\Gamma_S(p, p) = (1) \frac{\partial \Sigma(p^2)}{\partial \langle \sigma \rangle}, \quad (2.71)$$

were again  $\mathcal{Z}(p^2) = 1$  is assumed. However, these identities are not a straightforward consequence of the chiral Ward identity (2.52), but follow from the (presummed) analyticity of the generating functional  $Z[\mathbf{J}]$ , Eq. (2.6), in the sources  $\mathbf{J}$ , and the normalization  $Z[0] = 1$ .<sup>8</sup> The analyticity in sources requires that differentiations with respect to bare parameters ( $b_0$ ) of  $Z$  are zero at vanishing sources, *i.e.*,

$$\frac{\partial^n Z[\mathbf{J}]}{\partial b_0^n} \Big|_{\mathbf{J}=0} = 0, \quad b_0 = m_0, \alpha_0, \xi, \dots \quad (2.72)$$

Eq. (2.70) can be derived from the identity

$$\frac{\partial^2 Z[\mathbf{J}]}{\partial m_0^2} \Big|_{\mathbf{J}=0} = 0, \quad (2.73)$$

and, by making use of Eqs. (2.18), (2.19) and (2.25), Eq. (2.71) is obtained.

The relations given in this subsection are very important for the low-energy effective dynamics or the PCAC dynamics. Suppose that scalar and pseudoscalar propagators have the following low-energy or infra-red structure:

$$\Delta_S(q) = \frac{\tau_\sigma}{q^2 - m_\sigma^2}, \quad \Delta_P(q) = \frac{\tau_\pi}{q^2 - m_\pi^2}. \quad (2.74)$$

Then the mass-pole of the pseudoscalar at  $m_\pi$  also appears as a pole in the axial-vector vertex,  $\Gamma_5^\mu$ , and the residue  $\Pi_5(q^2)$  of Eq. (2.65) is related to the pion decay constant  $f_\pi$  in the following way, see *e.g.* Refs. [3, 74, 75, 76]:

$$\Pi_5(0) = \frac{f_\pi^2}{2\langle \sigma \rangle}, \quad (2.75)$$

The chiral WTI (2.66) using Eq. (2.74) at  $q^2 = 0$  implies that

$$\Pi_5(0) = \frac{2\langle \sigma \rangle}{\tau_\pi} \implies f_\pi = \frac{2\langle \sigma \rangle}{\tau_\pi^{1/2}}, \quad \tau_\pi \sim Z_\pi^2(0), \quad (2.76)$$

---

<sup>8</sup>This analyticity in the sources  $\mathbf{J}$  should not be confused with analyticity in bare parameters such as the gauge coupling  $\alpha_0$ , since the chiral phase transition is a consequence of nonanalyticity of  $Z$  in for instance  $\alpha_0$ .

where  $Z_\pi$  is the renormalization constant of the pseudoscalar field, Eq. (1.141). An approximation to  $f_\pi$  can be obtained by assuming that, for small  $q$ ,  $\Gamma_P(k+q, k) \approx \Gamma_P(k, k)$  in Eq. (2.65), this reproduces the well-known Pagels–Stokar’s [77] formula for  $f_\pi^2$ ,

$$f_\pi^2 = \left( -\frac{i}{2\pi^2} \right) \int \frac{d^4 k}{\pi^2} \frac{\Sigma(k^2)}{[k^2 - \Sigma^2(k^2)]^2} \left[ \Sigma(k^2) - \frac{k^2}{2} \Sigma'(k^2) \right]. \quad (2.77)$$

In the  $D\chi$ SB phase, in the chiral limit  $m_0 \rightarrow 0$ , Eq. (2.69) together with Eq. (2.66) relates the pion decay constant  $f_\pi$ , the fermion dynamical mass  $\Sigma$  and the vertex  $\Gamma_P$ , and can be considered as the generalization of the Goldenberger–Treiman relation in the GNJL, see for instance [3, 78]. Eq. (2.69) relates the pseudoscalar vertex to the dynamical mass function. Moreover Eq. (2.67) tells us that if we take the chiral limit, *i.e.*, the bare mass  $m_0 \rightarrow 0$ , the pseudoscalar propagator will describe a massless particle,  $m_\pi = 0$ , *i.e.* a Goldstone boson.

From the chiral WTI one can also derive the relation between UV behavior of the scalar and pseudoscalar propagators and the scalar and pseudoscalar vertices. It is to be expected that such Green functions are asymptotically degenerate, since the UV off-shell behavior of Green functions is not determined by the low-energy potential describing the dynamically broken chiral symmetry; it is determined by the behavior of the “potential” far above the minimum ( $q \gg m_\sigma$ ), where it still is chirally symmetric (there,  $\Delta_S$  and  $\Delta_P$  are degenerate).

## 2.3 Particles

In the GNJL model the particle spectrum contains in addition to the usual spin-1/2 fermions, and spin-1 gauge-bosons also the spinless composite states of fermion and anti-fermion, the scalars and pseudoscalars. Such particles or states are classified either as massive respectively massless stable particles, unstable particles (resonances), or as unphysical states called tachyons. Suppose we can write a particle propagator phenomenologically as

$$\Delta(p) \sim \frac{1}{p^2 - \mu^2}, \quad (2.78)$$

where for the time being we ignore spin-structure. The expression is valid for momenta close to the singularity  $p^2 \sim |\mu|^2$ . Stable particles are characterized by a real positive mass singularity  $\mu^2 \geq 0$ , resonances by a complex singularity  $\mu^2$  is complex, and tachyons by an imaginary pole  $\mu^2 < 0$ .

Masses and decay widths play an important role in the analytic structure of Green functions in the infra-red region. Where, by infra-red region, we refer to momenta close to being on-shell, *i.e.*  $p^2 \sim |\mu|^2$ . Intermediate and ultra-violet regions correspond to momenta which are highly off-shell or virtual,  $-p^2 \gg |\mu|^2$ . In

coordinate space, this means correlations are considered at distances much shorter than the correlation length  $\xi \sim 1/\mu$ .

It is believed that analysis of SDEs in Euclidean formulation gives reliable results in the ultra-violet regions and intermediate regions, *i.e.*, regions where the only relevant scale is the ultra-violet cutoff  $\Lambda$ . However to obtain results describing a correct analytic structure (from the physical point of view) of Green functions in the infra-red region requires in general a more delicate analysis, and, generally speaking, results are much more sensitive to the various approximations used, see, for a thorough discussion of complex branch-point singularities of fermion propagators in the framework of SDEs in QED and QCD, the thesis by Maris [79].

Below, a short overview is given of the various particles states that we will encounter throughout this thesis.

**Stable particles:** A stable physically observable particle, is believed to have an asymptotic in and out state and a Källen–Lehmann representation<sup>9</sup>, see [44]. A stable particle such as a fermion or a gauge boson in an Abelian theory is described by a particle propagator with a Lorentz structure defined by their spin, and has a real mass singularity  $p^2 = \mu^2 \geq 0$ . The mass singularity is a branch point on the positive real axis of the complex  $p^2$ -plane.

**Resonances:** A resonance is an unstable particle or bound state with a lifetime  $\tau \sim 1/\Gamma$ , where  $\Gamma$  is the width (or decay rate) of the resonance. A resonance of the Breit–Wigner type [80, 81, 79] is described by a complex pole in the particle or bound state propagator:

$$\Delta(p) \sim \frac{1}{p^2 - [M - (i/2)\Gamma]^2}, \quad (2.79)$$

which is supposed to be valid for  $p^2$  close to the resonance pole,  $p^2 \sim M^2$ . The resonance mass  $M$  and width  $\Gamma$  are defined to be real and positive. Unitarity of the S-matrix requires that the complex pole of the propagator lies on a second Riemann sheet of the complex plane of  $p^2$ , for an explanation of this point see for instance [81]. When we parametrize the resonance pole with a radius  $R$  and angle  $\theta$

$$p^2 = [M - (i/2)\Gamma]^2 \equiv R \exp(-i\theta), \quad (2.80)$$

then the condition

$$0 \leq \theta < \pi \quad (2.81)$$

---

<sup>9</sup>Contrary to QCD where there is no such thing as an asymptotic in or out quark propagator, and hence there is no Källen–Lehmann representation due to color confinement (breakdown of the cluster property), see [78].

ensures that the pole lies on the second Riemann sheet of  $p^2$ , where we have used that the width over mass ratio is positive,

$$\frac{\Gamma}{M} = \frac{2 \sin \theta}{1 + \cos \theta} \geq 0. \quad (2.82)$$

**Tachyons:** Tachyons are described by an imaginary mass pole, and are called unphysical states, they in fact correspond to particles moving faster than the speed of light. Although such tachyonic particle propagators sometimes occur as solutions of the SDEs, they usually correspond to unstable vacuum configurations, *i.e.*, they correspond to a local maximum instead of a local minimum of the action, and rearrangement of the vacuum will remove the tachyonic states from the physical particle spectrum. For a thorough discussion of tachyonic solutions of Bethe–Salpeter equations, see [3] and references therein.

### 2.3.1 The Wick rotation

The Schwinger–Dyson equation are formulated in Minkowski space, given by the indefinite metric  $g^{\mu\nu}$ . A four-momentum  $p_{\text{Mink}}^2 = p_0^2 - \vec{p}^2$  can either be positive or negative. However actual calculations of SDEs are preferably performed in Euclidean formulation, which has a definite positive metric,  $p_{\text{Eucl}}^2 \geq 0$ . The formulation in Euclidean space considerably simplifies the actual computation of Feynman graphs and henceforth the analysis of SDEs. Once Green functions have been obtained in Euclidean space (for space-like Minkowski momenta), they are rotated back to Minkowski space, after which they can be analytically continued into the time-like (physical) momentum region.

The transformation from Minkowski space to Euclidean space is called the Wick rotation, see Ref. [57], and rotates the zero-component or energy component of the four-momentum to the imaginary axis,  $p_0 \rightarrow ip_0$ . We then replace all Minkowski four-momenta with definite positive Euclidean momenta

$$-p_{\text{Mink}}^2 = p_0^2 + \vec{p}^2 \equiv p_{\text{Eucl}}^2. \quad (2.83)$$

The Wick rotation is allowed only if the Green functions do not have singularities in the second and fourth quadrant of the appropriate complex momentum plane. It is assumed for all practical purposes that this is the case in this thesis.

## Chapter 3

# Dynamical chiral symmetry breaking

Dynamical symmetry breaking is a special case of spontaneous symmetry breaking, where a continuous symmetry is broken through the appearance of a non-vanishing vacuum expectation value of a composite operator. Dynamical symmetry breaking is governed by the formation of bound states. As was mentioned in the introduction, the Bardeen-Cooper-Schrieffer (BCS) theory of superconductivity is one of earliest models of dynamical symmetry breaking and the first model with dynamical chiral symmetry breaking (D $\chi$ SB) in high energy particle physics is the Nambu–Jona-Lasinio model [1].

In this chapter we will discuss the chiral phase transition corresponding to the dynamical breakdown of the chiral symmetry in the GNJL model in the quenched ladder approximation treating the four-fermion interaction in the Hartree-Fock or mean field approximation. The quenched ladder approximation will be discussed in the next section. A combination of strong attractive four-fermion interaction and gauge interaction will turn out to break the chiral symmetry dynamically by the formation of a chiral condensate, where the chiral condensate Eq. (2.19) provides the order parameter of the DCSB. Since the chiral symmetry is a continuous symmetry, the DCSB gives rise to the Goldstone mechanism (see section 1.4), and PCAC dynamics through the formation of spinless bound states, see subsection 2.2.3. DCSB leads to a nonzero fermion dynamical mass  $m_{\text{dyn}}$  and to the appearance of pseudoscalar massless Nambu–Goldstone bosons composed of a massive fermion and a massive antifermion. Following Ref. [3], the massless NG bosons are characterized by a large binding energy, and it is argued that the dynamics producing such bound states should be rather strong.

The setup of this chapter is the following. First, the quenched ladder approximation is discussed, subsequently the gap equation for the fermion dynamical mass

$m_{\text{dyn}}$  following from the SDE for the fermion propagator is reviewed. In section 3.3, we derive the EOS for the GNJL model in analogy with Eq. (1.23). We discuss the solutions to the gap equation and the EOS, obtain the critical fixed point, and derive the scaling laws along with the critical exponents. In section 3.6, the concept of the conformal phase transition is introduced. Finally we discuss the RG flow and fine-tuning of the four-fermion coupling  $g_0$ , and compare the results obtained in the quenched ladder approximation with various lattice results.

### 3.1 The quenched ladder approximation

In the SD approach, the gap equation has been studied extensively in the so-called quenched-ladder, *i.e.* the quenched-planar approximation. In a quenched approximation only diagrams without fermion loops are taken into account, *i.e.* the fermion loops in the vacuum polarization of the photon propagator are neglected<sup>1</sup>. The quenched approximation can be considered as an approximation to a theory with an UV fixed point; at such a point the gauge coupling does not run, and the  $\beta$ -function of  $\alpha_0$  vanishes:

$$\beta_\alpha(\mu_0, g_0, \alpha_0) \equiv \Lambda \frac{d\alpha_0}{d\Lambda} = 0. \quad (3.1)$$

This is a rather crucial assumption, and the possible existence of an UV fixed point of Eq. (3.1) will be investigated in chapter 5.

The ladder or planar approximation is a replacement of the full photon-fermion vertex  $\Gamma^\mu$  of Eq. (2.29) by the bare vertex  $\gamma^\mu$  (photon lines don't cross), the replacement of the BS kernel  $K^{(2)}$ , Eq. (B.28), by a single photon exchange graph. Thus the ladder approximation is based on the following assumptions

$$\Gamma_{ab}^\mu(k, p) \approx \gamma_{ab}^\mu, \quad (3.2)$$

$$K_{cd,ab}^{(2)}(p, p+q, k+q) \approx D_{\mu\nu}(k-p)\gamma_{ad}^\mu\gamma_{cb}^\nu. \quad (3.3)$$

The ladder or planar approximation is assumed to be valid in the Landau gauge only ( $\xi = 0$ ) where  $\mathcal{Z}_{(f)} = 1$ , since then the vector WTI (2.50) and chiral WTI (2.62) are satisfied asymptotically.

In addition to the quenched ladder approximation, the four-fermion interactions are treated in the Hartree-Fock approximation.<sup>2</sup> This means that quantum corrections corresponding to four-fermion interactions are neglected beyond tree level in Feynman diagrams, and only the coupling to the chiral condensate represented by the tadpole graphs of Fig. 2.2 is taken into account. Hence, on the level of SDE for the fermion propagator, in the mean field approach contributions corresponding

<sup>1</sup>The quenched approximation can be considered as the limit of zero fermion flavors,  $N = 0$ , in the SDE for the photon propagator.

<sup>2</sup>The Hartree-Fock approximation is a specific mean field approach.

to exchanges of virtual scalars and pseudoscalars composites ( $\sigma$  and  $\pi$  bosons) are neglected.

## 3.2 The Gap equation

The SDE (2.23) for the fermion mass function  $\Sigma$  defined by Eq. (2.24) is commonly referred to as the gap equation in analogy with the equation for the energy gap near the Fermi surface of one-fermion excitations in the Bardeen–Cooper–Schrieffer (BCS) theory of superconductivity. Pioneering studies on the gap-equation in gauge theories were performed in Refs. [82, 8, 9]. These studies find a critical coupling  $\alpha_c \sim 1$  above which a nontrivial solution for the fermion dynamical mass exists in the chiral limit, *i.e.* zero bare mass  $m_0 = 0$ . As was shown in Refs. [83, 84, 85], the solution for the fermion propagator has moving branch-point singularities in the complex  $p^2$ -plane, instead of a real singularity (on physical grounds a real singularity is required). It is generally believed that the complex branch-points are an artifact of the ladder approximation. Extensive discussion of the gap equation in QED, QCD and the GNJL are given in *e.g.* [10, 19, 86, 3, 74, 39, 79]. In quenched QED, a nontrivial continuum limit can be reached [87, 88, 10, 11, 89].

After taking the trace of the SDE (2.23), performing a Wick rotation to Euclidean momentum  $x = p^2 \geq 0$ , and using Eq. (2.18), we obtain the well-known gap equation for the fermion mass function  $\Sigma$

$$\Sigma(x) = \langle \sigma \rangle + \frac{\lambda_0}{x} \int_0^x dy \frac{y \Sigma(y)}{y + \Sigma^2(y)} + \lambda_0 \int_x^{\Lambda^2} dy \frac{\Sigma(y)}{y + \Sigma^2(y)}, \quad (3.4)$$

$$\langle \sigma \rangle = m_0 + \frac{g_0}{\Lambda^2} \int_0^{\Lambda^2} dy \frac{y \Sigma(y)}{y + \Sigma^2(y)}, \quad (3.5)$$

where we recall that the dimensionless four-fermion coupling  $g_0$  is defined as

$$\frac{g_0}{\Lambda^2} \equiv \frac{G_0}{4\pi^2}, \quad \lambda_0 = \frac{3\alpha_0}{4\pi}, \quad (3.6)$$

with  $\Lambda$  the ultraviolet cutoff. The gap equation (3.4) can be written as a nonlinear second-order differential equation

$$x \frac{d^2}{dx^2} \Sigma(x) + 2 \frac{d}{dx} \Sigma(x) + \frac{\lambda_0 \Sigma(x)}{x + \Sigma^2(x)} = 0, \quad (3.7)$$

with an infrared boundary condition (IRBC),

$$0 = \left[ x^2 \frac{d}{dx} \Sigma(x) \right]_{x=0}, \quad (3.8)$$

and an ultraviolet boundary condition (UVBC),

$$m_0 = \left[ \left( 1 + \frac{g_0}{\lambda_0} \right) x \frac{d}{dx} \Sigma(x) + \Sigma(x) \right]_{x=\Lambda^2}. \quad (3.9)$$

At vanishing gauge coupling ( $\lambda_0 = 0$ ), the only possible solution to the gap equation is a constant  $\Sigma(x) = \Sigma_0$ . Hence, at  $\lambda_0 = 0$ , the gap equation reads

$$\frac{m_0}{\Lambda} = -(g_0 - 1) \frac{\Sigma_0}{\Lambda} + g_0 \frac{\Sigma_0^3}{\Lambda^3} \ln \left( \frac{\Lambda^2 + \Sigma_0^2}{\Sigma_0^2} \right). \quad (3.10)$$

This is the famous gap equation of Nambu and Jona-Lasinio [1].

For  $\lambda_0 > 0$ , the four-fermion coupling  $g_0$  comes into play via the UVBC, since Eq. (3.7) does not depend on  $g_0$ . At present no (nontrivial) analytic solution to the nonlinear second order differential equation Eq. (3.7) is known, except for the case of zero gauge coupling,  $\lambda_0 = 0$ , Eq. (3.10).

### 3.2.1 The linearized approximation

After approximating  $\Sigma^2(x)$  by  $\Sigma^2(0)$  in the denominator of Eq. (3.7), the gap equation becomes linear (though with a nonlinear UVBC) and can be solved straightforwardly [87, 10, 90]. In this so-called linearized approximation, the gap equation reads

$$x \frac{d^2}{dx^2} \Sigma(x) + 2 \frac{d}{dx} \Sigma(x) + \frac{\lambda_0 \Sigma(x)}{x + \Sigma_0^2} = 0, \quad (3.11)$$

where

$$\Sigma_0 \equiv \Sigma(0). \quad (3.12)$$

Clearly the linearized approximation is a good approximation in both the infrared ( $x \ll \Sigma_0^2$ ) and the ultraviolet ( $x \gg \Sigma_0^2$ ) regions. Moreover numerical analysis of *e.g.* Maris [79] shows that the linearized approximation is valid for the entire range of momenta, even for momenta close to the branch points ( $x \sim \Sigma_0^2$ ).

In terms of the variable  $u = -x/\Sigma_0^2$ , the equation can be written as a hypergeometric differential equation

$$u(1-u) \frac{d^2}{du^2} \Sigma(u) + 2(1-u) \frac{d}{du} \Sigma(u) - \lambda_0 \Sigma(u) = 0. \quad (3.13)$$

The hypergeometric differential equation is usually written as

$$z(1-z)w''(z) + (c - (1+a+b)z)w'(z) - abw(z) = 0, \quad (3.14)$$

which has the general solution in terms of hypergeometric functions

$$\begin{aligned} w(z) &= C_1 w_1(z) + C_2 w_2(z), \\ w_1(z) &= {}_2F_1(a, b, c; z), \\ w_2(z) &= z^{1-c} {}_2F_1(a - c + 1, b - c + 1, 2 - c; z), \end{aligned} \quad (3.15)$$

for  $c$  not integer  $\geq 2$ .

For the linearized gap equation, the values of  $a$ ,  $b$ , and  $c$  are

$$\begin{aligned} a &= (1 + \omega)/2, & b &= (1 - \omega)/2, & c &= 2, & (\alpha_0 \leq \alpha_c) \\ a &= (1 + i\nu)/2, & b &= (1 - i\nu)/2, & c &= 2, & (\alpha_0 > \alpha_c) \end{aligned} \quad (3.16)$$

where

$$\alpha_c \equiv \pi/3, \quad (3.17)$$

$$\omega \equiv \sqrt{1 - \alpha_0/\alpha_c} = \sqrt{1 - 4\lambda_0}, \quad (3.18)$$

$$\nu \equiv \sqrt{\alpha_0/\alpha_c - 1} = \sqrt{4\lambda_0 - 1}. \quad (3.19)$$

Thus, the point  $\alpha_0 = \alpha_c$  ( $\lambda_0 = 1/4$ ) is rather special, since at that point  $a$  and  $b$  change from real ( $\alpha_0 < \alpha_c$ ) to complex values ( $\alpha_0 > \alpha_c$ ). Therefore, we distinguish between four specific regimes of gauge coupling:

- A The pure Nambu–Jona-Lasinio (NJL) point:  $\alpha_0 = 0$ ,
- B The intermediate region:  $0 < \alpha_0 < \alpha_c$ ,
- C The QED critical point:  $\alpha_0 = \alpha_c$ ,
- D The strong QED region:  $\alpha_0 > \alpha_c$ .

For any (real positive) value of  $\alpha_0$ , the solution  $w_2(u)$  is irregular at  $u = 0$  ( $x = 0$ ), and does not satisfy the IRBC (3.8). Therefore the solution of the linearized gap-equation is

$$\frac{\Sigma(x)}{\Sigma_0} = \begin{cases} {}_2F_1((1 + \omega)/2, (1 - \omega)/2, 2; -x/\Sigma_0^2), & (\alpha_0 \leq \alpha_c) \\ {}_2F_1((1 + i\nu)/2, (1 - i\nu)/2, 2; -x/\Sigma_0^2), & (\alpha_0 > \alpha_c) \end{cases} \quad (3.20)$$

where  $\Sigma_0$  has to be determined from the UVBC. Thus the IRBC (3.8) determines uniquely the solution of the Eq. (3.11), leaving the value  $\Sigma_0 = \Sigma(0)$  as a free parameter. The UVBC (3.9) then gives a relation between  $\Sigma_0$ ,  $m_0$ ,  $g_0$ ,  $\alpha_0$ , and the ultraviolet cutoff  $\Lambda$ .

By making use of the identity

$$\begin{aligned} \frac{{}_2F_1(a, b, c; z)}{\Gamma(c)} &= \frac{\Gamma(b - a)}{\Gamma(b)\Gamma(c - a)}(-z)^{-a} {}_2F_1\left(a, 1 - c + a, 1 - b + a; \frac{1}{z}\right) \\ &+ \frac{\Gamma(a - b)}{\Gamma(a)\Gamma(c - b)}(-z)^{-b} {}_2F_1\left(b, 1 - c + b, 1 - a + b; \frac{1}{z}\right), \end{aligned} \quad (3.21)$$

$a - b$  not integer, and  $|\arg(-z)| < \pi$ , we get for  $|z| \gg 1$

$$\frac{{}_2F_1(a, b, c; -z)}{\Gamma(c)} \approx \frac{\Gamma(b-a)}{\Gamma(b)\Gamma(c-a)} z^{-a} + \frac{\Gamma(a-b)}{\Gamma(a)\Gamma(c-b)} z^{-b}, \quad |z| \gg 1. \quad (3.22)$$

For large momenta,  $x/\Sigma_0^2 \gg 1$ , and  $\alpha_0 < \alpha_c$  the fermion mass function is expressed as

$$\begin{aligned} \frac{\Sigma(x)}{\Sigma_0} &\approx c(\omega) \left( \frac{x}{\Sigma_0^2} \right)^{-(1-\omega)/2} - d(\omega) \left( \frac{x}{\Sigma_0^2} \right)^{-(1+\omega)/2} \\ &+ \mathcal{O} \left( (x/\Sigma_0^2)^{(\omega-3)/2} \right). \end{aligned} \quad (3.23)$$

with

$$c(\omega) = \frac{\Gamma(\omega)}{\Gamma(\frac{1+\omega}{2}) \Gamma(\frac{3+\omega}{2})}, \quad d(\omega) = -c(-\omega) > 0. \quad (3.24)$$

An analogous expression which is valid for  $\alpha_0 > \alpha_c$  is obtained by replacing  $\omega$  in Eq. (3.23) by  $i\nu$ . Special care should be taken at  $\alpha_0 = \alpha_c$  ( $\omega = 0$ ); at that point, we should expand Eq. (3.23) around  $\omega = 0$ .

To summarize, in the limit  $x/\Sigma_0^2 \gg 1$ , Eq. (3.20) can be written in the following form:

$$\frac{\Sigma(x)}{\Sigma_0} \approx \begin{cases} A(\alpha_0) (\Sigma_0^2/x)^{1/2} \sinh \left[ \frac{\omega}{2} \ln \frac{x}{\Sigma_0^2} + \omega \delta(\alpha_0) \right] / \omega, & (\alpha_0 < \alpha_c) \\ A(\alpha_c) (\Sigma_0^2/x)^{1/2} \left[ \frac{1}{2} \ln \frac{x}{\Sigma_0^2} + \delta(\alpha_c) \right], & (\alpha_0 = \alpha_c) \\ A(\alpha_0) (\Sigma_0^2/x)^{1/2} \sin \left[ \frac{\nu}{2} \ln \frac{x}{\Sigma_0^2} + \nu \delta(\alpha_0) \right] / \nu, & (\alpha_0 > \alpha_c) \end{cases} \quad (3.25)$$

with  $\omega$  and  $\nu$  given in Eqs. (3.18) and (3.19), and where

$$A(\alpha_0) = 2\omega \sqrt{c(\omega)d(\omega)} = \sqrt{\frac{8\omega \cot(\pi\omega/2)}{\pi(1-\omega^2)}}, \quad A(\alpha_c) = \frac{4}{\pi} \quad (3.26)$$

$$\delta(\alpha_0) = \frac{1}{2\omega} \ln \frac{c(\omega)}{d(\omega)}, \quad \delta(\alpha_c) = 2 \ln 2 - 1. \quad (3.27)$$

Here the real valued functions  $A$  and  $\delta$  are the “amplitude and the phase” of the solution, while  $\Sigma_0$  is the mass-scale, which depends on the bare mass  $m_0$ . Since the functions  $A$  and  $\delta$  are symmetric in  $\omega$ , they can be analytically continued to values  $\alpha_0 > \alpha_c$ , *i.e.*  $\omega$  is replaced by  $i\nu$ .

### 3.3 The equation of state

The relation between  $\Sigma_0$  and the chiral condensate  $\langle \sigma \rangle$  can be obtained from the gap equation (3.4)

$$\left[ x \frac{d}{dx} \Sigma(x) \right]_{x=\Lambda^2} = \frac{\lambda_0}{g_0} (m_0 - \langle \sigma \rangle) = \frac{3\pi\alpha_0}{\Lambda^2} \langle \bar{\psi}\psi \rangle, \quad (3.28)$$

see Eqs. (2.18) and (2.19). From the equation (3.28) for the order parameter  $\langle\bar{\psi}\psi\rangle$  and the UVBC (3.9), the fermion mass scale  $\Sigma_0$  can be eliminated. This yields a single equation between the order parameter  $\langle\bar{\psi}\psi\rangle$ , and the bare couplings  $g_0$ ,  $\alpha_0$  and the bare mass  $m_0$ , and the ultraviolet cutoff  $\Lambda$ . In analogy with statistical mechanics, such an equation is referred to as “the equation of state” (EOS).

For the intermediate region  $\alpha_0 < \alpha_c$ , with the assumption  $\Sigma_0 \ll \Lambda$ , the equation for the condensate  $\langle\bar{\psi}\psi\rangle$  can be obtained by substituting Eq. (3.23) in Eq. (3.28). Similarly, the UVBC can be solved by substituting Eq. (3.23) in Eq. (3.9). This gives the following EOS for  $\alpha_0 < \alpha_c$ :

$$\frac{m_0}{\Lambda} = \frac{\Sigma_0^2}{\Lambda^2} \left[ -\Delta g_0 C(\omega) \left( \frac{\Sigma_0}{\Lambda} \right)^{-\omega} + (\Delta g_0 + \omega) D(\omega) \left( \frac{\Sigma_0}{\Lambda} \right)^\omega \right], \quad (3.29)$$

$$\frac{\langle\bar{\psi}\psi\rangle}{\Lambda^3} = \frac{\Sigma_0^2}{\Lambda^2} \frac{1}{4\pi^2} \left[ -C(\omega) \left( \frac{\Sigma_0}{\Lambda} \right)^{-\omega} + D(\omega) \left( \frac{\Sigma_0}{\Lambda} \right)^\omega \right], \quad (\alpha_0 < \alpha_c) \quad (3.30)$$

where we have used that  $\lambda_0 = (1 - \omega^2)/4$ , and where

$$\Delta g_0 \equiv g_0 - \frac{(1 + \omega)^2}{4}, \quad (3.31)$$

and

$$C(\omega) = \frac{2}{1 + \omega} c(\omega), \quad D(\omega) = -C(-\omega). \quad (3.32)$$

At the critical gauge coupling  $\alpha_0 = \alpha_c$ , the EOS is obtained by substituting Eq. (3.25) in Eqs. (3.9) and (3.28). This gives

$$\frac{m_0}{\Lambda} = \frac{\Sigma_0^2}{\Lambda^2} A(\alpha_c) \left[ -\Delta g_0 \left[ \ln \frac{\Lambda^2}{\Sigma_0^2} + 2\delta(\alpha_c) \right] + 1 + 2\Delta g_0 \right], \quad (3.33)$$

$$\frac{\langle\bar{\psi}\psi\rangle}{\Lambda^3} = \frac{\Sigma_0^2}{\Lambda^2} \frac{A(\alpha_c)}{4\pi^2} \left[ -\ln \frac{\Lambda^2}{\Sigma_0^2} - 2\delta(\alpha_c) + 2 \right], \quad (\alpha_0 = \alpha_c) \quad (3.34)$$

where  $\Delta g_0 = g_0 - 1/4$  (at  $\alpha_0 = \alpha_c$ ).

For values of the gauge coupling larger than the critical value it is also convenient to use Eq. (3.25) to express the UVBC (3.9) and Eq. (3.28) as goniometric equations,

$$\frac{m_0}{\Lambda} = \frac{\Sigma_0^2}{\Lambda^2} \frac{2A(\alpha_0)}{(1 + \nu^2)\nu} [(\lambda_0 - g_0) \sin \theta + \nu(\lambda_0 + g_0) \cos \theta], \quad (3.35)$$

$$\frac{\langle\bar{\psi}\psi\rangle}{\Lambda^3} = \frac{\Sigma_0^2}{\Lambda^2} \frac{A(\alpha_0)}{2\pi^2(1 + \nu^2)\nu} [-\sin \theta + \nu \cos \theta], \quad (\alpha_0 > \alpha_c) \quad (3.36)$$

where  $\lambda_0 = (1 + \nu^2)/4$ , and where

$$\theta = \frac{\nu}{2} \ln \frac{\Lambda^2}{\Sigma_0^2} + \nu \delta(\alpha_0), \quad \nu = \sqrt{\alpha_0/\alpha_c - 1}. \quad (3.37)$$

The EOS for the pure NJL model ( $\alpha_0 = 0$ ) is given by Eq. (3.10), and the equation for the condensate follows from Eq. (3.5). Thus

$$\frac{m_0}{\Lambda} = \frac{\Sigma_0^2}{\Lambda^2} \left[ -\Delta g_0 \frac{\Lambda}{\Sigma_0} + (\Delta g_0 + 1) \frac{\Sigma_0}{\Lambda} \ln \frac{\Lambda^2}{\Sigma_0^2} \right], \quad (3.38)$$

$$\frac{\langle \bar{\psi} \psi \rangle}{\Lambda^3} = \frac{\Sigma_0^2}{\Lambda^2} \frac{1}{4\pi^2} \left[ -\frac{\Lambda}{\Sigma_0} + \frac{\Sigma_0}{\Lambda} \ln \frac{\Lambda^2}{\Sigma_0^2} \right], \quad (\alpha_0 = 0) \quad (3.39)$$

where  $\Delta g_0 = g_0 - 1$  (at  $\alpha_0 = 0$ ).

### 3.4 Scaling laws in the chiral limit

The UVBC (3.9) is an eigenvalue equation for  $\Sigma_0$ , and depends on the bare parameters  $\alpha_0$ ,  $g_0$ ,  $m_0$  and the UV cutoff. In the chiral limit we replace  $\Sigma_0$  by  $m_{\text{dyn}}$ , where  $m_{\text{dyn}}$  is called the dynamical mass, *i.e.*,  $m_{\text{dyn}}$  is generated purely by the dynamics (which is rather strong, since  $\alpha_0$ ,  $g_0$  are of order one).

Let us now consider the chiral limit  $m_0 \rightarrow 0$ , and look for a nontrivial solution to the UVBC. For the case of the pure NJL model ( $\alpha_0 = 0$ ), Eq. (3.10) has a nontrivial solution for  $g_0 > 1$ , for  $g_0 \leq 1$   $\Sigma_0 = 0$  is the solution. In the chiral limit we find the scaling law

$$\begin{aligned} (\Delta g_0 \leq 0) \quad \frac{m_{\text{dyn}}}{\Lambda} &= 0, \\ (\Delta g_0 > 0) \quad \frac{m_{\text{dyn}}}{\Lambda} &= \left[ \frac{\Delta g_0}{g_0 \ln(g_0/\Delta g_0)} \right]^{1/2}, \end{aligned} \quad (3.40)$$

where we assumed that  $\Delta g_0 = g_0 - 1 \ll 1$ . For the intermediate region ( $0 < \alpha_0 < \alpha_c$ ) we have nontrivial solution for  $\Sigma_0$  from Eq. (3.29) for values of the four-fermion coupling such that  $\Delta g_0 > 0$ . Since  $C(\omega)$  and  $D(\omega)$  are both positive in this region the solution to  $\Sigma_0 = m_{\text{dyn}}$  is

$$\begin{aligned} (\Delta g_0 \leq 0) \quad \frac{m_{\text{dyn}}}{\Lambda} &= 0, \\ (\Delta g_0 > 0) \quad \frac{m_{\text{dyn}}}{\Lambda} &= \left[ \frac{C(\omega)}{D(\omega)} \frac{\Delta g_0}{\Delta g_0 + \omega} \right]^{1/2\omega}, \end{aligned} \quad (3.41)$$

this scaling law has been obtained in ref. [91].

The sign of  $\Delta g_0$  determines whether there is a nontrivial solution or not. At the critical gauge coupling  $\alpha_0 = \alpha_c$ , we get the scaling law

$$\begin{aligned} (\Delta g_0 \leq 0) \quad \frac{m_{\text{dyn}}}{\Lambda} &= 0, \\ (\Delta g_0 > 0) \quad \frac{m_{\text{dyn}}}{\Lambda} &= \exp \left( \frac{1/4 + g_0}{1/4 - g_0} + \delta(\alpha_c) \right), \end{aligned} \quad (3.42)$$

where  $\Delta g_0 = g_0 - 1/4$ . Thus there is only a nontrivial solution at  $\alpha_c$  for  $g_0 > 1/4$ .

For values of  $\alpha_0 > \alpha_c$  the gauge coupling is strong enough by itself to give a nontrivial solution, so even for zero four-fermion coupling  $g_0$  we obtain a nontrivial solution. By putting  $m_0 = 0$  in Eq. (3.35) we find the following solutions:

$$\frac{m_{\text{dyn}}}{\Lambda} = \exp \left( -\frac{n\pi}{\nu} - \frac{\beta}{\nu} + \delta(\alpha_0) \right), \quad \nu = \sqrt{4\lambda_0 - 1}, \quad (3.43)$$

with

$$\beta = \tan^{-1} \left[ \frac{\nu(\lambda_0 + g_0)}{(g_0 - \lambda_0)} \right], \quad (3.44)$$

and where  $n$  is a positive integer ( $n = 1, 2, \dots$ ), since we have the physical constraint that  $\Sigma_0 < \Lambda$ . It is explained in [10, 3] and references therein that the largest value of  $m_{\text{dyn}}$  (*i.e.*,  $n = 1$ ) leads to the stable vacuum. By analysis of the BS equations for the bound state spectrum (in quenched-ladder QED) it is shown that the solutions with  $n \geq 2$  correspond to tachyonic bound states, whereas the  $n = 1$  solution describes a physical particle spectrum containing massless NG-bosons (pseudoscalars), and massive scalar particles.

Hence, when  $\nu \rightarrow 0$  ( $\alpha_0 \rightarrow \alpha_c$ ) we get

$$\frac{m_{\text{dyn}}}{\Lambda} = \exp \left( \frac{1/4 + g_0}{1/4 - g_0} + \delta(\alpha_c) \right) \exp \left( -\frac{\pi}{\sqrt{4\lambda_0 - 1}} \right). \quad (3.45)$$

This is the famous scaling law with the essential singularity, sometimes referred to as “Miransky” scaling. We will discuss this non-power-like scaling law more thoroughly in section 3.6.

**The critical line in the GNJL model.** From the considerations above it is clear that the GNJL model has a nontrivial chiral phase structure. The chiral symmetry is dynamically broken for values  $\Delta g_0 > 0$  or  $\alpha_0 > \alpha_c$ . We can now draw a critical line in the coupling constant plane  $(g_0, \alpha_0)$  separating the chiral symmetric phase from the chiral broken phase, see Fig. 3.1. The critical line is

$$g_c(\alpha_0) \equiv \frac{1}{4} \left( 1 + \sqrt{1 - \frac{\alpha_0}{\alpha_c}} \right)^2, \quad 0 \leq \alpha_0 < \alpha_c = \frac{\pi}{3} \quad (3.46)$$

at  $g_0 > 1/4$ , and

$$\alpha_0 = \alpha_c \quad (3.47)$$

at  $g_0 \leq 1/4$ , above which the gap equation for the fermion self-energy  $\Sigma(p)$  has a nontrivial solution. In the continuum formulation using the quenched-ladder approximation, the critical line was first obtained by Kondo *et al.* [19] and Appelquist

*et al.* [20]. More recently, a phase plot has been obtained in [92] using lattice simulations of the so-called noncompact GNJL model in a mean field approximation. The critical line obtained in the continuum formulation and the corresponding phase diagram obtained by the lattice simulations are in good qualitative agreement.

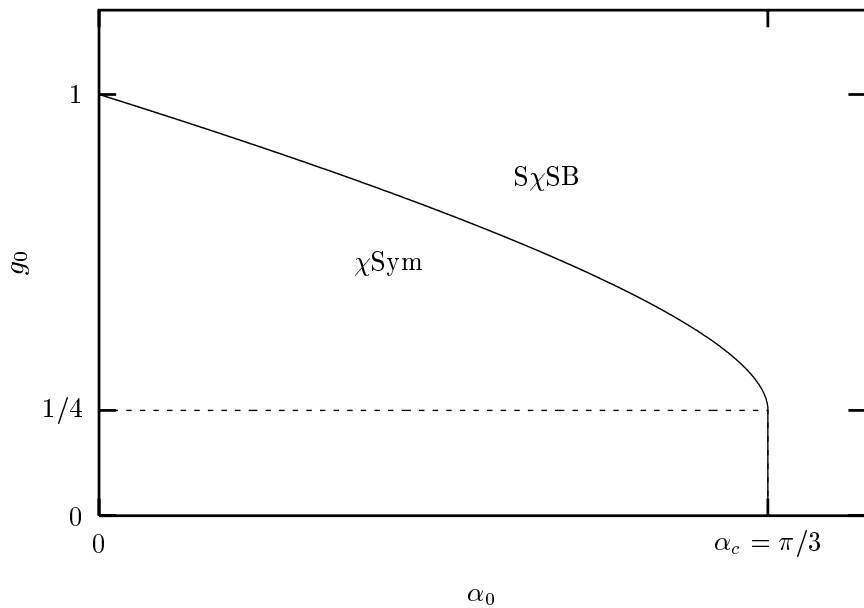


Figure 3.1: The critical curve in the  $(\alpha_0, g_0)$  plane separating a chiral symmetric phase ( $\chi$ Sym) from a spontaneous (dynamical) chiral symmetry broken phase ( $S\chi$ SB).

### 3.5 The critical exponents and scaling

An interesting one-to-one correspondence between the EOS of a magnet Eq. (1.24), and the EOS of the order parameter of chiral symmetry breaking in the GNJL model, *i.e.* Eqs. (3.29) and (3.30), was made independently in Refs. [24, 23], and later in Ref. [93].

Following Refs. [24, 23], we introduce the following correspondence:

- The analog of the magnetization  $M$  of Eq. (1.24) is the chiral condensate,

$$\mathcal{M} \equiv -4\pi^2 \langle \bar{\psi} \psi \rangle / \Lambda^3, \quad (3.48)$$

which is the order parameter.

- The analog of the external magnetic field  $h$  is the bare mass  $m_0$ .
- The analog of the temperature  $t = T - T_c$  is  $\Delta g_0 = g_0 - g_c$ .
- The analog of the magnetic susceptibility  $\chi$ , Eq. (1.28), is the chiral susceptibility

$$\chi \equiv \left. \frac{\partial \mathcal{M}}{\partial m_0} \right|_{m_0=0}. \quad (3.49)$$

The critical exponents  $\beta$ ,  $\gamma$ ,  $\delta$ ,  $\nu$  near the phase transition in a magnetic system were defined in Eqs. (1.27), (1.29), (1.26), and (1.39). Correspondingly, in the GNJL model, the critical exponents  $\beta$ ,  $\gamma$ ,  $\delta$ , and  $\nu$  are defined by the scalings:

$$\mathcal{M} \sim (\Delta g_0)^\beta \quad \text{at } m_0 = 0, \quad (3.50)$$

$$\chi \sim (\Delta g_0)^{-\gamma}, \quad (3.51)$$

$$\mathcal{M} \sim m_0^{1/\delta} \quad \text{at } \Delta g_0 = 0, \quad (3.52)$$

$$m_{\text{dyn}} \sim (\Delta g_0)^\nu \quad \text{at } m_0 = 0, \quad (3.53)$$

where the dynamical mass  $m_{\text{dyn}}$  can be considered as the inverse correlation length,  $m_{\text{dyn}} \sim \xi^{-1}$ , and  $\chi$  is defined by Eq. (3.49). Again we mention that the mass  $m_\sigma$  of the  $\sigma$  boson is the natural candidate for the inverse correlation length, since the  $\sigma$  boson propagator is the connected correlation function of the field  $\sigma$  describing correlations parallel to direction of symmetry breaking (*i.e.* parallel to the direction of long-range ordering given by the order parameter  $\langle \sigma \rangle$ ).

However it can be shown that in the broken phase  $m_\sigma$  scales in the same way as  $m_{\text{dyn}}$ . The symmetric phase will be analyzed more thoroughly in chapter 4.

Substituting Eq. (3.30) in (3.29), we can eliminate  $\Sigma_0$  and rewrite the EOS, in terms of  $\mathcal{M}$  (Eq. (3.48)), as

$$\begin{aligned} \frac{m_0}{\Lambda} &= \mathcal{F}(0)\mathcal{M}^{(2+\omega)/(2-\omega)} + \mathcal{F}'(0)\Delta g_0\mathcal{M} + \dots \\ &= \mathcal{M}^\delta \left[ \mathcal{F}(0) + \mathcal{F}'(0)\Delta g_0\mathcal{M}^{-1/\beta} + \dots \right] \sim \mathcal{M}^\delta \mathcal{F}(\Delta g_0\mathcal{M}^{-1/\beta}), \end{aligned} \quad (3.54)$$

from which the critical exponents  $\beta$  and  $\delta$  can be obtained (compare with Eq. (1.25))

$$\delta = \frac{2+\omega}{2-\omega}, \quad \beta = \frac{2-\omega}{2\omega}, \quad (3.55)$$

$$\mathcal{F}(0) = \omega D(\omega) [C(\omega)]^{(2-\omega)/(2+\omega)}, \quad \mathcal{F}'(0) = -1. \quad (3.56)$$

The dots in Eq. (3.54) represent subleading corrections under the assumption that

$$\Delta g_0 \ll \omega. \quad (3.57)$$

The critical exponent  $\gamma$  can also be obtained from Eq. (3.54) by differentiation with respect to  $m_0$ ,

$$\chi^{-1} \propto \delta \mathcal{M}^{\delta-1} \mathcal{F}(0) + \mathcal{F}'(0) \Delta g_0. \quad (3.58)$$

Using that

$$\mathcal{M}^{\delta-1} \sim (\Delta g_0)^{\beta(\delta-1)} = \Delta g_0. \quad (3.59)$$

We obtain

$$\gamma = 1. \quad (3.60)$$

Hence the hyperscaling equation (1.30)

$$\gamma = \beta(\delta - 1), \quad (3.61)$$

is satisfied.

The critical exponent  $\nu$  can be read off directly from the scaling law (3.41),

$$\nu = 1/2\omega. \quad (3.62)$$

Thus the hyperscaling equation

$$d\nu = 2\beta + \gamma, \quad (3.63)$$

is also satisfied in  $d = 4$  dimensions. This scaling law follows from scaling laws (1.36) and (1.44) after elimination of the critical exponent  $\alpha$ .

The four critical exponents  $\gamma$ ,  $\beta$ ,  $\delta$  and  $\nu$  satisfy the hyperscaling relations (3.61) and (3.63) in the intermediate region  $0 < \alpha_0 < \alpha_c$  ( $0 < \omega < 1$ ), hence only two of them are independent. In the intermediate region the critical exponents have non-mean field values, and the observation that the exponents satisfy the hyperscaling relations, suggest that the theory has a nontrivial continuum limit.

The situation changes at the NJL point ( $\alpha_0 = 0$ ). In the limit  $\omega \rightarrow 1$ , the expressions for the critical exponents Eqs. (3.55), (3.60), and (3.62) yield mean field (or gaussian) exponents ( $\gamma = 1$ ,  $\beta = 1/2$ ,  $\delta = 3$ ,  $\nu = 1/2$ )<sup>3</sup>.

However this result is not completely correct, since we should derive these exponents from Eqs. (3.38) and (3.39). Doing so, we obtain

$$\begin{aligned} \gamma &= 1, & \beta &= \frac{1}{2} + \frac{1}{4} \frac{1}{\ln(1/\mathcal{M})}, \\ \delta &= 3 - \frac{1}{\ln(1/\mathcal{M})}, & \nu &= \frac{1}{2} + \frac{1}{4} \frac{1}{\ln(1/\mathcal{M})}, \end{aligned} \quad (3.64)$$

---

<sup>3</sup> Mean field exponents follow from the mean field approach (or Landau's theory); an operator such as  $\bar{\psi}\psi$  is replaced by its average value, and fluctuations about that value are ignored, see [4].

where  $\mathcal{M}$  is the order parameter defined in Eq. (3.48). Hence the mean field critical exponents get logarithmic corrections. This result is well-known.

Due to the logarithmic corrections, the hyperscaling relations are violated, and we have the following inequalities:

$$4\nu > 2\beta + \gamma, \quad \gamma > \beta(\delta - 1). \quad (3.65)$$

This violation of hyperscaling is believed to be a sign of triviality meaning that the effective Yukawa-coupling (which couples Goldstone bosons to the fermions) vanishes in the continuum limit. The continuum limit is non-interacting, hence trivial. This can be seen in the following way. Assuming that in the low energy region the correlation length  $\xi$  is the only relevant length scale, we define an effective Yukawa-coupling  $g_Y$  by the zero-momentum limit of the scattering amplitude of two fermions exchanging a scalar bound state in the D $\chi$ SB phase

$$\frac{g_Y^2}{m_\sigma^2} \sim \xi^2 g_Y^2 \sim \Gamma_S(0,0) \Delta_S(0) \Gamma_S(0,0), \quad (3.66)$$

where  $\Gamma_S(0,0)$  and  $\Delta_S(0)$  are given by the PCAC relations Eqs. (2.70) and (2.71). Using the definition of the critical exponents (3.50)–(3.53),  $\xi \sim 1/m_{\text{dyn}} \sim 1/m_\sigma$ ,  $\langle \sigma \rangle \sim \mathcal{M}$ , we find that

$$g_Y^2 \sim \frac{1}{\xi^2} \left( \frac{\partial \Sigma_0}{\partial \langle \sigma \rangle} \right)^2 \frac{\partial \langle \sigma \rangle}{\partial m_0} \Big|_{m_0=0} \sim \xi^{(2\beta+\gamma-4\nu)/\nu}. \quad (3.67)$$

This expression is related to the definition of  $g_R \sim g_Y^2$  given in [94], and it is clear that the scaling inequalities (3.65) imply that  $g_Y^2 \rightarrow 0$  when  $\xi \rightarrow \infty$ . Thus, only if the hyperscaling relations are satisfied, a nonzero  $g_Y$  might be realized in the continuum limit ( $\xi \rightarrow \infty$ ), thereby giving rise to a nontrivial interacting theory. The Goldenberger–Treiman relation reads

$$g_Y \sim \frac{m_{\text{dyn}}}{f_\pi}, \quad (3.68)$$

with  $f_\pi$  given by Eq. (2.76). The scaling form for  $\tau_\sigma \sim Z_\sigma^2(0)$  of Eq. (2.74) can be derived from Eq. (2.70),

$$\tau_\sigma \sim \xi^{-\eta}, \quad (3.69)$$

thus  $\tau_\sigma \rightarrow 0$  for  $\xi \rightarrow \infty$ , which is referred to as the “compositeness” condition. Due to the chiral WTI,  $\tau_\pi$  of Eq. (2.74) scales, close to criticality, in the same manner as  $\tau_\sigma$ , *i.e.*  $\tau_\pi \sim \xi^{-\eta}$ . Then, with Eq. (2.76) and Eq. (1.42), we obtain that

$$f_\pi \sim \xi^{\eta/2-\beta/\nu} = \xi^{-1} \xi^{(4\nu-\gamma-2\beta)/2\nu}, \quad (3.70)$$

and thus Eq. (3.68) agrees with Eq. (3.67). Moreover Eq. (3.70) implies the existence of a scaling form for  $\Pi_5(q^2)$  of Eq. (2.65),

$$\Pi_5(q^2) \sim \Lambda(m_\sigma^2/\Lambda^2)^\epsilon \mathcal{F}(q^2/m_\sigma^2), \quad (3.71)$$

where the critical exponent  $\epsilon$  should satisfy  $\epsilon = \beta/2\nu - \eta/2$ , and  $\mathcal{F}$  is assumed to be finite at  $q^2 = 0$ .

Although the violations of the scaling laws for both fermions and magnets (fundamental scalars) is given by the inequalities (3.65), it is said [94] that the triviality of fermions and magnets are realized in a different manner. For instance, the logarithmic corrections to the critical exponent  $\delta$  have opposite sign; for fermions  $\delta < 3$  and for magnets  $\delta > 3$ .

The important difference is that the NG-bosons (pions etc) are composites of fermions, whereas the NG-bosons are fundamental in scalar fields theory. This issue is at the basis of determining whether the Higgs boson is a “fundamental” scalar field or some fermion composite.

If one takes the limit of  $\alpha_0 \rightarrow \alpha_c$ ,  $\omega$  vanishes, and the critical exponents  $\beta$  and  $\nu$  blow up. This can also be seen from the scaling law (3.42) which cannot be expressed as a power-law dependence Eq. (3.53). The phase transition at  $\alpha_0 = \alpha_c$  is rather special and we will discuss it more extensively in the next section.

### 3.6 The conformal phase transition

In the previous section we found that the critical exponents satisfy hyperscaling relations in the intermediate region  $0 < \alpha_0 < \alpha_c$ . Moreover, the Cornwall-Jackiw-Tomboulis (CJT)<sup>4</sup> effective potential  $V$  of the GNJL model in the intermediate region has been obtained by [24, 96, 97, 98, 39], and it can be shown that the effective potential for this range of gauge coupling constant is analogous to the “mexican hat” potential of the  $\sigma$ -model (the prototype potential for second-order phase transitions). However the phase transition at  $\alpha_0 = \alpha_c$  cannot be described by a  $\sigma$ -model type of effective potential. Although the chiral phase transition is continuous (not first order) it cannot be classified as a second order (or higher) phase transition ([99, 27]). The phase transition at  $\alpha_0 = \alpha_c$  is an example of a conformal phase transition (CPT).

The concept of the CPT was introduced and discussed in Ref. [27]. It embodies the classification of specific types of phase transitions. The main feature of the CPT is an abrupt change of the spectrum of light excitations (composites)<sup>5</sup> as the critical point is crossed, though the phase transition itself is continuous. This is connected with the nonperturbative breakdown of the conformal symmetry (scale invariance)

---

<sup>4</sup>See Ref. [95].

<sup>5</sup>By light excitations we mean excitations which have a small mass  $m$  compared with the cutoff  $\Lambda$ ,  $|m|/\Lambda \ll 1$ . In other words, the correlation lengths are large.

by marginal operators (*e.g.*,  $(\bar{\psi}\psi)^2 + (\bar{\psi}i\gamma_5\psi)^2$  in the GNJL model), which was illustrated in Ref. [27] by a study of the effective potentials in Gross-Neveu and GNJL models.

The concept of the CPT can be considered as an extension of the Berezinsky–Kosterlitz–Thouless (BKT) [25, 26] phase transition (taking place in two dimensions) to higher dimensions. Witten [100] has shown that the phase transition in the Gross–Neveu model<sup>6</sup> in  $d = 2$  is analogous to the BKT phase transition. Although due to the Mermin–Wagner theorem [101, 102] spontaneous symmetry breaking or long range order is not possible in  $d = 2$ , there is a generation of a fermion mass and “almost long range order”. The correlations below the critical temperature in the BKT type of models decrease with a (non-universal) power-law behavior instead of exponentially, hence there is a phase transition though the ground state is unique. Instead of a genuine NG-boson a BKT gapless mode appears. The correlation length  $\xi \sim 1/m$  in the Gross–Neveu model and in the models with BKT phase transition have a scaling law with essential singularity, similar to that of Eq. (3.45). This is the crucial property of the CPT; the presence of an essential singularity in the mass (energy) gap at the critical point.

In theories with chiral symmetry breaking in  $d > 2$ , the particle-spectrum consists of massless NG-bosons ( $\pi$ ), their chiral partners ( $\sigma$  bosons), and light<sup>7</sup> fermions (and massless gauge bosons) in the chiral symmetry broken phase. In case of a  $\sigma$ -model like phase transition, the particle spectrum would contain amongst massless fermions (and massless gauge bosons), also light  $\pi$  and  $\sigma$  resonances<sup>8</sup> in the symmetric phase. In case of the CPT, the spectrum in the symmetric phase only consists of massless fermions; light fermion-anti-fermion states are absent.

The absolute value of the mass  $m_\sigma$  of the  $\sigma$  boson is analogous to the inverse correlation length  $1/\xi$ , and the  $\pi$  boson plays the role of the Nambu–Goldstone-boson. In the symmetric phase, the  $\pi$  and  $\sigma$  bosons are degenerate, (*i.e.*,  $m_\pi = m_\sigma$ ). From the PCAC relations (see section 2.2.3) it follows that the  $\pi$  boson mass  $m_\pi$  vanishes in the non-symmetric phase (with zero bare mass  $m_0 = 0$ ). Thus we write, around a critical point  $z = z_c$ ,

$$m_\pi = 0, \quad m_\sigma/\Lambda = C_+(z)(z - z_c)^\nu, \quad z \geq z_c \quad \text{broken phase}, \quad (3.72)$$

$$m_\pi = m_\sigma, \quad m_\sigma/\Lambda = C_-(z)(z_c - z)^\nu, \quad z < z_c \quad \text{symmetric phase}, \quad (3.73)$$

where  $z$  is a generic notation for the parameters of the theory, *e.g.* the coupling constant  $\alpha_0$  or  $g_0$ , the number of fermion flavors  $N$  or temperature  $T$ . Moreover the factors  $C_+(z)$  and  $C_-(z)$  are functions of such parameters. Furthermore  $C_+$  is real (stable bound states) and  $C_-$  is complex valued (resonances). Since in general

$$\lim_{z \downarrow z_c} |C_+(z)| \neq \lim_{z \uparrow z_c} |C_-(z)|, \quad (3.74)$$

<sup>6</sup>The Gross–Neveu model or the Thirring model can be consider as the NJL model in two dimensions with  $N$  fermion flavors, see [67].

<sup>7</sup>By light particles we mean particles with masses much less than the cutoff  $\Lambda$ .

<sup>8</sup>The  $\pi$  and  $\sigma$  bosons can decay to massless fermions and anti-fermions.

the mass  $m_\sigma$ , although continuous, is nonanalytic in  $z = z_c$ . The explanation (see [27]) is that while in the symmetric phase, the  $\pi$  and  $\sigma$  bosons are described by BS equations with a zero fermion mass, in the non-symmetric phase they are described by BS equations with  $m_{\text{dyn}} \neq 0$ . Because of that, BS equations in the non-symmetric phase are not obtained by an analytic continuation of the equations in the symmetric phase. Again, this is reflection of the fact that a phase transition is described by non-analytic behavior in one (or more) of the parameters of the generating functional. Consequently the Green functions (or at least some of them) exhibit non-analyticity around the critical point.

It is clear from Eqs. (3.72) and (3.73) that close to criticality, *i.e.*  $z \sim z_c$ , the spectrum comprises of light bound states,  $|m_\pi|, |m_\sigma| \ll \Lambda$ . Moreover, the fermion dynamical mass  $m_{\text{dyn}}$ , which is given via the order parameter  $\mathcal{M} \sim \langle \psi \psi \rangle$ , vanishes in the symmetric phase. In the non-symmetric phase, the PCAC relations show that  $m_{\text{dyn}}$  scales in the same way as  $m_\sigma$ . We recall that, in the chiral limit ( $m_0 \rightarrow 0$ ), we have the scaling laws

$$m_{\text{dyn}} \sim m_\sigma, \quad \mathcal{M} \sim (z - z_c)^\beta, \quad z \geq z_c \quad \text{broken phase}, \quad (3.75)$$

$$m_{\text{dyn}} = 0, \quad \mathcal{M} = 0, \quad z < z_c \quad \text{symmetric phase}. \quad (3.76)$$

for models with  $d > 2$ . Thus close to criticality we can represent the mass spectrum of excitations by a universal scaling function  $f$

$$m_{\text{dyn}}, m_\sigma, m_\pi \sim \Lambda f(z), \quad (3.77)$$

around  $z = z_c$ . If the scaling function  $f$  is of the form  $f(z) \sim |z - z_c|^\nu$ , the spectrum consists of “light excitations” on both sides of the critical point.

The CPT is characterized by a scaling function  $f(z)$  which has an essential singularity at  $z = z_c$  and satisfies

$$\lim_{z \downarrow z_c} f(z) = 0, \quad z \geq z_c \quad \text{broken phase}, \quad (3.78)$$

$$\lim_{z \uparrow z_c} f(z) \neq 0, \quad z < z_c \quad \text{symmetric phase}. \quad (3.79)$$

The scaling law at  $\alpha_0 = \alpha_c$  of  $m_{\text{dyn}}$  in the GNJL model, see Eq. (3.45), is an example of a scaling law with such an essential singularity. Let us follow [27], and argue that the scaling law with essential singularity implies an abrupt change in the spectrum consisting of light excitations. The story is as follows. In the nonsymmetric phase, besides the solutions with  $m_{\text{dyn}} \neq 0$ , there are solutions with  $m_{\text{dyn}} = 0$ , which can be obtained by analytically continuing the solutions in the symmetric phase to the nonsymmetric phase. The solutions with  $m_{\text{dyn}} = 0$  in the broken phase are unstable or unphysical, in that case the  $\pi$  and  $\sigma$  bosons are tachyons:  $m_{\text{tach}}^2 \equiv m_\pi^2 = m_\sigma^2 < 0$ . It is shown in [3] that scaling law for the tachyonic masses has the same form as the scaling law for the dynamical fermion mass  $m_{\text{dyn}}$  in the broken phase:  $|m_{\text{dyn}}| \sim |m_{\text{tach}}|$ . The crucial point is that the

replacement of  $m_{\text{dyn}} \neq 0$  by  $m_{\text{dyn}} = 0$  does not change the ultraviolet properties of the theory. The analytic continuation of the scaling law for  $m_\sigma$  Eq. (3.73) from the symmetric phase ( $z < z_c$ ) to the broken phase ( $z > z_c$ ) gives the scaling law for the tachyonic mass

$$m_\sigma/\Lambda = C_-(z)(z_c - z)^\nu \sim f(z), \quad z < z_c, \quad (3.80)$$

$$m_{\text{tach}}/\Lambda = C_-(z)(z_c - z)^\nu \sim f(z), \quad z > z_c, \quad (3.81)$$

where  $m_{\text{tach}}^2 < 0$ ,  $m_{\text{dyn}} \sim |m_{\text{tach}}| = |m_\sigma|$ . Since the scaling law  $f(z)$  of the  $\sigma$ -model type approaches zero from both sides of the critical point  $z_c$ , it follows straightforwardly that the spectrum comprises of light excitations ( $|m_\sigma| = |m_\pi| \ll \Lambda$ ) in the symmetric phase. However in case of the CPT, when  $f(z)$  has an essential singularity (Eq. (3.79))  $f(z)$  does not approach zero from the symmetric side and the mass of the  $\sigma$  and  $\pi$  resonances will not be small ( $m_\sigma/\Lambda \sim \mathcal{O}(1)$ ). Thus the CPT is characterized by an abrupt change in the spectrum of light excitations across the critical point  $z = z_c$ .

What is the origin of the CPT? In case of the GNJL model with nonzero  $g_0$  and  $\alpha_0 < \alpha_c$  the model contains formally irrelevant four-fermion operators  $d_{(\bar{\psi}\psi)^2} > 4$  which become relevant operators  $d_{(\bar{\psi}\psi)^2} < 4$  near the critical curve due to the appearance of a large anomalous dimension for these operators. The relevant operators break the conformal symmetry (scale invariance) explicitly in the symmetric phase (close to criticality), and give rise to light  $\pi$  and  $\sigma$  resonances (which introduce a conformal symmetry breaking mass-scale into the theory). However at  $\alpha_0 = \alpha_c$  and  $g_0 < 1/4$  the four-fermion operators are marginal operators, and the theory is supposedly conformal invariant. Therefore in the symmetric phase it is consistent that we would expect only massless fermions and anti-fermions, and absence of light unstable  $\pi$  and  $\sigma$  bound states. In the symmetric phase the divergence of the dilatation current  $\mathcal{D}_\mu$  (see [6, 3] for exact definitions) vanishes, *i.e.*,  $\partial^\mu \mathcal{D}_\mu = 0$ . However dynamical breaking of the chiral symmetry introduces a new mass-scale, and introduces a conformal anomaly ( $\partial^\mu \mathcal{D}_\mu \neq 0$ )<sup>9</sup>. Hence, the origin of the CPT lies in the nonperturbative breakdown of conformal invariance.

Up till now, the CPT has been found in 2-dimensional Gross-Neveu model [100, 27], the GNJL model and quenched QED4 at  $\alpha_0 = \alpha_c$ , see for instance [11, 104]. More recently, the CPT was considered in  $SU(N_c)$  gauge theories (with  $N_c$  the number of colors) with  $N$  number of flavors [105, 106] by concluding the absence of light excitations in the symmetric phase. In QED<sub>3</sub> without Chern-Simons term a CPT like transition was found by [99] and [107], where Appelquist *et al.* considered the spectrum of excitations, and Gusynin *et al.* constructed the (CJT) effective potential. We will return to the concept of the CPT, when we discuss the propagator of the  $\sigma$  boson in section 4.6.

---

<sup>9</sup>It is said ([27]) that the specific form of the conformal anomaly implies a realization of the partial conservation of dilation current (PCDC) hypothesis, see for instance [103].

### 3.7 RG equations and fine-tuning

As was discussed in section 1.3, the concept of fine-tuning of relevant and marginal interactions is required for determining whether a nontrivial continuum limit exists. According to the renormalization group methods the bare couplings of a quantum field model run with the UV cutoff  $\Lambda$ . Referring to subsection 1.3.3, we recall that the bare relevant and marginal couplings (*e.g.*  $m_0$ ,  $\alpha_0$ ,  $g_0$ ) have to be fine-tuned sufficiently close to the critical point in order for scaling behavior to set in.

Near the critical point a new scale is generated, namely the correlation length which exist in case of for instance the  $\sigma$ -model type of phase transition on both sides (both phases) of the system. In the broken phase the inverse correlation length is real and can be considered as a physical mass of particles, for instance the mass of the scalar bound state (the  $\sigma$  boson)  $m_\sigma$ , or the mass of fermion  $m_{\text{dyn}}$ , whereas in the symmetric phase the correlation length is complex giving rise to resonances (scalar and pseudoscalar resonances), given by a mass and a width. It turns out that if hyperscaling relations are satisfied the absolute value of the mass of the resonance can be considered as the inverse correlation length, and the mass over width ratio (*i.e.*, the complex phase) will only depend on the critical exponents. In case of a CPT there are no resonances in the symmetric phase, and no new mass scale is introduced, hence there is absence of fine-tuning.

The fine-tuning depends on the eigenvalues of the couplings close to the critical point (see Eq. (1.84) and hence on the critical exponents (see Eq. (1.86)). These critical exponents follow in principle from the  $\beta$  functions for the coupling parameters  $\mu_0$ ,  $g_0$  and  $\alpha_0$ , which are defined by

$$\Lambda \frac{d\mu_0}{d\Lambda} = \beta_\mu(\mu_0, g_0, \alpha_0), \quad (3.82)$$

$$\Lambda \frac{dg_0}{d\Lambda} = \beta_g(\mu_0, g_0, \alpha_0), \quad (3.83)$$

$$\Lambda \frac{d\alpha_0}{d\Lambda} = \beta_\alpha(\mu_0, g_0, \alpha_0), \quad (3.84)$$

where  $\mu_0$  is the dimensionless bare mass

$$\mu_0 = m_0/\Lambda. \quad (3.85)$$

The first step is determine the fixed points  $(\mu^*, g^*, \alpha^*)$  of the RG equations (3.82), (3.83), and (3.84), *i.e.*

$$\beta_\mu(\mu^*, g^*, \alpha^*) = 0, \quad \beta_g(\mu^*, g^*, \alpha^*) = 0, \quad \beta_\alpha(\mu^*, g^*, \alpha^*) = 0. \quad (3.86)$$

In principle these RG equations follow from the regularized SDEs derived in chapter 2. As is well-known, the fixed point for  $\beta_\mu$  is  $\mu^* = 0$ , hence we can write

$$\Lambda \frac{d\mu_0}{d\Lambda} \approx -(1 + \gamma_m) \mu_0, \quad (3.87)$$

where  $\gamma_m$  is the anomalous dimension of the mass operator  $\bar{\psi}\psi$  evaluated at the fixed point  $(\mu^*, g^*, \alpha^*)$ , see again subsection 1.3.3. Equation (3.87) is in correspondence with Eqs. (1.98) and (1.100), since the canonical dimension of  $\bar{\psi}\psi$  is  $d^c = 3$  at  $d = 4$ . The critical exponent  $\eta$  (see Eq. (1.100)) of  $\mu_0$  is negative (for  $\gamma_m > -1$ ), thus the dimensionless bare mass  $\mu$  is a relevant coupling, and requires fine-tuning.

After setting  $\mu_0 = \mu^* = 0$ , the problem reduces to the determination of the UV fixed points for the subset

$$\beta_g(g_0, \alpha_0) = 0, \quad (3.88)$$

$$\beta_\alpha(g_0, \alpha_0) = 0, \quad (3.89)$$

of the  $\beta$  functions. The quenched ladder approximation simplifies the solutions of Eqs. (3.88), and (3.89) considerably since the quenched hypothesis Eq. (3.1) explicitly sets  $\beta_\alpha = 0$ . In this way, as we will show in a moment, the critical fixed point of Eq. (3.88) is given by Eq. (3.46):

$$g^* = g_c(\alpha_0), \quad \beta_g(g_c(\alpha_0), \alpha_0) = 0. \quad (3.90)$$

Therefore we can address the problem of finding critical fixed points beyond the quenched approximation as was proposed at the end of subsection 1.3.2. Thus the analysis of solutions  $(g^*, \alpha^*)$  of Eqs. (3.88) and (3.89) is performed by first assuming that a solution of

$$\beta_g(g_0, \alpha_0) = 0 \quad (3.91)$$

exists and can be expressed as  $g^* = g_c(\alpha_0)$ . Then the equation (3.89) should be reconsidered. In chapter 5 the equation (3.89) will be analyzed beyond the quenched approximation, and we will indeed try to solve

$$\beta_\alpha(g_c(\alpha_0), \alpha_0) = 0. \quad (3.92)$$

In what follows, we derive the expression for the anomalous dimension  $\gamma_m$  of  $\bar{\psi}\psi$  and find an expression for the  $\beta$  function,  $\beta_g$ , of  $g_0$ .

### 3.7.1 RG flow in the broken phase

In the broken phase the mass of the scalar  $m_\sigma$  scales in the same way as the dynamical fermion mass. Hence we assume that in the chiral limit ( $m_0 \rightarrow 0$ ) the dynamical mass  $m_{\text{dyn}} \sim \Sigma_0$  is related to some physical mass scale and thus independent of the UV cutoff  $\Lambda$ . The dynamical mass is given by the scaling law (3.41), so we assume that

$$\Lambda \frac{dm_{\text{dyn}}}{d\Lambda} = 0. \quad (3.93)$$

Since in the broken phase  $m_{\text{dyn}} \neq 0$ , we get

$$\Lambda \frac{dm_{\text{dyn}}}{d\Lambda} = m_{\text{dyn}} \left[ 1 + \frac{\beta_g(g_0, \alpha_0)}{2\Delta g_0(\Delta g_0 + \omega)} \right], \quad (3.94)$$

where the  $\beta$ -function of  $g_0$  is defined in Eq. (3.83). The left-hand side is zero, so this gives the following condition for the  $\beta$ -function in the broken phase ( $\Delta g_0 > 0$ ):

$$\beta_g(g_0, \alpha_0) = -2\Delta g_0(\Delta g_0 + \omega). \quad (3.95)$$

An additional fine-tuning condition is that the bare mass  $m_0$  is supposed to be much smaller than the dynamically generated mass  $m_{\text{dyn}}$ ,

$$m_0 \ll m_{\text{dyn}} \sim \Sigma_0 \ll \Lambda. \quad (3.96)$$

An expression for the anomalous dimension  $\gamma_m$  of the mass operator  $\bar{\psi}\psi$  which is defined in Eq. (3.87), can be obtained by differentiating Eq. (3.29) with respect to  $\Lambda$  and assuming the fine-tuning condition (3.96). We obtain

$$\begin{aligned} \frac{dm_0}{d\Lambda} &= -\Delta g_0 C(\omega) \left( \frac{\Sigma_0}{\Lambda} \right)^{2-\omega} \left[ \frac{\beta_g(g_0, \alpha_0)}{\Delta g_0} - (1 - \omega) \right] \\ &+ (\Delta g_0 + \omega) D(\omega) \left( \frac{\Sigma_0}{\Lambda} \right)^{2+\omega} \left[ \frac{\beta_g(g_0, \alpha_0)}{\Delta g_0 + \omega} - (1 + \omega) \right]. \end{aligned} \quad (3.97)$$

Using now the equation for the  $\beta$ -function Eq. (3.95) we get, for the anomalous dimension in the broken phase,

$$\gamma_m = 1 + \omega + 2\Delta g_0, \quad (3.98)$$

near the critical curve.

### 3.7.2 RG flow in the symmetric phase

In the symmetric phase ( $\Delta g_0 < 0$ ), the only scale besides the UV cutoff and the bare mass  $m_0$  is the scale set by the mass and width of the scalar and pseudoscalar resonances, *i.e.*  $|m_\sigma| = |m_\pi|$  the absolute value of the complex mass pole of  $\Delta_S$ . The mass and the width of the scalar and pseudoscalar resonances (analogous of the correlation length in the symmetric phase) should be considered as the physical mass scales which in principle can be obtained from experiment. We set  $\mu \sim |m_\sigma|$ .

The fine-tuning condition or RG flow of the bare four-fermion coupling  $g_0$  in the symmetric phase is obtained from the condition

$$0 = \Lambda \frac{d}{d\Lambda} \left[ \left( \frac{\Lambda}{\mu} \right)^{2\omega} \left( \frac{1}{g_0} - \frac{1}{g_c} \right) \right] = -\Lambda \frac{d}{d\Lambda} \left[ \frac{\Delta g_0}{g_0 g_c} \left( \frac{\Lambda}{\mu} \right)^{2\omega} \right], \quad (3.99)$$

where  $\mu$  is some infrared renormalization scale related to  $m_\sigma$  (by definition independent of  $\Lambda$ ). We assume also that the scale of the bare mass is much smaller than the physical infrared scale  $\mu$ , thus in the chiral limit,  $\mu \gg m_0$ . At the moment the fine-tuning condition seems a bit arbitrary, however in the next chapter when we explicitly renormalize the scalar propagator in the symmetric phase, the fine-tuning condition (3.99) turns out to be quite natural.

Thus Eq. (3.99) gives the RG flow or the  $\beta$ -function in the symmetric phase

$$\beta_g(g_0, \alpha_0) = -2\omega \frac{g_0}{g_c} \Delta g_0. \quad (3.100)$$

The anomalous dimension follows from Eq. (3.29) under the assumption that

$$-\Delta g_0 \sim (\mu/\Lambda)^{2\omega} \gg (\Sigma_0/\Lambda)^{2\omega}, \quad (3.101)$$

since  $\Sigma_0$  is the fermion mass in the symmetric phase which vanishes in the chiral limit, thus  $\Sigma_0 \rightarrow 0$  when  $m_0 \rightarrow 0$ . We get

$$\frac{m_0}{\Lambda} \approx -\Delta g_0 C(\omega) (\Sigma_0/\Lambda)^{2-\omega}. \quad (3.102)$$

Differentiating with respect to  $\Lambda$  and using Eq. (3.100) gives

$$\gamma_m = 1 - \omega + 2\omega \frac{g_0}{g_c}. \quad (3.103)$$

At the critical line  $g_0 = g_c = (1 + \omega)^2/4$  the anomalous dimension is

$$\gamma_m = 1 + \omega, \quad \Delta g_0 = 0. \quad (3.104)$$

The expression for  $\gamma_m$  in the broken phase were firstly obtained by Miransky and Yamawaki [21]. Later it was shown by Kikukawa and Yamawaki [108] in  $d < 4$  dimensional NJL models and by Kondo *et al.* [39] that the anomalous dimension is continuous (but in fact non-analytic) across the critical curve, by identifying the fine tuning of  $g_0$ .

## 3.8 Lattice simulations of strong coupling QED

Lattice simulations of strong coupling QED and the GNJL models are usually performed in the noncompact formulation, (*i.e.*, the gauge fields are noncompact). In such a formulation the pure gauge sector is free of topological excitations. The main reason for using the noncompact formulation of the gauge group is the observation that it appears to have a second order chiral phase transition [38], whereas the compact formulation exhibits a first order chiral phase transition [109]. The latter, therefore, is not a realistic candidate for a relativistic continuum quantum field theory.

The scaling law with essential singularity (Miransky scaling) at the critical coupling  $\alpha_0 = \alpha_c$  has been studied by Kogut *et al.* [110, 111]. However later simulations questioned the existence of Miransky scaling on the lattice, see for instance the discussion in [23] and [92].

Early studies of strong QED with four-fermion coupling on the lattice were done by [23, 112]. The conclusions of [23] are in agreement with [24]; the critical exponents have nonmean field values and satisfy hyperscaling in the intermediate region ( $0 < \alpha_0 < \alpha_c$ ) (in quenched approximation). Furthermore it was argued in [23] that from the RG point of view it is essential that the critical exponent  $\gamma = 1$ . It means one has the factorization  $\eta_{(\bar{\psi}\psi)^2} = 2\eta_{(\bar{\psi}\psi)}$ . Hence the anomalous dimension of the operator  $(\bar{\psi}\psi)^2$  is twice the anomalous dimension of the mass operator  $\bar{\psi}\psi$ . A renormalization of the chiral condensate simultaneously renormalizes the propagators  $\Delta_S$  and  $\Delta_P$ . Indeed the lattice computations of the critical exponent  $\gamma$  reported in [23, 112] showed strong evidence for  $\gamma = 1$ .

Moreover it was argued that it is natural for the lattice-regulated form of QED to incorporate four-fermion interactions. The Illinois group ([23, 112]) obtained a critical point  $(0.44\alpha_c, 0.76)$  in the  $(\alpha_0, g_0)$  plane, which fits nicely on the critical line Eq. (3.46). However it was not possible at that time to investigate with lattice simulations the phase transition along the critical line.

Later, the GNJL model was studied on the lattice in noncompact formulation using some mean field approach for the fermions, by Azcoiti *et al.* [92]. They obtained a critical line qualitatively similar to the SDE approach Eq. (3.46), and nonmean field critical exponents.

Studies of the compact GNJL model [113] (with torus topology) showed to have both a first order transition as well a second order phase transition similar to the continuous transition in the noncompact formulation [92, 113]. Also in these studies ([92]) it was shown that the critical exponents have nonmean field values and satisfy hyperscaling.

Simulations of noncompact full (unquenched) QED on the lattice (with flavors,  $N = 2$  and  $N = 4$ ) are controversial [114]. The Illinois group [115, 116] (see also [117, 118]) and the Zaragoza group [119, 120], find power-law scaling and nonmean field critical exponents, signaling a possible nontrivial continuum limit for the strong coupling broken phase, whereas [121, 122, 114] obtain mean field behavior (mean field critical exponents with logarithmic corrections). Thus Göckeler *et al.* find a vanishing renormalized gauge coupling and a vanishing effective Yukawa coupling (defined by the Goldberger–Treiman relation), and they conclude that lattice QED is trivial, see for their most recent result Ref. [123].

The authors of [124, 115, 116] found indications that monopole condensation and chiral symmetry transitions were coincident. These results suggested that theories of fundamental charges and monopoles provide a natural scenario for nontrivial ultraviolet behavior. However later analysis of [125] and the discussion in [126] put in doubt the initial ideas on the role of monopole condensation driving the chiral

phase transition.

In [94] it was argued that the triviality of  $\lambda\phi^4$  theory cannot be a good guide to understanding the possible triviality of the pure NJL or spinor QED. The main reason is that the Nambu-Goldstone bosons in models with fundamental fermions which undergo (dynamical) chiral symmetry breaking are composite, and their propagators have a large anomalous dimension, whereas they are fundamental in theories with scalars that exhibit a magnetic type of phase transition, and the anomalous dimension is small. The consequence is the following. Although both the NJL model and  $\lambda\phi^4$  theory violate hyperscaling due to the appearance of logarithmic corrections, and hence are trivial, the bounds on the critical exponents are different. In NJL type of models the logarithmic violations reduce the critical exponent  $\delta$  below its mean field value  $\delta < 3$ , whereas in scalar models the critical exponent exceeds its mean field value  $\delta > 3$ . Such logarithmic violations<sup>10</sup> of scaling and the direction of violation were tested in [127], and [128].

Studies of unquenched QED or GNJL model in the continuum (both analytic and numerical studies), see Refs. [129, 130, 131], commonly use a one-loop vacuum polarization in the SDE for the fermion propagator and gap equation. The effect of the inclusion of screening effects on the phase transition is that instead of the scaling law with essential singularity, the scaling appears to be of the mean field type, as one would expect for a trivial theory (With a one-loop vacuum polarization incorporated QED is shown to be explicitly trivial).

### 3.9 Beyond the ladder approximation

In the previous section we have pointed out the qualitative agreement of the SD quenched-ladder approximation with the quenched lattice simulations. But we would like to mention other attempts to study the gap equation beyond the ladder approximation in framework of the SD approach. In Refs.[132, 133] the validity of the ladder approximation is analyzed by including the effects of *e.g.* crossed photon exchange graphs. Moreover, Holdom [133] gives strong arguments that the scaling law for the fermion dynamical mass  $m_{\text{dyn}}$  in the quenched theory (including also crossed photon graphs, and vertex corrections) is of the same form as the scaling law obtained in the quenched-ladder approximation given by Eq. (3.45). This is analogous to the statement that the anomalous dimension is one ( $\gamma_m = 1$ ) in quenched QED.

In addition, the nonperturbative renormalization group methods (NPRG) of Refs. [41, 132] provide a way to check the quenched-ladder approximation in the GNJL model by including the effect of crossed photon exchange graphs, and four-fermion interactions in the RG flow of coupling constants. The basic principle of the NPRG methods is to write down the equation for the so-called shell-mode

---

<sup>10</sup>Logarithmic scaling is rather complicated to investigate on the lattice due to the finiteness of the system.

effective action, which follows from varying the cutoff of the Wilsonian effective action, see *e.g.* Eq. (1.55). In principle the NPRG method is exact, but unsolvable in practice, since it involves the computation of the RG flows of an infinite set of operators and couplings. The systematic approximation is to write down the NPRG equations for a suitable finite set of local operators, which is called the local potential approximation (LPA). The next step is that the solutions obtained in the LPA have to be checked for stability with respect to enlargement of the set of operators.

In Ref. [134] the critical line in the full quenched GNJL model is obtained in a particular LPA, which incorporates besides crossed photon exchange graphs also four-fermion exchanges beyond the mean field approach. The equation for the critical line obtained by Aoki *et al.* reads

$$g_c(\alpha_0) = \frac{1}{3} \left( 1 + \sqrt{1 - \frac{\alpha_0}{\alpha_c}} \right)^2, \quad (3.105)$$

and in comparison with Eq. (3.46) the difference is just an overall factor  $3/4$ . Thus these studies support the reliability of the ladder approximation. Moreover in Ref. [134] it is shown that the critical exponents agree rather well with the quenched-ladder results for small values of  $\alpha_0$ . However, for values of the gauge coupling  $\alpha_0$  close to the CPT point  $\alpha_0 = \alpha_c$ , a small quantitative difference in the values of the critical exponents emerges.

Let us mention some other attempts to study D $\chi$ SB in quenched QED beyond the ladder approximation. In Refs. [135, 136, 137, 138, 139, 140] various Ansätze for the photon-fermion vertex have been constructed and analyzed. The main motivation for the construction of such Ansätze is the formulation of a gauge independent approach to D $\chi$ SB. In the ladder approximation the full photon-fermion vertex is approximated by the bare vertex and the approximation is believed to be reliable only in Landau gauge  $\xi = 0$ . Since, there, the gauge-dependent anomalous dimension of the fermion wave function  $\mathcal{Z}$  (Eq. (2.24)) vanishes, and  $\mathcal{Z} = 1$ . Consequently the WTI for the photon-fermion vertex, Eq. (2.50), is satisfied asymptotically, *i.e.* for momenta  $|p| \gg |m_{\text{dyn}}|$ . Two crucial constraints on the vertex Ansätze are the WTI and power-law behavior for the fermion wave function. The power-law behavior for  $\mathcal{Z}$  is motivated and derived from the multiplicative renormalizability of perturbation theory for arbitrary gauge-parameters  $\xi$ .

## Chapter 4

# Scalar composites in the symmetric phase

### 4.1 Introduction

In the ladder approximation, and using the Hartree-Fock (mean field) approximation for the four-fermion coupling it has been shown [96, 97, 104, 39] that the GNJL model in four dimensions is indeed renormalizable, and that the anomalous dimension of  $\bar{\psi}\psi$  is large, turning the formally irrelevant four-fermion operators into relevant operators. Fine-tuning the coupling  $g_0$  to  $g_c$  in  $S\chi SB$  phase in such a way that  $m_d/\Lambda \ll 1$ , where  $m_d \equiv \Sigma(0)$  is the dynamical mass of a fermion, a nontrivial continuum limit ( $m_d/\Lambda \rightarrow 0$ ) can be reached just as in pure quenched QED [87, 10, 11, 89]. The spectrum of such a theory contains pseudoscalar ( $\pi$ ) and scalar ( $\sigma$ ) bound states which become light and dynamically active in the vicinity of the critical line. Since the phase transition is second order along the part Eq. (3.46) of the critical curve, scalar and pseudoscalar resonances have been shown to be produced on the symmetric side of the curve, whose masses approach zero as the critical curve is approached [22]. The resonances are of the Breit-Wigner type (see section 2.3) and described by a complex pole (on a second Riemann sheet) in their respective propagators.

The part of the critical curve, Eq. (3.47), with  $\alpha_0 = \alpha_c$  is rather special. For example, an abrupt change of the spectrum of light excitations occurs when the line  $\alpha_0 = \alpha_c$ ,  $g_0 < 1/4$  is crossed: while light scalar and pseudoscalar excitations still persist in the broken phase, there are no such light excitations in the symmetric phase [104, 105]. A similar behavior has been revealed also in  $\text{QED}_3$  [99]. This peculiar phase transition was referred to as a conformal phase transition (CPT) [27].

In this chapter we study scalar composites ( $\sigma$  and  $\pi$  bosons) in the symmetric

$$\text{---} \circledS \text{---}^{-1} = \text{---} \text{---}^{-1} - \text{---} \text{---} \text{---} \text{---} \text{---}$$


Figure 4.1: The SDE for the scalar propagator  $\Delta_S(p)$ .

$$\begin{array}{c} \text{Diagram 1} \\ \text{Diagram 2} \\ \text{Diagram 3} \end{array}$$

Figure 4.2: The SDE for the scalar vertex  $\Gamma_S(p+q, p)$ . The shaded circle with the 2 represents the two-fermion one-boson irreducible fermion-fermion scattering kernel.

phase of the GNJL model. Computing the scalar propagator, see Eqs. (2.25)–(2.26) and Fig. 4.1, requires knowledge of the full scalar-fermion-antifermion vertex  $\Gamma_S(p + q, p)$  (the Yukawa vertex) which in turn satisfies the Bethe-Salpeter (BS) equation 2.40 and is displayed in Fig. 4.2. We solve this BS equation in the ladder approximation (Fig. 4.3) but differ from the corresponding studies in Refs. [39, 22] who used an approximation for  $\Gamma_S(p + q, p)$  with zero boson momentum ( $q = 0$ ). A technique of expansion in Chebyshev polynomials is introduced for solving the Yukawa vertex with nonzero boson momentum and consequently an explicit analytical expression is derived for the propagator of the  $\sigma$  boson valid along the entire critical curve. Our main physical conclusions are the same as in Refs. [104, 22, 105]: in the region  $\alpha_0 < \alpha_c$ ,  $g_0 > 1/4$ , in the symmetric phase, a spectrum of light resonances exists while at  $\alpha_0 < \alpha_c$ ,  $g_0 < 1/4$  there are no light resonances. Having

$$\begin{array}{c} \text{Diagram 1} \\ \hline
 \text{Diagram 2} = \text{Diagram 3} + \text{Diagram 4}
 \end{array}$$

Figure 4.3: The SDE for the scalar vertex in the quenched-ladder approximation.

obtained an analytical expression for the scalar propagator, we can analytically continue it into the region  $\alpha_0 > \alpha_c$  and find light tachyons there, signaling the instability of the symmetric solution.

The plan of the present chapter is as follows. First we solve the equation for the Yukawa vertex with nonzero boson momentum in section 4.2 keeping only the zero order Chebyshev harmonics. In section 4.3 we obtain an analytical expression for the  $\sigma$  boson propagator valid along the entire critical line and analyze its behavior in different asymptotical regimes. Section 4.4 is devoted to comparing our results for the Yukawa vertex and boson propagator with the corresponding ones in Refs. [39, 22]. In section 4.5 we discuss the behavior of the scalar propagator near the critical line (3.46) in the symmetric phase and, in particular, the mass and the width of resonances. The analysis of the scalar composites near the critical line (3.47) is given in section 4.6, where we show the absence of light excitations at  $\alpha_0 \leq \alpha_c$  while analytically continuing the symmetric phase propagator into the region  $\alpha_0 \geq \alpha_c$  leads to the appearance of tachyonic states. We discuss this behavior from the viewpoint of the CPT conception proposed in Ref. [27] and section 4.6. A summary is given in section 4.8 and in appendix D we give an analysis of the contribution of higher order Chebyshev harmonics into the Yukawa vertex equation and scalar vacuum polarization. The results of this chapter were published in Ref. [40].

## 4.2 Scalar vertex in quenched-ladder approximation

In this section we discuss the SDEs for the scalar propagator and the scalar vertex in the well-known quenched-ladder approximation and introduce an approximation scheme for solving the SDE for the scalar vertex. For the time being we consider one flavor of fermions,  $N = 1$ . Then the SDE for  $\sigma$  boson reads

$$\Delta_S^{-1}(p) = -\frac{1}{G_0} + \Pi_S(p^2), \quad (4.1)$$

where the scalar vacuum polarization  $\Pi_S(q^2)$  is given by

$$\Pi_S(p^2) = i \int_{\Lambda} \frac{d^4 k}{(2\pi)^4} \text{Tr} [S(k+p)\Gamma_S(k+p, k)S(k)], \quad (4.2)$$

and for the Yukawa vertex  $\Gamma_S$  we have

$$\begin{aligned} -i\Gamma_{Sab}(p+q, p) &= (-i\mathbf{1})_{ab} + \int_{\Lambda} \frac{d^4 r}{(2\pi)^4} [iS(r+q)(-i)\Gamma_S(r+q, r)iS(r)]_{dc} \\ &\times (-ie_0^2)K_{cd,ab}^{(2)}(r, r+q, p+q) \end{aligned} \quad (4.3)$$

(see Fig. 4.2), and where  $\Lambda$  is the UV cutoff. We recall that in the symmetric phase of the GNJL the pseudoscalar and scalar propagators are degenerate, so are the pseudoscalar vertex and scalar vertex.

The ladder approximation is obtained by replacing the Bethe-Salpeter kernel  $K^{(2)}$  of Eq. (B.28) by the one photon exchange graph,

$$(-ie_0^2)K_{ab,cd}^{(2)}(k,p,p+q) = (-ie_0)\gamma_{cb}^\lambda iD_{\lambda\sigma}(q)(-ie_0)\gamma_{ad}^\sigma. \quad (4.4)$$

Furthermore the photon propagator is considered as quenched, *i.e.*, vacuum polarization effects are turned off, and thus the gauge coupling does not run (as explained earlier), we again assume

$$\beta_\alpha(\alpha_0) \approx 0. \quad (4.5)$$

In principle the Bethe-Salpeter kernel also contains scalar and pseudoscalar exchanges. One question is whether such exchanges can be neglected, this question will be addressed in the next chapter. The answer not only depends on the short-distance behavior of the full scalar propagators and Yukawa vertex which we will try to solve in this chapter, but also on the representation of the chiral symmetry. In the next chapter we will argue that, provided scalars and pseudoscalars are considered both in the adjoint representation of the chiral symmetry, the neglect of scalar and pseudoscalar exchanges in the kernel  $K^{(2)}$  seems reasonable for the SDE for the Yukawa vertices  $\Gamma_S$  and  $\Gamma_P$ . Hence we will treat the four-fermion interactions again in the Hartree-Fock approximation, a sort of mean field approach, and postpone discussions of validity and self-consistency to the chapter 5.

The SDE equation for the scalar vertex in the ladder approximation can be written as

$$\begin{aligned} \Gamma_S(p+q,p) &= \mathbf{1} + ie_0^2 \int_\Lambda \frac{d^4r}{(2\pi)^4} \\ &\times \gamma^\lambda S(r+q)\Gamma_S(r+q,r)S(r)\gamma^\sigma D_{\lambda\sigma}(r-p) \end{aligned} \quad (4.6)$$

(see Fig. 4.3). The SDE for the scalar propagator, Eq. (4.2), is left unchanged. In the symmetric phase, the equation for the scalar vertex, Eq. (4.6), is a self-contained equation, if we note that in the Landau gauge the fermion propagator is  $S(p) = 1/\hat{p}$ . We recall that in the Landau gauge the ladder approximation respects the chiral and vector Ward-Takahashi identities. The SDEs in ladder approximation for scalar propagator and vertex, Eqs. (4.2) and (4.6), have been studied extensively in the literature [39, 22, 141, 142, 98], but mainly for the case of zero-transfer boson momentum ( $q = 0$ ).

In what follows, we present a method for solving the scalar vertex with nonzero boson momentum. The starting point is a general structure of the scalar vertex and pseudoscalar vertex. The scalar and pseudoscalar vertices in momentum space can be decomposed over four spinor structures with dimensionless scalar functions as

given in Eqs. (2.42) and (2.43). In the symmetric phase, the scalar and pseudoscalar vertex functions coincide, *i.e.*, we set  $F_i \equiv F_i^{(s)} = F_i^{(p)}$ ,  $i = 1, 2$ . The straightforward consequence is that the scalar and pseudoscalar propagators are also identical (degenerate) in the symmetric phase, just a reflection of the chiral symmetry. Thus we have the structure

$$\Gamma_S(p+q, p) = \mathbf{1} [F_1 + (\hat{q}\hat{p} - \hat{p}\hat{q}) F_2 + (\hat{p} + \hat{q}) F_3 + \hat{p} F_4]. \quad (4.7)$$

Furthermore, because of the absence of a dynamical mass in the symmetric phase, the equations for the scalar functions  $F_3$  and  $F_4$  decouple from the equations for  $F_1$  and  $F_2$ . Moreover,  $F_3$  and  $F_4$  do not contribute in scalar and pseudoscalar vacuum polarizations. In fact the integral equations for these functions are homogeneous ones and in the symmetric phase we can always take the solution  $F_3 = F_4 = 0$  which is a consistent one.

So the problem is reduced to solving a coupled set of integral equations for two scalar functions  $F_1, F_2$ , which has the form (after making a standard Wick rotation [143])

$$F_i(p+q, p) = \delta_{i1} + \lambda_0 \sum_{j=1}^2 \int_{\Lambda} dr^2 \int \frac{d\Omega_r}{2\pi^2} K_{ij}(p, q, r) F_j(r+q, r), \quad i = 1, 2, \quad (4.8)$$

where  $\lambda_0 = 3\alpha_0/4\pi$ , and

$$K_{11}(p, q, r) = \frac{(r^2 + q \cdot r)}{(r+q)^2(r-p)^2}, \quad (4.9)$$

$$K_{12}(p, q, r) = \frac{2[(q \cdot r)^2 - r^2 q^2]}{(r+q)^2(r-p)^2}, \quad (4.10)$$

$$K_{21}(p, q, r) = \frac{1}{6} \frac{\kappa(p, q, r)}{(r+q)^2(r-p)^4[(p \cdot q)^2 - p^2 q^2]}, \quad (4.11)$$

$$K_{22}(p, q, r) = \frac{1}{3} \frac{\kappa(p, q, r)(r^2 + q \cdot r)}{(r+q)^2(r-p)^4[(p \cdot q)^2 - p^2 q^2]}, \quad (4.12)$$

with

$$\begin{aligned} \kappa(p, q, r) = & p^2 p \cdot r q^2 - p^2 p \cdot q q \cdot r - 2p \cdot q p \cdot r q \cdot r + 2p^2 (q \cdot r)^2 \\ & + 2(p \cdot q)^2 r^2 - 2p^2 q^2 r^2 + p \cdot r q^2 r^2 - p \cdot q q \cdot r r^2, \end{aligned} \quad (4.13)$$

and  $\int d\Omega_r$  denotes the usual angular part of the four-dimensional integration.

The SDE for Yukawa vertex is quite similar to a Bethe-Salpeter equation (BSE) for bound state wave function  $\chi$  ( $\chi \sim S\Gamma_S S$ ). The essential difference of course is that the SDE for  $\Gamma_S$  is an inhomogeneous equation, whereas the homogeneous BSE describing bound states is an eigenvalue equation.

The equations (4.8) are still very complicated due to the fact that the angular part of the integration cannot be performed in explicit form, since the angular dependence of the Yukawa vertex is unknown. Without any further approximations it seems impossible to solve the equations analytically. Our primary interest is the scalar propagator defined by the vacuum polarization Eq. (4.2). The equation for the scalar vacuum polarization is

$$\Pi_S(q^2) = \frac{1}{4\pi^2} \int_0^{\Lambda^2} dk^2 \int \frac{d\Omega_k}{2\pi^2} \left[ A_1(k, q) F_1(k+q, k) + A_2(k, q) F_2(k+q, k) \right], \quad (4.14)$$

where

$$A_1(k, q) \equiv \frac{k^2 + k \cdot q}{(k+q)^2}, \quad A_2(k, q) \equiv \frac{2[(k \cdot q)^2 - k^2 q^2]}{(k+q)^2}. \quad (4.15)$$

The method to tackle the angular dependence is to expand in terms of Chebyshev polynomials of the second kind  $U_n(x)$ , a method which was used before, for instance in Ref [10].

We define the following Chebyshev expansions. For the vertex function  $F_1$  and  $F_2$  we define

$$F_1(p+q, p) = \sum_{n=0}^{\infty} f_n(p^2, q^2) U_n(\cos \alpha), \quad (4.16)$$

$$F_2(p+q, p) = \sum_{n=0}^{\infty} g_n(p^2, q^2) U_n(\cos \alpha), \quad (4.17)$$

for the kernels of the  $\Pi_S$ , Eq. (4.15)

$$A_1(p, q) = \sum_{n=0}^{\infty} a_n(p^2, q^2) U_n(\cos \alpha), \quad (4.18)$$

$$A_2(p, q) = \sum_{n=0}^{\infty} b_n(p^2, q^2) U_n(\cos \alpha), \quad (4.19)$$

and for the kernels, Eqs. (4.9)–(4.12)

$$K(p, q, r) = \sum_{n,m,l=0}^{\infty} K_{nml}(p^2, q^2, r^2) U_n(\cos \alpha) U_m(\cos \beta) U_l(\cos \gamma), \quad (4.20)$$

where

$$\cos \alpha = \frac{p \cdot q}{pq}, \quad \cos \beta = \frac{p \cdot r}{pr}, \quad \cos \gamma = \frac{q \cdot r}{qr} \quad (4.21)$$

(for the coefficients  $K_{nml}(p^2, q^2, r^2)$  see appendix D). After that the angular integration can be done explicitly leading to an infinite chain of equations for harmonics  $f_n(p^2, q^2)$  and  $g_n(p^2, q^2)$ . The important thing is that only the harmonics  $f_0$  contains an inhomogeneous term in the equation for it (the constant 1 in Eq. (4.8)), while other harmonics can be found iteratively once  $f_0$  is computed. In other words, for the vertex function  $F_1$  the scale is set by the bare vertex, *i.e.*, such a function has nonhomogeneous ultraviolet boundary conditions. For the vertex function  $F_2$  there is no such inhomogeneous term other than given indirectly by the coupling to vertex function  $F_1$ .

We assume that the scalar vertex function  $F_1(p + q, p)$  depends only weakly on the angle between fermion and scalar-boson momentum  $p \cdot q$ , so that an infinite set of equations for  $f_n$  and  $g_n$  is replaced by the equation for the zeroth-order Chebyshev coefficient function  $f_0$  which we shall solve exactly. The main approximation is to replace the Yukawa vertex by the angular average of the vertex function  $F_1$ ,

$$\Gamma_S(p + q, p) \approx \mathbf{1} \int \frac{d\Omega_p}{2\pi^2} F_1(p + q, p) = \mathbf{1} f_0(p^2, q^2), \quad (4.22)$$

since Chebyshev polynomials of the second kind are precisely orthogonal with respect to such integration. Then we write

$$f_0(p^2, q^2) \equiv F_{\text{IR}}(p^2, q^2)\theta(q^2 - p^2) + F_{\text{UV}}(p^2, q^2)\theta(p^2 - q^2). \quad (4.23)$$

The functions  $F_{\text{IR}}$  and  $F_{\text{UV}}$  are respectively referred to as the IR channel (infrared), and the UV channel (ultraviolet).

If the scalar vertex indeed weakly depends on angle between scalar-boson and fermion momentum  $p$  flowing through the Yukawa vertex, these channel functions should have the limits

$$\lim_{p^2 \gg q^2} \Gamma_S(p + q, p) = \mathbf{1} \lim_{p^2 \gg q^2} F_{\text{UV}}(p^2, q^2), \quad (4.24)$$

$$\lim_{q^2 \gg p^2} \Gamma_S(p + q, p) = \mathbf{1} \lim_{q^2 \gg p^2} F_{\text{IR}}(p^2, q^2), \quad (4.25)$$

*i.e.*, the asymptotics of the scalar vertex are independent of the angle between  $p$  and  $q$ . Hence the UV channel contains a limit of the Yukawa vertex with the boson momentum  $q$  that is much smaller than both fermion momenta ( $q \ll p$ ), and the IR channel contains a limit of the vertex with the fermion momentum  $p$  that is much smaller than the boson momentum ( $q \gg p$ ). The connection between the Yukawa vertex  $\Gamma_S$  and these two channel functions is illustrated in Fig. 4.4.

The expansion in Chebyshev polynomials is discussed in detail in appendix D. Moreover, the error, due to our approximation, Eq. (4.22), in the computation of the scalar vacuum polarization, is estimated in that appendix.

The zeroth-order Chebyshev or the two channel approximation of Eq. (4.23)

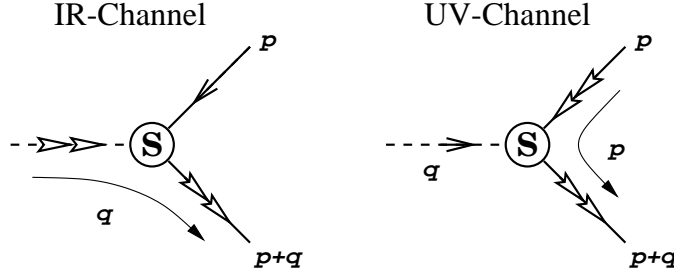


Figure 4.4: The two-channel approximation.

gives the following equation for the vertex function  $f_0(p^2, q^2)$ :

$$f_0(p^2, q^2) = 1 + \lambda_0 \int_0^{\Lambda^2} dr^2 N_0(r^2, p^2) a_0(r^2, q^2) f_0(r^2, q^2), \quad (4.26)$$

where

$$N_0(r^2, p^2) = \frac{\theta(r^2 - p^2)}{r^2} + \frac{\theta(p^2 - r^2)}{p^2} \quad (4.27)$$

and

$$a_0(r^2, q^2) = \frac{1}{2} \left[ \left( 2 - \frac{q^2}{r^2} \right) \theta(r^2 - q^2) + \frac{r^2}{q^2} \theta(q^2 - r^2) \right] \quad (4.28)$$

(see also appendix D). The equation for the scalar vacuum polarization in this approximation Eq. (4.14) takes the form

$$\Pi_S(q^2) = \frac{1}{4\pi^2} \int_0^{\Lambda^2} dk^2 a_0(k^2, q^2) f_0(k^2, q^2). \quad (4.29)$$

With the Eqs. (4.27) and (4.28) for  $N_0$  and  $a_0$ , respectively, and the definition of the channel functions Eq. (4.23), we get two coupled integral equations for the IR-UV channels:

$$(s < t) \quad F_{\text{IR}}(s, t) = 1 + \lambda_0 \int_0^s du \frac{u}{2st} F_{\text{IR}}(u, t) + \lambda_0 \int_s^t du \frac{1}{2t} F_{\text{IR}}(u, t)$$

$$+ \lambda_0 \int_t^{\Lambda^2} du \frac{2u-t}{2u^2} F_{UV}(u, t), \quad (4.30)$$

$$(s > t) \quad F_{UV}(s, t) = 1 + \lambda_0 \int_0^t du \frac{u}{2st} F_{IR}(u, t) + \lambda_0 \int_t^s du \frac{2u-t}{2su} F_{UV}(u, t) \\ + \lambda_0 \int_s^{\Lambda^2} du \frac{2u-t}{2u^2} F_{UV}(u, t), \quad (4.31)$$

where  $s = p^2$ ,  $t = q^2$ , and  $u = r^2$ . For the vacuum polarization, Eq. (4.29), we obtain the equation

$$\Pi_S(t) = \frac{1}{4\pi^2} \left[ \int_0^t du \frac{u}{2t} F_{IR}(u, t) + \int_t^{\Lambda^2} du \frac{2u-t}{2u} F_{UV}(u, t) \right], \quad t = q^2. \quad (4.32)$$

Using Eq. (4.31) with  $s = \Lambda^2$  provides a simple relation between the vacuum polarization and the UV-channel function

$$\Pi_S(q^2) = \frac{\Lambda^2}{4\pi^2} \frac{1}{\lambda_0} [F_{UV}(\Lambda^2, q^2) - 1], \quad (4.33)$$

which is different from the functional form proposed in Ref. [39].

The integrals equations for  $F_{IR}$  and  $F_{UV}$  are equivalent to two second order differential equations with four appropriate boundary conditions. We get for the IR channel:

$$s^2 \frac{d^2}{ds^2} F_{IR}(s, t) + 2s \frac{d}{ds} F_{IR}(s, t) + \frac{\lambda_0}{2t} s F_{IR}(s, t) = 0, \quad (4.34)$$

and for the UV channel

$$s^2 \frac{d^2}{ds^2} F_{UV}(s, t) + 2s \frac{d}{ds} F_{UV}(s, t) + \lambda_0 \frac{2s-t}{2s} F_{UV}(s, t) = 0. \quad (4.35)$$

The infrared and ultraviolet boundary conditions (IRBC), respectively, (UVBC) are

$$\left[ s^2 \frac{d}{ds} F_{IR}(s, t) \right]_{s=0} = 0, \quad \left[ F_{UV} + s \frac{d}{ds} F_{UV} \right]_{s=\Lambda^2} = 1. \quad (4.36)$$

Moreover we get a continuity and differentiability equation at  $s = t$

$$F_{IR}(t, t) = F_{UV}(t, t), \quad \left. \frac{d}{ds} F_{IR}(s, t) \right|_{s=t} = \left. \frac{d}{ds} F_{UV}(s, t) \right|_{s=t}. \quad (4.37)$$

The differential equations can be solved straightforwardly. The equation for  $F_{\text{IR}}$  can be written as a Bessel equation, and the equation for  $F_{\text{UV}}$  as a modified Bessel equation (see Ref. [144] for mathematical details). The general solutions of the differential equations are

$$\begin{aligned} F_{\text{IR}}(s, t) &= c_3(t/\Lambda^2, \omega) \left(\frac{t}{s}\right)^{1/2} J_1\left(\sqrt{2\lambda_0 s/t}\right) \\ &+ c_4(t/\Lambda^2, \omega) \left(\frac{t}{s}\right)^{1/2} Y_1\left(\sqrt{2\lambda_0 s/t}\right), \end{aligned} \quad (4.38)$$

$$\begin{aligned} F_{\text{UV}}(s, t) &= c_1(t/\Lambda^2, \omega) \left(\frac{t}{s}\right)^{1/2} I_{-\omega}\left(\sqrt{2\lambda_0 t/s}\right) \\ &+ c_2(t/\Lambda^2, \omega) \left(\frac{t}{s}\right)^{1/2} I_{\omega}\left(\sqrt{2\lambda_0 t/s}\right), \end{aligned} \quad (4.39)$$

with  $J_1$  and  $Y_1$  the Bessel functions of first and second kind, respectively, and where  $I_{\pm\omega}$  are modified Bessel functions and  $\omega = \sqrt{1 - 4\lambda_0}$ , see also Eq. (3.18). We note that since Eqs. (4.34), (4.35) are scale invariant their solutions are functions of the ratio  $s/t$  and the scale invariance is violated by the UV boundary condition (4.36) only.

The IRBC for the IR channel requires  $c_4(t/\Lambda^2, \omega) = 0$ , since the Bessel function  $Y_n(z)$  is irregular at  $z = 0$ , the other coefficients are fixed by the remaining three boundary conditions and the solutions are

$$c_1(t/\Lambda^2, \omega) = \frac{\pi\gamma(\omega)}{2\sin\omega\pi} Z^{-1}(t/\Lambda^2, \omega), \quad (4.40)$$

$$c_2(t/\Lambda^2, \omega) = c_1(t/\Lambda^2, -\omega), \quad (4.41)$$

$$c_3(t/\Lambda^2, \omega) = Z^{-1}(t/\Lambda^2, \omega), \quad (4.42)$$

where

$$Z(q^2/\Lambda^2, \omega) \equiv \frac{\pi}{2\sin\omega\pi} [\gamma(\omega)G(q^2/\Lambda^2, -\omega) - \gamma(-\omega)G(q^2/\Lambda^2, \omega)], \quad (4.43)$$

and

$$\gamma(\omega) \equiv \sqrt{2\lambda_0} \left[ J_1(\sqrt{2\lambda_0}) I'_{\omega}(\sqrt{2\lambda_0}) + J'_1(\sqrt{2\lambda_0}) I_{\omega}(\sqrt{2\lambda_0}) \right], \quad (4.44)$$

$$G(q^2/\Lambda^2, \omega) \equiv \frac{1}{2} \sqrt{\frac{q^2}{\Lambda^2}} \left[ I_{\omega}\left(\sqrt{\frac{2\lambda_0 q^2}{\Lambda^2}}\right) - \sqrt{\frac{2\lambda_0 q^2}{\Lambda^2}} I'_{\omega}\left(\sqrt{\frac{2\lambda_0 q^2}{\Lambda^2}}\right) \right]. \quad (4.45)$$

Summarizing, the solution of scalar vertex in terms of channel functions is

$$F_{\text{IR}}(p^2, q^2) = Z^{-1}\left(\frac{q^2}{\Lambda^2}, \omega\right) \left(\frac{q^2}{p^2}\right)^{1/2} J_1\left(\sqrt{\frac{2\lambda_0 p^2}{q^2}}\right), \quad (4.46)$$

$$\begin{aligned}
F_{\text{UV}}(p^2, q^2) &= \frac{\pi}{2 \sin \omega \pi} Z^{-1} \left( \frac{q^2}{\Lambda^2}, \omega \right) \left( \frac{q^2}{p^2} \right)^{1/2} \\
&\times \left[ \gamma(\omega) I_{-\omega} \left( \sqrt{\frac{2\lambda_0 q^2}{p^2}} \right) - \gamma(-\omega) I_\omega \left( \sqrt{\frac{2\lambda_0 q^2}{p^2}} \right) \right]. \quad (4.47)
\end{aligned}$$

It is easy to verify that at zero boson momentum one gets

$$\Gamma_S(p, p) \equiv F_{\text{UV}}(p^2, q^2 = 0) = \frac{2}{1 + \omega} \left( \frac{p^2}{\Lambda^2} \right)^{-(1-\omega)/2}, \quad (4.48)$$

which coincides with the zero transfer vertex of Refs. [39, 22]. In the limit of pure NJL model,  $\alpha_0 \rightarrow 0$  ( $\omega \rightarrow 1$ ), the vertex is equal, of course, to the bare vertex,  $\Gamma_S = 1 = F_{\text{UV}} = F_{\text{IR}}$ . To study the vertex at critical gauge coupling  $\alpha_0 = \alpha_c$  ( $\omega = 0$ ) we expand the Bessel functions in small  $\omega$  using the following property of the modified Bessel functions:

$$I_\omega(x(\omega)) \approx I_0(x(0)) - \omega K_0(x(0)) + \mathcal{O}(\omega^2), \quad (4.49)$$

where  $x(\omega) \propto \sqrt{1 - \omega^2}$ . Then the expressions for  $F_{\text{IR}}$ ,  $F_{\text{UV}}$ , Eqs. (4.46), (4.47), take the following form at  $\alpha_0 \rightarrow \alpha_c$ :

$$F_{\text{IR}}(p^2, q^2) = Z^{-1} \left( \frac{q^2}{\Lambda^2}, 0 \right) \left( \frac{q^2}{p^2} \right)^{1/2} J_1 \left( \sqrt{\frac{p^2}{2q^2}} \right), \quad (4.50)$$

$$\begin{aligned}
F_{\text{UV}}(p^2, q^2) &= Z^{-1} \left( \frac{q^2}{\Lambda^2}, 0 \right) \left( \frac{q^2}{p^2} \right)^{1/2} \\
&\times \left[ \epsilon_1 K_0 \left( \sqrt{\frac{q^2}{2p^2}} \right) - \epsilon_2 I_0 \left( \sqrt{\frac{q^2}{2p^2}} \right) \right], \quad (4.51)
\end{aligned}$$

where

$$\begin{aligned}
Z^{-1} \left( \frac{q^2}{\Lambda^2}, 0 \right) &= \frac{1}{2} \left( \frac{q^2}{\Lambda^2} \right)^{1/2} [\epsilon_1 K_0(x) + \epsilon_1 x K_1(x) \\
&\quad - \epsilon_2 I_0(x) - \epsilon_2 x I'_0(x)], \quad (4.52) \\
x &= \sqrt{q^2/2\Lambda^2},
\end{aligned}$$

and where

$$\epsilon_1 = \sqrt{1/2} (J_1(\sqrt{1/2}) I'_0(\sqrt{1/2}) + J'_1(\sqrt{1/2}) I_0(\sqrt{1/2})), \quad (4.53)$$

$$\epsilon_2 = \sqrt{1/2} (J_1(\sqrt{1/2}) K'_0(\sqrt{1/2}) + J'_1(\sqrt{1/2}) K_0(\sqrt{1/2})), \quad (4.54)$$

and  $K_i$  is the modified Bessel function of the third kind. Note that when we expand the UV channel function, ( $p^2 \gg q^2$ ), Eq. (4.51), we get

$$F_{\text{UV}}(p^2, q^2) = 2 \left( \frac{p^2}{\Lambda^2} \right)^{-1/2} \left[ \frac{\epsilon_3 - 2 + \ln(p^2/q^2)}{\epsilon_3 - \ln(q^2/\Lambda^2)} + \mathcal{O}(q^2/p^2 \ln(q^2/p^2)) \right], \quad (4.55)$$

where

$$\epsilon_3 = 2(1 - \gamma) + 3 \ln 2 - 2 \frac{\epsilon_2}{\epsilon_1} \approx 3.2 \quad (4.56)$$

and  $\gamma$  is the Euler gamma. The expression (4.55) is of the same form as obtained in Ref. [39] (their formula (2.88)).

### 4.3 Analytic structure of the scalar propagator

In the previous section we obtained an analytical expression for the scalar vertex by assuming that the vertex only weakly depends on the angle between boson momentum and fermion momentum. The expression for the scalar vacuum polarization in such an approximation takes the form of Eq. (4.32). The main object of investigation is scalar compositeness near the critical line. In the neighborhood of the critical line, the tendency of fermion-antifermion pairs to form bound states under the influence of strong attractive four-fermion forces becomes apparent.

Since we are in the symmetric phase of the GNJL model (there is no dynamical mass), the only important variable is the scalar boson momentum over cutoff  $t = q^2/\Lambda^2$ . Equation (4.32) shows that the vacuum polarization depends only on the UV channel with fermion momentum at  $\Lambda^2$ , Eq. (4.33). Substituting the expressions obtained for the vertex function Eq. (4.39) in the equation for the vacuum polarization Eq. (4.33), we obtain

$$\Pi_S(q^2) = \frac{\Lambda^2}{4\pi^2} \frac{1}{\lambda_0} \left[ \frac{\gamma(\omega)H(q^2/\Lambda^2, -\omega) - \gamma(-\omega)H(q^2/\Lambda^2, \omega)}{\gamma(\omega)G(q^2/\Lambda^2, -\omega) - \gamma(-\omega)G(q^2/\Lambda^2, \omega)} \right], \quad (4.57)$$

where  $\gamma$  and  $G$  are given by Eqs. (4.44) and (4.45), and where

$$H(q^2/\Lambda^2, \omega) \equiv \frac{1}{2} \sqrt{\frac{q^2}{\Lambda^2}} \left[ I_\omega \left( \sqrt{\frac{2\lambda_0 q^2}{\Lambda^2}} \right) + \sqrt{\frac{2\lambda_0 q^2}{\Lambda^2}} I'_\omega \left( \sqrt{\frac{2\lambda_0 q^2}{\Lambda^2}} \right) \right]. \quad (4.58)$$

This expression is valid along the entire critical curve in the symmetric phase. Note that the vacuum polarization is symmetric in  $\omega$  which means that we can analytically continue it to values  $\alpha_0 > \alpha_c$ .

Equation (4.57) is a rather complicated expression, and we will first investigate some specific limits:

- (A) The pure NJL limit, where the gauge interaction is turned off, *i.e.*, the case where  $\alpha_0 = 0$ , thus  $\omega = 1$ .
- (B) Asymptotic behavior of  $\Pi_S$ , the infrared behavior  $q^2/\Lambda^2 \ll 1$  in such a manner, so that  $(q^2/\Lambda^2)^\omega \gg q^2/\Lambda^2$ .
- (C) The behavior at the critical gauge coupling  $\alpha_0 = \alpha_c$ , thus  $\omega = 0$ .
- (D) The behavior of  $\Pi_S$  for  $\alpha_0 > \alpha_c$ ,  $\omega = i\nu$ ,  $\nu = \sqrt{\alpha_0/\alpha_c - 1}$ , *i.e.*, analytic continuation across the critical curve at  $\alpha_0 = \alpha_c$ .

### 4.3.1 The pure NJL limit

The pure Nambu–Jona-Lasinio limit is the case where the gauge interaction is completely turned off, possible bound states in such a model are purely due to the four-fermion interaction. So  $\alpha_0 \rightarrow 0$ , and therefore  $\omega \rightarrow 1$ . The scalar vertex at  $\alpha_0 = 0$  is just equal to the bare vertex,  $\Gamma_S = 1 = F_{UV} = F_{IR}$ . The pure NJL limit can be correctly obtained from Eq. (4.57) by making expansions of the Bessel functions keeping sufficient number of terms, and then performing an expansion in  $(1 - \omega)$  to zeroth order. Hence with  $\alpha_0 = 0$ ,  $\omega = 1$  in Eq. (4.57), we get

$$\Pi_S(q^2) = \frac{\Lambda^2}{4\pi^2} \left[ 1 + \frac{q^2}{2\Lambda^2} \ln \left( \frac{q^2}{\Lambda^2} \right) - \frac{3q^2}{4\Lambda^2} \right]. \quad (4.59)$$

The log term is a consequence of the “hard” fermion loop which also ruins the renormalizability of the pure NJL model.

### 4.3.2 Asymptotic behavior of the $\sigma$ boson vacuum polarization

The asymptotic behavior  $0 < \omega < 1$  so that  $(q^2/\Lambda^2)^\omega \gg q^2/\Lambda^2$  can be obtained by considering first the  $q^2 \ll \Lambda^2$  limit of  $Z$ , Eq. (4.43):

$$Z \approx \frac{\pi}{2 \sin \omega \pi} \sqrt{h(\omega)h(-\omega)(1 - \omega^2)} \left( \frac{q^2}{\Lambda^2} \right)^{1/2} \sinh \left[ \frac{\omega}{2} \ln \left( \frac{\Lambda^2}{q^2} \right) + \delta(\omega) \right], \quad (4.60)$$

where

$$\delta(\omega) \equiv \frac{1}{2} \ln \frac{h(\omega)(1 + \omega)}{h(-\omega)(1 - \omega)} - \omega \ln \sqrt{2\lambda_0}, \quad h(\omega) \equiv \frac{\gamma(\omega)2^\omega}{\Gamma(1 - \omega)}. \quad (4.61)$$

Then the UV-channel function with fermion momentum  $p^2 = \Lambda^2$  can be expressed, in this limit, as

$$F_{UV}(\Lambda^2, q^2) \approx \frac{2}{1 + \omega} + \frac{2\omega}{1 - \omega^2} (1 - \coth y), \quad y = \frac{\omega}{2} \ln \left( \frac{\Lambda^2}{q^2} \right) + \delta(\omega). \quad (4.62)$$

Hence

$$\Pi_S(q^2) \approx \frac{\Lambda^2}{4\pi^2} \left[ \frac{1}{g_c(\omega)} + \frac{8\omega}{(1-\omega^2)^2} (1 - \coth y) \right], \quad q^2 \ll \Lambda^2. \quad (4.63)$$

However, the above expression does not reproduce the correct leading term of the NJL limit ( $\omega \rightarrow 1$ ), for that we should use the expression (4.57). In order to obtain such an expression which contains properly the pure NJL limit, we have to keep more terms in the expansion of  $Z$ . We then get for the scalar vacuum polarization

$$\begin{aligned} \Pi_S(q^2) \approx & \frac{\Lambda^2}{4\pi^2} \left[ \frac{1}{g_c(\omega)} - B(\omega) \left( \frac{q^2}{\Lambda^2} \right)^\omega + A(\omega) \frac{q^2}{\Lambda^2} \right. \\ & \left. + \mathcal{O}((q^2/\Lambda^2)^{2\omega}) + \mathcal{O}((q^2/\Lambda^2)^{1+\omega}) \right], \end{aligned} \quad (4.64)$$

where

$$A(\omega) \equiv \frac{1}{2g_c(\omega)(1-\omega)}, \quad B(\omega) = \frac{16\omega}{(1-\omega^2)^2} \frac{\gamma(-\omega)}{\gamma(\omega)} \frac{\Gamma(2-\omega)}{\Gamma(2+\omega)} \left( \frac{\lambda_0}{2} \right)^\omega. \quad (4.65)$$

For Eq. (4.64) to be valid, it is assumed that  $\omega > 1/2$ . It is straightforward to check that this expression satisfies the NJL limit ( $\omega \rightarrow 1$ ).

This is a suitable point to refer to appendix D for an analysis of the reliability of Eq. (4.64), where it is shown that the leading and next-to-leading terms in  $q^2/\Lambda^2$  of  $\Pi_S$  (*i.e.*, the first two terms on the right-hand side of Eq. (4.64)) are indeed correctly obtained by our approximation, see Eq. (D.36).

### 4.3.3 The $\sigma$ boson at critical gauge coupling

At critical gauge coupling  $\alpha_0 = \alpha_c$  ( $\omega = 0$ ) is the onset of the scalar compositeness originating purely from electromagnetic forces. The expression for  $F_{\text{UV}}$ , Eq. (4.51), has the form at  $\alpha_0 = \alpha_c$

$$\begin{aligned} F_{\text{UV}}(p^2, q^2) = & 2 \left( \frac{p^2}{\Lambda^2} \right)^{-1/2} \\ & \times \left[ \frac{\epsilon_2 I_0(y) - \epsilon_1 K_0(y)}{\epsilon_2 I_0(x) - \epsilon_2 x I_1(x) - \epsilon_1 K_0(x) - \epsilon_1 x K_1(x)} \right], \end{aligned} \quad (4.66)$$

where  $x = \sqrt{q^2/2\Lambda^2}$  and  $y = \sqrt{q^2/2p^2}$ . This gives

$$\Pi_S(q^2) = \frac{\Lambda^2}{4\pi^2} \left[ 4 + \frac{8 [\epsilon_2 x I_1(x) + \epsilon_1 x K_1(x)]}{\epsilon_2 I_0(x) - \epsilon_2 x I_1(x) - \epsilon_1 K_0(x) - \epsilon_1 x K_1(x)} \right]. \quad (4.67)$$

### 4.3.4 Analytic continuation across the critical curve

Since the expression for the scalar vacuum polarization is symmetric in  $\omega$ , Eq. (4.57), it can be analytically continued to the values  $\alpha_0 > \alpha_c$ . This holds in replacing  $\omega$  by  $i\nu$  in Eq. (4.57), where

$$\nu = \sqrt{\alpha_0/\alpha_c - 1}. \quad (4.68)$$

The four specific limits of the scalar vacuum polarization described above are very useful for studying the resonance structure of the bound states which will be done in section 4.5, and for the study of the CPT which will be done in section 4.6. But first we shall compare our result for  $\Delta_S$  with that one obtained by other authors in the next section.

## 4.4 Comparison with earlier work

In this section we discuss the earlier work of Appelquist, Terning, and Wijewardhana [22] and related work based on that by Kondo, Tanabashi, and Yamawaki [39] on the scalar composites in the GNJL model. The method used by these authors to solve the coupled set of scalar vertex and scalar vacuum polarization is the following. They consider a Taylor-series expansion about  $q = 0$  of the scalar vacuum polarization  $\Pi_S(q^2)$ . In the ladder approximation, such a series has the property that the  $n$ th derivative can be written as

$$\begin{aligned} \left( \frac{\partial}{\partial q} \right)^n \Pi_S(q^2) &\sim \int_{\Lambda} \frac{d^4 k}{(2\pi)^4} \sum_{m=0}^{n-1} C_m \text{Tr} \left[ \left( \frac{\partial^m}{\partial q^m} \Gamma_S(k+q, k) \right) \right. \\ &\quad \times \left. \frac{1}{\hat{k}} \Gamma_S(k, k+q) \frac{\partial^{n-m}}{\partial q^{n-m}} \frac{1}{\hat{k} - \hat{q}} \right]. \end{aligned} \quad (4.69)$$

Their basic assumption is then that derivatives of the scalar vertex  $\Gamma_S$  can be neglected with respect to  $\Gamma_S$  for small  $\alpha_0$ ,

$$\left. \frac{\partial^n \Gamma_S(k+q, k)}{\partial q^n} \right|_{q=0} \sim \frac{1}{k^n} \frac{\alpha_0}{4\alpha_c} \Gamma_S(k, k). \quad (4.70)$$

Subsequently the Taylor series is resummed using the assumption stated above to obtain

$$\Pi_S(q^2) \sim \int_{\Lambda} \frac{d^4 k}{(2\pi)^4} \text{Tr} \left[ \Gamma_S(k, k) \frac{1}{\hat{k}} \Gamma_S(k, k) \frac{1}{\hat{k} - \hat{q}} \right], \quad (4.71)$$

which yields in terms of Euclidean momentum,

$$\Pi_S(q^2) = \frac{\Lambda^2}{4\pi^2} \left[ \frac{1}{g_c(\omega)} - b(\omega) \left( \frac{q^2}{\Lambda^2} \right)^\omega + a(\omega) \frac{q^2}{\Lambda^2} \right], \quad (4.72)$$

where

$$a(\omega) = \frac{1}{2g_c(\omega)(1-\omega)}, \quad b(\omega) = \frac{1}{g_c(\omega)\omega(1-\omega^2)}, \quad g_c = \frac{(1+\omega)^2}{4}. \quad (4.73)$$

How does their result compare to ours? From our expression for the asymptotic behavior of  $\Pi_S$ , Eq. (4.64), and the result obtained in Refs. [22] and [39], Eq. (4.72), the leading power of momentum is the same, namely,  $(q^2/\Lambda^2)^\omega$ . However, the  $\omega$ -dependent factors in front of the leading and next-to-leading powers are different. At the same time the pure NJL limit is obtained correctly in Refs. [22] and [39]. The differences are rather small for values of  $\omega$  close to 1, *i.e.* the coefficients are

$$A(\omega) = a(\omega), \quad B(\omega) = b(\omega) [1 + \mathcal{O}((1-\omega)^2)]. \quad (4.74)$$

Hence the approach to the NJL point  $\omega = 1$  of both approximations is equal. However, for smaller values of  $\omega$  the coefficient  $B$  obtained in the present chapter starts to deviate from the one obtained in Ref. [22]. Then for such values of  $\omega$ ,  $b(\omega) > B(\omega)$ .

What is the origin of this difference? The first point is that the expression derived in Refs. [22] and [39] is valid for  $\alpha_0$  not too large. Secondly, from their answer Eq. (4.72) it is clear that a Taylor series of the scalar propagator about  $q = 0$  is not well defined due to the noninteger power behavior for values  $0 < \omega < 1$ . This is reflected also in their assumption regarding the derivatives of the scalar vertex at  $q = 0$ , Eq. (4.70). The expression for the scalar vertex obtained in section 4.2 shows that in general, for  $0 < \omega < 1$ , the assumption (4.70) is not true. Such derivatives of  $\Gamma_S$  are singular at  $q = 0$  due to the fact that they depend on noninteger powers of  $q$ , which can be seen from Eq. (4.39).

The scalar vertex for small  $q \ll p$  is of the form  $\Gamma_S(p+q, p) \sim F_{UV}(p^2, q^2)$ , and

$$\begin{aligned} F_{UV}(p^2, q^2) \approx & \left( \frac{p^2}{\Lambda^2} \right)^{-1/2+\omega/2} \left\{ \frac{2}{(1+\omega)} + \frac{q^2}{p^2} \left[ \frac{1}{4} + \frac{(1-\omega)}{4(1+\omega)} \frac{p^2}{\Lambda^2} \right] \right. \\ & - 2 \left( \frac{q^2}{p^2} \right)^\omega \frac{\gamma(-\omega)}{\gamma(\omega)} \frac{\Gamma(1-\omega)}{\Gamma(2+\omega)} \left[ 1 - \frac{(1-\omega)}{(1+\omega)} \left( \frac{p^2}{\Lambda^2} \right)^\omega \right] \left( \frac{\lambda_0}{2} \right)^\omega \\ & \left. + \mathcal{O}((q^2/p^2)^\omega (q^2/\Lambda^2)^\omega) + \mathcal{O}((q^2/p^2)^{1+\omega}) + \dots \right\}, \end{aligned} \quad (4.75)$$

which is consistent with Eq. (4.64) for  $p^2 = \Lambda^2$ , because of Eq. (4.33). Of course at  $q = 0$  our result coincides with that of the other authors. But for nonzero  $q$  this expression clearly shows that for  $0 < \omega < 1$  the vertex contains noninteger powers of  $q$ . Hence the assumption made in Refs. [39, 22] is not true in general, since higher derivatives of the scalar vertex with respect to  $q$  are singular at  $q = 0$ .

## 4.5 Light scalar resonances near criticality

In this section we discuss the behavior of the scalar propagator near the critical line in the symmetric phase  $g_0 \leq g_c$ . In the symmetric phase the scalar and pseudoscalar composites, the  $\sigma$  and  $\pi$  bosons are degenerate. Near the critical curve, a combination of strong four-fermion coupling and gauge coupling will tend to bind fermions and antifermions into these scalar composites. Since the chiral symmetry is unbroken the  $\sigma$  and  $\pi$  bosons decay to massless fermions and antifermions. Hence the scalar composites are resonances which are described by a complex pole in their propagators. The complex pole determines the mass and the width of the resonances.

In what follows, we redo the computation of the complex poles of the  $\sigma$  boson which was performed by Appelquist *et al.* in Ref. [22] using the expression for  $\Delta_S$ , Eq. (4.57), obtained with the two-channel approximation of the Yukawa vertex. The expressions obtained in section 4.3 for  $\Pi_S(p^2)$  in various regimes are rotated back to Minkowski momentum  $p^2 \rightarrow p_M^2 \exp(-i\pi)$ . Then the complex poles are given by

$$p_M^2 = p_0^2 \exp(-i\theta), \quad \Delta_S^{-1}(p_M) = -\frac{\Lambda^2}{4\pi^2 g_0} + \Pi_S(p_0^2 \exp(-i\theta)) = 0. \quad (4.76)$$

We can also parametrize the location of a pole by a mass and a width, *i.e.*,  $p_0^2 \exp(-i\theta) = [M_\sigma - (i/2)\Gamma_\sigma]^2$ , which yields

$$M_\sigma = p_0 \left[ \frac{1 + \cos \theta}{2} \right]^{1/2}, \quad \frac{\Gamma_\sigma}{M_\sigma} = \frac{2 \sin \theta}{1 + \cos \theta}. \quad (4.77)$$

If  $\theta$  is small, then  $\Gamma_\sigma/M_\sigma \approx \theta$ .

Near the Nambu–Jona-Lasinio point ( $\alpha_0 = 0$ ) our expression for the vacuum polarization coincides with that obtained by Appelquist *et al.*, Eq. (4.59), and we get the following equations for the resonances:

$$\frac{c\Lambda^2}{p_0^2} = \cos \theta \left[ \ln(\Lambda^2/p_0^2) + 3/2 \right], \quad c = \frac{2(1 - g_0)}{g_0}, \quad (4.78)$$

and

$$\pi + \theta = \left[ \ln(\Lambda^2/p_0^2) + \frac{3}{2} \right] \tan \theta. \quad (4.79)$$

If now  $g_0$  is tuned close enough to the critical value  $g_c = 1$ , so that  $\ln 1/c \gg 1$ , the solution is approximately

$$p_0^2 \approx \frac{2(1 - g_0)}{g_0 \ln [g_0/2(1 - g_0)]} \Lambda^2 \quad (4.80)$$

and we find a narrow width

$$\theta \approx \frac{\pi}{\ln [g_0/2(1 - g_0)]}. \quad (4.81)$$

These results are nothing else than the familiar NJL results. For intermediate values of the gauge coupling,  $0 < \alpha_0 < \alpha_c$  ( $0 < \omega < 1$ ), we assume the poles of  $\Delta_S$  are small,  $p_0/\Lambda \ll 1$ , so that

$$(p_0/\Lambda)^\omega \ll 1. \quad (4.82)$$

Then, from Eq. (4.64) we get the following equation for the real part of the pole:

$$0 \approx -\frac{1}{g_0} + \frac{1}{g_c} - B(\omega) \left( \frac{p_0^2}{\Lambda^2} \right)^\omega \cos \omega(\theta + \pi). \quad (4.83)$$

The equation for the imaginary part reads

$$0 \approx \sin \omega(\theta + \pi), \quad (4.84)$$

where  $B(\omega)$  is given by Eq. (4.65).

The solution is

$$\theta = \frac{\pi(n - \omega)}{\omega}, \quad (4.85)$$

and  $n$  is odd integer, so that  $\cos \omega(\theta + \pi) = -1$ , thus

$$p_0 \approx \Lambda \left[ \frac{(1 - g_0/g_c)}{g_0 B(\omega)} \right]^{1/2\omega}. \quad (4.86)$$

Hence  $\theta$  is only small if  $\omega \sim 1$  for  $n = 1$ . The result obtained in Ref. [22], see Eq. (4.73), gives a mass

$$p_0 \approx \Lambda \left[ \frac{(1 - g_0/g_c)}{g_0 b(\omega)} \right]^{1/2\omega}, \quad b(\omega) = \frac{1}{g_c \omega (1 - \omega^2)}. \quad (4.87)$$

The pole obtained in Ref. [22] is of the same order as Eq. (4.86) for values of  $\omega$  close to 1 (see also discussion in the previous section). For more intermediate values of  $\omega$  the poles obtained in our approximation are somewhat bigger, since  $b(\omega) > B(\omega)$  for  $0 < \omega < 1$ . The quantitative difference between the result of Ref. [22] and that obtained in this chapter for resonance structures are visualized in Fig. 4.5. In Fig. 4.5 the imaginary part of  $\Delta_S$  given by Eq. (4.57) and Eq. (4.1) is plotted versus  $p/M$  where the tuning of the four-fermion to the critical line is  $g_0/g_c = 0.999$ , and  $M/\Lambda = (1 - g_0/g_c)^{1/2}$ . From Fig. 4.5 it is clear that the position of the peak of the resonant curve is slightly shifted to the right in our case at a fixed ratio

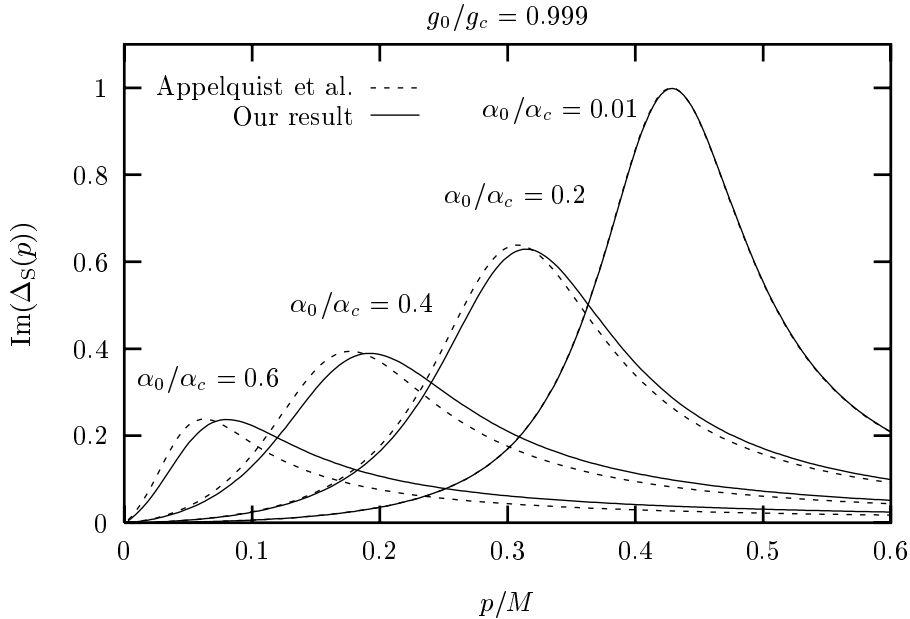


Figure 4.5: A comparison of our result with Appelquist *et al.* Graphs of  $\text{Im}(\Delta_S(p))$  for different values of  $\alpha_0/\alpha_c$ . The curves are normalized so that the peak of the  $\alpha_0/\alpha_c = 0.01$  curve equals 1.

$\alpha_0/\alpha_c \sim \mathcal{O}(1)$  (intermediate or small values of  $\omega$ ), while the width over mass ratio remains comparable. Near the pure NJL point  $\omega \sim 1$  both results coincide.

As was pointed out in the previous section, and following from the restriction Eq. (4.82), these results are only valid for  $\alpha_0/\alpha_c$  small. For larger values of the gauge coupling,  $\omega \rightarrow +0$ , the widths become larger, and Eq. (4.82) is no longer satisfied. This can also be seen in Fig. 4.5. As the ratio  $\alpha_0/\alpha_c$  increases the width increases too, and the position of the peak becomes more difficult to define.

## 4.6 Again: the conformal phase transition

In this section we analyze the scalar composites near the critical gauge coupling  $\alpha_0 = \alpha_c$ , with the purpose of investigating the conformal phase transition, which was introduced in section 3.6. We recall that the main feature of the CPT is an abrupt change of the spectrum of light excitations (composites) as the critical point is crossed, though the phase transition itself is continuous.

In the previous section we encountered a no-CPT,  $\sigma$ -model-like phase transition

for values of  $\alpha_0 < \alpha_c$ . The masses of light excitations<sup>1</sup> are continuous functions across the critical curve (though non-analytic); there is no abrupt change in the spectrum of light excitations. In the broken phase the  $\pi$  boson becomes a massless Nambu-Goldstone boson, while the fermion and  $\sigma$  boson acquire a dynamical mass which is small with respect to the cutoff  $\Lambda$  near criticality.

The pole at the critical gauge coupling  $\alpha_0 = \alpha_c$  is determined by Eq. (4.67), which is rather complicated but we only need to study the IR limit, so we assume that the pole is small  $p_0^2 \ll \Lambda^2$ . The infrared limit obtained from Eq. (4.67) is

$$\Pi_S(q^2) \approx \frac{\Lambda^2}{4\pi^2} \left[ 4 + \frac{16}{\ln(q^2/\Lambda^2) - \epsilon_3} + \mathcal{O}(q^2/\Lambda^2 \ln(q^2/\Lambda^2)) \right]. \quad (4.88)$$

We then find zeros of  $\Delta_S^{-1}(p)$  at

$$0 \approx \left( \frac{1}{g_0} - 4 \right) + \frac{16(\ln(\Lambda^2/p_0^2) + \epsilon_3)}{(\ln(\Lambda^2/p_0^2) + \epsilon_3)^2 + (\theta + \pi)^2}, \quad (4.89)$$

$$0 \approx \theta + \pi. \quad (4.90)$$

Thus  $\theta \approx -\pi$ , and from Eq. (4.89) it is clear that if  $g_0 \leq g_c = 1/4$  both terms on the right-hand side are positive, and there is no solution for the pole with  $p_0/\Lambda \ll 1$ . Hence if there is a pole it will be heavy, *i.e.*,  $p_0/\Lambda = \mathcal{O}(1)$ . Therefore at  $\alpha_0 = \alpha_c$  no light resonances are present in the spectrum for  $g_0 \leq g_c = 1/4$ . The imaginary phase  $\theta$  approaches  $-\pi$  which means the heavy pole occurs at “Euclidean” momentum, a sign of tachyonic states.

The statement above can be made more explicit. If we analytically continue the scalar propagator to the values of  $\alpha_0 > \alpha_c$ , then we end up in the “wrong vacuum” and we should get tachyonic states. In the broken phase ( $\alpha_0 > \alpha_c$ ), a chiral symmetric solution still exists, but it is unstable. The  $\pi$  and  $\sigma$  bosons are tachyons for such a solution. The unstable symmetric solution is obtained by analytic continuation of the solution in the symmetric phase across the critical curve (at  $\alpha_c$ ). The scaling law is determined by the UV properties of the theory and therefore the scaling law of the tachyonic masses is the same as that of the fermion and  $\sigma$ -boson mass in the broken phase.

Tachyons are described by an imaginary mass  $m^2 < 0$ . This means the scalar propagator must have a real pole for Euclidean momentum. If the pole  $p_0$  is small,  $p_0 \ll \Lambda$ , we analytically continue Eq. (4.63) to  $\alpha_0 > \alpha_c$  by replacing  $\omega$  by  $i\nu$ ,

$$\omega \rightarrow i\nu \equiv i\sqrt{4\lambda_0 - 1}. \quad (4.91)$$

We then obtain

$$\Pi_S(q^2) = \frac{\Lambda^2}{\pi^2} \frac{1 - \nu^2 - 2\nu \cot y}{(1 + \nu^2)^2}, \quad y = \frac{\nu}{2} \ln \left( \frac{\Lambda^2}{q^2} \right) + \nu\phi(\nu^2), \quad (4.92)$$

---

<sup>1</sup> The scalar composites, *i.e.*, the  $\pi$  and  $\sigma$  bosons are light resonances,  $|m_\pi| = |m_\sigma| \ll \Lambda$ .

where

$$\phi(\nu^2) \equiv \frac{1}{2i\nu} \ln \frac{h(i\nu)(1+i\nu)}{h(-i\nu)(1-i\nu)} - \ln \sqrt{2\lambda_0}. \quad (4.93)$$

The tachyonic pole is then given by the root of the equation

$$-\frac{\Lambda^2}{4\pi^2 g_0} + \Pi_S(p_0^2) = 0, \quad (4.94)$$

which gives

$$\frac{p_0}{\Lambda} = \exp \left( -\frac{n\pi}{\nu} - \frac{\beta}{\nu} + \phi(\nu^2) \right), \quad (4.95)$$

where  $n$  is a positive integer and

$$\beta = \tan^{-1} \frac{\nu g_0}{g_0 - 2\lambda_0(g_0 + \lambda_0)}. \quad (4.96)$$

The tachyon with largest  $p_0$  in the physical region  $p_0 < \Lambda$  corresponds to  $n = 1$ . If we now consider the limit  $\nu \rightarrow 0$  ( $\lambda_0 \rightarrow 1/4$ ), we get

$$\beta \approx \frac{2\nu g_0}{g_0 - 1/4}, \quad \phi(\nu^2) \approx 1 - \gamma - \frac{1}{2} \ln 2 - \frac{\epsilon_2}{\epsilon_1} + \mathcal{O}(\nu^2). \quad (4.97)$$

In this case,

$$\frac{p_0}{\Lambda} \approx \exp \left( \frac{2g_0}{1/4 - g_0} + \phi(0) \right) \exp \left( -\frac{\pi}{\sqrt{4\lambda_0 - 1}} \right), \quad (4.98)$$

which is proportional to the well-known scaling law of quenched QED. Thus the scalar propagator giving the tachyon pole equation, Eq. (4.98), reproduces the scaling law with essential singularity (compare with Eq. (3.45)), which is another confirmation of the CPT.

## 4.7 Renormalization and the scaling hypothesis

In what follows, we discuss the results from the viewpoint of the renormalizability of the GNJL model. The renormalization is performed by a suitable redefinition of the composite or auxiliary fields  $\sigma$  and  $\pi$  (see Eq. (1.141)):

$$\sigma_R \equiv [Z_\sigma^{(\mu)}]^{-1} \sigma, \quad \pi_R \equiv [Z_\pi^{(\mu)}]^{-1} \pi, \quad (4.99)$$

where  $\mu$  is related to some physical scale, which should be independent of  $\Lambda$ . The renormalization factors of the scalar and pseudoscalar fields  $Z_\sigma^{(\mu)}$ , respectively,  $Z_\pi^{(\mu)}$

can be chosen to coincide both in the symmetric and broken phase, and the renormalized auxiliary fields  $\sigma_R$  and  $\pi_R$  define the renormalized scalar propagator

$$\Delta_S^R(q) = \left[ Z_\sigma^{(\mu)} \right]^{-2} \Delta_S(q) \quad (4.100)$$

and the renormalized scalar vertex

$$\Gamma_S^R(p+q, p) = Z_\sigma^{(\mu)} \Gamma_S(p+q, p). \quad (4.101)$$

In order to renormalize the scalar propagator and Yukawa vertex simultaneously (see also Eqs. (4.64) and (4.75)), the wave function renormalization factor at some renormalization scale  $\mu$  should be of the form

$$Z_\sigma^{(\mu)} \propto \left( \frac{\mu^2}{\Lambda^2} \right)^{(1-\omega)/2}. \quad (4.102)$$

Freedom in the choice of renormalization scheme allows us to take the factor  $Z$  defined in Eq. (4.43) as the wave function renormalization factor, since

$$Z_\sigma^{(\mu)} = Z(\mu^2/\Lambda^2, \omega) \approx \frac{\pi}{2 \sin \omega \pi} \frac{\gamma(\omega)}{2} \frac{(1+\omega)}{\Gamma(1-\omega)} \left( \frac{\lambda_0}{2} \right)^{-\omega/2} \left( \frac{\mu^2}{\Lambda^2} \right)^{(1-\omega)/2}. \quad (4.103)$$

Hence it follows that four-fermion scattering amplitudes, for instance one-scalar exchange amplitudes are renormalization group (RG) invariant, *i.e.*

$$\Gamma_S^R(p_1+q, p_1) \Delta_S^R(q) \Gamma_S^R(p_2, p_2+q) \sim \Gamma_S(p_1+q, p_1) \Delta_S(q) \Gamma_S(p_2, p_2+q), \quad (4.104)$$

(*e.g.* see again [22]). Consider the case where  $p_1^2, p_2^2 \gg q^2$ , so that the scalar vertices are described by the UV channels, and suppose that we are sufficiently close to the critical line (the fine-tuning condition Eq. (3.99))

$$-\frac{\Delta g_0}{g_0 g_c} \equiv \frac{1}{g_0} - \frac{1}{g_c} \ll \left( \frac{q^2}{\Lambda^2} \right)^\omega \implies -\frac{\Delta g_0}{g_0 g_c} \sim \left( \frac{\mu^2}{\Lambda^2} \right)^\omega, \quad \mu^2 \ll q^2, \quad (4.105)$$

where  $\Delta g_0 \equiv g_0 - g_c$ , then from Eqs. (4.1) and (4.64) the scalar propagator has the asymptotic behavior

$$\Delta_S(q) \approx -\frac{4\pi^2}{\Lambda^2} \frac{1}{B(\omega)} \left( \frac{\Lambda^2}{q^2} \right)^\omega. \quad (4.106)$$

Such a specific power-law behavior for the scalar propagator is essential for the renormalizability of the GNJL model as is shown in Refs. [96, 22, 97, 104, 39].

Thus, from Eq. (4.102) and Eq. (4.75), we get

$$\Delta_S^R(q) \propto -\frac{1}{\mu^2} \left( \frac{\mu^2}{q^2} \right)^\omega, \quad (4.107)$$

$$\begin{aligned} F_{\text{UV}}^R(p^2, q^2) &\propto \frac{2}{(1+\omega)} \left( \frac{p^2}{\mu^2} \right)^{-(1-\omega)/2} \\ &\times \left[ 1 - 2 \left( \frac{q^2}{p^2} \right)^\omega \frac{\gamma(-\omega)}{\gamma(\omega)} \frac{\Gamma(1-\omega)}{\Gamma(2+\omega)} \left( \frac{\lambda_0}{2} \right)^\omega \right]. \end{aligned} \quad (4.108)$$

With these expressions, it is straightforward to check that Eq. (4.104) is indeed independent of  $\Lambda$  and  $\mu$ . Hence the renormalization of the auxiliary fields  $\sigma$  and  $\pi$ , Eq. (4.99), simultaneously renormalizes the Yukawa vertex and the scalar propagator.

The above considerations can be made more explicit by writing the scalar propagator according to the scaling hypothesis Eq. (1.37) (in Euclidean formulation). The scaling hypothesis states that the propagator should have the following form:

$$\Delta_S(q) = \frac{1}{\Lambda^2} \left( \frac{\Lambda^2}{q^2} \right)^{1-\eta/2} \mathcal{F}_\Delta(|m_\sigma|^2/q^2), \quad (4.109)$$

where  $\eta$  is by definition the anomalous dimension. We write  $|m_\sigma| = p_0$ , with  $p_0$  given by Eq. (4.86), where  $|m_\sigma|$  is the analog of the inverse correlation length  $|m_\sigma| = 1/\xi$ , and  $\xi \sim (\Delta g_0)^{-\nu}$ . Then

$$\Delta_S(q) = -\frac{4\pi^2}{\Lambda^2} \frac{1}{B(\omega)} \left( \frac{\Lambda^2}{q^2} \right)^\omega \left[ 1 + \left( \frac{|m_\sigma|^2}{q^2} \right)^\omega - \frac{A(\omega)}{B(\omega)} \left( \frac{q^2}{\Lambda^2} \right)^{\sigma_1} + \dots \right]^{-1} \quad (4.110)$$

where the exponent  $\sigma_1 > 0$  for  $0 < \omega < 1$ . From this we read off that the anomalous dimension  $\eta$  is given by

$$2\omega = 2 - \eta \implies \eta = 2(1 - \omega), \quad (4.111)$$

and that the scaling function is (provided  $|m_\sigma|^2, q^2 \ll \Lambda^2$ )

$$\mathcal{F}_\Delta(x) \approx -\frac{4\pi^2}{B(\omega)} \frac{1}{1+x^\omega}. \quad (4.112)$$

Thus indeed if  $q^2 \gg |m_\sigma|^2$  we obtain Eq. (4.106), and when  $q^2 \ll |m_\sigma|^2$  we get

$$\Delta_S(0) = \frac{4\pi^2}{\Lambda^2} \frac{g_0 g_c}{\Delta g_0} \sim (\Delta g_0)^{-\gamma} \sim \chi = \left. \frac{\partial \mathcal{M}}{\partial m_0} \right|_{m_0=0}, \quad (4.113)$$

supporting the fact that the critical exponent  $\gamma = 1$ . Within the quenched-ladder approximation, Eq. (4.113) agrees with the PCAC relation (2.67) and the analyticity

condition (2.70). The PCAC relation for the pseudoscalar propagator is

$$-\frac{\langle \sigma \rangle}{m_0} = \frac{\Delta_P(0)}{G_0}. \quad (4.114)$$

Using the EOS Eqs. (3.29) and (3.30) and the fact that in the symmetric phase (in the chiral limit)

$$-\Delta g_0 \gg (\Sigma_0/\Lambda)^{2\omega}, \quad (4.115)$$

see Eq. (3.101), we get that

$$\frac{\Delta_P(0)}{G_0} = \frac{g_c}{\Delta g_0}. \quad (4.116)$$

Same can be done for  $\Delta_S(0)$  (of course  $\Delta_S = \Delta_P$  in the symmetric phase), thus

$$\frac{\Delta_S(0)}{G_0} = \frac{\Delta_P(0)}{G_0} = \frac{g_c}{\Delta g_0}. \quad (4.117)$$

Hence, with  $G_0 = 4\pi^2 g_0/\Lambda^2$ , Eq. (4.113) is obtained.

Since the absolute value of the resonance *i.e.*,  $|m_\sigma|$  is now the new scale (besides the UV cutoff) generated close to the critical curve, it is natural to take it to be a physical scale, which by definition should be independent of  $\Lambda$ . Using Eq. (4.86), we get the fine-tuning condition

$$0 = \Lambda \frac{d|m_\sigma|}{d\Lambda} \sim \Lambda \frac{d}{d\Lambda} \left[ \Lambda \left( \frac{-\Delta g_0}{g_0} \right)^{1/2\omega} \right] \Rightarrow \beta_g(g_0) = -2\omega \frac{g_0}{g_c} (g_0 - g_c), \quad (4.118)$$

which is equivalent to the fine-tuning condition given in [39], and Eq. (3.99).<sup>2</sup> Hence the critical curve  $g_0 = g_c$  is an UV fixed point  $\beta_g(g_c) = 0$  ( $\beta'_g(g_c) < 0$ ) of the renormalization group flow.

## 4.8 Summary of results

In this chapter we studied the scalar composites near criticality in the GNJL model. We obtained an analytic expression for the scalar propagator describing the composite states which is valid along the entire critical curve of the GNJL model. We presented a method for solving the Yukawa vertex in the GNJL in the quenched-ladder approximation. The crucial assumption was that such a vertex depends only weakly on the angle between  $\sigma$ -boson momentum and fermion momentum. The method presented here incorporated the infrared boundary condition in a more

---

<sup>2</sup>Again it is assumed that  $\beta_\alpha(\alpha_0) \approx 0$ .

natural way than previous attempts in this direction. Also the observation that derivatives of the Yukawa vertex are singular at zero  $\sigma$ -boson momentum transfer is a warning that derivative expansions and Taylor series could fail. Moreover this is reflected by the property of the scalar composites having noninteger power-law behavior, which means that, although these states are tightly bound, they are not pointlike.

The conclusion of the comparison of the method presented here and work done previously on the  $\sigma$ -boson propagator is the following. Qualitatively the results obtained by Appelquist *et al.*, Kondo *et al.* and by our approximation are in agreement. Both methods yield a renormalizable  $\sigma$ -boson propagator and Yukawa vertex near criticality and find light resonances for gauge coupling  $0 < \alpha_0 < \alpha_c$ . Quantitatively, at a fixed value of the gauge coupling, the scalar composites computed in our case are slightly heavier with comparable width, as is illustrated in Fig. 4.5.

In addition, the scalar composites propagator were examined for values of the coupling near the critical gauge coupling  $\alpha_c$ . Near the critical line  $\alpha_0 = \alpha_c, g_0 < \frac{1}{4}$  the conformal phase transition is encountered and the spectrum of light excitations (resonances) in the symmetric phase disappears. Moreover the well-known scaling law with essential singularity, which is characteristic for the CPT, was recovered by analytic continuation of the  $\sigma$ -boson propagator across the critical curve at  $\alpha_0 = \alpha_c$ .



## Chapter 5

# On the existence of ultra-violet fixed points

### 5.1 Beyond the quenched approximation

The general consensus on  $U(1)$  gauge theories such as the GNJL model is that they are trivial. Once fermion-loops are present the electromagnetic charge will be screened completely in the continuum limit ( $\Lambda \rightarrow \infty$ ). But we argue that (pseudo)scalar degrees of freedom play an important role, and in case of the GNJL model, provided the number of fermion flavors  $N$  exceeds some critical value, ultra-violet (UV) fixed points can be realized. The existence of UV fixed points gives rise to a non-trivial theory.

The crucial mechanism responsible for the realization of such a nontrivial root of the  $\beta$  function of the gauge coupling is given by the formation of tight scalar and pseudoscalar resonances in the symmetric phase or bound states in the broken phase near the critical line. In other words, the formation, due to the strong coupling chiral symmetry breaking dynamics, of neutral scalars and pseudoscalar composites reduces the screening of charge.

As a perturbation theory, QED has been proven to be a successful gauge field theory, tested at extremely high precision. However, in the language of the renormalization group, perturbative QED appears to be a trivial theory in four dimensions (see Ref. [42]). In the continuum limit, taking the cutoff  $\Lambda$  to infinity, the effective or running gauge coupling vanishes, and the theory becomes a free field (*i.e.* trivial) theory.

In the renormalized theory, triviality represents itself in the form of the so-called Landau ghost, which is a singularity in the RG transformation for the gauge coupling  $\alpha_0$  at  $\Lambda = \Lambda_{LG}$ , see Refs. [42, 145, 146]. The renormalized theory should then be considered as an effective theory, which is not defined for distances shorter

than  $1/\Lambda_{LG}$ , see Ref. [2]. In QED the Landau ghost  $\Lambda_{LG}$  lies far beyond the Planck scale, and is not of practical importance.

The triviality of QED originates from the screening of charged particles by their interactions with virtual fermion anti-fermion pairs from the vacuum. Such charge screening is described by the vacuum polarization  $\Pi$ , Eq. (2.22), and the implications of the one-loop leading contribution were discussed in Refs. [147, 148, 149]:

$$\Pi(q^2) = \frac{N\alpha_0}{3\pi} \log \frac{\Lambda^2}{q^2}, \quad (5.1)$$

where  $N$  is the number of fermion flavors. The QED vacuum is not a perfect insulator and can be considered as a medium of dipoles, where the dipoles represent the virtual fermion anti-fermion pairs (*i.e.* the fermion loops in the vacuum polarization). This logarithmic screening effect is sufficient to cause the complete screening of charge in the continuum limit.

The charge screening and charge renormalization give rise to a running gauge coupling, *i.e.*  $\alpha_0$  depends on the cut-off  $\Lambda$ , and the roots  $\alpha_0$  of the  $\beta$  function,

$$\beta_\alpha(\alpha_0) \equiv \Lambda \frac{d\alpha_0}{d\Lambda} = 0, \quad (5.2)$$

are essential in the renormalization group analysis. Such a root is either a Gaussian fixed point corresponding to a trivial theory or an UV fixed point (*i.e* critical fixed point) corresponding to a nontrivial continuum limit. In case of perturbative QED, the only zero of  $\beta_\alpha$  is the origin  $\alpha_0 = 0$ , the Gaussian fixed point. In case of asymptotic free theories such as QCD the origin is an UV fixed point. A nontrivial (interacting) theory arises whenever  $\beta_\alpha$  has a root which is an UV fixed point. The first formulation of the renormalization group for the gauge coupling  $\alpha_0$  of QED and speculations about the existence of a fixed point was given in Ref. [16].

Although the conclusions concerning QED are usually drawn from the one-loop results, the two-loop computations of Ref. [150] and the three-loop (quenched) computations of Refs. [151, 152] are consistent with the view that QED is trivial. In this context we should mention that the effort of Johnson, Baker, Willey, and Adler [46, 153, 154, 155] to find a finite nontrivial continuum limit of QED was inspired by the simplicity and the negative sign of the three-loop result of Rosner. No realization of the scenario presented by Johnson *et al.* has been found, mainly because they were looking for a perturbative resolution. The problem is that for a possible nontrivial continuum limit of QED, critical and hence nonperturbative dynamics is required.

Therefore, the discovery of dynamical chiral symmetry breaking in the strong-coupling phase of QED and the existence of an UV fixed point in the quenched-ladder approximation sheds new light on the nonperturbative nature of QED. The fundamental notion is that composite degrees of freedom play an important role in resolving the scaling behavior of the theory near criticality. The GNJL model is the

generalization of strong coupling QED analysis taking into account the composite degrees of freedom.

An interesting attempt to incorporate the dynamics of chiral symmetry breaking (*e.g.* the formation of bound states) was made in Ref. [156]. Kocić *et al.* argued that magnetic effects described by parts of the transverse vertex (the vertex function  $\tau_5$ ) could prevent the total screening of charge. However, we think that the analysis of Kocić *et al.* lacks an inhomogeneous term in the equation for the transverse vertex function. It is precisely the inhomogeneous term that introduces boundary conditions which eliminate the nontrivial solution for the transverse vertex function obtained by Kocić *et al.*, henceforth, their scenario is not suitable to resolve the triviality problem.

Magnetic effects described by the transverse vertex can only be proportional to the fermion dynamical mass; singular solutions of the type proposed by Kocić *et al.* are eliminated by ultraviolet boundary conditions. Since the fermion dynamical mass vanishes close to criticality (large correlation length), it is unlikely that magnetic effects are important for the study of charge screening.

We speculate therefore that some other mechanism is responsible for the possible realization of an UV fixed point, and the absence of charge screening, in the unquenched GNJL model. Formally irrelevant four-fermion interactions become relevant near the critical line of the chiral phase transition,

$$g_c(\omega) = (1 + \omega)^2/4, \quad \omega = \sqrt{1 - \alpha_0/\alpha_c}, \quad (5.3)$$

and the dynamics of the composite states described by the four-fermion interactions might play a crucial role in the phenomenon of charge screening.

Dynamical symmetry breaking is an inherently nonperturbative phenomenon, and, due to the lack of other solvable approximations, has been predominantly studied in the framework of SDEs in the quenched-ladder approximation. As was mentioned in chapter 3, the physical implications and the consistency of the quenched-ladder results with many quenched lattice simulations, and with the nonperturbative RG techniques, support the view that the qualitative features of the approach might be realistic and describe properties of the full theory. Moreover the ladder approach respects the vector and axial Ward–Takahashi identities.

The quenched approximation is analogous to the assumption that the full gauge boson propagator  $D_{\mu\nu}(k)$  can be approximated by the bare or canonical propagator (for large momenta),

$$D_{\mu\nu}(k) = \left( -g_{\mu\nu} + \frac{k_\mu k_\nu}{k^2} \right) \frac{1}{k^2}, \quad (5.4)$$

in the Landau gauge. The quenched approximation is only consistent when the vacuum polarization is finite in the continuum limit, *i.e.* the logarithmic running of the coupling is absent. This is the case at an UV fixed point of the  $\beta$  function Eq. (5.2) of  $\alpha_0$ . The assumption that such a critical fixed point exists, and that

it lies somewhere on the critical curve (5.3) is the starting point for many studies of dynamical chiral symmetry breaking in context of the GNJL model. In fact the quenched hypothesis is only consistent when the bare gauge coupling  $\alpha_0$  is the UV fixed point of the theory,  $\beta_\alpha(\alpha_0) = 0$ .

Attempts to include a logarithmic running of the coupling drastically changes the chiral phase transition and the critical line, see Refs. [129, 130, 131, 157]. It was shown in Refs. [131, 93, 158, 159] that  $\gamma_m = 2$ , which is analogous to the vanishing of the anomalous dimension of the scalar propagator,  $\eta = 2(2 - \gamma_m) = 0$  (*e.g.* see Eq. (4.109)). Consequently, the critical exponents turn out to be of the mean field type. The quenched theory and the theory with the logarithmically running coupling seem to be two different theories.

It is essential to incorporate the composite degrees of freedom and their effective interactions to properly understand the scaling structure of the full unquenched GNJL model. In case of the GNJL model, the four-fermion interactions are treated in a mean field approach known as the Hartree–Fock approximation, see also section 3.1. We recall that by mean field approach, we refer to approximations which neglect quantum corrections corresponding to four-fermion interactions beyond tree level.

The merit of the mean field approximation is the decoupling of SDEs. Clearly it is necessary to check the consistency between the initial assumptions and the final result. As long as four-fermion interactions are irrelevant the mean-field approach for these operators is justified. However the conclusions of Refs.[24, 23] are that the quenched-ladder approximations with four-fermion interactions in the mean field approach satisfy the hyperscaling equations for the critical exponents, suggesting that the four-fermion operators become relevant due to the appearance of large anomalous dimensions. In other words, the mean field approach yields nonmean-field exponents, thereby being inconsistent (*e.g.* see Refs.[4, 92]).

The fluctuations of the gauge field for the composite degrees of freedom are essential and cannot be neglected; they give rise to a large anomalous dimension turning irrelevant four-fermion interaction into relevant ones implying that such interactions give nontrivial quantum corrections (they cannot be neglected beyond tree level.) This is supported by the computations of the anomalous scaling laws for the Yukawa vertices and the propagators of the scalar and pseudoscalar composite states, *i.e.* the  $\sigma$  and  $\pi$  bosons of chapter 4. In fact, as was discussed in section 3.5, the hyperscaling relations imply the existence of a nontrivial Yukawa interaction describing the interaction between fermions and  $\sigma$  and  $\pi$  composites in the GNJL model.

The question is; how to modify the mean field approach? An appropriate answer depends on the following three concepts: skeleton expansions, the  $1/N$  expansion (with  $N$  the number of fermion flavors), and the specific form of the chiral symmetry. Clearly going beyond the quenched approximation seems only interesting once four-fermion interactions are treated beyond the mean field approach.

## 5.2 Beyond the mean field approach

Let us first review the concept of the so-called skeleton expansions. The anomalous dimensions follow from the scaling structure of the fully dressed Yukawa vertices and  $\sigma$  and  $\pi$  propagators, hence it is necessary to incorporate the full Green functions corresponding to the four-fermionic composite degrees of freedom (or at least the leading or asymptotic parts of these functions). Therefore it is crucial to study such issues in a renormalization group (RG) invariant manner. This can be done on the level of the Bethe-Salpeter fermion–anti-fermion scattering kernels in the skeleton expansion (see *e.g.* Bjorken and Drell [44]).

Analogous to the pure QED kernels we define the one-boson irreducible kernel  $K^{(1)}$ , and the two-fermion one-boson irreducible kernel  $K^{(2)}$ , where these kernels now also include the  $\sigma$  and  $\pi$  composites. For both type of kernels a skeleton expansion exists, and the integral equation between  $K^{(1)}$  and  $K^{(2)}$  is known as the Bethe-Salpeter equation. The skeleton expansion is a series in topologically distinct Feynman diagrams with all vertices and propagators fully dressed. Each term in the skeleton expansion of the BS kernel is RG invariant, up to fermion wave function factors, *i.e.* the expansion is independent of the renormalization factors  $Z_3$  and  $Z = Z_\sigma = Z_\pi$  (see Eqs. (1.140) and (1.141)) of, respectively, the gauge field and the composite fields  $\sigma$  and  $\pi$ . The two  $Z^{-1}$  factors with anomalous dimensions of each Yukawa vertex cancel with the  $Z^2$  factors of the  $\sigma$  and  $\pi$  propagators. Since in the quenched approximation the renormalization constant of the gauge field is one ( $Z_3 = 1$ ), the quenched-ladder approximation is consistent from the RG point of view.

The GNJL model, with  $N$  number of fermion flavors, is taken to be invariant under global  $U_L(N) \times U_R(N)$  chiral transformations, so that both the scalar and pseudoscalar four-fermion interactions are in the adjoint representation, and, consequently, the number of scalar composites ( $N^2$ ) equals the number of pseudoscalar composites ( $N^2$ ). In this way, when  $N$  is large we can use the  $1/N$  expansion introduced by 't Hooft [45]. The  $1/N$  expansion states that planar, *i.e.* ladder, graphs describe the dominant contribution to Green functions. The  $1/N$  expansion will be discussed in the next section.

With the gauge interaction treated in the ladder approximation each full Yukawa vertex and  $\sigma$ ,  $\pi$  boson propagator can be written as

$$\Gamma_{S_{ij}^{ab}}^\alpha(k, p) = \tau_{ij}^\alpha \Gamma_{Sab}(k, p), \quad \Delta_S^{(\alpha)}(q) = \Delta_S(q). \quad (5.5)$$

So that

$$\begin{aligned} & \sum_{\alpha=0}^{N^2-1} \Gamma_{S_{ij}^{ab}}^\alpha(k+q, k) \Delta_S^{(\alpha)}(q) \Gamma_{S_{kl}^{cd}}^\alpha(p, p+q) \\ &= \delta_{il} \delta_{kj} \Gamma_{Sab}(k+q, k) \Delta_S(q) \Gamma_{Scd}(p, p+q), \end{aligned} \quad (5.6)$$

where we have used the Fierz identity

$$\sum_{\alpha=0}^{N^2-1} \tau_{ij}^{\alpha} \tau_{kl}^{\alpha} = \delta_{il} \delta_{kj}, \quad (5.7)$$

with  $\tau$  the generators of the  $U(N)$  symmetry. Then the first term of the skeleton expansion for  $K^{(2)}$  is the following single boson exchange term:

$$\begin{aligned} (-ie_0^2) K_{i_1 j_1, i_2 j_2}^{(2)} (k, p, p+q) = & \\ & \delta_{i_2 j_1} \delta_{i_1 j_2} (-ie_0) \Gamma_{cb}^{\lambda} (p+q, p) i D_{\lambda\sigma} (q) (-ie_0) \Gamma_{ad}^{\sigma} (k, k+q) \\ & + \delta_{i_1 j_1} \delta_{i_2 j_2} (-i) \Gamma_{Scb} (p+q, p) i \Delta_S (q) (-i) \Gamma_{Sad} (k, k+q) \\ & + \delta_{i_1 j_1} \delta_{i_2 j_2} (-i) \Gamma_{Pcb} (p+q, p) i \Delta_P (q) (-i) \Gamma_{Pad} (k, k+q), \end{aligned} \quad (5.8)$$

where the labels  $i$ s and  $j$ s are flavor labels.

As a result of the chiral symmetry the contributions of four-fermion interactions, which are represented by  $\sigma$  and  $\pi$  exchanges, exhibit two distinct features depending on whether they are incorporated in SDEs describing quantities connected with so-called zero-spin structures<sup>1</sup> (*e.g.* the dynamical mass  $\Sigma$ , the Yukawa vertices  $\Gamma_S$ ,  $\Gamma_P$ , and the  $\sigma$  and  $\pi$  propagators  $\Delta_S$ ,  $\Delta_P$ ), or whether the exchanges are included in SDEs describing nonzero-spin structures (anti-commuting with  $\gamma_5$ ) (*e.g.* the vacuum polarization  $\Pi$ , the photon-fermion vertex  $\Gamma^{\mu}$ , and the fermion wave function  $\mathcal{Z}$ ). Henceforth, we refer to (non)zero-spin functions, and their equations as (non)zero-spin channels.

The chiral symmetry gives rise to the following properties:

1. In spin-zero-channels, the contribution of planar diagrams (*i.e.* planar in  $\sigma$  and  $\pi$  exchanges) vanishes due to the fact that the exchange of a  $\sigma$  has an opposite sign with respect to a  $\pi$  exchange. Why? Let us consider a planar contribution to the scalar vacuum polarization which contains (amongst others) a  $\pi$  exchange. Both  $\gamma_5$  matrices corresponding to this particular planar  $\pi$  exchange can be eliminated from the fermion trace of the scalar vacuum polarization by moving them to right-hand side of the trace. For planar diagrams such a process involves the interchange of the  $\gamma_5$  matrix with an even number of fermion propagators, and an arbitrary number of Yukawa vertices. Since the Yukawa vertices commute with the  $\gamma_5$  matrix, and  $\gamma_5$  anti-commutes with the fermion propagator<sup>2</sup>  $S$ , the process of moving the  $\gamma_5$  to the right does not introduce an overall minus sign. Now using that  $(i\gamma_5)(i\gamma_5) = -(\mathbf{1})(\mathbf{1})$ , we see that such a specific  $\pi$  exchange is identical to minus the same diagram with the  $\pi$  exchange replaced by a  $\sigma$  exchange. Since each diagram containing a  $\pi$  exchange has a scalar counter part (*i.e.* an analogous diagram with a  $\sigma$  instead

<sup>1</sup>Such structures are characterized by spinor matrices which commute with the  $\gamma_5$  matrix.

<sup>2</sup>In the symmetric phase  $\gamma_5 S = -S\gamma_5$ .

of a  $\pi$  exchange), the sum of all planar diagrams, with a particular number of exchanges, vanishes. Thus in channels with spin-zero matrix structures (*i.e.* channels which correspond to vertices which commute with  $\gamma_5$ ) scalar forces appear to be opposite to pseudoscalar forces.

2. In nonzero-spin channels (think of  $\Pi$ ,  $\Gamma^\mu$ , etc.) containing vertices which anti-commute with the  $\gamma_5$  matrix, the situation is different: planar  $\sigma$  and  $\pi$  exchanges contribute with identical sign. Let us now consider a planar contribution to the (photon) vacuum polarization containing a  $\pi$  exchange. If we again move the  $\gamma_5$  matrices to the right-hand side of the trace, we get an overall minus sign due to the anti-commutation of  $\gamma_5$  with  $\gamma^\mu$ . This means that any planar diagram in the vacuum polarization containing a  $\pi$  exchange is identical to the same diagram with the  $\pi$  exchange replaced by a  $\sigma$  exchange. Hence, in channels connected with spin structures anti-commuting with  $\gamma_5$ ,  $\sigma$  and  $\pi$  exchanges behave identical. In other words, in such channels, pseudoscalar and scalar forces act in the same direction (instead of canceling).

The properties described above are, strictly speaking, only valid in the symmetric (massless) phase, where the  $\sigma$  and  $\pi$  bosons are degenerate. However, in the broken phase, the properties are valid whenever momenta larger than the dynamical mass  $\Sigma$  or inverse correlation length  $\xi^{-1} \sim m_\sigma$  are considered, because then the degeneracy emerges too.

These properties also provide us with a general argument why the mean field approach for four-fermion operators for Green functions corresponding to spin-zero channels (*e.g.*  $\Gamma_S$  and  $\Delta_S$  of chapter 4) is reliable. For such channels planar contributions vanish and the next non-vanishing contributions (such as contributions containing crossed  $\sigma$  and  $\pi$  exchanges) are proportional to  $1/N$ , thus small for large  $N$ . This suggests that quantities such as the critical curve, dynamical mass, anomalous dimensions etc., are nearly independent of  $N$ , and are described rather well by the mean field approach.

However, such a cancellation of scalars against pseudoscalars degrees of freedom does not occur in nonzero-spin channels, such as the vacuum polarization  $\Pi$ . In the vacuum polarization it turns out that  $\sigma$  and  $\pi$  exchanges are attractive and virtual fermion anti-fermion pairs from vacuum fluctuations are constrained by these forces, reducing their capability to screen.

### 5.3 The $1/N$ expansion

The  $1/N$  expansion of 't Hooft (see Refs. [45, 160]) provides us with a useful non-perturbative tool to incorporate four-fermion interactions beyond the mean field approach. As mentioned previously, the  $1/N$  expansion states that the planar (*i.e.* ladder) diagrams, with fermions at the edges, describe the leading or dominant contributions to Green functions. The interesting feature of the  $1/N$  expansion

is that Feynman diagrams can be classified in terms of two-dimensional surfaces with specific topology. Diagrams with other (than planar) topological structures are multiplied by factors of  $1/N$ , and in the limit of large  $N$ , their contribution can be neglected with respect to planar graphs.

In the formulation of the  $1/N$  expansion of 't Hooft, the planar graphs coincide with ladder graphs in case of the GNJL model. One important rule is to draw Feynman graphs with fermion loops forming the boundary of the graph (if possible). In this way, vertex corrections are not necessarily classified as being planar, *e.g.* see Fig. 9 of section 3.1 of the book by Coleman [160].

In the context of the paper by 't Hooft which deals mainly with QCD, we should consider internal or virtual  $\sigma$  and  $\pi$  exchanges analogous to gluon exchanges, with the important difference that due to the chiral symmetry we have two types of particles both being in the adjoint representation ( $N^2$  scalars and  $N^2$  pseudoscalars).

Suppose we can define an “effective” Yukawa coupling  $g_Y$  describing the interaction of scalars and pseudoscalar with fermions. For the time being we leave unspecified such a coupling. Let us consider  $N$  large with  $g_Y^2 N$  is fixed and of order one

$$g_Y^2 N \sim \mathcal{O}(1). \quad (5.9)$$

If the theory under consideration is rewritten in terms of the coupling constant  $g_N^2 \equiv g_Y^2 N$ , a  $1/N$  expansion can be formulated straightforwardly.

Then, by keeping track of the flavor indices within a particular Feynman diagram, we can count factors of  $1/N$ . Each fermion carries a flavor index ( $i$ ), which runs from 1 to  $N$ . A virtual  $\sigma, \pi$  exchange carries two flavor indices. This follows from Eq. (5.6) and the Fierz identity (5.7). Each virtual  $\sigma, \pi$  exchange is associated with two Yukawa vertices, therefore giving rise to a pair of Kronecker delta functions connecting the flavor indices of the scattered fermions. In the context of flavor indices, either a  $\sigma$  or  $\pi$  boson can be considered as a propagating fermion-anti-fermion pair carrying double flavor indices.

Whenever a trace over a flavor Kronecker delta function enters into the expression for a particular Feynman diagram, we speak of an index loop. An index loop is easily identified by using the double-line representation of 't Hooft. A fermion propagator is represented by a single index-line (*i.e.* fermion line), whereas each internal scalar, respectively, pseudoscalar propagator is represented by a double index-line. Consequently, whenever, after drawing a particular Feynman diagram, an index-line closes, it forms an index loop giving rise to a factor

$$N = \text{Tr } \delta = \sum_{i=1}^N \delta_{ii}. \quad (5.10)$$

A particular Feynman diagram containing a number of virtual  $\sigma$  and  $\pi$  exchanges is associated with a factor

$$r = g_Y^V N^I, \quad (5.11)$$

where  $V$  is the number of Yukawa vertices, and  $I$  the number of index loops. The factor  $r$  can be written as

$$r = (g_Y^2 N)^{V/2} N^\chi = g_Y^V N^\chi, \quad (5.12)$$

where the Euler characteristic  $\chi$  is given by

$$\chi = 2 - 2H - B, \quad (5.13)$$

with  $H$  the number of “handles”, and  $B$  the number of “holes” of the two dimensional surface to which the Feynman diagram can be associated. The Euler characteristic  $\chi$  is a topological invariant. For instance, the vacuum polarization has the topology of a sphere with a single hole (*i.e.* a disk), where the fermion-loop forms the boundary (*i.e.* hole) of the graph. Thus planar diagrams in the vacuum polarization with  $n$  exchanges of  $\sigma$ ’s and  $\pi$ ’s are associated with a factor

$$r = N(g_Y^2 N)^n. \quad (5.14)$$

Other types of diagrams, *e.g.* diagrams with one crossed  $\sigma$ , respectively,  $\pi$  exchange have the topology of a disk with a handle, hence giving rise to a factor

$$r = N^{-1}(g_Y^2 N)^2. \quad (5.15)$$

However, the sum of such type of vacuum polarization diagrams is zero due to the chiral symmetry.

Since planar diagrams vanish in spin-zero channels such as the SDE for the dynamical mass, the first nonzero contribution is given by diagrams with crossed  $\sigma$  and  $\pi$  exchanges, and vertex corrections. Those type of diagrams have one extra handle as compared with planar graphs. Therefore in zero-spin channels, we should compare *e.g.* graphs with a single handle with the gauge interaction in the planar (ladder) approximation. Furthermore, each handle correspond to a factor  $g_Y^4$ , and since  $g_Y$  is small because of the assumption (5.9),  $g_Y^4$  should be compared with the gauge coupling  $\alpha_0$ . Then, if the following inequality holds

$$\alpha_0 \gg \lambda_Y^2/\pi, \quad \lambda_Y = g_Y^2/4\pi, \quad (5.16)$$

the gauge interaction dominates over four-fermion interactions, and we have an argument supporting the validity of the mean field approach in such channels.

## 5.4 Regularization and the fermion wave function

The inclusion of relevant four-fermion interactions beyond the mean field approach requires a reinvestigation of the SDE for the fermion wave function  $\mathcal{Z}$ . In QED in the quenched approximation, the fermion wave function has a gauge dependent

anomalous dimension. In the Landau gauge, this anomalous dimension vanishes and the fermion wave function equals one ( $\mathcal{Z} = 1$ ). We conjecture that the inclusion of relevant four-fermion interactions does not introduce an anomalous dimension for the fermion wave function other than already introduced by the gauge interactions. Thus, in the Landau gauge, the wave function  $\mathcal{Z}$  is finite though it might deviate from unity. The argument in support of the conjecture stated above is that only one full Yukawa vertex appears in the self-energy part, which means that anomalous dimensions of four-fermion interactions are not canceled. Only two fully dressed Yukawa vertices and a fully dressed scalar composite are renormalization group invariant (anomalous dimensions cancel!).

The consequence is that a remnant power of the cutoff (related to anomalous dimension of a Yukawa vertex) lowers the degree of divergence of the self-energy part from a logarithmic divergence to a finite integral. The question is how to compute the finite correction to  $\mathcal{Z}$ .

The problem of the self-energy SDEs lies in regulating it. In case of the fermion-loops appearing in vacuum polarizations it is possible to introduce Pauli-Villars fields which will regulate the fermion loops. However an additional regularization and fields are needed in order to regulate self-energy parts of the fermion, especially the wave function, since the SDE is naively linearly divergent, and shifts in momentum integration variables are tricky. A momentum shift invariant regularization is by no means trivial to implement. At the moment we do not know how to properly regularize the SDE for  $\mathcal{Z}$ , and how to compute a possible deviation of  $\mathcal{Z}$  from unity in the Landau gauge.

We believe that the conjecture holds irrespectively of the regularization method. Therefore throughout this chapter we assume  $\mathcal{Z} = 1$ . Eventually, a deviation from unity might change the results presented here quantitatively, although this is not expected, since we will use a nonperturbative method introduced by Johnson, Willey, and Baker [46], which is independent of  $\mathcal{Z}$ . The nice feature of the assumption that  $\mathcal{Z} = 1$  is that with the gauge interaction treated in the quenched-ladder approach the chiral and vector Ward–Takahashi identities are preserved, since in channels with spin-zero the planar  $\sigma$  and  $\pi$  exchanges cancel each other.

## 5.5 Scalars, pseudoscalars, and charge screening

Since, in the GNJL model, the scalars and pseudoscalars are neutral states which therefore do not couple to the photon field, their contribution to the vacuum polarization is described indirectly in terms of photon-fermion vertex corrections, and fermion self-energy corrections. Hence, in order to gain some intuition for the role of scalar degrees of freedom on the mechanism of charge screening, we analyze the two-loop contribution arising from  $\sigma$  and  $\pi$  exchanges to the vacuum polarization.

Let us consider a gauge–Higgs–Yukawa type of interaction described by the

Lagrangian

$$\begin{aligned}\mathcal{L}_{GHY} = & -\frac{1}{4}F_{\mu\nu}F^{\mu\nu} + \bar{\psi}i\gamma^\mu\partial_\mu\psi + \frac{1}{2}(\partial_\mu\sigma)^2 + \frac{1}{2}(\partial_\mu\pi)^2 \\ & - e_0\bar{\psi}\gamma^\mu A_\mu\psi - g_Y\bar{\psi}(\sigma + i\gamma_5\pi)\psi - V(\sigma, \pi),\end{aligned}\quad (5.17)$$

where the potential  $V$  contains *e.g.* mass terms, and a  $\sigma^4$  type of interaction (*i.e.* a quartic scalar interaction). For simplicity, we take  $N = 1$ , and we ignore the effect of the potential  $V$ .

The Lagrangian  $\mathcal{L}_{GHY}$  gives rise to the following bare or free propagators for the scalar and pseudoscalar bosons:

$$\Delta_P(p) = \Delta_S(p) = \frac{1}{p^2}. \quad (5.18)$$

In appendix E, the two-loop contribution has been computed for the special case of  $N = 1$  and is given by Eq. (E.49). If the scalar and pseudoscalar fields in Eq. (5.17) are both in the adjoint representation of  $U(N)$ , the result, for arbitrary  $N$ , reads

$$\Pi(q^2) \approx \frac{N\alpha_0}{2\pi} \left( \frac{2}{3} + \frac{\alpha_0}{2\pi} - \frac{N\lambda_Y}{2\pi} \right) \log \left( \frac{\Lambda^2}{q^2} \right) + (\alpha_0/\pi)\mathcal{O}(1), \quad (5.19)$$

with  $\lambda_Y = g_Y^2/4\pi$ . The  $\beta$  function corresponding to such a vacuum polarization is

$$\beta_\alpha(\alpha_0, \lambda_Y) = \frac{N\alpha_0^2}{\pi} \left[ \frac{2}{3} + \frac{\alpha_0}{2\pi} - \frac{N\lambda_Y}{2\pi} \right]. \quad (5.20)$$

The interesting result of this computation is difference in sign between terms corresponding to photon exchanges, and terms corresponding to (pseudo)scalar exchanges. Furthermore, we might be tempted to conclude that a nontrivial root of Eq. (5.20) could be realized whenever  $N\lambda_Y/2\pi \sim 2/3$ . However, the complete situation is more involved. The RG equation for *e.g.*  $\lambda_Y$  should be considered too, *i.e.* we should compute the  $\beta$  functions of  $\lambda_Y$ , and of any quartic scalar coupling. If and only if a nontrivial (nonzero) UV fixed point for  $\lambda_Y$  exists, the realization of a zero of Eq. (5.20) becomes a realistic option. In other words, such a scenario is only possible if the Yukawa interaction  $\lambda_Y$  is nontrivial. The discussion in section 3.5 suggests that in order to obtain a nontrivial Yukawa coupling, the hyperscaling laws should be obeyed.

In this context, we mention that the renormalization of Gauge-Higgs-Yukawa models, with a non-Abelian gauge interaction, has been considered extensively in Ref. [161]. In that paper, it was shown that special nontrivial cases of gauge-Higgs-Yukawa models are equivalent to GNJL models with non-Abelian (asymptotically free) gauge interaction (see also Ref. [162]), hence proving the renormalizability of non-Abelian GNJL models.

Moreover, in appendix E it is shown explicitly that when gauge-invariant four-fermion interactions are treated perturbatively (thus their anomalous dimensions are small), they do not contribute to the vacuum polarization, and consequently  $\beta_\alpha$ . In fact, the conclusion can be drawn beforehand, since the RG of Wilson states that irrelevant interactions cannot affect low-energy effective quantities.

Summarizing, we have illustrated that fundamental scalars and pseudoscalars in a gauge-Higgs-Yukawa system tend to decrease charge screening. On the other-hand, perturbatively irrelevant four-fermion interaction do not contribute to the vacuum polarization. The idea is that, nonperturbatively, close to the critical curve in the GNJL model, the scalar and pseudoscalar Yukawa interactions are nontrivial, and kinetic terms for the scalar and pseudoscalar composites are effectively induced via the appearance of a large anomalous dimension.

## 5.6 The vacuum polarization in the $1/N$ expansion

In studying the vacuum polarization, the usual assumption is to neglect vacuum polarization corrections to internal photon propagators. As explained earlier, such a quenching of internal photon propagators is supposed to be valid close to a fixed point. Thus, following Ref. [46], with the replacement of full photon propagators by the bare ones (*e.g.* Eq. (5.4)), the vacuum polarization should be of the form:

$$\Pi(\mu^2) = \Pi[\mu/\Lambda, \alpha_0] \approx f(\alpha_0) \log \frac{\Lambda^2}{\mu^2} + \mathcal{O}(1). \quad (5.21)$$

The vacuum polarization contains only a single power of  $\log \Lambda$ . Higher powers of  $\log \Lambda$ , which correspond to a higher number of fermion-loops, are absent. Furthermore, the constant term and other small corrections to  $\Pi$  are irrelevant for the question of screening. The vacuum polarization defines a running coupling  $\alpha(\mu)$ ,

$$\alpha(\mu) = \frac{\alpha_0}{1 + \Pi[\mu/\Lambda, \alpha_0]}, \quad (5.22)$$

where we define  $\alpha_0 = \alpha(\Lambda)$ , and the  $\beta$  function Eq. (5.2) at  $\alpha(\mu)$  is

$$\beta_\alpha(\alpha(\mu)) \equiv \mu \frac{d\alpha(\mu)}{d\mu}. \quad (5.23)$$

Since the bare coupling is independent of  $\mu$ , we have the identity

$$\beta_\alpha(\alpha_0) = \lim_{\mu \rightarrow \Lambda} \mu \frac{d\alpha(\mu)}{d\mu} = 2\alpha_0 f(\alpha_0). \quad (5.24)$$

Thus the function  $f(\alpha_0)$  is proportional to the  $\beta$  function, and since it is a non-singular function in  $\alpha_0$  clearly the  $\beta$  function has a Gaussian or trivial fixed point

at  $\alpha_0 = 0$ , *i.e.*,  $\beta_\alpha(0) = 0$ . To obtain an UV fixed point it is essential that, for  $\alpha < \alpha_z$  (where  $\alpha_z$  is a root of  $\beta_\alpha$ ), the  $\beta$  function is positive. Hence, the equation (see Eq. (1.76))

$$\beta_\alpha(\alpha_z) = 0, \quad \beta'_\alpha(\alpha_z) < 0, \quad (5.25)$$

determines an UV fixed point  $\alpha_z$ .

The function  $f(\alpha_0)$  has been studied thoroughly by Johnson *et al.* in Refs. [46, 153, 155] and by Adler [154] in the context of massless QED, these authors write (according to Johnson *et al.* [46])

$$f(\alpha_0) = \frac{N\alpha_0}{2\pi} \left[ \frac{2}{3} + \Phi(\alpha_0) \right], \quad (5.26)$$

where the term with the  $2/3$  is the one-loop vacuum polarization. Johnson *et al.* derived an expression for  $\Phi(\alpha_0)$  in terms of the Bethe-Salpeter (BS) kernel  $K^{(2)}$  as the single unknown Green function. In defining the BS kernels we follow the definitions of Björken and Drell [44]. We mention that, although the strong belief of Johnson *et al.* in the possible existence of an UV fixed point for  $\alpha_0$ , might seem poorly motivated from the point of view of Wilson's RG methods (see Ref [15])<sup>3</sup>, their methods and techniques are still valid and directly applicable to the GNJL model.

The BS kernel  $K^{(1)}$  is defined as the one-boson irreducible fermion-fermion scattering kernel, and the BS kernel  $K^{(2)}$  as the two-fermion one-boson irreducible fermion-fermion scattering kernel. The integral equation between  $K^{(1)}$  and  $K^{(2)}$  is the Bethe-Salpeter equation, which is depicted in Fig. B.2. In appendix F we give a derivation of the Johnson-Willey-Baker (JWB) equation for  $\Phi$ , their result is

$$\Phi(\alpha_0) = \frac{\phi_1 + \phi_2(2 + \phi_2)}{1 - \phi_1} + \phi_3, \quad (5.27)$$

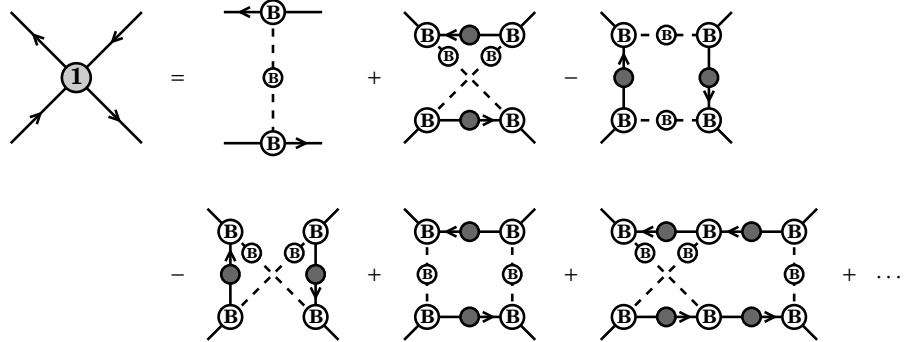
where the functions  $\phi_j$  are identical to the functions  $f_j$  defined by JWB, with

$$\begin{aligned} \phi_1(\alpha_0) &\equiv \sum_{\text{flavors}} -\frac{ie_0^2}{48} \int \frac{d^4 p}{(2\pi)^4} \\ &\times \text{Tr} \left[ \frac{(\gamma^\mu \hat{p} \gamma^\alpha - \gamma^\alpha \hat{p} \gamma^\mu)}{2p^4} K^{(2)}(p, k)(\gamma_\mu \hat{k} \gamma_\alpha - \gamma_\alpha \hat{k} \gamma_\mu) \right], \end{aligned} \quad (5.28)$$

$$\phi_2(\alpha_0) \equiv \sum_{\text{flavors}} -\frac{ie_0^2}{48} \int \frac{d^4 p}{(2\pi)^4} \text{Tr} \left[ \frac{\hat{p} \gamma^\mu \hat{p}}{p^4} K^{(2)\alpha}(p, k)(\gamma_\mu \hat{k} \gamma_\alpha - \gamma_\alpha \hat{k} \gamma_\mu) \right], \quad (5.29)$$

$$\phi_3(\alpha_0) \equiv \sum_{\text{flavors}} \frac{ie_0^2}{48} \int \frac{d^4 p}{(2\pi)^4} \text{Tr} \left[ \frac{\hat{p} \gamma^\mu \hat{p}}{p^4} K_\alpha^{(2)\alpha}(p, k) \hat{k} \gamma_\mu \hat{k} \right]. \quad (5.30)$$

<sup>3</sup>Johnson *et al.* don't explain the dynamical origin of the singular critical behavior, which would be required for the realization of an UV fixed point in QED.

Figure 5.1: Skeleton expansion for  $K^{(1)}$ .

The derivatives of the BS kernels  $K^{(2)}$  are defined in appendix F. Furthermore, Eqs. (5.24), (5.26), and (5.27) give rise to the following  $\beta$  function:

$$\beta_\alpha(\alpha_0) = \frac{N\alpha_0^2}{\pi} \left[ \frac{2}{3} + \frac{\phi_1 + \phi_2(2 + \phi_2)}{1 - \phi_1} + \phi_3 \right]. \quad (5.31)$$

For the BS kernels there exists a so-called skeleton expansion (see also [44]), which is an expansion in topologically distinct Feynman diagrams with all vertices and propagators fully dressed. The skeleton expansion is a special way of resumming the entire set of Feynman diagrams in a consistent manner, *i.e.*, without double counting. The lowest order terms (“lowest” in terms of loops) of the skeleton expansions for  $K^{(1)}$ , respectively,  $K^{(2)}$  are illustrated in Fig. 5.1, respectively, Fig. 5.2.

As was pointed out in section 5.3, the  $1/N$  expansion states that the planar diagrams for the  $\sigma$  and  $\pi$  exchanges are dominant. The approximation for the BS kernel  $K^{(2)}$ , which generates the entire set of planar scalar and pseudoscalar skeleton diagrams for the vacuum polarization is the following: the BS kernel  $K^{(2)}$  is approximated by its “lowest” order skeleton graph, *i.e.*,

$$\begin{aligned} K_{cd,ab}^{(2)}(p, p+q, k+q) &= \frac{\delta_{il}\delta_{kj}}{e_0^2} \left[ \Gamma_{Scb}(k+q, p+q)\Delta_S(k-p)\Gamma_{Sad}(p, k) \right. \\ &\quad + \left. \Gamma_{Pcb}(k+q, p+q)\Delta_P(k-p)\Gamma_{Pad}(p, k) \right] \\ &\quad + \delta_{ij}\delta_{kl}\gamma_{ad}^\mu\gamma_{cb}^\nu D_{\mu\nu}(k-p). \end{aligned} \quad (5.32)$$

The decomposition of the Yukawa vertices in terms of scalar functions is given by Eqs. (2.42) and (2.43). First of all, as was explained in chapter 4, in the symmetric phase the Yukawa vertex structure function  $F_3$  and  $F_4$  are zero, and the scalar and pseudoscalar vertex functions are identical

$$F_1^{(s)} = F_1^{(p)} = F_1, \quad F_2^{(s)} = F_2^{(p)} = F_2, \quad (5.33)$$

and so are the  $\sigma$  and  $\pi$  propagators,  $\Delta_S = \Delta_P$ . Secondly, it was shown in appendix D that the structure function  $F_2$  is rather small compared to the leading structure function  $F_1$ . (it is assumed that  $F_1$  describes the leading asymptotic behavior of the Yukawa vertices). Therefore, we neglect contributions related to the scalar structure function  $F_2$ . Although it might be possible that the contribution coming from gauge interactions is smaller, than corrections resulting from this structure function  $F_2$ , we keep the gauge interaction in order to compare with results mentioned in the literature. Thus, we take for  $K^{(2)}$

$$\begin{aligned} K_{cd,ab}^{(2)}(p, p+q, k+q) &\approx \frac{\delta_{il}\delta_{kj}}{e_0^2} F_1(k+q, p+q) F_1(p, k) \Delta_S(k-p) \\ &\times [\mathbf{1}_{ad}\mathbf{1}_{cb} + i\gamma_5{}_{ad}i\gamma_5{}_{cb}] \\ &+ \delta_{ij}\delta_{kl}D_{\mu\nu}(k-p)\gamma_{ad}^\mu\gamma_{cb}^\nu, \end{aligned} \quad (5.34)$$

where  $F_1$  is given by the ladder SDE (4.8), and  $\Delta_S$  by Eq. (4.1) and (4.14).

With this truncation for the BS kernel  $K^{(2)}$ , we can actually compute the  $\phi_j$  functions (5.28)–(5.30), and subsequently analyze the  $\beta$  function (5.31). We recall that, in the vacuum polarization, the scalars and pseudoscalars give the same contribution in the functions  $\phi_j$ . Moreover the sum over flavor indices yields a factor of  $N$  in the expressions for  $\phi_j$  for contributions corresponding to  $\sigma$  and  $\pi$  exchanges.

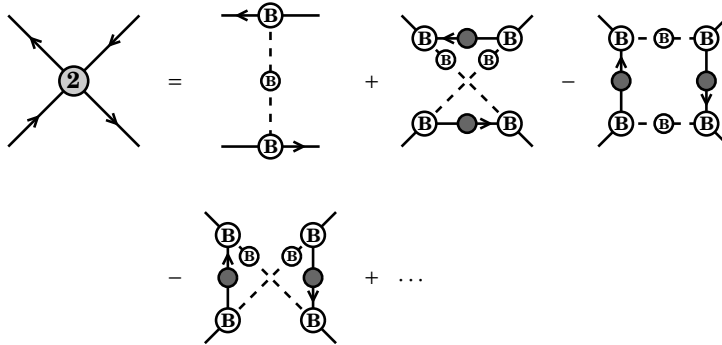


Figure 5.2: Skeleton expansion for  $K^{(2)}$ .

## 5.7 Analysis of the Johnson–Willey–Baker functions

In computing the functions  $\phi_j$ , we initially neglect the ladder photon exchange in Eq. (5.34). Since such contributions were already computed by Johnson *et al.* [46], it will be rather easy to include them later on in the analysis.

It is straightforward to show that, within the proposed approximations,  $\phi_2$  vanishes. Using Eq. (5.34), we obtain that

$$\text{Tr} \left[ \hat{p} \gamma^\mu \hat{p} K^\alpha(p, k) (\gamma_\mu \hat{k} \gamma_\alpha - \gamma_\alpha \hat{k} \gamma_\mu) \right] \propto \text{Tr} \left[ \hat{p} \gamma^\mu \hat{p} (\gamma_\mu \hat{k} \gamma_\alpha - \gamma_\alpha \hat{k} \gamma_\mu) \right] = 0. \quad (5.35)$$

Thus,

$$\phi_2(\alpha_0) = 0. \quad (5.36)$$

What remains is the evaluation of  $\phi_1$  and  $\phi_3$ . With

$$\text{Tr} \left[ (\gamma_\mu \hat{p} \gamma_\alpha - \gamma_\alpha \hat{p} \gamma_\mu) (\gamma^\mu \hat{k} \gamma^\alpha - \gamma^\alpha \hat{k} \gamma^\mu) \right] = -96 p \cdot k, \quad (5.37)$$

the equation for  $\phi_1$  Eq. (5.28) reads

$$\begin{aligned} \phi_1(\alpha_0) &= 2Ni \int_{\Lambda} \frac{d^4 p}{(2\pi)^4} \frac{p \cdot k}{p^4} [F_1(p, k)]^2 \Delta_S(p - k) \\ &= 2Ni \int_{\Lambda} \frac{d^4 p}{(2\pi)^4} \frac{(p + k) \cdot k}{(p + k)^4} [F_1(k + p, k)]^2 \Delta_S(p), \end{aligned} \quad (5.38)$$

where in last step, we have performed a supposedly “harmless”<sup>4</sup> shift of integration, and used the fact that  $F_1$  is symmetric in the fermion momenta,  $F_1(p, k) = F_1(k, p)$ , because of charge conjugation properties, see Eq. (2.44). The factor  $N$  results from the trace of the flavor Kronecker  $\delta$  function, *i.e.* an index line which closes. After a usual Wick rotation

$$\phi_1(\alpha_0) = \frac{N}{8\pi^2} \int_0^{\Lambda^2} dp^2 \int \frac{d\Omega_p}{2\pi^2} \frac{p^2(p \cdot k + k^2)}{(p + k)^4} [F_1(k + p, k)]^2 \Delta_S(p). \quad (5.39)$$

Since the integrals for the functions  $\phi_j$  are finite, the cutoff can be taken to infinity (the continuum limit). This can be written as

$$\lim_{\Lambda \rightarrow \infty} \phi_1(\alpha_0) \approx -N \int_0^{\infty} du G_1(u) + \mathcal{O}((k/\Lambda)_1^\sigma), \quad (5.40)$$

---

<sup>4</sup>The integral is naively logarithmically divergent, therefore translationally invariant.

where  $\sigma_1$  is (again) some positive power,  $u = p^2/k^2$ , and

$$G_1(p^2/k^2) \equiv -\lim_{\Lambda \rightarrow \infty} \frac{1}{8\pi^2} \int \frac{d\Omega_p}{2\pi^2} \frac{k^2 p^2 (k \cdot p + k^2)}{(k + p)^4} [F_1(k + p, k)]^2 \Delta_S(p). \quad (5.41)$$

The function  $G_1$  is defined with a minus sign to make it a positive function, as will be shown to be the case later. The angular integral can be performed if we define the following Chebyshev expansion

$$\frac{k^2(k \cdot p + k^2)}{(k + p)^4} = \sum_{n=0}^{\infty} c_n(k^2, p^2) U_n(\cos \alpha), \quad \cos \alpha = \frac{k \cdot p}{kp}, \quad (5.42)$$

where

$$c_n(k^2, p^2) = \frac{2}{\pi} \int_0^{\pi} d\alpha \sin^2 \alpha U_n(\cos \alpha) \frac{k^2(k \cdot p + k^2)}{(k + p)^4}, \quad (5.43)$$

$$c_n(k^2, p^2) = \frac{(-1)^n}{2} \left[ (2 + n)\theta(k^2 - p^2) \left(\frac{p}{k}\right)^n - n\theta(p^2 - k^2) \left(\frac{k}{p}\right)^{n+2} \right] \quad (5.44)$$

The Chebyshev expansion for the function  $F_1$  was already introduced in Eq. (4.16) (and [40]), and reads

$$F_1(k + p, k) = \sum_{n=0}^{\infty} f_n(k^2, p^2) U_n(\cos \alpha). \quad (5.45)$$

Thus, following analogous derivations in appendix D, the function  $G_1$  can be expressed as

$$G_1(p^2/k^2) = -\lim_{\Lambda \rightarrow \infty} \frac{p^2 \Delta_S(p)}{8\pi^2} \sum_{l,m,n=0}^{\infty} C_{lmn} c_l(k^2, p^2) f_m(k^2, p^2) f_n(k^2, p^2), \quad (5.46)$$

where the constants  $C_{lmn}$  are given in Eq. (D.17). We approximate  $G_1$  by keeping only the lowest order term in the Chebyshev expansion,

$$G_1(p^2/k^2) \approx -\lim_{\Lambda \rightarrow \infty} \frac{p^2 \Delta_S(p)}{8\pi^2} c_0(k^2, p^2) [f_0(k^2, p^2)]^2, \quad (5.47)$$

where  $f_0$  is decomposed into the two channel functions  $F_{\text{UV}}$  and  $F_{\text{IR}}$ , see Eq. (4.23). Then, the asymptotics,  $k^2 \gg p^2$ , respectively,  $p^2 \gg k^2$ , of  $G_1$  are well approximated by the lowest order Chebyshev term (5.47). Again, this is the two channel approximation for the Yukawa vertices of chapter 4. However for momenta  $k^2 \sim p^2$  the channel approximation is not necessarily valid. So, how about  $G_1(1)$ ? Since, from the appendix D, Eq. (D.32), it follows that

$$f_{2n}(k^2, p^2) \geq 0, \quad f_{2n+1}(k^2, p^2) \leq 0, \quad (5.48)$$

from Eq. (D.17) that

$$C_{(2l+1)(2m+1)(2n+1)} = C_{(2l+1)(2m)(2n)} = 0, \quad \forall l, m, n, \quad (5.49)$$

and from Eq. (D.9) that

$$c_n(k^2, k^2) = \frac{(-1)^n}{2} \longrightarrow c_{2n}(k^2, k^2) \geq 0, \quad c_{2n+1}(k^2, k^2) \leq 0. \quad (5.50)$$

Hence, we conclude that all terms of the series

$$\sum_{l,m,n=0}^{\infty} C_{lmn} c_l(k^2, k^2) f_m(k^2, k^2) f_n(k^2, k^2), \quad (5.51)$$

of  $G_1$  are positive, and the lowest order term gives a lower bound on the series,

$$c_0(k^2, k^2) [f_0(k^2, k^2)]^2 \leq \sum_{l,m,n=0}^{\infty} C_{lmn} c_l(k^2, k^2) f_m(k^2, k^2) f_n(k^2, k^2). \quad (5.52)$$

Therefore, the approximation Eq. (5.47) is reliable for the asymptotics  $k^2 \gg p^2$ , and  $p^2 \gg k^2$ . Moreover, Eq. (5.47) is a lower bound on Eq. (5.46) at  $k^2 = p^2$ , so that at least we won't overestimate the contribution of scalar and pseudoscalar composites to the vacuum polarization.

The function  $G_1$  can now be computed, since  $f_0$  is expressed in terms of the channel functions  $F_{\text{UV}}$  and  $F_{\text{IR}}$  of chapter 4. Furthermore, from Eq. (5.44) we see that

$$c_0(k^2, p^2) = \theta(k^2 - p^2). \quad (5.53)$$

and the only nonzero contribution to  $G_1$  of Eq. (5.47) comes from the momenta  $k^2 \geq p^2$ . Thus, using Eqs. (5.47), (5.53), and (4.23), we find

$$G_1(p^2/k^2) \approx -\lim_{\Lambda \rightarrow \infty} \frac{p^2 \Delta_S(p)}{8\pi^2} [F_{\text{UV}}(k^2, p^2)]^2 \theta(k^2 - p^2). \quad (5.54)$$

The ultraviolet channel function  $F_{\text{UV}}$  is proportional to the factor  $Z^{-1}(p^2/\Lambda^2, \omega)$ , Eq. (4.43), and the scalar propagator is proportional to  $Z^2$ . Thus the  $Z$  factors in Eq. (5.54) cancel as was expected and the angular integral Eq. (5.41) can indeed be written in terms of a function which depends only on the ratio of  $p^2/k^2$ .

Recall that the scaling form for the scalar propagator is

$$\frac{p^2 \Delta_S(p)}{8\pi^2} \approx -\frac{1}{2B(\omega)} \left( \frac{p^2}{\Lambda^2} \right)^{1-\omega}, \quad (5.55)$$

where  $B(\omega)$  is given by Eq. (4.65), and  $p^2/\Lambda^2 \ll 1$ . The channel function  $F_{\text{UV}}$  is given by Eq. (4.47), and using the asymptotic form for  $Z(p^2/\Lambda^2, \omega)$  given in Eq. (4.103), the scaling form for  $F_{\text{UV}}$  is

$$\begin{aligned} F_{\text{UV}}(k^2, p^2) &\approx \frac{2}{\gamma(\omega)} \frac{\Gamma(1-\omega)}{(1+\omega)} \left(\frac{\lambda_0}{2}\right)^{\omega/2} \left(\frac{p^2}{\Lambda^2}\right)^{-(1-\omega)/2} \\ &\times \left(\frac{p^2}{k^2}\right)^{1/2} \left[ \gamma(\omega) I_{-\omega} \left(\sqrt{\frac{2\lambda_0 p^2}{k^2}}\right) - \gamma(-\omega) I_\omega \left(\sqrt{\frac{2\lambda_0 p^2}{k^2}}\right) \right], \end{aligned} \quad (5.56)$$

with  $p^2 \leq k^2 \ll \Lambda^2$ . Inserting Eqs. (5.55) and (5.56) in (5.54), we obtain for  $G_1$

$$\begin{aligned} G_1(u) &= \frac{\Gamma(2-\omega)\Gamma(2+\omega)}{8\omega\gamma(\omega)\gamma(-\omega)} \\ &\times u \left[ \gamma(\omega) I_{-\omega} \left(\sqrt{2\lambda_0 u}\right) - \gamma(-\omega) I_\omega \left(\sqrt{2\lambda_0 u}\right) \right]^2 \theta(1-u), \end{aligned} \quad (5.57)$$

where  $u = p^2/k^2$ . Thus Eq. (5.40) is

$$\lim_{\Lambda \rightarrow \infty} \phi_1(\alpha_0) \approx -N\zeta_1(\alpha_0), \quad (5.58)$$

where

$$\zeta_1(\alpha_0) = \int_0^1 du G_1(u) \geq 0. \quad (5.59)$$

The function  $G_1$  is positive, hence  $\phi_1$  is negative. The integral over the function  $G_1$  can be done explicitly by making use of the integral identity 2.15.19.1 in Volume 2 of Prudnikov *et al.* [163]. The result is

$$\begin{aligned} \zeta_1(\alpha_0) &= \frac{1}{\omega} \frac{\lambda_0}{2} \left\{ \frac{1}{(2+\omega)} \frac{\Gamma(1-\omega)\gamma(-\omega)}{\Gamma(1+\omega)\gamma(\omega)} \left(\frac{\lambda_0}{2}\right)^\omega \right. \\ &\times {}_2F_3(2+\omega, 1/2+\omega; 3+\omega, 1+2\omega, 1+\omega; 2\lambda_0) \\ &- {}_2F_3(2, 1/2; 3, 1+\omega, 1-\omega; 2\lambda_0) \\ &+ \frac{1}{(2-\omega)} \frac{\Gamma(1+\omega)\gamma(\omega)}{\Gamma(1-\omega)\gamma(-\omega)} \left(\frac{\lambda_0}{2}\right)^{-\omega} \\ &\times \left. {}_2F_3(2-\omega, 1/2-\omega; 3-\omega, 1-2\omega, 1-\omega; 2\lambda_0) \right\}. \end{aligned} \quad (5.60)$$

The above analysis of the function  $\phi_1$  is repeated for the function  $\phi_3$ . The second derivative of the BS kernel,  $K_\alpha^\alpha(p, k)$  of Eq. (5.34), is

$$K_\alpha^\alpha(p, k) \propto \lim_{q \rightarrow 0} \frac{\partial^2}{\partial q^\alpha \partial q_\alpha} F_1(k+q, p+q). \quad (5.61)$$

The SDE for  $F_1$  (in quenched-ladder approximation) is given by Eq. (4.8)

$$\begin{aligned} F_1(k+q, p+q) &= 1 - i\lambda_0 \int_{\Lambda} \frac{d^4 r}{\pi^2} \frac{(r^2 + (k-p) \cdot r)}{r^2(r+k-p)^2(r-p-q)^2} \\ &\times F_1(r+k-p, r), \end{aligned} \quad (5.62)$$

where we neglect the vertex function  $F_2$ . Thus

$$\begin{aligned} \lim_{q \rightarrow 0} \frac{\partial^2}{\partial q^\alpha \partial q_\alpha} F_1(k+q, p+q) &= -i\lambda_0 \int_{\Lambda} \frac{d^4 r}{\pi^2} \frac{(r^2 + (k-p) \cdot r)}{r^2(r+k-p)^2} F_1(r+k-p, r) \\ &\times \lim_{q \rightarrow 0} \frac{\partial^2}{\partial q^\alpha \partial q_\alpha} \frac{1}{(r-p-q)^2}. \end{aligned} \quad (5.63)$$

By making use of the identity

$$\frac{\partial}{\partial q^\alpha} \frac{\partial}{\partial q_\alpha} \frac{1}{q^2} = -4\pi^2 i \delta^4(q), \quad (5.64)$$

we obtain

$$\begin{aligned} K_\alpha^\alpha(p, k) &= \frac{\delta\delta}{e_0^2} \left[ -4\lambda_0 \frac{p \cdot k}{p^2 k^2} \right] [F_1(p, k)]^2 \Delta_S(p-k) \\ &\times [\mathbf{1}_{ad} \mathbf{1}_{cb} + i\gamma_5{}_{ad} i\gamma_5{}_{cb}], \end{aligned} \quad (5.65)$$

in Minkowsky formulation. Inserting the above expression in Eq. (5.30) the equation  $\phi_3(\alpha_0)$  takes the form

$$\phi_3(\alpha_0) = -\frac{\alpha_0}{\pi} \frac{N}{8\pi^2} \int_0^{\Lambda^2} dp^2 \int \frac{d\Omega_p}{2\pi^2} \frac{p^2}{k^2} \frac{(p \cdot k + k^2)^3}{(p+k)^6} [F_1(k+p, k)]^2 \Delta_S(p). \quad (5.66)$$

Then

$$\lim_{\Lambda \rightarrow \infty} \phi_3(\alpha_0) \approx N \int_0^\infty du G_3(u) + \mathcal{O}((k/\Lambda)^\sigma), \quad (5.67)$$

where  $u = p^2/k^2$ , and

$$G_3(p^2/k^2) \equiv \lim_{\Lambda \rightarrow \infty} -\frac{\alpha_0}{\pi} \frac{1}{8\pi^2} \int \frac{d\Omega_p}{2\pi^2} \frac{p^2(k \cdot p + k^2)^3}{(k+p)^6} [F_1(k+p, k)]^2 \Delta_S(p). \quad (5.68)$$

We define the following Chebyshev expansion

$$\frac{(k \cdot p + k^2)^3}{(k+p)^6} = \sum_{n=0}^{\infty} d_n(k^2, p^2) U_n(\cos \alpha), \quad \cos \alpha = \frac{k \cdot p}{kp}, \quad (5.69)$$

where

$$d_n(k^2, p^2) = \frac{2}{\pi} \int_0^\pi d\alpha \sin^2 \alpha U_n(\cos \alpha) \frac{(p \cdot k + k^2)^3}{(p + k)^6}, \quad (5.70)$$

$$d_0(k^2, p^2) = \left(1 - \frac{3p^2}{4k^2}\right) \theta(k^2 - p^2), \quad (5.71)$$

$$\begin{aligned} d_n(k^2, p^2) &= \frac{(-1)^n}{8} \left\{ n + 1 + \left[ 6 + \sum_{l=0}^{n-1} (4+l) \right] \left(1 - \frac{p^2}{k^2}\right) \right\} \theta(k^2 - p^2) \left(\frac{p}{k}\right)^n \\ &- \frac{(-1)^n}{8} \left\{ n + 1 - \left[ \sum_{l=0}^{n-1} (2-l) \right] \left(1 - \frac{k^2}{p^2}\right) \right\} \theta(p^2 - k^2) \left(\frac{k}{p}\right)^n, \\ n &\geq 1. \end{aligned} \quad (5.72)$$

The function  $G_3$  can be expressed as

$$G_3(p^2/k^2) = \lim_{\Lambda \rightarrow \infty} -\frac{\alpha_0}{\pi} \frac{p^2 \Delta_S(p)}{8\pi^2} \sum_{l,m,n=0}^{\infty} C_{lmn} d_l(k^2, p^2) f_m(k^2, p^2) f_n(k^2, p^2). \quad (5.73)$$

We also approximate  $G_3$  by keeping only the lowest order term in the Chebyshev expansion,

$$G_3(p^2/k^2) \approx \lim_{\Lambda \rightarrow \infty} -\frac{\alpha_0}{\pi} \frac{p^2 \Delta_S(p)}{8\pi^2} d_0(k^2, p^2) [f_0(k^2, p^2)]^2. \quad (5.74)$$

Then, again the asymptotics,  $k^2 \gg p^2$ , respectively,  $p^2 \gg k^2$ , of  $G_3$  are well approximated by the lowest order Chebyshev term (5.47). Moreover, for momenta  $k^2 = p^2$  the approximation Eq. (5.74) is exact, since

$$d_n(k^2, k^2) = 0, \quad \forall n \geq 1. \quad (5.75)$$

Therefore, the approximation Eq. (5.74) is even better than the analogous approximation, Eq. (5.47), to  $G_1$ . Furthermore, from Eq. (5.71) we see that the only nonzero contributions to  $G_3$  of Eq. (5.74) are given by momenta  $k^2 \geq p^2$ . Thus, using Eqs. (5.74), (5.71), and (4.23), we find

$$G_3(p^2/k^2) \approx \lim_{\Lambda \rightarrow \infty} -\frac{\alpha_0}{\pi} \left(1 - \frac{3p^2}{4k^2}\right) \frac{p^2 \Delta_S(p)}{8\pi^2} [F_{UV}(k^2, p^2)]^2 \theta(k^2 - p^2). \quad (5.76)$$

Substituting Eqs. (5.55) and (5.56) in Eq. (5.76), we obtain for  $G_3$

$$\begin{aligned} G_3(u) &= \frac{\alpha_0}{\pi} \left(1 - \frac{3u}{4}\right) \frac{\Gamma(2-\omega)\Gamma(2+\omega)}{8\omega\gamma(\omega)\gamma(-\omega)} \\ &\times u \left[ \gamma(\omega)I_{-\omega}(\sqrt{2\lambda_0 u}) - \gamma(-\omega)I_\omega(\sqrt{2\lambda_0 u}) \right]^2 \theta(1-u), \end{aligned} \quad (5.77)$$

where  $u = p^2/k^2$ . Thus Eq. (5.67) is

$$\lim_{\Lambda \rightarrow \infty} \phi_3(\alpha_0) \approx N\zeta_3(\alpha_0), \quad (5.78)$$

where

$$\zeta_3(\alpha_0) = \int_0^1 du G_3(u) \geq 0. \quad (5.79)$$

The function  $\phi_3$  is positive, and can be computed in the same way as  $\phi_1$ . The result is

$$\zeta_3(\alpha_0) = \frac{\alpha_0}{\pi} [\zeta_1(\alpha_0) - \tau(\alpha_0)], \quad (5.80)$$

where

$$\begin{aligned} \tau(\alpha_0) = & \frac{3}{4\omega} \frac{\lambda_0}{2} \left\{ \frac{1}{(3+\omega)} \frac{\Gamma(1-\omega)\gamma(-\omega)}{\Gamma(1+\omega)\gamma(\omega)} \left(\frac{\lambda_0}{2}\right)^\omega \right. \\ & \times {}_2F_3(3+\omega, 1/2+\omega; 4+\omega, 1+2\omega, 1+\omega; 2\lambda_0) \\ & - \frac{2}{3} {}_2F_3(3, 1/2; 4, 1+\omega, 1-\omega; 2\lambda_0) \\ & + \frac{1}{(3-\omega)} \frac{\Gamma(1+\omega)\gamma(\omega)}{\Gamma(1-\omega)\gamma(-\omega)} \left(\frac{\lambda_0}{2}\right)^{-\omega} \\ & \left. \times {}_2F_3(3-\omega, 1/2-\omega; 4-\omega, 1-2\omega, 1-\omega; 2\lambda_0) \right\}. \end{aligned} \quad (5.81)$$

## 5.8 UV fixed points

In the computation of the functions  $\phi_1$ ,  $\phi_2$ , and  $\phi_3$  the ladder (planar) photon exchanges have been neglected. After reinstating the ladder photon exchange term in Eq. (5.34), we obtain, together with Eqs. (5.58) and (5.78), that

$$\phi_1(\alpha_0) = \frac{\alpha_0}{2\pi} - N\zeta_1(\alpha_0), \quad \phi_2(\alpha_0) = 0, \quad \phi_3(\alpha_0) = N\zeta_3(\alpha_0). \quad (5.82)$$

The ladder photon exchange only contributes to  $\phi_1$ , see again [46]. After substitution of Eq. (5.82) in Eq. (5.31), the  $\beta$  function reads

$$\beta_\alpha(\alpha_0) = \frac{N\alpha_0^2}{\pi} \left[ \frac{2}{3} + \frac{\alpha_0/2\pi - N\zeta_1(\alpha_0)}{1 - \alpha_0/2\pi + N\zeta_1(\alpha_0)} + N\zeta_3(\alpha_0) \right], \quad (5.83)$$

where explicit expressions for  $\zeta_1$  and  $\zeta_3$  are given by Eq. (5.60) and Eq. (5.80).

Let us start analyzing Eq. (5.83) by first considering the properties of the functions  $\zeta_1(\alpha_0)$  and  $\zeta_3(\alpha_0)$ . These functions have been plotted versus  $\alpha_0/\alpha_c$  in Fig. 5.3.

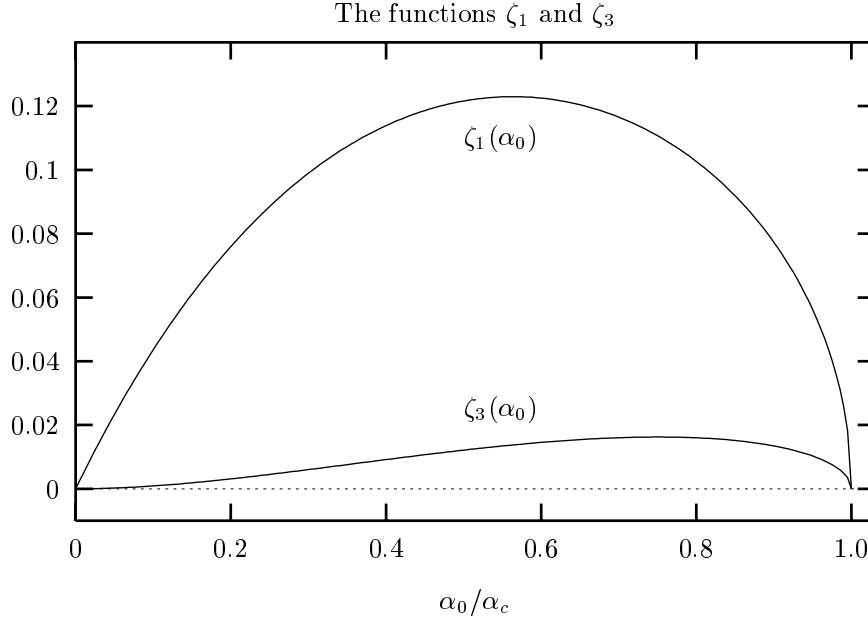


Figure 5.3: The functions  $\zeta_1$  and  $\zeta_3$  plotted versus  $\alpha_0/\alpha_c$ .

Firstly, it is clear that the  $\zeta_1$  and  $\zeta_3$ , are positive, and have a maximum at some intermediate value of  $0 < \alpha_0 < \pi/3$ . For instance,  $\zeta_1$  has a maximum  $\zeta_1 \approx 0.123$  at  $\alpha_0/\alpha_c \approx 0.58$  ( $\omega \approx 0.65$ ). Secondly, the functions  $\zeta_1$  and  $\zeta_3$  vanish at the pure NJL point  $\alpha_0 = 0$ , and at the CPT point  $\alpha_0 = \alpha_c = \pi/3$ . At  $\alpha_0 = 0$ , we can consider this as a reflection of the fact that hyperscaling breaks down due to logarithmic corrections; the ‘‘effective’’ Yukawa coupling is trivial, therefore vanishes, see again the discussion in section 3.5. At  $\alpha_0 = \alpha_c$ , where the critical exponents become singular, the vanishing of  $\zeta_1$  and  $\zeta_3$  is related to the dynamics of the CPT, see sections 3.6 and 4.6. There are no light  $\sigma$  and  $\pi$  exchanges in the symmetric phase which consequently implies the absence of effective Yukawa interactions.<sup>5</sup>

Let us illustrate this by comparing the  $\beta$  function (5.83) with the  $\beta$  function of the gauge-Higgs-Yukawa model (5.17) in the  $1/N$  expansion. Then, the entire set of planar  $\sigma$  and  $\pi$  exchanges is generated by the kernel

$$K_{cd,ab}^{(2)}(p, p+q, k+q) \approx \delta_{il}\delta_{kj} \frac{g_Y^2}{e_0^2} \Delta_S(k-p) [\mathbf{1}_{ad}\mathbf{1}_{cb} + i\gamma_{5ad}i\gamma_{5cb}], \quad (5.84)$$

---

<sup>5</sup>Moreover at the CPT point four-fermion interaction are marginal instead of relevant, and start to mix with the gauge interaction, hence the analysis becomes considerably more complicated.

$$\Delta_S(k-p) = \frac{1}{(k-p)^2}.$$

With such a kernel,  $\phi_2$  and  $\phi_3$  are zero, because the right-hand side of Eq. (5.84) does not depend on the momentum  $q$ . The equation for  $\phi_1$  reads

$$\phi_1 = 2N g_Y^2 i \int_{\Lambda} \frac{d^4 p}{(2\pi)^4} \frac{p \cdot k}{p^4} \frac{1}{(p-k)^2}. \quad (5.85)$$

After a standard Wick rotation, the integral can be performed in the standard way:

$$\begin{aligned} \phi_1 &= -\frac{N\lambda_Y}{2\pi} \int_0^{\Lambda^2} dp^2 \int \frac{d\Omega_p}{2\pi^2} \frac{p \cdot k}{p^2} \frac{1}{(p-k)^2} \\ &= -\frac{N\lambda_Y}{4\pi} \left[ \int_0^{k^2} dp^2 \frac{1}{k^2} + \int_{k^2}^{\Lambda^2} dp^2 \frac{k^2}{p^4} \right] = -\frac{N\lambda_Y}{4\pi} \left[ 2 - \frac{k^2}{\Lambda^2} \right]. \end{aligned} \quad (5.86)$$

Then, taking the cutoff to infinity, we obtain

$$\phi_1(\lambda_Y) = -\frac{N\lambda_Y}{2\pi}. \quad (5.87)$$

Again we introduce the ladder photon exchanges by the replacement

$$\phi_1(\lambda_Y) \longrightarrow \phi_1(\alpha_0, \lambda_Y) = \frac{\alpha_0}{2\pi} - \frac{N\lambda_Y}{2\pi}. \quad (5.88)$$

Hence, in this case, the  $\beta$  function is

$$\beta_{\alpha}(\alpha_0, \lambda_Y) = \frac{N\alpha_0^2}{\pi} \left[ \frac{2}{3} + \frac{\alpha_0/2\pi - N\lambda_Y/2\pi}{1 - \alpha_0/2\pi + N\lambda_Y/2\pi} \right]. \quad (5.89)$$

Comparing the  $\beta$  functions (5.83) and (5.89) leads to the suggestion that  $\zeta_1(\alpha_0)$  is analogous to the Yukawa coupling  $\lambda_Y$  in a gauge-Higgs-Yukawa model,

$$\zeta_1(\alpha_0) \sim \frac{\lambda_Y}{2\pi}. \quad (5.90)$$

This is a crucial point. The general consensus is that for a gauge-Higgs-Yukawa model the Yukawa interaction  $\lambda_Y$  is trivial, thus  $\lambda_Y \rightarrow 0$  in Eq. (5.89). However, the situation is essentially different for  $\zeta_1$  in the GNJL model. There the “effective” coupling  $\zeta_1$  is formed by the exchange of  $\sigma$  and  $\pi$  bosons, with the Yukawa vertices, and (pseudo)scalar propagators fully dressed (*i.e.* the skeleton expansion). The cancellation of the  $Z$  factors, see Eq. (4.104), which is related to the fact that the hyperscaling equations are satisfied, gives rise to a finite nonzero  $\zeta_1(\alpha_0)$  at the

critical curve for  $0 < \alpha_0 < \alpha_c$ . The other nonzero function  $\zeta_3$  results from taking into account fully dressed Yukawa vertices.

Let us now discuss the possible existence of UV fixed points. A necessary but not a sufficient condition for the realization of an UV fixed point is that  $N\zeta_1$  has to be larger than both  $N\zeta_3$  and  $\alpha_0/2\pi$ , and  $N\zeta_1 \sim \mathcal{O}(1)$ . For large  $N$ , the contribution of the planar photon exchanges (represented by the  $\alpha_0/2\pi$  terms) is negligible with respect to  $N\zeta_1$  and  $N\zeta_3$ . Moreover Fig. 5.3 shows, for  $\alpha_0$  small, that  $\zeta_1$  is considerably larger than  $\zeta_3$ . This suggests that only for flavors  $N$  larger than some critical value  $N_c$  UV fixed points can be obtained.

By substituting the expressions (5.60) and (5.80) for  $\zeta_1$  and  $\zeta_3$  in Eq. (5.83), we can straightforwardly analyze the  $\beta$  function graphically. In Fig. 5.4 the  $\beta$  function is plotted for various values of  $N$ . Fig. 5.4 shows that for values of  $N > N_c$ , with  $55 > N_c > 54$ , UV fixed points exists, the largest being  $\alpha_0 \approx 0.14$ ,

$$N = 55 : \quad \beta_\alpha(0.14) \approx 0, \quad (5.91)$$

$$N = 60 : \quad \beta_\alpha(0.1) \approx 0. \quad (5.92)$$

The general pattern is clear; the larger  $N$ , with  $N > N_c$ , the smaller will be the

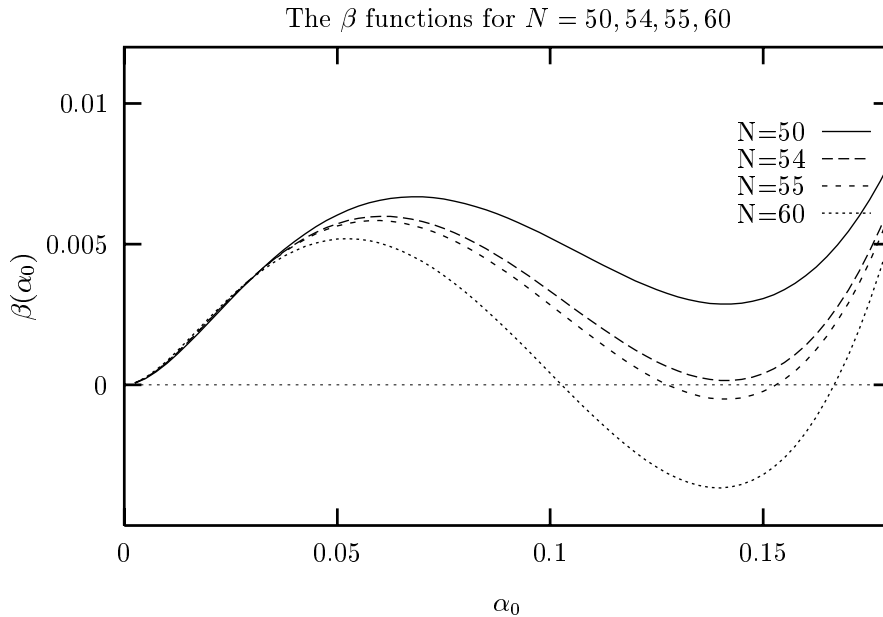


Figure 5.4: Plot of the function  $\beta_\alpha$  versus the gauge coupling  $\alpha_0$  for various values of the fermion flavor number  $N$ .

UV fixed point. Moreover, Fig. 5.4 suggests that the UV fixed points are first order zeros of  $\beta$ , and clearly satisfy Eq. (5.25).

Since we have made use of results obtained in the quenched approximation, we mention that the plots of the  $\beta$  function are (at the most) reliable at or in the vicinity of the UV fixed points at which the quenched approach is self consistent.

In Fig. 5.5, the case of  $N = 60$  fermion flavors is compared with the one-loop  $\beta$  function of QED. For very small values of  $\alpha_0 < 1/100$  indeed the one-loop QED result coincides with that of the GNJL model, however for larger values of  $\alpha_0$  the  $\beta$  function (5.83) deviates from the one-loop expression, and eventually an UV fixed point is realized at  $\alpha_0 \approx 0.1$ .

The analysis shows that a rather large number of flavors,

$$N > N_c \approx 54, \quad (5.93)$$

is required to obtain UV fixed points. From the point of view of the  $1/N$  expansion this seems a consistent result, since other than planar contributions are suppressed by at least factors of (say)  $1/N_c$ . However, from the phenomenological point of view, the result is unsatisfactory, since it implies that the unquenched GNJL model

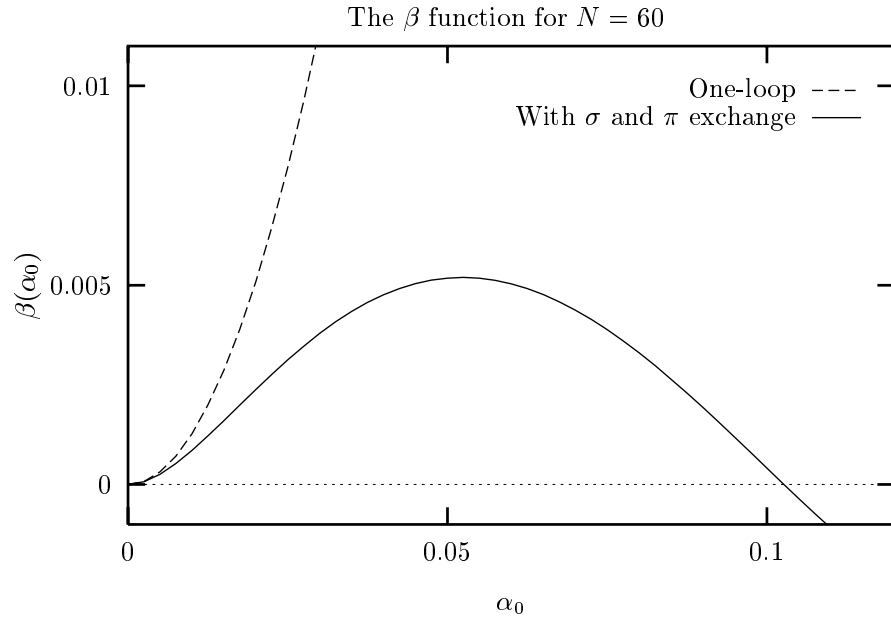


Figure 5.5: The one-loop  $\beta$  function for  $N = 60$  compared with the  $\beta$  function including four-fermion interactions.

(exhibiting UV fixed points) is only practically applicable for models which have at least  $N_c$  fermion flavors (fractions rounded up). Therefore, it is appropriate to discuss how  $N_c$  depends on the approximation.

Firstly, we stress that the second term on the right-hand side in Eq. (5.83) containing the  $\zeta_1$  function causes the suppression of charge screening and is responsible for the possible realization of an UV fixed point. The denominator in the second term is a direct consequence of the resummation of the infinite ladder  $\sigma$  and  $\pi$  exchanges, and it is mainly due to this denominator  $1 + N\zeta_1$  that the critical number of fermion flavors  $N_c$  is large.

Secondly, the existence of an UV fixed point for a specific number of fermion flavors  $N$  depends on the interplay between the functions  $\zeta_1$  and  $\zeta_3$ , which are given in terms of integrals of the functions  $G_1$  and  $G_3$ . Let us recall that the lowest order Chebyshev expansion for  $G_1$ , Eq. (5.47) is a lower bound on  $G_1$  of Eq. (5.46), since all terms of the Chebyshev expansion are positive at  $k^2 = p^2$ , the same cannot be said about  $G_3$  of Eq. (5.74). Thus keeping more terms in the Chebyshev expansion leads to an increase of  $\zeta_1$ , whereas the effect on  $\zeta_3$  is less clear, because of the alternating Chebyshev series for  $\zeta_3$ . Therefore, an improvement of the computation of  $\zeta_1$  will most likely lead to a decrease of the critical flavor number  $N_c$ .

Moreover in computation of the functions  $\zeta_1$  and  $\zeta_3$  we have used Yukawa vertices ( $\Gamma_S$ ) and  $\sigma$  and  $\pi$  propagators ( $\Delta_S$ ) which were obtained in the quenched-ladder approximation. It is an interesting question, whether the improvement of the ladder approximation for the gauge interaction (*e.g.* by including crossed photon exchanges) leads to a increase of  $\zeta_1$ , and thus a decrease of  $N_c$ .

Finally, we recall that we have neglected the effect of the Yukawa vertex function  $F_2$  (Eq. (4.7)), but clearly the inclusion of  $F_2$  in the analysis could change the results quantitatively. Whether such an improvement will tend to increase or decrease  $N_c$  remains unclear at this stage.

### 5.8.1 Close to the NJL point

Let us analyze the interplay between  $\zeta_1$  and  $\zeta_3$  in more detail close to the pure NJL point (*i.e.* for small values of  $\alpha_0$ ) by expanding these functions in  $\alpha_0$ . The computation of the lowest order terms in  $\alpha_0$  of Eqs. (5.60) and (5.80) is laborious but straightforward, therefore we mention just the final results:

$$\zeta_1(\alpha_0) \approx \frac{3\alpha_0}{2\pi} + \mathcal{O}(\alpha_0^2), \quad (5.94)$$

$$\zeta_3(\alpha_0) \approx \frac{15}{16} \frac{\alpha_0^2}{\pi^2} + \mathcal{O}(\alpha_0^3). \quad (5.95)$$

With these expansions in  $\alpha_0$ , the  $\beta$  function Eq. (5.83) reads

$$\beta_\alpha(\alpha_0) = \frac{N\alpha_0^2}{\pi} \left[ \frac{2}{3} - \frac{(3N-1)\alpha_0/2\pi}{1 + (3N-1)\alpha_0/2\pi} + N \frac{15}{16} \frac{\alpha_0^2}{\pi^2} \right]. \quad (5.96)$$

Let us write the  $\beta$  function in terms of the variable

$$x \equiv N\alpha_0/\alpha_c, \quad \alpha_c = \pi/3, \quad (5.97)$$

then

$$\beta_\alpha(\alpha_0) = \frac{N\alpha_0^2}{\pi} \left[ \frac{2}{3} - \frac{(1-1/3N)x}{2+(1-1/3N)x} + \frac{5}{48} \frac{x^2}{N} \right]. \quad (5.98)$$

The equation for the zero of  $\beta_\alpha$  is a third order equation, and a UV fixed point is given by the lowest positive root satisfying Eq. (1.76). The equation is

$$4 - (1-\epsilon)x + \frac{15}{8}\epsilon x^2 + \frac{15}{16}\epsilon(1-\epsilon)x^3 = 0, \quad \epsilon \equiv \frac{1}{3N}. \quad (5.99)$$

The expression for the relevant root is rather ugly. However, in the limit  $N \rightarrow \infty$  keeping  $x$  fixed, the solution is

$$x = \frac{N\alpha_0}{\alpha_c} \approx \left[ 4 + \frac{94}{3} \frac{1}{N} \right], \quad N \rightarrow \infty, \quad x = \text{constant}. \quad (5.100)$$

The critical number of flavors  $N_c$ , below which no UV fixed point can be realized, is given by the following expression

$$\begin{aligned} \frac{1}{N_c} &= \frac{3}{64} \left[ 2209 + 285\sqrt{57} - \sqrt{9505410 + 1259130\sqrt{57}} \right] \implies \\ N_c &\approx 45.42. \end{aligned} \quad (5.101)$$

This  $N_c$  is slightly smaller than the critical number  $N_c \approx 54$ , which was obtained graphically from Fig. 5.4. The value of the root  $x$  at this critical number  $N_c$  is

$$x \approx 6.32131 \implies \alpha_0 \approx 0.146. \quad (5.102)$$

Summarizing, we find, that for  $N > N_c \approx 45$  UV fixed points  $\alpha_0$  ( $\alpha_0 < 0.146$ ) are obtained. Moreover, with the identification Eq. (5.90),  $\lambda_Y = g_Y^2/4\pi$  and the fact that  $\zeta_1$  is of order  $\alpha_0$  the inequality (5.16) is satisfied for  $\alpha_0$  sufficiently small.

## 5.9 Discussion

Relevant four-fermion interactions in four dimensions are possible at the chiral phase transition in the GNJL model. The main objective of this chapter was to study the effect of such “relevant” four-fermion dynamics on the vacuum polarization and to reinvestigate the problem of triviality of  $U(1)$  gauge theories.

To obtain new results, the four-fermion interactions had to be incorporated beyond the commonly used Hartree–Fock or mean-field approach. At the chiral

phase transition (*e.g.* the critical curve Eq. (3.46)) in the quenched GNJL model, the appearance of a large anomalous dimension is believed to turn naively irrelevant interactions into relevant ones.

The crucial feature of the GNJL model is that a nontrivial Yukawa interaction (*i.e.* an interaction between (pseudo)scalars and fermions) exists for  $0 < \alpha_0 < \alpha_c$ . The existence of such a nontrivial Yukawa interaction requires the cancellation of  $Z$  factors<sup>6</sup> in fermion–anti-fermion scattering amplitudes such as the BS kernel  $K^{(2)}$ , and is analogous to the requirement of hyperscaling (see section 3.5). If the hyperscaling equations are satisfied, then only two of the critical exponents are independent, namely  $\eta$  and  $\gamma$ , with

$$\gamma = 1, \quad \eta = 2(1 - \omega), \quad \omega = \sqrt{1 - \alpha_0/\alpha_c}, \quad (5.103)$$

see Eqs. (3.60) and (4.111). We recall that the anomalous dimension  $\eta$  is defined at the critical point, whereas  $\gamma$  describes scaling in the neighborhood of the critical point.<sup>7</sup>

The skeleton expansion for the BS kernel  $K^{(2)}$  provides a natural framework to take into account the anomalous dimension of Yukawa vertices and  $\sigma$  and  $\pi$  propagators. Within the skeleton expansion,  $\sigma$  and  $\pi$  exchanges are described in terms of fully dressed Yukawa vertices and  $\sigma$  and  $\pi$  propagators. The actual computation of the anomalous dimension, and the resolution of the scaling form requires a solution of the SDEs for Yukawa vertices, and  $\sigma$  and  $\pi$  bosons.

In previous work such fully dressed Yukawa vertices and  $\sigma$  and  $\pi$  propagators have been analyzed in the quenched-ladder approximation, see chapter 4, Ref. [40], and references therein. To make use of these results consistently, we used the following approximations. Firstly, we assumed that all dynamics takes place in a region close to an UV fixed point,  $\beta_\alpha(\alpha_0) \approx 0$ . In that case, the quenched approximation is self-consistent. Secondly, the gauge-interaction is considered in the ladder form, with bare vertices. Thirdly, we used the  $1/N$  expansion (with  $N$  the number of fermion flavors) which states that planar  $\sigma$  and  $\pi$  exchanges describe the leading contribution to Green functions for large  $N$ . Then, due to the specific form of the chiral symmetry with both scalars and pseudoscalar in the adjoint representation, we argued that in so-called zero-spin channels (such as Yukawa vertices and  $\sigma$  and  $\pi$  propagators) the planar  $\sigma$  and  $\pi$  exchanges cancel each other for momenta larger than the inverse correlation length (in fact in the symmetric phase this cancellation is exact). The inverse correlation length in the GNJL model is the mass of the  $\sigma$  boson,  $\xi^{-1} = m_\sigma$ . Moreover, an important property of the planar (ladder) approximations is that such truncations respect the vector and chiral Ward–Takahashi identities.

---

<sup>6</sup>The  $Z$  factor is the wave function renormalization constant of the  $\sigma$  and  $\pi$  fields.

<sup>7</sup>These values of the critical exponents are in rather good agreement with lattice simulations, and results obtained by nonperturbative RG techniques, see the discussions in sections 3.8 and 3.9.

The so-called JWB method [46], which is a nonperturbative framework independent of the fermion wave function  $\mathcal{Z}$ , allowed us to compute the contributions of the infinite set of planar  $\sigma$  and  $\pi$  exchanges to the vacuum polarization. The result of the computations is that the GNJL model exhibits an UV fixed point,  $\beta_\alpha(\alpha_0) = 0$ , for any value of  $N$  that exceeds some critical value  $N_c$  ( $N > N_c$ ). This critical number of flavors turned out to be  $N_c \approx 54$ . The larger the number of fermion flavors, the smaller the UV fixed point  $\alpha_0$  will be, provided  $N > N_c$ .

The large value for  $N_c$  puts questions to the applicability of the GNJL. However, we have given a few arguments in the previous section suggesting that  $N_c$  could be rather sensitive to approximations, and that an improvement of the approximations and calculations will probably lead to a smaller value for  $N_c$ .

The mechanism responsible for the realization of an UV fixed point is illustrated by the observation that contributions of planar  $\sigma$  and  $\pi$  exchanges to the vacuum polarization have identical sign, and tend to reduce screening. The four-fermion interactions describe attractive forces between virtual fermion–anti-fermion pairs in the vacuum polarization.

The conventional leading term in the vacuum polarization is the one-loop correction describing the creation of fermion–anti-fermion pairs. These virtual pairs can be considered as dipoles causing the screening; the vacuum is a medium of the insulator type. Such a screening is proportional to the coupling  $\alpha_0$  and proportional to the number of fermion flavors  $N$ . However, if a particular fraction of the total amount of fermion–anti-fermion pairs created are correlated by attractive four-fermion interactions, represented by  $\sigma$  and  $\pi$  exchanges, then clearly these composite neutral states are not capable of screening. Thus the negative term  $N\zeta_1$  in the  $\beta$  function (5.83) represents the contributions and the attractive nature of four-fermion interactions in the vacuum polarization.

It is known that in the quenched approximation, the critical curve and critical exponents are independent of the number of fermion flavors. In the quenched-ladder approximation using the mean-field approach for the four-fermion interactions it is straightforward to derive that this is indeed the case. Clearly, the mechanism of charge screening is flavor dependent, since the total number of virtual fermion–anti-fermion pairs is proportional to  $N$  and the total number of composite scalars and pseudoscalars grows as  $2N^2$ . The larger the number of flavors, the stronger the effect of four-fermion interactions. The fixed point appears when the virtual pairs completely loose the ability to screen.

The existence of an UV fixed point implies a nontrivial continuum limit of the GNJL model with a  $U(1)$  gauge interaction. The analysis presented here suggest that in the full unquenched GNJL model the critical line is replaced by an UV fixed point somewhere on the critical line depending on the number of fermion flavors. If the number of fermion flavors is below some specific value, the critical four-fermion dynamics are not sufficient to yield an UV fixed point. In that case the unquenched GNJL model only has a trivial (IR) fixed point.

Finally, let us briefly compare our results with that obtained by lattice simulations and nonperturbative RG techniques. Although there still is some controversy between different groups performing lattice computations, the standard conclusion of the Desy group (Göckeler *et al.*) is that QED is trivial and that the chiral phase transition is of the mean field type. Our results agree with these conclusions for  $N < N_c$ .

Using nonperturbative RG techniques, it was found in Refs. [41, 134], that within a particular local potential approach the gauge coupling  $\alpha_0$  in GNJL model is trivial. Again for  $N < N_c$  the results agree. However, for large  $N$ , we think that, in order to compare such type of approaches with our results, the RG flows of operators corresponding to the dynamical nature of  $\sigma$  and  $\pi$  exchanges should be taken into account. In the context of NPRG techniques, we think this probably involves taking into account higher (than 6) dimensional chiral invariant operators containing derivatives, such as  $(\partial_\mu(\bar{\psi}\gamma^\mu\psi))^2$ .



## Appendix A

# GNJL model with $U(N)$ symmetry

The gauged NJL model with a global  $U_V(N) \times U_A(N)$  symmetry is described by the Lagrangian (see [3])

$$\begin{aligned} \mathcal{L}_1 = & \bar{\psi}_i (i\gamma^\mu D_\mu - M)_{ij} \psi_j - \frac{1}{4} F_{\mu\nu} F^{\mu\nu} \\ & + \frac{G_0}{2} \sum_{\alpha=0}^{N^2-1} \left[ (\bar{\psi}_i \tau_{ij}^\alpha \psi_j)^2 + (\bar{\psi}_i \tau_{ij}^\alpha (i\gamma_5) \psi_j)^2 \right], \end{aligned} \quad (\text{A.1})$$

where  $D_\mu = \partial_\mu + ie_0 A_\mu$  and where the flavor labels  $i, j$  run from 1 to  $N$ . Of course the symmetry only applies when the (bare) mass matrix  $M$  vanishes. The generators,  $\tau$ , of the  $U(N)$  Lie algebra have the following properties:

$$\tau^{\alpha\dagger} = \tau^\alpha, \quad \text{Tr } \tau^\alpha \tau^\beta = \delta^{\alpha\beta}, \quad (\text{A.2})$$

$$\sum_{\alpha=0}^{N^2-1} \tau_{ij}^\alpha \tau_{kl}^\alpha = \delta_{il} \delta_{kj}. \quad (\text{A.3})$$

The last identity is called the Fierz identity. The Lagrangian is invariant under global  $U_V(N)$  transformations <sup>1</sup>:

$$\psi \longrightarrow \psi'_i = [\exp(i\theta^\alpha \tau^\alpha)]_{ij} \psi_j, \quad (\text{A.4})$$

$$\bar{\psi} \longrightarrow \bar{\psi}'_i = \bar{\psi}_j [\exp(-i\theta^\alpha \tau^\alpha)]_{ji}. \quad (\text{A.5})$$

and under global  $U_A(N)$  transformations:

$$\psi(x) \longrightarrow \psi'_i(x) = [\exp(i\gamma_5 \theta^\alpha \tau^\alpha)]_{ij} \psi_j(x), \quad (\text{A.6})$$

---

<sup>1</sup>We use the standard summation convention, *i.e.* sum over all double indices.

$$\bar{\psi}(x) \longrightarrow \bar{\psi}'_i(x) = \bar{\psi}_j(x) [\exp(i\gamma_5\theta^\alpha\tau^\alpha)]_{ji}. \quad (\text{A.7})$$

In terms of auxiliary spinless fields,  $\sigma^\alpha$  and  $\pi^\alpha$ , the Lagrangian Eq. (A.1) is rewritten as

$$\begin{aligned} \mathcal{L}_2 &= \sum_{i=1}^N \bar{\psi}_i i\gamma^\mu D_\mu \psi_i - \frac{1}{4} F_{\mu\nu} F^{\mu\nu} - \sum_{i,j=1}^N \sum_{\alpha=0}^{N^2-1} \bar{\psi}_i \tau_{ij}^\alpha (\sigma^\alpha + i\gamma_5 \pi^\alpha) \psi_j \\ &- \frac{1}{2G_0} \sum_{\alpha=0}^{N^2-1} [(\sigma^\alpha)^2 + (\pi^\alpha)^2] - 2c^\alpha \sigma^\alpha, \end{aligned} \quad (\text{A.8})$$

where the Euler–Lagrange equations for the auxiliary fields are constraints

$$\sigma^\alpha = -G_0 \bar{\psi}_i \tau_{ij}^\alpha \psi_j, \quad (\text{A.9})$$

$$\pi^\alpha = -G_0 \bar{\psi}_i \tau_{ij}^\alpha (i\gamma_5) \psi_j, \quad (\text{A.10})$$

and  $c^\alpha = \text{Tr}[M\tau^\alpha]$ .

The infinitesimal  $U_V(N)$  transformations for the Lagrangian Eq. (A.8) are

$$\delta\psi_i(x) = i\theta^\beta \tau_{ij}^\beta \psi_j(x), \quad \delta\bar{\psi}_i(x) = -\bar{\psi}_j(x) i\theta^\beta \tau_{ji}^\beta, \quad (\text{A.11})$$

$$\delta\sigma^\alpha(x) = f^{\alpha\beta\gamma} i\theta^\beta \sigma^\gamma(x), \quad \delta\pi^\alpha(x) = f^{\alpha\beta\gamma} i\theta^\beta \pi^\gamma(x), \quad (\text{A.12})$$

where  $\theta$  is small, and the infinitesimal  $U_A(N)$  transformations are

$$\delta\psi_i(x) = i\gamma_5 \theta^\beta \tau_{ij}^\beta \psi_j(x), \quad \delta\bar{\psi}_i(x) = \bar{\psi}_j(x) i\gamma_5 \theta^\beta \tau_{ji}^\beta, \quad (\text{A.13})$$

$$\delta\sigma^\alpha(x) = g^{\alpha\beta\gamma} \theta^\beta \sigma^\gamma(x), \quad \delta\pi^\alpha(x) = -g^{\alpha\beta\gamma} \theta^\beta \pi^\gamma(x). \quad (\text{A.14})$$

The structure constants are defined as

$$[\tau^\alpha, \tau^\beta] = f^{\alpha\beta\gamma} \tau^\gamma, \quad (\text{A.15})$$

$$\{\tau^\alpha, \tau^\beta\} = g^{\alpha\beta\gamma} \tau^\gamma. \quad (\text{A.16})$$

## Appendix B

# Green functions, propagators, and proper vertices

In this appendix we define the Green function, connected Green functions both in coordinate and momentum space, and we define the propagators and proper vertices of the GNJL model. The fermion fields are labeled with a Dirac index (first subscript  $a, b, c, d$ ) and a flavor index (second subscript  $f, i, j, l, k$ ). The scalar and pseudoscalar fields are labeled with flavor indices  $\alpha$  and  $\beta$ . Spinor indices run from 1 to 4, fermion flavor indices from 1 to  $N$  and scalar resp. pseudoscalar indices from 0 to  $N^2 - 1$ .

In what follows  $\mathbf{J}$  represents the set of sources  $\mathbf{J} = (J, \eta, \bar{\eta}, J_\sigma, J_\pi)$ .

### B.1 Green functions of the GNJL model

The Green function are defined as time order vacuum-to-vacuum expectation values of the fields. First we define the appropriate one-point Green functions:

$$iD_{\alpha}^{(1)} = \langle 0 | \sigma^\alpha | 0 \rangle = \frac{1}{i} \frac{\delta Z[\mathbf{J}]}{\delta J_\sigma^\alpha(x)} \Big|_{\mathbf{J}=0}, \quad (\text{B.1})$$

$$iD_{\alpha}^{(1)} = \langle 0 | \pi^\alpha | 0 \rangle = \frac{1}{i} \frac{\delta Z[\mathbf{J}]}{\delta J_\pi^\alpha(x)} \Big|_{\mathbf{J}=0}. \quad (\text{B.2})$$

The one-point function are independent of coordinates  $x$  due to invariance under space-time translation. The two point Green functions are

$$iD_{\mu\nu}^{(2)}(z, z') \equiv \langle 0 | T(A_\mu(z) A_\nu(z')) | 0 \rangle$$

$$= \left( \frac{1}{i} \right)^2 \frac{\delta^2 Z[\mathbf{J}]}{\delta J^\nu(z') \delta J^\mu(z)} \Big|_{\mathbf{J}=0}, \quad (\text{B.3})$$

$$\begin{aligned} iD_{\frac{ab}{ij}}^{(2)}(x, y) &\equiv \langle 0 | T(\psi_{ai}(x) \bar{\psi}_{bj}(y)) | 0 \rangle \\ &= \left( \frac{1}{i} \right)^2 \frac{\delta^2 Z[\mathbf{J}]}{\delta \eta_{bj}(y) \delta \bar{\eta}_{ai}(x)} \Big|_{\mathbf{J}=0}, \end{aligned} \quad (\text{B.4})$$

$$\begin{aligned} iD_{\frac{SS}{\alpha\beta}}^{(2)}(x, y) &\equiv \langle 0 | T(\sigma^\alpha(x) \sigma^\beta(y)) | 0 \rangle \\ &= \left( \frac{1}{i} \right)^2 \frac{\delta^2 Z[\mathbf{J}]}{\delta J_\sigma^\beta(y) \delta J_\sigma^\alpha(x)} \Big|_{\mathbf{J}=0}, \end{aligned} \quad (\text{B.5})$$

$$\begin{aligned} iD_{\frac{PP}{\alpha\beta}}^{(2)}(x, y) &\equiv \langle 0 | T(\pi^\alpha(x) \pi^\beta(y)) | 0 \rangle \\ &= \left( \frac{1}{i} \right)^2 \frac{\delta^2 Z[\mathbf{J}]}{\delta J_\pi^\beta(y) \delta J_\pi^\alpha(x)} \Big|_{\mathbf{J}=0}, \end{aligned} \quad (\text{B.6})$$

the three-point Green functions are

$$\begin{aligned} iD_{\frac{ab}{ij}\mu}^{(3)}(x, y, z) &\equiv \langle 0 | T(\psi_{ai}(x) \bar{\psi}_{bj}(y) A_\mu(z)) | 0 \rangle \\ &= \left( \frac{1}{i} \right)^3 \frac{\delta^3 Z[\mathbf{J}]}{\delta J^\mu(z) \delta \eta_{bj}(y) \delta \bar{\eta}_{ai}(x)} \Big|_{\mathbf{J}=0}, \end{aligned} \quad (\text{B.7})$$

$$\begin{aligned} iD_{\frac{abS}{ij\alpha}}^{(3)}(x, y, z) &\equiv \langle 0 | T(\psi_{ai}(x) \bar{\psi}_{bj}(y) \sigma^\alpha(z)) | 0 \rangle \\ &= \left( \frac{1}{i} \right)^3 \frac{\delta^3 Z[\mathbf{J}]}{\delta J_\sigma^\alpha(z) \delta \eta_{bj}(y) \delta \bar{\eta}_{ai}(x)} \Big|_{\mathbf{J}=0}, \end{aligned} \quad (\text{B.8})$$

$$\begin{aligned} iD_{\frac{abP}{ij\alpha}}^{(3)}(x, y, z) &\equiv \langle 0 | T(\psi_{ai}(x) \bar{\psi}_{bj}(y) \pi^\alpha(z)) | 0 \rangle \\ &= \left( \frac{1}{i} \right)^3 \frac{\delta^3 Z[\mathbf{J}]}{\delta J_\pi^\alpha(z) \delta \eta_{bj}(y) \delta \bar{\eta}_{ai}(x)} \Big|_{\mathbf{J}=0}, \end{aligned} \quad (\text{B.9})$$

and the four-point Green function is

$$\begin{aligned} iD_{\frac{ab,cd}{i_1j_1,i_2j_2}}^{(4)}(x_1, y_1, x_2, y_2) &\equiv \langle 0 | T(\psi_{ai_1}(x_1) \psi_{ci_2}(x_2) \bar{\psi}_{bj_1}(y_1) \bar{\psi}_{dj_2}(y_2)) | 0 \rangle \\ &= \left( \frac{1}{i} \right)^4 \frac{\delta^4 Z[\mathbf{J}]}{\delta \eta_{dj_2}(y_2) \delta \eta_{bj_1}(y_1) \delta \bar{\eta}_{ci_2}(x_2) \delta \bar{\eta}_{ai_1}(x_1)} \Big|_{\mathbf{J}=0}. \end{aligned} \quad (\text{B.10})$$

## B.2 Connected Green functions

By making use of Wick's theorem, we derive the connected Green functions from the Green function of the previous section by subtracting all disconnected parts, for

instance:

$$\begin{aligned} \langle 0 | T(\sigma^\alpha(x)\sigma^\beta(y)) | 0 \rangle &= \langle 0 | \sigma^\alpha(x) | 0 \rangle \langle 0 | \sigma^\beta(y) | 0 \rangle \\ &+ \langle 0 | T(\sigma^\alpha(x)\sigma^\beta(y)) | 0 \rangle_{\text{connected}}. \end{aligned} \quad (\text{B.11})$$

Thus we define

$$iD_{\mu\nu}(z - z') = iD_{\mu\nu}^{(2)}(z, z'), \quad (\text{B.12})$$

$$\delta_{ij}iS_{ab}^{(i)}(x - y) = iD_{\frac{ab}{ij}}^{(2)}(x, y), \quad (\text{B.13})$$

$$i\Delta_S^{(\alpha)}(x - y) = iD_{\frac{ss}{\alpha\alpha}}^{(2)}(x, y) - \langle 0 | \sigma^\alpha | 0 \rangle^2, \quad (\text{B.14})$$

$$i\Delta_P^{(\alpha)}(x - y) = iD_{\frac{pp}{\alpha\alpha}}^{(2)}(x, y) - \langle 0 | \pi^\alpha | 0 \rangle^2, \quad (\text{B.15})$$

$$\delta_{ij}iC_{ab\mu}^{(3)(i)}(x, y, z) = iD_{\frac{ab}{ij}\mu}^{(3)}(x, y, z), \quad (\text{B.16})$$

$$iC_{\frac{ab}{ij}\alpha}^{(3)}(x, y, z) = iD_{\frac{ab}{ij}\alpha}^{(3)}(x, y, z) - \delta_{ij}iS_{ab}^{(i)}(x - y)\langle 0 | \sigma^\alpha | 0 \rangle, \quad (\text{B.17})$$

$$iC_{\frac{ab}{ij}\alpha}^{(3)}(x, y, z) = iD_{\frac{ab}{ij}\alpha}^{(3)}(x, y, z) - \delta_{ij}iS_{ab}^{(i)}(x - y)\langle 0 | \pi^\alpha | 0 \rangle, \quad (\text{B.18})$$

and the connected four-point function

$$\begin{aligned} iC_{\frac{ab}{ij_1}\frac{cd}{ij_2}}^{(4)}(x_1, y_1, x_2, y_2) &= iD_{\frac{ab}{ij_1}\frac{cd}{ij_2}}^{(4)}(x_1, y_1, x_2, y_2) \\ &- \delta_{ij_2} \delta_{ij_1} iS_{cb}^{(i_2)}(x_2 - y_1) iS_{ad}^{(i_1)}(x_1 - y_2) \\ &+ \delta_{ij_1} \delta_{ij_2} iS_{ab}^{(i_1)}(x_1 - y_1) iS_{cd}^{(i_2)}(x_2 - y_2). \end{aligned} \quad (\text{B.19})$$

### B.3 Fourier transforms

For the two-point functions, we have the following Fourier transforms:

$$iD_{\mu\nu}(z - z') = \int \frac{d^4 k}{(2\pi)^4} e^{-ik(z-z')} iD_{\mu\nu}(k), \quad (\text{B.20})$$

$$iS_{ab}^{(f)}(x - y) = \int \frac{d^4 k}{(2\pi)^4} e^{-ik(x-y)} iS_{ab}^{(f)}(k), \quad (\text{B.21})$$

$$i\Delta_S^{(\alpha)}(x - y) = \int \frac{d^4 k}{(2\pi)^4} e^{-ik(x-y)} i\Delta_S^{(\alpha)}(k), \quad (\text{B.22})$$

$$i\Delta_P^{(\alpha)}(x - y) = \int \frac{d^4 k}{(2\pi)^4} e^{-ik(x-y)} i\Delta_P^{(\alpha)}(k). \quad (\text{B.23})$$

The Fourier transform of the vertices are

$$iC_{ab\mu}^{(3)(f)}(x, y, z) = \int \frac{d^4 k d^4 p}{(2\pi)^8} e^{-ik(x-z)+ip(y-z)} iD_{\nu\mu}(k - p)$$

$$\times \left[ iS^{(f)}(k)(-ie_0)\Gamma^{(f)\nu}(k,p)iS^{(f)}(p) \right]_{ab}, \quad (\text{B.24})$$

$$\begin{aligned} iC_{\substack{abS \\ ij\alpha}}^{(3)}(x,y,z) &= \int \frac{d^4k d^4p}{(2\pi)^8} e^{-ik(x-z)+ip(y-z)} i\Delta_S^{(\alpha)}(k-p) \\ &\times \left[ iS^{(i)}(k)(-i)\Gamma_{Sij}^{\alpha}(k,p)iS^{(j)}(p) \right]_{ab}, \end{aligned} \quad (\text{B.25})$$

$$\begin{aligned} iC_{\substack{abS \\ ij\alpha}}^{(3)}(x,y,z) &= \int \frac{d^4k d^4p}{(2\pi)^8} e^{-ik(x-z)+ip(y-z)} i\Delta_P^{(\alpha)}(k-p) \\ &\times \left[ iS^{(i)}(k)(-i)\Gamma_{Pij}^{\alpha}(k,p)iS^{(j)}(p) \right]_{ab}, \end{aligned} \quad (\text{B.26})$$

where the  $\Gamma$ 's represent the amputated vertices or proper vertices in momentum space. Finally, the connected four-point function has the Fourier transform

$$\begin{aligned} iC_{\substack{ab,cd \\ i_1 j_1, i_2 j_2}}^{(4)}(x_1, y_1, x_2, y_2) &= \int \frac{d^4k_1 d^4p_1 d^4k_2}{(2\pi)^{12}} e^{-ik_1(x_1-y_2)+ip_1(y_1-y_2)-ik_2(x_2-y_2)} \\ &\times iS_{aa'}^{(i_1)}(k_1)iS_{cc'}^{(i_2)}(k_2)(-ie_0^2)K_{\substack{a'b',c'd' \\ i_1 j_1, i_2 j_2}}^{(0)}(k_1, p_1, k_2)iS_{b'b}^{(j_1)}(p_1)iS_{d'd}^{(j_2)}(k_1 - p_1 + k_2). \end{aligned} \quad (\text{B.27})$$

## B.4 The Bethe–Salpeter scattering kernel

The 2-fermion 1-photon-scalar-pseudoscalar irreducible Bethe–Salpeter kernel is defined via the Bethe–Salpeter equation

$$\begin{aligned} (-ie_0^2)K_{\substack{ab,cd \\ i_1 j_1, i_2 j_2}}^{(1)}(k_1, p_1, k_2) &= (-ie_0^2)K_{\substack{ab,cd \\ i_1 j_1, i_2 j_2}}^{(2)}(k_1, p_1, k_2) \\ &+ \sum_{l=1}^N \sum_{m=1}^N \int \frac{d^4r}{(2\pi)^4} (-ie_0^2)K_{\substack{ab,c'd' \\ i_1 j_1, l m}}^{(1)}(k_1, p_1, r + p_1)iS_{d'a'}^{(m)}(r + k_1) \\ &\times (-ie_0^2)K_{\substack{a'b',cd \\ ml, i_2 j_2}}^{(2)}(r + k_1, r + p_1, k_2)iS_{b'c'}^{(l)}(r + p_1), \end{aligned} \quad (\text{B.28})$$

where  $K^{(1)}$  is defined as the 1-particle irreducible part of  $K^{(0)}$ , and is defined explicitly as follows:

$$\begin{aligned} (-ie_0^2)K_{\substack{ab,cd \\ i_1 j_1, i_2 j_2}}^{(0)}(k_1, p_1, k_2) &= (-ie_0^2)K_{\substack{ab,cd \\ i_1 j_1, i_2 j_2}}^{(1)}(k_1, p_1, k_2) \\ &- \delta_{i_1 j_1}(-ie_0)\Gamma_{ab}^{(i_1)\mu}(k_1, p_1)iD_{\mu\nu}(k_1 - p_1)\delta_{i_2 j_2}(-ie_0)\Gamma_{cd}^{(i_2)\nu}(k_2, k_1 - p_1 + k_2) \\ &- \sum_{\alpha=0}^{N^2-1} (-i)\Gamma_{S_{i_1 j_1}^{ab}}^{(\alpha)}(k_1, p_1)i\Delta_S^{(\alpha)}(k_1 - p_1)(-i)\Gamma_{S_{i_2 j_2}^{cd}}^{(\alpha)}(k_2, k_1 - p_1 + k_2) \\ &- \sum_{\alpha=0}^{N^2-1} (-i)\Gamma_{P_{i_1 j_1}^{ab}}^{(\alpha)}(k_1, p_1)i\Delta_P^{(\alpha)}(k_1 - p_1)(-i)\Gamma_{P_{i_2 j_2}^{cd}}^{(\alpha)}(k_2, k_1 - p_1 + k_2). \end{aligned} \quad (\text{B.29})$$

Note that the minus signs in the three one-particle exchange graphs on the righthand side come from the fact that such types of diagrams are related to the expectation value  $\langle \psi_a \bar{\psi}_b \psi_c \bar{\psi}_d \rangle = -\langle \psi_a \psi_c \bar{\psi}_b \bar{\psi}_d \rangle$ .

Eqs. (B.29) and (B.28) are depicted in Figs. B.1 and B.2.

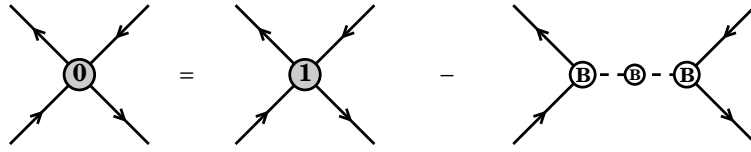


Figure B.1: Definition of the 1-boson irreducible scattering kernel,  $K^{(1)}$ .

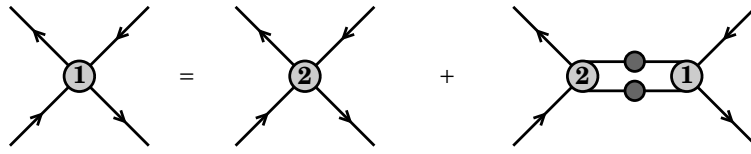


Figure B.2: Definition of the Bethe–Salpeter kernel,  $K^{(2)}$ .



# Appendix C

## Feynman rules

- The bare fermion propagator:

$$\overrightarrow{b_j} \xrightarrow{p} \overrightarrow{a_i} = i\delta_{ij} \frac{(\hat{p} + m_{(i)})_{ab}}{p^2 - m_{(i)}^2}, \quad (\text{C.1})$$

where  $M_{ij} = m_{(i)}\delta_{ij}$ , the diagonal mass matrix.

- The full fermion propagator:

$$\overrightarrow{b_j} \xrightarrow{p} \bullet \xrightarrow{p} \overrightarrow{a_i} = i\delta_{ij} S_{ab}^{(i)}(p). \quad (\text{C.2})$$

- The bare photon propagator:

$$\overbrace{\mu}^{\text{wavy}} \xrightarrow{q} \overbrace{\nu}^{\text{wavy}} = \frac{i}{q^2} \left[ -g_{\mu\nu} + \frac{q_\mu q_\nu}{q^2} \right], \quad (\text{C.3})$$

in the Landau gauge.

- The full photon propagator:

$$\overbrace{\mu}^{\text{wavy}} \bullet \overbrace{\nu}^{\text{wavy}} = iD_{\mu\nu}(q). \quad (\text{C.4})$$

- The bare scalar and pseudoscalar propagators are identical:

$$\overbrace{\alpha}^{\text{dashed}} \cdots \overbrace{\alpha}^{\text{dashed}} = -iG_0. \quad (\text{C.5})$$

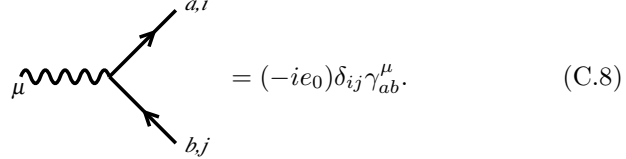
- The full scalar propagator:

$$\overbrace{\alpha}^{\text{dashed}} \cdots \bullet \overbrace{\alpha}^{\text{dashed}} = i\Delta_S^{(\alpha)}(q). \quad (\text{C.6})$$

- The full pseudoscalar propagator:

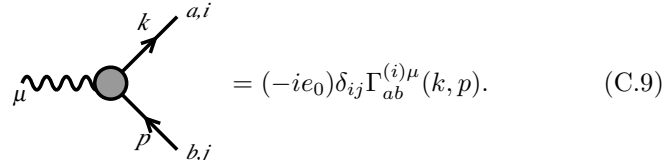
$$\overline{\alpha} \cdots \textcircled{P} \cdots \alpha = i\Delta_P^{(\alpha)}(q). \quad (\text{C.7})$$

- The bare photon-fermion vertex:



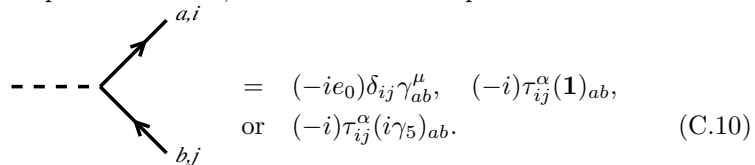
$$= (-ie_0)\delta_{ij}\gamma_{ab}^\mu. \quad (\text{C.8})$$

- The full photon-fermion vertex:



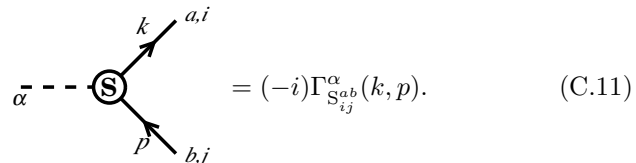
$$= (-ie_0)\delta_{ij}\Gamma_{ab}^{(i)\mu}(k, p). \quad (\text{C.9})$$

- Either the bare photon-fermion, bare scalar or bare pseudoscalar vertex:



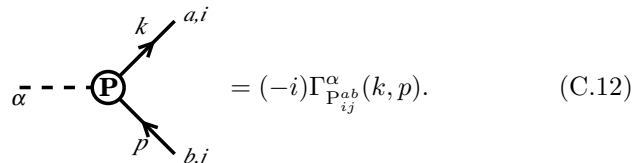
$$= (-ie_0)\delta_{ij}\gamma_{ab}^\mu, \quad (-i)\tau_{ij}^\alpha(\mathbf{1})_{ab}, \\ \text{or} \quad (-i)\tau_{ij}^\alpha(i\gamma_5)_{ab}. \quad (\text{C.10})$$

- The full scalar vertex:



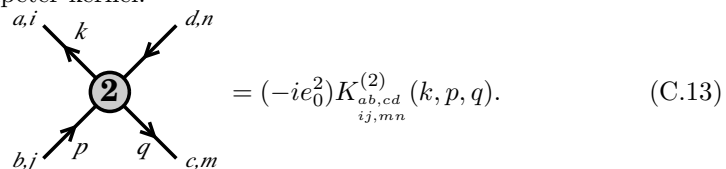
$$= (-i)\Gamma_{S_{ij}^{ab}}^\alpha(k, p). \quad (\text{C.11})$$

- The full pseudoscalar vertex:



$$= (-i)\Gamma_{P_{ij}^{ab}}^\alpha(k, p). \quad (\text{C.12})$$

- The Bethe-Salpeter kernel:



$$= (-ie_0^2)K_{ij, mn}^{(2)}(k, p, q). \quad (\text{C.13})$$

- A Minkowskian four-momentum integral for each closed loop:

$$\int_{\Lambda} \frac{d^4 k}{(2\pi)^4} \quad (C.14)$$

- An extra minus sign for each closed fermion-loop:

$$(-1) \quad \quad \quad (C.15)$$

- For each internal fermion line a sum over all flavors:

$$\sum_{i=1}^N \quad \quad \quad (C.16)$$

- For each internal ‘boson’ line a sum over all bosonic propagators:

$$\text{---} \text{---} \textcircled{\text{B}} \text{---} \overset{q}{\text{---}} = iD_{\mu\nu}(q) + \sum_{\alpha=0}^{N^2-1} \left[ i\Delta_{\text{S}}^{(\alpha)}(q) + i\Delta_{\text{P}}^{(\alpha)}(q) \right]. \quad (\text{C.17})$$

- The ‘boson’ vertex, internal or external, represents either one of the vertices:



$$= (-ie_0)\delta_{ij}\Gamma_{ab}^{(i)\mu}(k, p), \quad (-i)\Gamma_{S_{ij}^{ab}}^{\alpha}(k, p),$$

or  $(-i)\Gamma_{P_{ij}^{ab}}(k, p).$  (C.18)

- The bare axial-vector vertex:

$$\mu = (-i)(\gamma^\mu \gamma_5)_{ab}. \quad (\text{C.19})$$

- The full axial-vector vertex ( $N = 1$ ):

$$= (-i)\Gamma_{5ab}^\mu(k, p). \quad (\text{C.20})$$



## Appendix D

# Analysis of the Chebyshev expansion

In this appendix we discuss the validity of the zeroth-order Chebyshev expansion for the Yukawa vertex function  $F_1$  introduced in section 4.2. The problem of angular dependence in the SDEs for the Yukawa vertex functions  $F_1$  and  $F_2$  is replaced by an infinite set of Chebyshev harmonics. Subsequently this set is truncated to the lowest order harmonic of  $F_1$ , which is the only harmonic having nonhomogeneous ultraviolet boundary conditions because of the presence of the (angular independent) inhomogeneous term 1.

As mentioned previously, the method of using expansions in terms of Chebyshev polynomials  $U_n(x)$  (of the second kind) was used before [10, 164, 165]. These polynomials are orthogonal with respect to the angular integration  $\int d\Omega$ . In the analysis of BSEs in Ref. [10] a  $CP$  invariant Chebyshev expansion was used, which has the nice property of keeping only even terms in the expansion. However, we use a slightly different expansion (not explicitly  $CP$  invariant) which has the disadvantage of also including odd terms in the Chebyshev expansion, but the advantages that the integral equation for the zeroth order harmonic is more “friendly” and the zeroth order harmonic coincides with both the large fermion momentum limit ( $p^2 \gg q^2$ ) as well the large boson-momentum limit ( $q^2 \gg p^2$ ) of the Yukawa vertex, see Fig. 4.4.

Thus the vertex functions satisfying the SDEs (4.8) are expanded in the angle between fermion momentum  $p$  and scalar boson  $q$ , *i.e.*,  $p \cdot q$ , in the following way:

$$F_1(p+q, p) = \sum_{n=0}^{\infty} f_n(p^2, q^2) U_n(\cos \alpha), \quad (\text{D.1})$$

$$F_2(p+q, p) = \sum_{n=0}^{\infty} g_n(p^2, q^2) U_n(\cos \alpha), \quad (\text{D.2})$$

$$\frac{1}{(r-p)^2} = \sum_{n=0}^{\infty} N_n(r^2, p^2) U_n(\cos \beta), \quad (\text{D.3})$$

$$A_1(r, q) = \sum_{n=0}^{\infty} a_n(r^2, q^2) U_n(\cos \gamma), \quad (\text{D.4})$$

$$A_2(r, q) = \sum_{n=0}^{\infty} b_n(r^2, q^2) U_n(\cos \gamma), \quad (\text{D.5})$$

where

$$\cos \alpha = \frac{p \cdot q}{pq}, \quad \cos \beta = \frac{p \cdot r}{pr}, \quad \cos \gamma = \frac{q \cdot r}{qr}. \quad (\text{D.6})$$

The vertex functions and kernels  $A_1$  and  $A_2$  were defined in Eq. (4.7), respectively, Eq. (4.15). The coefficients  $N_n$ ,  $a_n$ , and  $b_n$  are

$$N_n(r^2, p^2) = \frac{\theta(r^2 - p^2)}{r^2} \left(\frac{p}{r}\right)^n + \frac{\theta(p^2 - r^2)}{p^2} \left(\frac{r}{p}\right)^n, \quad (\text{D.7})$$

and

$$a_0(r^2, q^2) = \frac{1}{2} \left[ \left(2 - \frac{q^2}{r^2}\right) \theta(r^2 - q^2) + \frac{r^2}{q^2} \theta(q^2 - r^2) \right], \quad (\text{D.8})$$

$$a_n(r^2, q^2) = (-1)^n \frac{(r^2 - q^2)}{2} \left[ \frac{\theta(r^2 - q^2)}{r^2} \left(\frac{q}{r}\right)^n + \frac{\theta(q^2 - r^2)}{q^2} \left(\frac{r}{q}\right)^n \right], \quad n \geq 1, \quad (\text{D.9})$$

and

$$b_0(r^2, q^2) = \frac{1}{2} \left[ \frac{q^2(q^2 - 3r^2)}{r^2} \theta(r^2 - q^2) + \frac{r^2(r^2 - 3q^2)}{q^2} \theta(q^2 - r^2) \right], \quad (\text{D.10})$$

$$b_1(r^2, q^2) = -\frac{1}{2} \left[ \frac{q^3(q^2 - 2r^2)}{r^3} \theta(r^2 - q^2) + \frac{r^3(r^2 - 2q^2)}{q^3} \theta(q^2 - r^2) \right], \quad (\text{D.11})$$

$$b_n(r^2, q^2) = (-1)^n \frac{(r^2 - q^2)^2}{2} \left[ \frac{\theta(r^2 - q^2)}{r^2} \left(\frac{q}{r}\right)^n + \frac{\theta(q^2 - r^2)}{q^2} \left(\frac{r}{q}\right)^n \right], \quad n \geq 2. \quad (\text{D.12})$$

The equations for the scalar vertex functions (4.8) and scalar vacuum polarization (4.14) are expressed in terms of an infinite set of equations between the harmonics. Hence

$$\Pi_S(q^2) = \frac{1}{4\pi^2} \int_0^{\Lambda^2} dk^2 \sum_{n=0}^{\infty} [a_n(k^2, q^2) f_n(k^2, q^2) + b_n(k^2, q^2) g_n(k^2, q^2)], \quad (\text{D.13})$$

and with Eqs. (4.9) and (4.10) using Eqs. (D.3) and (D.5), we get for the harmonics of  $F_1$

$$\begin{aligned} f_l(p^2, q^2) &= \delta_{0,l} + \frac{\lambda_0}{(l+1)} \int_0^{\Lambda^2} dr^2 N_l(r^2, p^2) \sum_{m=0}^{\infty} \sum_{n=0}^{\infty} C_{lmn} \\ &\times [a_m(r^2, q^2) f_n(r^2, q^2) + b_m(r^2, q^2) g_n(r^2, q^2)], \end{aligned} \quad (\text{D.14})$$

where

$$C_{lmn} \equiv \frac{2}{\pi} \int_0^{\pi} d\gamma \sin^2 \gamma U_l(\cos \gamma) U_m(\cos \gamma) U_n(\cos \gamma). \quad (\text{D.15})$$

In the derivation of Eq. (D.14) use has been made of the fact that

$$\frac{1}{\pi \sin \gamma} \int_{-1}^1 d \cos \alpha \int_{\cos(\alpha+\gamma)}^{\cos(\alpha-\gamma)} d \cos \beta U_m(\cos \alpha) U_n(\cos \beta) = \delta_{m,n} \frac{U_n(\cos \gamma)}{n+1}. \quad (\text{D.16})$$

The symmetric index  $C_{lmn}$  can be calculated using product properties of the Chebyshev polynomials, giving

$$\begin{aligned} C_{(2l)mn} &= \sum_{k=0}^l (\delta_{2k,|m-n|} - \delta_{2k,n+m+2}), \\ C_{(2l+1)mn} &= \sum_{k=0}^l (\delta_{2k+1,|m-n|} - \delta_{2k+1,n+m+2}), \quad l = 0, 1, 2, \dots \end{aligned} \quad (\text{D.17})$$

Then the first two equations for the coefficients  $f_n(p^2, q^2)$  of vertex function  $F_1$  read

$$\begin{aligned} f_0(s, t) &= 1 + \lambda_0 \int_0^{\Lambda^2} du N_0(u, s) \sum_{m=0}^{\infty} \left[ a_m(u, t) f_m(u, t) \right. \\ &\quad \left. + b_m(u, t) g_m(u, t) \right], \end{aligned} \quad (\text{D.18})$$

$$\begin{aligned} f_1(s, t) &= \frac{\lambda_0}{2} \int_0^{\Lambda^2} du N_1(u, s) \sum_{m=0}^{\infty} \left[ a_{m+1}(u, t) f_m(u, t) + a_m(u, t) f_{m+1}(u, t) \right. \\ &\quad \left. + b_{m+1}(u, t) g_m(u, t) + b_m(u, t) g_{m+1}(u, t) \right], \end{aligned} \quad (\text{D.19})$$

where we have introduced the variables

$$s = p^2, \quad t = q^2, \quad u = r^2. \quad (\text{D.20})$$

In principle there is an equivalent set of equations for the coefficients  $g_n$  of  $F_2$ . However we did not succeed in finding explicit expression for these, due to our inability to compute explicitly the angular integrals given by kernels  $K_{21}$  and  $K_{22}$  of Eqs. (4.11) and (4.12). The problem is to compute the integrals

$$\int \frac{d\Omega_p}{2\pi^2} \int \frac{d\Omega_r}{2\pi^2} U_n(\cos \alpha) K_{21}(p, q, r), \quad \int \frac{d\Omega_p}{2\pi^2} \int \frac{d\Omega_q}{2\pi^2} U_n(\cos \alpha) K_{21}(p, q, r). \quad (\text{D.21})$$

The main approximation used in chapter 4 is Eq. (4.22), *i.e.* the replacement of the Yukawa vertex by the zeroth-order harmonic of  $F_1$ . In what follows we estimate the error made by such an approximation. We define the error  $E(q^2)$  in computation of the scalar vacuum polarization Eq. (D.13) as follows:

$$\Pi_S(q^2) = \frac{1}{4\pi^2} \int_0^{\Lambda^2} dk^2 a_0(k^2, q^2) f_0(k^2, q^2) + E(q^2), \quad (\text{D.22})$$

where

$$E(q^2) \equiv \frac{1}{4\pi^2} \int_0^{\Lambda^2} dk^2 \left[ \sum_{n=1}^{\infty} a_n(k^2, q^2) f_n(k^2, q^2) + \sum_{n=0}^{\infty} b_n(k^2, q^2) g_n(k^2, q^2) \right]. \quad (\text{D.23})$$

For an estimation of  $E(q^2)$  we need to know more about the harmonics  $f_n$ ,  $n \geq 1$ , and  $g_n$ ,  $n \geq 0$ . The solution to these harmonics is assumed to be governed by the harmonic  $f_0$  only, since the integral over the harmonic  $f_0$  acts as the largest inhomogeneous term in the integral equations for the higher order harmonics. So the equations for the higher order harmonics are approximated by

$$g_n(p^2, q^2) \approx \lambda_0 \int_0^{\Lambda^2} dr^2 \int \frac{d\Omega_p}{2\pi^2} \int \frac{d\Omega_r}{2\pi^2} U_n(\cos \alpha) K_{21}(p, q, r) f_0(r^2, q^2), \quad (\text{D.24})$$

$$f_n(p^2, q^2) \approx \frac{\lambda_0}{(n+1)} \int_0^{\Lambda^2} dr^2 N_n(r^2, p^2) a_n(r^2, q^2) f_0(r^2, q^2), \quad n \geq 1. \quad (\text{D.25})$$

Unfortunately there is no explicit expression for Eq. (D.24) for the reason described above. However it is possible to approximate the angular average by considering either one of the three momenta in  $K_{21}(p, q, r)$  to be much smaller than the other two. Then the dependence on one of the three angles between the momenta is lost,

and the integration can be performed explicitly. The result for the lowest harmonic of  $F_2$ , *i.e.*,  $g_0$  given by Eq. (D.24), is

$$(s < t) \quad g_0(s, t) \approx \frac{\lambda_0}{12} \int_0^s du \frac{u}{s^2 t} F_{\text{IR}}(u, t) + \frac{\lambda_0}{12} \int_s^t du \frac{1}{st} F_{\text{IR}}(u, t) \\ + \frac{\lambda_0}{12} \int_t^{\Lambda^2} du \frac{1}{u^2} F_{\text{UV}}(u, t), \quad (\text{D.26})$$

$$(s > t) \quad g_0(s, t) \approx \frac{\lambda_0}{12} \int_0^t du \frac{u}{s^2 t} F_{\text{IR}}(u, t) + \frac{\lambda_0}{12} \int_t^s du \frac{1}{s^2} F_{\text{UV}}(u, t) \\ + \frac{\lambda_0}{12} \int_s^{\Lambda^2} du \frac{1}{u^2} F_{\text{UV}}(u, t), \quad (\text{D.27})$$

and for Eq. (D.25) with Eqs (D.7) and (D.9)

$$(s < t) \quad f_1(s, t) \approx -\frac{\lambda_0}{4} \int_0^s du \frac{u-t}{st} \sqrt{\frac{u^2}{st}} F_{\text{IR}}(u, t) \\ - \frac{\lambda_0}{4} \int_s^t du \frac{u-t}{ut} \sqrt{\frac{s}{t}} F_{\text{IR}}(u, t) \\ - \frac{\lambda_0}{4} \int_t^{\Lambda^2} du \frac{u-t}{u^2} \sqrt{\frac{st}{u^2}} F_{\text{UV}}(u, t), \quad (\text{D.28})$$

$$(s > t) \quad f_1(s, t) \approx -\frac{\lambda_0}{4} \int_0^t du \frac{u-t}{st} \sqrt{\frac{u^2}{st}} F_{\text{IR}}(u, t) \\ - \frac{\lambda_0}{4} \int_t^s du \frac{u-t}{us} \sqrt{\frac{t}{s}} F_{\text{UV}}(u, t) \\ - \frac{\lambda_0}{4} \int_s^{\Lambda^2} du \frac{u-t}{u^2} \sqrt{\frac{st}{u^2}} F_{\text{UV}}(u, t), \quad (\text{D.29})$$

where  $s = p^2$ ,  $t = q^2$ , and we have used Eq. (4.23). These equations can be analyzed in detail once the solutions for the channel functions, Eqs. (4.46) and (4.47), are known. But for obtaining the asymptotic behavior of the harmonics  $g_0$  and  $f_1$  it is sufficient to use the asymptotics of the channels, *i.e.*, take  $F_{\text{IR}}(p^2, q^2) \rightarrow F_{\text{IR}}(0, q^2) \propto (q^2/\Lambda^2)^{\omega/2-1/2}$ ,  $F_{\text{UV}}(p^2, q^2) \rightarrow F_{\text{UV}}(p^2, 0) \propto (p^2/\Lambda^2)^{\omega/2-1/2}$ . This gives for the harmonics

$$g_0(p^2, q^2) \propto \lambda_0 \frac{1}{p^2} F_{\text{UV}}(p^2, 0), \quad f_1(p^2, q^2) \propto \lambda_0 \frac{q}{p} F_{\text{UV}}(p^2, 0), \quad p^2 \gg q^2 \quad (\text{D.30})$$

$$g_0(p^2, q^2) \propto \lambda_0 \frac{1}{p^2} F_{\text{IR}}(0, q^2), \quad f_1(p^2, q^2) \propto \lambda_0 \frac{p}{q} F_{\text{IR}}(0, q^2), \quad q^2 \gg p^2. \quad (\text{D.31})$$

The above equations give the leading behavior (in either  $q/p \ll 1$  or  $p/q \ll 1$ ) of the harmonics  $g_0$ ,  $f_1$  in terms of  $f_0$  up to some  $\lambda_0$ -dependent factor, which is  $\mathcal{O}(1)$

(thus nonsingular in  $\lambda_0$ ). Furthermore, from Eq. (D.25) we get the relation

$$\frac{f_{n+1}(p^2, q^2)}{f_n(p^2, q^2)} \propto -\frac{q}{p}, \quad p^2 \gg q^2, \quad \frac{f_{n+1}(p^2, q^2)}{f_n(p^2, q^2)} \propto -\frac{p}{q}, \quad q^2 \gg p^2, \quad (\text{D.32})$$

and we assume a similar relation to hold between the harmonics  $g_{n+1}$  and  $g_n$ . Thus the series

$$S(p^2, q^2) \equiv \sum_{m=0}^{\infty} [a_m(p^2, q^2)f_m(p^2, q^2) + b_m(p^2, q^2)g_m(p^2, q^2)], \quad (\text{D.33})$$

which occurs both in the equation for  $f_0$ , Eq. (D.18), and for  $\Pi_S$ , Eq. (D.13), will be rapidly converging for either  $p^2 \gg q^2$  or  $p^2 \ll q^2$ , since

$$\frac{a_{n+1}(p^2, q^2)f_{n+1}(p^2, q^2)}{a_n(p^2, q^2)f_n(p^2, q^2)} \approx \frac{\min(p^2, q^2)}{\max(p^2, q^2)} \ll 1, \quad (\text{D.34})$$

and again a similar equation for the part containing the harmonics  $g_n$ . At  $p^2 = q^2$  only three terms of the series  $S$ , Eq. (D.33), contribute, since  $a_n(p^2, p^2) = 0$  for  $n \geq 1$  and  $b_n(p^2, p^2) = 0$  for  $n \geq 2$ . Hence, a straightforward approximation for the series  $S$  is

$$S(p^2, q^2) \approx a_0(p^2, q^2)f_0(p^2, q^2) + \mathcal{O}(a_1(p^2, q^2)f_1(p^2, q^2)) + \mathcal{O}(b_0(p^2, q^2)g_0(p^2, q^2)), \quad (\text{D.35})$$

supporting Eq. (4.22). With the expressions obtained for  $f_1$  and  $g_0$ , Eqs. (D.30) and (D.31), the leading term of the error  $E$  defined in Eq. (D.23) can be estimated. The leading term of the error  $E(q^2)$  is given by

$$\begin{aligned} E(q^2) &\approx \frac{1}{4\pi^2} \int_0^{\Lambda^2} dk^2 [a_1(k^2, q^2)f_1(k^2, q^2) + b_0(k^2, q^2)g_0(k^2, q^2)] \\ &\sim \lambda_0 \int_{q^2}^{\Lambda^2} dk^2 \frac{q^2}{k^2} F_{\text{UV}}(k^2, q^2 = 0) + \text{next-to-leading} \\ &\sim \Lambda^2 \left[ (1 + \mathcal{O}(\lambda_0)) \left( \frac{q^2}{\Lambda^2} \right)^{\omega/2+1/2} - (1 + \mathcal{O}(\lambda_0)) \frac{q^2}{\Lambda^2} \right], \end{aligned} \quad (\text{D.36})$$

where we have kept only leading terms and for  $F_{\text{UV}}(p^2, 0) = F_1(p, p)$  given by Eq. (4.48). Recall that  $\omega = \sqrt{1 - 4\lambda_0}$ . The estimation of Eq. (D.36) can be checked more explicitly by using the solutions obtained in section 4.2 for the channel functions  $F_{\text{IR}}$ ,  $F_{\text{UV}}$ , Eqs. (4.46) and (4.47).

Eq. (D.36) shows that when  $\lambda_0 = 0$ ,  $\omega = 1$ , the error  $E$  vanishes, and when  $\omega < 1$  clearly the terms in the error can be neglected with respect to the first two terms on the right-hand side of  $\Pi_S(q^2)$ , see Eq. (4.64). Thus this analysis supports the assumption Eq. (4.22) made in section 4.2 and the error  $E$  contributes only to next-to-next-to-leading order in  $q^2/\Lambda^2$ . And therefore we may conclude that our approximation gives correct leading and next-to-leading behavior of  $\Pi_S(q^2)$ .



## Appendix E

# Two-loop vacuum polarization

In this appendix we compute two-loop vacuum polarization corrections including  $\sigma$  and  $\pi$  exchanges.

### E.1 Two-loop vacuum polarization

In this section, we compute the two-loop vacuum polarization in QED. We derive the two-loop contribution by making use of the one-loop computation of the photon-fermion vertex [69, 70].

The SDE for vacuum polarization tensor reads

$$\Pi^{\mu\nu}(q^2) = ie_0^2 \int_{\Lambda} \frac{d^4 k}{(2\pi)^4} \text{Tr} [\gamma^\mu S(k+q) \Gamma^\nu(k+q, k) S(k)]. \quad (\text{E.1})$$

Assuming that the WTIs are respected, the vacuum polarization tensor is transverse:

$$\Pi^{\mu\nu}(q^2) = [-q^2 g^{\mu\nu} + q^\mu q^\nu] \Pi(q^2) \quad (\text{E.2})$$

If so, we find that

$$\Pi(q^2) = -\frac{ie_0^2}{3q^2} \int_{\Lambda} \frac{d^4 k}{(2\pi)^4} \text{Tr} [\gamma_\mu S(k+q) \Gamma^\mu(k+q, k) S(k)]. \quad (\text{E.3})$$

Let us write and denote the one-loop vertex and self-energy corrections with a subscript (1) as follows

$$\Gamma^\mu(k, p) = \gamma^\mu + \Gamma_{(1)}^\mu(k, p), \quad S(p) = \frac{\hat{p}}{p^2} [1 + \mathcal{Z}_{(1)}(p^2)]. \quad (\text{E.4})$$

The vacuum polarization up to two-loop corrections can be expressed as

$$\Pi(q^2) = \Pi_{(1)}(q^2) + \Pi_{(2a)}(q^2) + \Pi_{(2b)}(q^2), \quad (\text{E.5})$$

where

$$\Pi_{(1)}(q^2) = -\frac{ie_0^2}{3q^2} \int_{\Lambda} \frac{d^4 k}{(2\pi)^4} \frac{\text{Tr} \left[ \gamma_{\mu}(\hat{k} + \hat{q}) \gamma^{\mu} \hat{k} \right]}{(k + q)^2 k^2}, \quad (\text{E.6})$$

$$\begin{aligned} \Pi_{(2a)}(q^2) &= -\frac{ie_0^2}{3q^2} \int_{\Lambda} \frac{d^4 k}{(2\pi)^4} \frac{\text{Tr} \left[ \gamma_{\mu}(\hat{k} + \hat{q}) \gamma^{\mu} \hat{k} \right]}{(k + q)^2 k^2} \\ &\quad \times \left[ \mathcal{Z}_{(1)}((k + q)^2) + \mathcal{Z}_{(1)}(k^2) \right], \end{aligned} \quad (\text{E.7})$$

$$\Pi_{(2b)}(q^2) = -\frac{ie_0^2}{3q^2} \int_{\Lambda} \frac{d^4 k}{(2\pi)^4} \frac{\text{Tr} \left[ \gamma_{\mu}(\hat{k} + \hat{q}) \Gamma_{(1)}^{\mu}(k + q, k) \hat{k} \right]}{(k + q)^2 k^2}. \quad (\text{E.8})$$

The one-loop vacuum polarization  $\Pi_{(1)}$  can be computed straightforwardly

$$\Pi_{(1)}(q^2) = \frac{\alpha_0}{3\pi} \left[ \log \left( \frac{\Lambda^2}{q^2} \right) - 2 \frac{\Lambda^2}{q^2} + \mathcal{O}(1) \right], \quad (\text{E.9})$$

where  $q^2$  is an Euclidean momentum. The quadratically divergent contribution  $\Lambda^2/q^2$  is a notorious artifact of computing vacuum polarization corrections in the presence of a hard cutoff (*i.e.* an explicit cutoff in the momentum integrations instead of Pauli–Villars regularization, see for a recent discussion Ref. [59]). The quadratically divergent term is proportional to the  $g_{\mu\nu}$  tensor in the vacuum polarization tensor, and it ruins the transversality of  $\Pi_{\mu\nu}$ . This cutoff problem can be circumvented by making use of a projector  $g_{\mu\nu} - 4q_{\mu}q_{\nu}/q^2$ , which by contraction with the vacuum polarization tensor eliminates the term in  $\Pi_{\mu\nu}$  proportional to the  $g_{\mu\nu}$  tensor. With such a projector we obtain

$$\Pi_{(1)}(q^2) = \frac{\alpha_0}{3\pi} \left[ \log \left( \frac{\Lambda^2}{q^2} \right) + \mathcal{O}(1) \right], \quad (\text{E.10})$$

which is the well-known one-loop vacuum polarization.

We write

$$\Gamma_{(1)}^{\mu}(k, p) = \Gamma_{L(1)}^{\mu}(k, p) + \Gamma_{R(1)}^{\mu}(k, p) + \Gamma_{I(1)}^{\mu}(k, p), \quad (\text{E.11})$$

where  $\Gamma_{L(1)}^{\mu}$  is the one-loop longitudinal part of the vertex, and where  $\Gamma_{R(1)}$  and  $\Gamma_{I(1)}^{\mu}$  are one-loop transverse parts:

$$\Gamma_{R(1)}^{\mu}(k, p) = T_8^{\mu}(k, p) \tau_8(k^2, p^2, q^2), \quad (\text{E.12})$$

$$\begin{aligned} \Gamma_{I(1)}^{\mu}(k, p) &= T_2^{\mu}(k, p) \tau_2(k^2, p^2, q^2) + T_3^{\mu}(k, p) \tau_3(k^2, p^2, q^2) \\ &\quad + T_6^{\mu}(k, p) \tau_6(k^2, p^2, q^2), \quad q^2 = (k - p)^2. \end{aligned} \quad (\text{E.13})$$

Furthermore, we write

$$\Pi_{(2b)}(q^2) = \Pi_{(2L)}(q^2) + \Pi_{(2R)}(q^2) + \Pi_{(2I)}(q^2), \quad (\text{E.14})$$

where

$$\Pi_{(2j)}(q^2) = -\frac{ie_0^2}{3q^2} \int_{\Lambda} \frac{d^4 k}{(2\pi)^4} \frac{\text{Tr} \left[ \gamma_{\mu}(\hat{k} + \hat{q}) \Gamma_{j(1)}^{\mu}(k + q, k) \hat{k} \right]}{(k + q)^2 k^2}, \quad (\text{E.15})$$

with  $j = L, R, I$ .

As was shown by Ball and Chiu [69], the (one-loop) longitudinal vertex can be written as

$$\begin{aligned} \Gamma_{L(1)}^{\mu}(k, p) &= \frac{\gamma^{\mu}}{2} \left[ -\mathcal{Z}_{(1)}(k^2) - \mathcal{Z}_{(1)}(p^2) \right] \\ &+ \frac{(k + p)^{\mu}(\hat{k} + \hat{p})}{2(k^2 - p^2)} \left[ -\mathcal{Z}_{(1)}(k^2) + \mathcal{Z}_{(1)}(p^2) \right]. \end{aligned} \quad (\text{E.16})$$

By construction, the Ball–Chiu expression for the longitudinal vertex satisfies the WTI

$$q_{\mu} \Gamma_{L(1)}^{\mu}(k, p) = -\hat{k} \mathcal{Z}_{(1)}(k^2) + \hat{p} \mathcal{Z}_{(1)}(p^2). \quad (\text{E.17})$$

For QED, the one-loop vertex and self-energy corrections are

$$\Gamma_{(1)}^{\mu}(k, p) = -ie_0^2 \int_{\Lambda} \frac{d^4 w}{(2\pi)^4} \frac{\gamma^{\lambda}(\hat{k} - \hat{w}) \gamma^{\mu}(\hat{p} - \hat{w}) \gamma_{\lambda}}{(k - w)^2 (p - w)^2 w^2}, \quad (\text{E.18})$$

and

$$\hat{p} \mathcal{Z}_{(1)}(p^2) = -ie_0^2 \int_{\Lambda} \frac{d^4 w}{(2\pi)^4} \frac{\gamma^{\lambda}(\hat{p} - \hat{w}) \gamma_{\lambda}}{(p - w)^2 w^2}, \quad (\text{E.19})$$

in the Feynman gauge.

How can one compute the contributions given in Eq. (E.15)? Since the one-loop transverse vertex functions themselves are finite, *i.e.* these function are independent of the cut-off  $\Lambda$ , the leading logarithmic contributions to the vacuum polarization result from integrations over momenta  $k^2 \gg q^2$  in  $\Pi_{(2R)}$  and  $\Pi_{(2I)}$ . These leading logarithmic contribution can be found by first deriving the  $k^2 \gg q^2$  asymptotic behavior of the transverse structure functions, after which the integration over angles can be performed. In the Feynman gauge  $\xi = 1$ , the asymptotic behavior  $k^2 \gg q^2$  of the  $\tau$ 's is

$$\tau_2 \approx \frac{\alpha_0}{24\pi} \frac{1}{k^4}, \quad (\text{E.20})$$

$$\tau_3 \approx \frac{\alpha_0}{6\pi} \frac{1}{k^2} \log\left(\frac{q^2}{k^2}\right) - \frac{29}{72} \frac{\alpha_0}{\pi} \frac{1}{k^2}, \quad (\text{E.21})$$

$$\tau_6 \approx \frac{(2k \cdot q + q^2)}{2} \frac{\alpha_0}{24\pi} \frac{1}{k^4}, \quad (\text{E.22})$$

$$\tau_8 \approx -\frac{\alpha_0}{2\pi} \frac{1}{k^2}, \quad (\text{E.23})$$

where  $k^2$  is a Minkowskian momentum. Using such asymptotic expressions, the integration over angles in  $\Pi_{(2R)}$  and  $\Pi_{(2I)}$  can be performed straightforwardly, and the integrations over momenta  $k^2 \geq q^2$  leads to logarithmic corrections. Let us give an example, and compute, in this way,  $\Pi_{(2R)}$ . After evaluating the trace in Eq. (E.15) (with  $j = R$ ), and Wick rotating to Euclidean momenta, the expression for  $\Pi_{(2R)}$  reads

$$\begin{aligned} \Pi_{(2R)}(q^2) &= \frac{2\alpha_0}{3\pi} \int_0^{\Lambda^2} dk^2 \int \frac{d\Omega_k}{2\pi^2} \left[ \frac{k^2 q^2 - (k \cdot q)^2}{q^2(k+q)^2} \right] \tau_8(-(k+q)^2, -k^2, -q^2) \\ &\approx \frac{2\alpha_0}{3\pi} \int_{q^2}^{\Lambda^2} dk^2 \frac{3}{4} \frac{\alpha_0}{2\pi} \frac{1}{k^2} \approx \frac{\alpha_0^2}{\pi^2} \left[ \frac{1}{4} \log\left(\frac{\Lambda^2}{q^2}\right) + \mathcal{O}(1) \right]. \end{aligned} \quad (\text{E.24})$$

The result is that the logarithmic corrections of  $\tau_2$  and  $\tau_6$  cancel each other, and that the contributions of  $\tau_3$  contain a  $\log^2$  term:

$$\Pi_{(2I)}(q^2) \approx \frac{\alpha_0^2}{\pi^2} \left[ \frac{1}{24} \log^2\left(\frac{\Lambda^2}{q^2}\right) + \frac{29}{144} \log\left(\frac{\Lambda^2}{q^2}\right) + \mathcal{O}(1) \right]. \quad (\text{E.25})$$

An analogous computation can be performed for the self-energy and longitudinal vertex corrections.

Due to the Ball–Chiu expression (E.16) for  $\Gamma_{L(1)}^\mu$ , the contributions  $\Pi_{(2a)}$  and  $\Pi_{(2L)}$  depend on the one-loop computation of the self-energy  $\mathcal{Z}_{(1)}$ . Since we have chosen  $w$  to be the photon momentum in Eq. (E.19), we find that

$$\mathcal{Z}_{(1)}(p^2) = -\frac{\alpha_0}{4\pi} \left[ \log\left(\frac{\Lambda^2}{-p^2}\right) + \frac{3}{2} \right]. \quad (\text{E.26})$$

After expanding  $\mathcal{Z}_{(1)}((k+q)^2)$  for  $k^2 \gg q^2$ ,

$$\begin{aligned} \mathcal{Z}_{(1)}((k+q)^2) &\approx \mathcal{Z}_{(1)}(k^2) + (2k \cdot q + q^2) \mathcal{Z}'_{(1)}(k^2) \\ &+ \frac{1}{2} (2k \cdot q + q^2)^2 \mathcal{Z}''_{(1)}(k^2) + \frac{1}{6} (2k \cdot q + q^2)^3 \mathcal{Z}'''_{(1)}(k^2), \end{aligned} \quad (\text{E.27})$$

and using that  $\mathcal{Z}_{(1)}((k+q)^2) \approx \mathcal{Z}_{(1)}(q^2)$  for  $q^2 \gg k^2$ , the angular integration can be performed, and the logarithmic corrections can be computed. The result is

$$\Pi_{(2a)}(q^2) + \Pi_{(2L)}(q^2) \approx \frac{\alpha_0^2}{\pi^2} \left[ -\frac{1}{24} \log^2\left(\frac{\Lambda^2}{q^2}\right) - \frac{29}{144} \log\left(\frac{\Lambda^2}{q^2}\right) + \mathcal{O}(1) \right]. \quad (\text{E.28})$$

Thus, comparing this expression with Eq. (E.25), we see that the “overlapping divergencies” (*i.e.* the  $\log^2$ ) cancel

$$\Pi_{(2a)}(q^2) + \Pi_{(2L)}(q^2) + \Pi_{(2I)}(q^2) \approx (\alpha_0^2/\pi^2)\mathcal{O}(1). \quad (\text{E.29})$$

Such a cancellation occurs in a similar manner in any covariant gauge  $\xi$ . Thus, the two-loop contribution contribution to  $\Pi$  is described solely by the part of the transverse vertex containing the  $T_8^\mu$  tensor, *i.e.*  $\Pi_{(2R)}$ , and, after adding all the pieces, we find that

$$\Pi(q^2) \approx \frac{\alpha_0}{2\pi} \left( \frac{2}{3} + \frac{\alpha_0}{2\pi} \right) \log \left( \frac{\Lambda^2}{q^2} \right) + (\alpha_0/\pi)\mathcal{O}(1). \quad (\text{E.30})$$

As was shown in [70], the particular transverse structure function  $\tau_8$  does not depend on the gauge parameter  $\xi$ . This observation agrees with the JBW computation of vacuum polarization effects.

## E.2 Scalar and pseudoscalar contributions

The two-loop contributions of scalars and pseudoscalars to the vacuum polarization can be computed rather easily by making use of the results of the previous section. Besides the photon exchange, we now take into account also scalar and pseudoscalar exchanges in the one-loop vertex, and self-energy defined in Eq. (E.4), *i.e.*,

$$\Gamma_{(1)}^\mu(k, p) = \Lambda_{(V)}^\mu(k, p) + \Lambda_{(S)}^\mu(k, p) + \Lambda_{(P)}^\mu(k, p), \quad (\text{E.31})$$

$$\hat{p}\mathcal{Z}_{(1)}(p^2) = -\Sigma_{(V)}(p) - \Sigma_{(S)}(p) - \Sigma_{(P)}(p). \quad (\text{E.32})$$

With one-loop vertex corrections

$$(-ie_0)\Lambda_{(V)}^\mu(k, p) = \int_\Lambda \frac{d^4w}{(2\pi)^4} (-ie_0)\gamma^\lambda iS(k-w) \times (-ie_0)\gamma^\mu iS(p-w)(-ie_0)\gamma^\sigma iD_{\lambda\sigma}(w), \quad (\text{E.33})$$

$$(-ie_0)\Lambda_{(S)}^\mu(k, p) = \int_\Lambda \frac{d^4w}{(2\pi)^4} (-ig_Y)\mathbf{1}iS(k-w) \times (-ie_0)\gamma^\mu iS(p-w)(-ig_Y)\mathbf{1}i\Delta_S(w), \quad (\text{E.34})$$

$$(-ie_0)\Lambda_{(P)}^\mu(k, p) = \int_\Lambda \frac{d^4w}{(2\pi)^4} (-ig_Y)i\gamma_5 iS(k-w) \times (-ie_0)\gamma^\mu iS(p-w)(-ig_Y)i\gamma_5 i\Delta_P(w), \quad (\text{E.35})$$

and the self-energies

$$i\Sigma_{(V)}(p) = \int_\Lambda \frac{d^4k}{(2\pi)^4} (-ie_0)\gamma^\mu iS(k)(-ie_0)\gamma^\nu iD_{\mu\nu}(k-p), \quad (\text{E.36})$$

$$i\Sigma_{(S)}(p) = \int_{\Lambda} \frac{d^4 k}{(2\pi)^4} (-ig_Y) \mathbf{1} iS(k) (-ig_Y) \mathbf{1} i\Delta_S(k-p), \quad (E.37)$$

$$i\Sigma_{(P)}(p) = \int_{\Lambda} \frac{d^4 k}{(2\pi)^4} (-ig_Y) i\gamma_5 iS(k) (-ig_Y) i\gamma_5 i\Delta_P(k-p), \quad (E.38)$$

Taking free massless scalar and pseudoscalar propagator, and the photon propagator in the Feynman gauge,

$$D_{\mu\nu}(q) = -\frac{g_{\mu\nu}}{q^2}, \quad \Delta_S(q) = \Delta_P(q) = \frac{1}{q^2}. \quad (E.39)$$

the one-loop vertices can be expressed as

$$\Lambda_{(V)}^{\mu}(k, p) = -ie_0^2 \int_{\Lambda} \frac{d^4 w}{(2\pi)^4} \frac{\gamma^{\lambda}(\hat{k} - \hat{w})\gamma^{\mu}(\hat{p} - \hat{w})\gamma_{\lambda}}{(k - w)^2(p - w)^2w^2}, \quad (E.40)$$

$$\Lambda_{(S)}^{\mu}(k, p) = ig_Y^2 \int_{\Lambda} \frac{d^4 w}{(2\pi)^4} \frac{(\hat{k} - \hat{w})\gamma^{\mu}(\hat{p} - \hat{w})}{(k - w)^2(p - w)^2w^2}, \quad (E.41)$$

$$\Lambda_{(P)}^{\mu}(k, p) = \Lambda_{(S)}^{\mu}(k, p), \quad (E.42)$$

where the last identity is obtained from Eq. (E.35) by using  $\gamma_5\gamma^{\mu} = -\gamma^{\mu}\gamma_5$ . Using Eq. (E.19), the self-energy contributions read

$$\begin{aligned} \Sigma_{(V)}(p) + \Sigma_{(S)}(p) + \Sigma_{(P)}(p) &= 2(e_0^2 + g_Y^2) \left[ -i \int_{\Lambda} \frac{d^4 w}{(2\pi)^4} \frac{(\hat{p} - \hat{w})}{(p - w)^2w^2} \right] \\ &= 2(e_0^2 + g_Y^2) \frac{\hat{p}}{32\pi^2} \left[ \log \left( \frac{\Lambda^2}{-p^2} \right) + \frac{3}{2} \right], \end{aligned} \quad (E.43)$$

The sum of one-loop vertex corrections can be rewritten as

$$\Lambda_{(V)}^{\mu}(k, p) + 2\Lambda_{(S)}^{\mu}(k, p) = 2[e_0^2 - g_Y^2] R^{\mu}(k, p) + 2[e_0^2 + g_Y^2] S^{\mu}(k, p), \quad (E.44)$$

where

$$R^{\mu}(k, p) = -i \int_{\Lambda} \frac{d^4 w}{(2\pi)^4} \frac{\gamma^{\mu}(\hat{p} - \hat{w})(\hat{k} - \hat{w})/2 - (\hat{k} - \hat{w})(\hat{p} - \hat{w})\gamma^{\mu}/2}{(k - w)^2(p - w)^2w^2}, \quad (E.45)$$

$$\begin{aligned} S^{\mu}(k, p) &= -i \int_{\Lambda} \frac{d^4 w}{(2\pi)^4} \left[ \frac{(k - w) \cdot (p - w)\gamma^{\mu}}{(k - w)^2(p - w)^2w^2} - \frac{(k - w)^{\mu}(\hat{p} - \hat{w})}{(k - w)^2(p - w)^2w^2} \right. \\ &\quad \left. - \frac{(p - w)^{\mu}(\hat{k} - \hat{w})}{(k - w)^2(p - w)^2w^2} \right]. \end{aligned} \quad (E.46)$$

The vertex part  $R^{\mu}$  is defined so that it is proportional to the transverse vertex with the  $T_8^{\mu}$  tensor:

$$2e_0^2 R^{\mu}(k, p) = \Gamma_{R(1)}^{\mu}(k, p) = \tau_8(k^2, p^2, q^2) T_8^{\mu}(k, p), \quad q^2 = (k - p)^2. \quad (E.47)$$

Thus we see that the part of Eq. (E.44), that is proportional to  $\Gamma_{R(1)}^\mu$ , and which turned out to be responsible for the two-loop contribution to the vacuum polarization, has a difference in sign between terms corresponding to photon exchanges, and terms corresponding to (pseudo)scalar exchanges.

Clearly the vertex part  $S^\mu$  must be

$$2e_0^2 S^\mu(k, p) = \Gamma_{L(1)}^\mu(k, p) + \Gamma_{I(1)}^\mu(k, p), \quad (\text{E.48})$$

with  $\Gamma_{L(1)}^\mu$  and  $\Gamma_{I(1)}^\mu$  given by Eqs. (E.16) and (E.13). Since we already computed the contributions of  $\Sigma_{(V)}$ ,  $\Gamma_{L(1)}^\mu$ ,  $\Gamma_{R(1)}^\mu$ , and  $\Gamma_{I(1)}^\mu$  to the vacuum polarization in Eqs. (E.28), (E.25), and (E.24), we deduce that

$$\Pi(q^2) \approx \frac{\alpha_0}{2\pi} \left( \frac{2}{3} + \frac{\alpha_0}{2\pi} - \frac{\lambda_Y}{2\pi} \right) \log \left( \frac{\Lambda^2}{q^2} \right) + (\alpha_0/\pi)\mathcal{O}(1), \quad (\text{E.49})$$

with

$$\lambda_Y = \frac{g_Y^2}{4\pi}. \quad (\text{E.50})$$

So from the point of view of two-loop correction to the vacuum polarization, the negative sign of the scalar and pseudoscalar interactions in Eq. (E.49) suggests that these type of interactions tend to reduce the screening, *i.e.* represents the attractive nature of forces between virtual fermion pairs in the vacuum polarization.

### E.3 Perturbative four-fermionic contributions

In this section, we compute the two-loop contributions of four-fermion interactions to the vacuum polarization. The four-fermion interactions are treated in a perturbation expansion in the dimensionless four-fermion coupling  $g_0$  defined in Eq. (3.6). Then in the lowest order approximation, the  $\sigma$  and  $\pi$  exchanges corresponding to the four-fermion interactions are described by the bare or free propagators

$$\Delta_S(q) = \Delta_P(q) = -G_0. \quad (\text{E.51})$$

With such  $\sigma$  and  $\pi$  propagators, the one-loop vertex and self-energy corrections are given by

$$\Gamma_{(1)}^\mu(k, p) = -iG_0 \int_\Lambda \frac{d^4w}{(2\pi)^4} \frac{(\hat{k} - \hat{w})\gamma^\mu(\hat{p} - \hat{w})}{(k - w)^2(p - w)^2}, \quad (\text{E.52})$$

$$\hat{p}\mathcal{Z}_{(1)}(p^2) = -iG_0 \int_\Lambda \frac{d^4w}{(2\pi)^4} \frac{(\hat{p} - \hat{w})}{(p - w)^2}. \quad (\text{E.53})$$

The one-loop vertex can be decomposed into

$$\Gamma_{(1)}^\mu(k, p) = \frac{G_0}{16\pi^2} \left[ \hat{k}\gamma^\mu \hat{p} I(k, p) - (\gamma_\lambda \gamma^\mu \hat{p} + \hat{k}\gamma^\mu \gamma_\lambda) I_\lambda(k, p) + I_{\lambda\sigma}(k, p) \right], \quad (\text{E.54})$$

where

$$I(k, p) = -i \int_\Lambda \frac{d^4 w}{\pi^2} \frac{1}{(k-w)^2 (p-w)^2}, \quad (\text{E.55})$$

$$I_\lambda(k, p) = -i \int_\Lambda \frac{d^4 w}{\pi^2} \frac{w_\lambda}{(k-w)^2 (p-w)^2}, \quad (\text{E.56})$$

$$I_{\lambda\sigma}(k, p) = -i \int_\Lambda \frac{d^4 w}{\pi^2} \frac{w_\lambda w_\sigma}{(k-w)^2 (p-w)^2}. \quad (\text{E.57})$$

Let us write

$$I = I_0, \quad I_\lambda = (k_\lambda + p_\lambda) J_0, \quad (\text{E.58})$$

$$I_{\lambda\sigma} = g_{\lambda\sigma} K_0 + (k_\lambda k_\sigma + p_\lambda p_\sigma) K_1 + (p_\lambda k_\sigma + k_\lambda p_\sigma) K_2, \quad (\text{E.59})$$

and with the help of Ref. [166], we find

$$I_0 = \log \left( \frac{\Lambda^2}{-q^2} \right) + 1, \quad J_0 = \frac{1}{2} \left[ \log \left( \frac{\Lambda^2}{-q^2} \right) + \frac{1}{2} \right], \quad (\text{E.60})$$

$$K_0 = -\frac{\Lambda^2}{4} - \frac{q^2}{2} \log \left( \frac{\Lambda^2}{-q^2} \right) + \frac{5q^2}{72} - \frac{(k^2 + p^2)}{12}, \quad (\text{E.61})$$

$$K_1 = \frac{1}{3} \log \left( \frac{\Lambda^2}{-q^2} \right) + \frac{1}{9}, \quad K_2 = \frac{1}{6} \log \left( \frac{\Lambda^2}{-q^2} \right) - \frac{1}{36}, \quad (\text{E.62})$$

Again it is useful to decompose the one-loop vertex into transverse and longitudinal parts, just as in Eq. (E.11). The result is

$$\Gamma_{R(1)}^\mu(k, p) = \frac{G_0}{16\pi^2} [2J_0 - I_0] T_8^\mu(k, p) = c_8 T_8^\mu(k, p), \quad (\text{E.63})$$

$$\begin{aligned} \Gamma_{I(1)}^\mu(k, p) &= \frac{G_0}{16\pi^2} \left[ \frac{I_0}{2} - K_1 + K_2 \right] T_3^\mu(k, p) \\ &= \frac{G_0}{16\pi^2} \left[ \frac{1}{3} \log \left( \frac{\Lambda^2}{-q^2} \right) + c_3 \right] T_3^\mu(k, p), \end{aligned} \quad (\text{E.64})$$

where  $c_3$  and  $c_8$  are constants whose exact values are irrelevant for the computation. Since the four-fermion interactions are gauge-invariant, we assume that the Ball-Chiu Ansatz is also valid in this case. We find for the longitudinal vertex part

$$\Gamma_{L(1)}^\mu(k, p) = \frac{G_0}{16\pi^2} \left[ (k^2 + p^2) (2J_0 - \frac{I_0}{2} - K_1 - K_2) + q^2 (K_1 - J_0) - 2K_0 \right] \gamma^\mu$$

$$\begin{aligned}
&+ \frac{G_0}{16\pi^2} \left[ \frac{I_0}{2} - 2J_0 + K_1 + K_2 \right] (k+p)^\mu (\hat{k} + \hat{p}) \\
&\approx \frac{G_0}{16\pi^2} \left\{ \left[ \frac{\Lambda^2}{2} + \mathcal{O} \left( q^2 \log \left( \frac{\Lambda^2}{-q^2} \right) \right) \right] \gamma^\mu + \frac{1}{12} (k+p)^\mu (\hat{k} + \hat{p}) \right\}.
\end{aligned} \tag{E.65}$$

The self-energy contribution is

$$\mathcal{Z}_{(1)}(p^2) \approx \frac{G_0}{16\pi^2} \left[ -\frac{\Lambda^2}{2} + \mathcal{O} \left( p^2 \log \left( \frac{\Lambda^2}{-p^2} \right) \right) \right] \approx -\frac{g_0}{8}, \tag{E.66}$$

where  $G_0 = 4\pi^2 g_0/\Lambda^2$ . With the one-loop vertex and self-energy corrections given above, we can proceed in the same manner as in the previous section, and obtain from Eqs. (E.7), (E.10), (E.15), and (E.66) that:

$$\Pi_{(2a)}(q^2) + \Pi_{(2L)}(q^2) \approx -\frac{g_0}{8} \Pi_{(1)}(q^2) = \frac{\alpha_0 g_0}{\pi} \left[ -\frac{1}{24} \log \left( \frac{\Lambda^2}{q^2} \right) + \mathcal{O}(1) \right]. \tag{E.67}$$

The contributions of the one-loop transverse vertex parts to the vacuum polarization can be performed exactly, since the angular integral can be done, the result is

$$\Pi_{(2I)}(q^2) = \frac{\alpha_0 g_0}{\pi} \left[ \frac{1}{24} \log \left( \frac{\Lambda^2}{q^2} \right) + \mathcal{O}(1) \right], \quad \Pi_{(2R)}(q^2) = (\alpha_0 g_0 / \pi) \mathcal{O}(1). \tag{E.68}$$

Hence

$$\Pi(q^2) = \frac{\alpha_0}{3\pi} \log \left( \frac{\Lambda^2}{q^2} \right) + (\alpha_0 g_0 / \pi) \mathcal{O}(1), \tag{E.69}$$

and the four-fermion interaction treated in a perturbative way do not give contributions to the  $\beta$  function. Thus again in this case too, the contributions of the longitudinal vertex cancel the contributions of the transverse vertex part which are proportional to the  $T_3^\mu$  tensor. In this case, however, the transverse part connected with  $T_8^\mu$  does not give a logarithmic contribution to screening.

The four-fermion interactions treated in a perturbative way are irrelevant, and, according to the RG of Wilson, these interactions do not contribute to the low-energy effective dynamics such as charge screening.



## Appendix F

# A derivation of the JWB equation

In this appendix we review the derivation of equation (5.27) for the  $f$  function given by Eq. (5.26) (and thus the  $\beta$  function) of QED introduced by Johnson, Willey, and Baker [46]. Since their result is formulated in terms of the BS fermion-fermion scattering kernel  $K^{(2)}$  their method is also applicable to the GNJL model.

In order to derive the JWB result, the following is assumed:

- The fermion wave function equals one,  $\mathcal{Z} = 1/A = 1$ , in the Landau gauge. In principle, this assumption is redundant since the JWB result is valid in any gauge, as long as the WTI is satisfied.
- The quenched approximation is assumed to be consistent. Internal photon propagators are quenched. Only a single fermion loop, thus a single power of  $\log \Lambda$  contributes to the vacuum polarization. Such an approximation is assumed to be valid close to an ultraviolet fixed point.
- Translational invariance of naively logarithmically divergent and finite momentum space integrals is assumed. This is an important point, since such translational invariance is lost in naively linear divergent integrals, such as the integral in the SDE for the fermion wave function  $\mathcal{Z}$ .
- Also it is assumed that we are in the scaling region of the theory, where the only relevant dimensionless variable is  $q^2/\Lambda^2$ . Thus the momenta are assumed to be larger than the particle masses or bound states masses in the model.

Hence,

$$\mathcal{Z}(k^2) = 1/A(k^2) = 1, \quad S(k) = \frac{\hat{k}}{k^2}, \quad \Gamma^\mu(k, k) = \gamma^\mu. \quad (\text{F.1})$$

The vacuum polarization tensor is

$$\Pi^{\mu\nu}(q) = \frac{iN\alpha_0}{4\pi^3} \int d^4k \text{Tr} [S(k+q)\Gamma^\mu(k+q,k)S(k)\gamma^\nu]. \quad (\text{F.2})$$

Since vacuum polarization tensor is transverse,  $\Pi_{\mu\nu}(q) = (-g_{\mu\nu}q^2 + q_\mu q_\nu)\Pi(q^2)$ , and the only relevant momentum variable is  $q^2/\Lambda^2$ , the equation for the vacuum polarization can be written as

$$\Pi(\mu^2) = -\lim_{q^2 \rightarrow \mu^2} \frac{1}{6} \frac{q^\mu q^\nu}{q^2} \frac{\partial^2}{\partial q_\alpha q^\alpha} \Pi_{\mu\nu}(q) + \mathcal{O}(1) + \mathcal{O}((\mu/\Lambda)^\sigma), \quad (\text{F.3})$$

where  $\mu$  is some infrared reference scale,  $\mu^2 \ll \Lambda^2$ , *e.g.*  $\mu \sim m_\sigma$ , and  $\sigma$  is some positive power. After inserting Eq. (F.2), and setting  $\mu^2 = 0$  in the integrand, and using  $\mu^2$  as the infrared cutoff in the momentum integral, we obtain

$$\begin{aligned} \Pi(\mu^2) = & -\lim_{q^2 \rightarrow \mu^2} \frac{1}{6} \frac{q_\mu q_\nu}{q^2} \frac{iN\alpha_0}{4\pi^3} \int_\mu d^4k \text{Tr} [S_\alpha^\alpha(k)\Gamma^\mu(k)S(k)\gamma^\nu \\ & + 2S_\alpha(k)\Gamma^{\mu,\alpha}(k)S(k)\gamma^\nu + S(k)\Gamma_\alpha^{\mu,\alpha}(k)S(k)\gamma^\nu] \\ & + \mathcal{O}(\mu^2/\Lambda^2), \end{aligned} \quad (\text{F.4})$$

where the derivatives are defined as follows:

$$S_\alpha(k) \equiv \frac{\partial}{\partial k^\alpha} S(k) = -\frac{\hat{k}\gamma_\alpha\hat{k}}{k^4}, \quad S_\alpha^\alpha(k) \equiv \frac{\partial^2}{\partial k_\alpha \partial k^\alpha} S(k) = -\frac{4\hat{k}}{k^4}, \quad (\text{F.5})$$

$$\Gamma_{\mu,\alpha}(k) \equiv \frac{\partial}{\partial q^\alpha} \Gamma_\mu(k+q,k) \Big|_{q=0}, \quad \Gamma_{\mu,\alpha}^\alpha(k) \equiv \frac{\partial^2}{\partial q_\alpha \partial q^\alpha} \Gamma_\mu(k+q,k) \Big|_{q=0}, \quad (\text{F.6})$$

and  $\Gamma^\mu(k) \equiv \Gamma^\mu(k,k)$ . Since the integral Eq. (F.4) can only be proportional to  $g^{\mu\nu}$ , it reduces to

$$\begin{aligned} \Pi(\mu^2) = & -\lim_{q^2 \rightarrow \mu^2} \frac{iN\alpha_0}{96\pi^3} \int_\mu d^4k \text{Tr} [S_\alpha^\alpha(k)\Gamma^\mu(k)S(k)\gamma_\mu \\ & + 2S_\alpha(k)\Gamma^{\mu,\alpha}(k)S(k)\gamma_\mu + S(k)\Gamma_\alpha^{\mu,\alpha}(k)S(k)\gamma_\mu] \\ & + \mathcal{O}(\mu^2/\Lambda^2). \end{aligned} \quad (\text{F.7})$$

The SDE for the vertex  $\Gamma^\mu$  reads, in terms of  $K^{(2)}$

$$\begin{aligned} \Gamma_{ab}^\mu(k+q,k) = & \gamma_{ab}^\mu + \sum_{\text{flavors}} (ie_0^2) \int_\Lambda \frac{d^4p}{(2\pi)^4} [S(p+q)\Gamma^\mu(p+q,p)S(p)]_{dc} \\ & \times K_{cd,ab}^{(2)}(p,p+q,k+q). \end{aligned} \quad (\text{F.8})$$

The first derivative of the vertex is anti-symmetric in  $\alpha$  and  $\mu$ , because of the assumption Eq. (F.1). Furthermore,  $CP$ -invariance implies that the only nonzero

contribution to the first derivative of  $\Gamma^\mu$  must be proportional to the tensor  $(\gamma_\mu \hat{k} \gamma_\alpha - \gamma_\alpha \hat{k} \gamma_\mu)$ . Thus we write

$$\Gamma_{[\mu,\alpha]}(k) \equiv \Gamma_{\mu,\alpha}(k) - \Gamma_{\alpha,\mu}(k) = \frac{(\gamma_\mu \hat{k} \gamma_\alpha - \gamma_\alpha \hat{k} \gamma_\mu)}{k^2} \Gamma', \quad (\text{F.9})$$

$$\Gamma_{(\mu,\alpha)}(k) \equiv \Gamma_{\mu,\alpha}(k) + \Gamma_{\alpha,\mu}(k) = S_{\mu\alpha}^{-1}(k). \quad (\text{F.10})$$

The dimensionless scalar function  $\Gamma'$  is related to the transverse structure function  $\tau_8(k^2, k^2, 0)$ , see ref. [70],

$$\Gamma' = -k^2 \tau_8(k^2, k^2, 0). \quad (\text{F.11})$$

Since  $S_{\nu\mu}^{-1}(k) = 0$  due to the Ward-Takahashi identity for the vertex, and Eq. (F.1). We find that

$$\Gamma_{\mu,\alpha}(k) = \frac{1}{2} \Gamma_{[\mu,\alpha]}(k) + \frac{1}{2} \Gamma_{(\mu,\alpha)}(k) = \frac{1}{2} \Gamma_{[\mu,\alpha]}(k) = \frac{(\gamma_\mu \hat{k} \gamma_\alpha - \gamma_\alpha \hat{k} \gamma_\mu)}{2k^2} \Gamma'. \quad (\text{F.12})$$

Differentiating now the SDE (F.8) with respect to  $q$ , and setting  $q = 0$ , we obtain

$$\begin{aligned} \Gamma_{\mu,\alpha}(k) &= \sum_{\text{flavors}} (ie_0^2) \int_\Lambda \frac{d^4 p}{(2\pi)^4} \left[ S(p) \Gamma_{\mu,\alpha} S(p) K^{(2)}(p, k) \right. \\ &\quad \left. + S_\alpha(p) \Gamma_\mu(p) S(p) K^{(2)}(p, k) + S(p) \Gamma_\mu(p) S(p) K_\alpha^{(2)}(p, k) \right]. \end{aligned} \quad (\text{F.13})$$

This gives

$$\Gamma_{\mu,\alpha}(k) = [\phi_1(\alpha_0) + \phi_2(\alpha_0) + \Gamma' \phi_1(\alpha_0)] \frac{(\gamma_\mu \hat{k} \gamma_\alpha - \gamma_\alpha \hat{k} \gamma_\mu)}{2k^2}. \quad (\text{F.14})$$

Thus

$$\Gamma' = \phi_1 + \phi_2 + \Gamma' \phi_1. \quad (\text{F.15})$$

The following identities have been used

$$\text{Tr} \left[ (\gamma_\mu \hat{k} \gamma_\alpha - \gamma_\alpha \hat{k} \gamma_\mu) (\gamma^\mu \hat{k} \gamma^\alpha - \gamma^\alpha \hat{k} \gamma^\mu) \right] = -96k^2, \quad (\text{F.16})$$

$$S_\alpha(p) \Gamma_\mu(p) S(p) = -S(p) \Gamma_\mu(p) S_\alpha(p) = \frac{(\gamma_\mu \hat{p} \gamma_\alpha - \gamma_\alpha \hat{p} \gamma_\mu)}{2p^4}, \quad (\text{F.17})$$

$$S(p) \Gamma_{\mu,\alpha}(p) S(p) = \Gamma' \frac{(\gamma_\mu \hat{p} \gamma_\alpha - \gamma_\alpha \hat{p} \gamma_\mu)}{2p^4}. \quad (\text{F.18})$$

Furthermore, the functions  $\phi_j$  are defined as follows:

$$\phi_1(\alpha_0) \equiv \sum_{\text{flavors}} -\frac{ie_0^2}{48} \int \frac{d^4 p}{(2\pi)^4}$$

$$\times \text{Tr} \left[ \frac{(\gamma^\mu \hat{p} \gamma^\alpha - \gamma^\alpha \hat{p} \gamma^\mu)}{2p^4} K^{(2)}(p, k) (\gamma_\mu \hat{k} \gamma_\alpha - \gamma_\alpha \hat{k} \gamma_\mu) \right], \quad (\text{F.19})$$

$$\phi_2(\alpha_0) \equiv \sum_{\text{flavors}} -\frac{ie_0^2}{48} \int \frac{d^4 p}{(2\pi)^4} \text{Tr} \left[ \frac{\hat{p} \gamma^\mu \hat{p}}{p^4} K^{(2)\alpha}(p, k) (\gamma_\mu \hat{k} \gamma_\alpha - \gamma_\alpha \hat{k} \gamma_\mu) \right], \quad (\text{F.20})$$

$$\phi_3(\alpha_0) \equiv \sum_{\text{flavors}} \frac{ie_0^2}{48} \int \frac{d^4 p}{(2\pi)^4} \text{Tr} \left[ \frac{\hat{p} \gamma^\mu \hat{p}}{p^4} K_\alpha^{(2)\alpha}(p, k) \hat{k} \gamma_\mu \hat{k} \right], \quad (\text{F.21})$$

where the trace over spinor indices is defined as

$$\text{Tr} [L(p)K(p, k)R(k)] \equiv L_{dc} K_{cd,ab}(p, k) R_{ba}(k), \quad (\text{F.22})$$

with  $L$  and  $R$  some projectors. The derivatives of the BS kernel  $K^{(2)}$  are

$$K_{cd,ab}^{(2)}(p, k) \equiv K_{cd,ab}^{(2)}(p, p+q, k+q) \Big|_{q=0}, \quad (\text{F.23})$$

$$K_\alpha^{(2)}{}_{cd,ab}(p, k) \equiv \frac{\partial}{\partial q^\alpha} K_{cd,ab}^{(2)}(p, p+q, k+q) \Big|_{q=0}, \quad (\text{F.24})$$

$$K_\alpha^{(2)\alpha}{}_{cd,ab}(p, k) \equiv \frac{\partial^2}{\partial q^\alpha \partial q_\alpha} K_{cd,ab}^{(2)}(p, p+q, k+q) \Big|_{q=0}. \quad (\text{F.25})$$

Assuming that  $K^{(2)}$  is translationally invariant, we can derive the following properties:

$$\int d^4 p \text{Tr} [L(p)K(p, k)R(k)] = \int d^4 p \text{Tr} [R(k)K(k, p)L(p)], \quad (\text{F.26})$$

$$\int d^4 p \text{Tr} [L(p)K_\alpha(p, k)R(k)] = - \int d^4 p \text{Tr} [R(k)K_\alpha(k, p)L(p)], \quad (\text{F.27})$$

$$\int d^4 p \text{Tr} [L(p)K_\alpha^\alpha(p, k)R(k)] = \int d^4 p \text{Tr} [R(k)K_\alpha^\alpha(k, p)L(p)]. \quad (\text{F.28})$$

By making use of the full SDE for the vertex, the second derivative  $\Gamma_\alpha^{\mu,\alpha}(k)$  can be eliminated in Eq. (F.4). The second derivative of the vertex is

$$\begin{aligned} \Gamma_\alpha^{\mu,\alpha}(k) &= \sum_{\text{flavors}} (ie_0^2) \int_\Lambda \frac{d^4 p}{(2\pi)^4} \left[ S(p) \Gamma_\alpha^{\mu,\alpha}(p) S(p) K^{(2)}(p, k) \right. \\ &+ 2S_\alpha(p) \Gamma^{\mu,\alpha}(p) S(p) K^{(2)}(p, k) + S_\alpha^\alpha(p) \Gamma^\mu(p) S(p) K^{(2)}(p, k) \\ &+ 2S(p) \Gamma^{\mu,\alpha}(p) S(p) K_\alpha^{(2)}(p, k) + 2S^\alpha(p) \Gamma^\mu(p) S(p) K_\alpha^{(2)}(p, k) \\ &\left. + S(p) \Gamma^\mu(p) S(p) K_\alpha^{(2)\alpha}(p, k) \right]. \end{aligned} \quad (\text{F.29})$$

Since  $\Gamma^\mu(k) = \gamma^\mu$ , and using Eq. (F.29) for  $\Gamma_\alpha^{\mu,\alpha}(k)$ , the second derivative of  $\Gamma_\alpha^{\mu,\alpha}$  in Eq. (F.7) can be eliminated. The result is

$$\Pi(\mu^2) = \frac{N\alpha_0}{2\pi} \left[ \sum_{n=1}^5 I_n(\alpha_0, \mu^2/\Lambda^2) + \mathcal{O}(\mu^2/\Lambda^2) \right], \quad (\text{F.30})$$

where

$$I_1 \equiv -\frac{i}{48} \int_\mu \frac{d^4 k}{\pi^2} \text{Tr} [S_\alpha^\alpha(k) \gamma^\mu S(k) \gamma_\mu], \quad (\text{F.31})$$

$$I_2 \equiv -\frac{i}{24} \int_\mu \frac{d^4 k}{\pi^2} \text{Tr} [S_\alpha(k) \Gamma^{\mu,\alpha}(k) S(k) \gamma_\mu], \quad (\text{F.32})$$

$$I_3 \equiv \frac{e_0^2}{24} \int_\mu \frac{d^4 k}{\pi^2} \int_\mu \frac{d^4 p}{(2\pi)^4} \times \text{Tr} \left[ S(p) \Gamma_{\mu,\alpha}(p) S(p) K^{(2)\alpha}(p, k) S(k) \gamma^\mu S(k) \right], \quad (\text{F.33})$$

$$I_4 \equiv \frac{e_0^2}{24} \int_\mu \frac{d^4 k}{\pi^2} \int_\mu \frac{d^4 p}{(2\pi)^4} \text{Tr} \left[ S_\alpha(p) \gamma_\mu S(p) K^{(2)\alpha}(p, k) S(k) \gamma^\mu S(k) \right], \quad (\text{F.34})$$

$$I_5 \equiv \frac{e_0^2}{48} \int_\mu \frac{d^4 k}{\pi^2} \int_\mu \frac{d^4 p}{(2\pi)^4} \text{Tr} \left[ S(p) \gamma_\mu S(p) K_\alpha^{(2)\alpha}(p, k) S(k) \gamma^\mu S(k) \right]. \quad (\text{F.35})$$

Using Eqs. (F.26)–(F.28), we find

$$\begin{aligned} I_1 &= \frac{2}{3} \int_{\mu^2}^{\Lambda^2} \frac{dk^2}{k^2} + \mathcal{O}(1), & I_2 &= \Gamma' \int_{\mu^2}^{\Lambda^2} \frac{dk^2}{k^2} + \mathcal{O}(1), \\ I_3 &= \Gamma' \phi_2 \int_{\mu^2}^{\Lambda^2} \frac{dk^2}{k^2} + \mathcal{O}(1), & I_4 &= \phi_2 \int_{\mu^2}^{\Lambda^2} \frac{dk^2}{k^2} + \mathcal{O}(1), \\ I_5 &= \phi_3 \int_{\mu^2}^{\Lambda^2} \frac{dk^2}{k^2} + \mathcal{O}(1). \end{aligned} \quad (\text{F.36})$$

Thus

$$\Pi(\mu^2) = \frac{N\alpha_0}{2\pi} \left[ \frac{2}{3} + \Phi(\alpha_0) \right] \log \frac{\Lambda^2}{\mu^2} + \text{finite}, \quad (\text{F.37})$$

where, inserting Eq. (F.15),

$$\Phi = \frac{\phi_1 + \phi_2(2 + \phi_2)}{1 - \phi_1} + \phi_3. \quad (\text{F.38})$$

In fact, Eq. (F.38) is the main result of [46]. The entire derivation did not yet specify the BS kernel  $K^{(2)}$ , and the JWB equation is applicable to the GNJL model as well. The crucial approximation is that internal gauge bosons are taken to be quenched, *i.e.*,  $D_{\mu\nu}(p) = (-g_{\mu\nu} + p_\mu p_\nu / p^2) / p^2$ , which is considered to be reasonable near a fixed point.

# References

- [1] Y. Nambu and G. Jona-Lasinio, Phys. Rev. **122**, 345 (1961).
- [2] C. Itzykson and J.-B. Zuber, *Quantum Field Theory*, McGraw-Hill, New York, 1980.
- [3] V.A. Miransky, *Dynamical Symmetry Breaking in Quantum Field Theories*, World-Scientific, Singapore, 1993.
- [4] N. Goldenfeld, *Lectures on Phase Transitions and the Renormalization Group*, Addison-Wesley Publishing Company, Reading, 1992.
- [5] D.J. Amit, *Field Theory, the Renormalization Group, and Critical Phenomena*, World Scientific, Singapore, revised second edition, 1989.
- [6] J. Zinn-Justin, *Quantum Field Theory and Critical Phenomena*, Clarendon Press, Oxford, 1989.
- [7] C.N. Yang and T.D. Lee, Phys. Rev. **87**, 404 (1952).
- [8] P.I. Fomin and V.A. Miransky, Phys. Lett. **B64**, 166 (1976).
- [9] P.I. Fomin, V.P. Gusynin, V.A. Miransky, and Yu.A. Sitenko, Nucl. Phys. **B110**, 445 (1976).
- [10] P.I. Fomin, V.P. Gusynin, V.A. Miransky, and Yu.A. Sitenko, Riv. Nuovo Cim. **6**, 1 (1983).
- [11] V.A. Miransky, Nuovo Cim. A **90**, 149 (1985).
- [12] W.A. Bardeen, C.N. Leung, and S.T. Love, Phys. Rev. Lett. **56**, 1230 (1986).
- [13] C.N. Leung, S.T. Love, and W.A. Bardeen, Nucl. Phys. **B273**, 649 (1986).
- [14] K.G. Wilson, Phys. Rev. **B4**, 3174, 3184 (1971).
- [15] K.G. Wilson and J.B. Kogut, Phys. Rep. **C12**, 75 (1974).

- [16] M. Gell-Mann and F.E. Low, Phys. Rev. **95**, 1300 (1954).
- [17] L.P. Kadanoff, Physics **2**, 263 (1966).
- [18] T. Appelquist and J. Carazzone, Phys. Rev. **D11**, 2856 (1975).
- [19] K-I. Kondo, H. Mino, and K. Yamawaki, Phys. Rev. **D39**, 2430 (1989).
- [20] T. Appelquist, M. Soldate, T. Takeuchi, and L.C.R. Wijewardhana, In *Proceedings of John Hopkins Workshop On Current Problems in Particle Theory*, G. Domokos and S. Kovesi-Domokos, editors, Singapore, 1988. World Scientific.
- [21] V.A. Miransky and K. Yamawaki, Mod. Phys. Lett. **A4**, 129 (1989).
- [22] T. Appelquist, J. Terning, and L.C.R. Wijewardhana, Phys. Rev. **D44**, 871 (1991).
- [23] A. Kocić, S. Hands, J.B. Kogut, and E. Dagotto, Nucl. Phys. **B347**, 217 (1990).
- [24] W.A. Bardeen, S.T. Love, and V.A. Miransky, Phys. Rev. **D42**, 3514 (1990).
- [25] V.L. Berezinskii, Sov. Phys. JETP **32**, 493 (1970).
- [26] J.M. Kosterlitz and D.J. Thouless, J. Phys. C. **6**, 1181 (1973).
- [27] V.A. Miransky and K. Yamawaki, Phys. Rev. **D55**, 5051 (1997).
- [28] B. Holdom, Phys. Lett. **B150**, 301 (1985).
- [29] T. Appelquist, M.B. Einhorn, T. Takeuchi, and L.C.R. Wijewardhana, Phys. Lett. **B220**, 223 (1989).
- [30] T. Appelquist, M.B. Einhorn, T. Takeuchi, and L.C.R. Wijewardhana, Phys. Lett. **B232**, 211 (1989).
- [31] V.A. Miransky, M. Tanabashi, and K. Yamawaki, Phys. Lett. **B221**, 177 (1989).
- [32] V.A. Miransky, M. Tanabashi, and K. Yamawaki, Mod. Phys. Lett. **A4**, 1043 (1989).
- [33] W.A. Bardeen, C.T. Hill, and M. Lindner, Phys. Rev. **D41**, 1647 (1990).
- [34] B. Holdom, Phys. Rev. **D24**, 1441 (1981).
- [35] K. Yamawaki, M. Bando, and K. Matumoto, Phys. Rev. Lett. **56**, 1335 (1986).
- [36] K. Yamawaki, M. Bando, and K. Matumoto, Phys. Lett. **B178**, 308 (1986).

- [37] T. Akiba and T. Yanagida, Phys. Lett. **B169**, 432 (1986).
- [38] J.B. Kogut, E. Dagotto, and A. Kocić, Phys. Rev. Lett. **60**, 772 (1988).
- [39] K-I. Kondo, M. Tanabashi, and K. Yamawaki, Prog. Theor. Phys. **89**, 1249 (1993).
- [40] V.P. Gusynin and M. Reenders, Phys. Rev. **D57**, 6356 (1998).
- [41] K-I. Aoki, K. Morikawa, J-I. Sumi, H. Terao, and M. Tomoyose, Prog. Theor. Phys. **97**, 479 (1997).
- [42] L.D. Landau and I.Ya. Pomeranchuk, Dokl. Akad. Nauk. **102**, 489 (1955).
- [43] V.A. Miransky, Int. J. Mod. Phys. **A6**, 1641 (1991).
- [44] J.D. Bjorken and S.D. Drell, *Relativistic Quantum Fields*, McGraw-Hill, New York, 1965.
- [45] G. 't Hooft, Nucl. Phys. **B75**, 461 (1974).
- [46] K. Johnson, R. Willey, and M. Baker, Phys. Rev. **163**, 1699 (1967).
- [47] T.E. Clark, S.T. Love, and W.A. Bardeen, Phys. Lett. **B237**, 235 (1990).
- [48] S. Bornholdt and C. Wetterich, Phys. Lett. **B282**, 399 (1992).
- [49] R.P. Feynman, Rev. Mod. Phys. **20**, 367 (1948).
- [50] R.P. Feynman, Phys. Rev. **76**, 769 (1949).
- [51] J. Glimm and A. Jaffe, *Quantum physics; a functional integral point of view*, Springer-Verlag, New-York, 1981.
- [52] O. de Mirleau, *Foundations of Functional Integration and the Schwinger-Dyson equation*, PhD thesis, University of Amsterdam, 1997.
- [53] F.J. Dyson, Phys. Rev. **75**, 1736 (1949).
- [54] J. Schwinger, Proc. Nat. Acad. Sc. **37**, 452 and 455 (1951).
- [55] B. Widom, J. Chem. Phys. **43**, 3892, 3898 (1965).
- [56] J. Polchinski, Nucl. Phys. **B231**, 269 (1984).
- [57] G.C. Wick, Phys. Rev. **96**, 1124 (1954).
- [58] W. Pauli and F. Villars, Rev. Mod. Phys. **21**, 434 (1949).
- [59] K. Fujikawa, Nucl. Phys. **B428**, 169 (1994).

- [60] S.L. Adler, Phys. Rev. **177**, 2426 (1969).
- [61] J.S. Bell and R. Jackiw, Nuovo Cimento **60A**, 47 (1969).
- [62] C.G. Callan, Phys. Rev. **D2**, 1541 (1970).
- [63] K. Symanzik, Comm. Math. Phys. **18**, 227 (1970).
- [64] M. Henneaux and C. Teitelboim, *Quantization of Gauge Systems*, Princeton University Press, Princeton, 1992.
- [65] J. Goldstone, Nuovo Cimento **19**, 154 (1961).
- [66] J. Goldstone, A. Salam, and S. Weinberg, Phys. Rev. **127**, 965 (1962).
- [67] D. Gross and A. Neveu, Phys. Rev. **D10**, 3235 (1974).
- [68] J.F. Cartier, A.A. Broyles, R.M. Placido, and H.S. Green, Phys. Rev. **D30**, 1742 (1984).
- [69] J.S. Ball and T-W. Chiu, Phys. Rev. **D22**, 2542 (1980).
- [70] A. Kizilersü, M. Reenders, and M.R. Pennington, Phys. Rev. **D52**, 1242 (1995).
- [71] K. Fujikawa, Phys. Rev. Lett. **42**, 1195 (1979).
- [72] K. Fujikawa, Phys. Rev. **D21**, 2848 (1980).
- [73] A.H. Hams, *Dyson–Schwinger equations and Ward–Takahashi identities*, Unpublished, a derivation of the ABJ anomaly from Dyson–Schwinger formalism, private communication.
- [74] V.P. Gusynin, *Low-Energy Chiral Lagrangian from the Gauged Nambu–Jona–Lasinio model*, RUG internal report 256, University of Groningen (1992).
- [75] M. Hashimoto, Phys. Lett. **B441**, 389 (1998).
- [76] P. Maris, C.D. Roberts, and P.C. Tandy, Phys. Lett. **B420**, 267 (1998).
- [77] H. Pagels and S. Stokar, Phys. Rev. **D20**, 2947 (1979).
- [78] C.D. Roberts and A.G. Williams, Prog. Part. Nucl. Phys. **33**, 477 (1994).
- [79] P. Maris, *Nonperturbative Analysis of the Fermion Propagator: complex singularities and dynamical mass generation*, PhD thesis, University of Groningen, 1993.
- [80] L.D. Landau and E.M. Lifshitz, *Quantum Mechanics*, Pergamon Press, Oxford, 1958.

- [81] R.G. Newton, *Scattering theory of waves and particles*, McGraw-Hill, New York, 1966.
- [82] T. Maskawa and H. Nakajima, *Prog. Theor. Phys.* **52**, 1326 (1974).
- [83] R. Fukuda and T. Kugo, *Nucl. Phys.* **B117**, 250 (1976).
- [84] D. Atkinson and D.W.E. Blatt, *Nucl. Phys.* **B151**, 342 (1979).
- [85] A.T. Filippov, *Sov. J. Part. Nucl.* **11**, 293 (1980).
- [86] T. Takeuchi, *Phys. Rev.* **D40**, 2697 (1989).
- [87] P.I. Fomin, V.P. Gusynin, and V.A. Miransky, *Phys. Lett.* **B78**, 136 (1978).
- [88] V.A. Miransky, *Phys. Lett.* **B91**, 421 (1980).
- [89] V.A. Miransky, *Sov. Phys. JETP* **61**, 905 (1985).
- [90] V.A. Miransky and P.I. Fomin, *Sov. J. Part. Nucl.* **16**, 203 (1985).
- [91] V.P. Gusynin, V.A. Kushnir, and V.A. Miransky, *Phys. Lett.* **B220**, 635 (1989).
- [92] V. Azcoiti, G. Di Carlo, A. Galante, A.F. Grillo, V. Laliena, and C.E. Piedrafita, *Phys. Lett.* **B355**, 270 (1995).
- [93] K-I. Kondo, *Int. J. Mod. Phys.* **A6**, 5447 (1991).
- [94] A. Kocić and J.B. Kogut, *Nucl. Phys.* **B422**, 593 (1994).
- [95] J.M. Cornwall, R. Jackiw, and E. Tomboulis, *Phys. Rev.* **D10**, 2428 (1974).
- [96] V.P. Gusynin and V.A. Miransky, *Mod. Phys. Lett.* **A6**, 2443 (1991).
- [97] V.P. Gusynin and V.A. Miransky, *Sov. Phys. JETP* **74**, 216 (1992).
- [98] W.A. Bardeen and S.T. Love, *Phys. Rev.* **D45**, 4672 (1992).
- [99] T. Appelquist, J. Terning, and L.C.R. Wijewardhana, *Phys. Rev. Lett.* **75**, 2081 (1995).
- [100] E. Witten, *Nucl. Phys.* **B145**, 110 (1978).
- [101] N.D. Mermin and H. Wagner, *Phys. Rev. Lett.* **17**, 1133 (1966).
- [102] S. Coleman, *Commun. Math. Phys.* **31**, 259 (1973).
- [103] V.A. Miransky and V.P. Gusynin, *Prog. Theor. Phys.* **81**, 426 (1989).
- [104] V.A. Miransky, *Int. J. Mod. Phys. A* **8**, 135 (1993).

- [105] T. Appelquist, J. Terning, and L.C.R. Wijewardhana, Phys. Rev. Lett. **77**, 1214 (1996).
- [106] T. Appelquist, A. Ratnaweera, J. Terning, and L.C.R. Wijewardhana, hep-ph/9806472, (1998).
- [107] V.P. Gusynin, V.A. Miransky, and A.V. Shpigin, Phys. Rev. **D58**, 085023 (1998).
- [108] Y. Kikukawa and K. Yamawaki, Prog. Lett. **B234**, 497 (1990).
- [109] J.B. Kogut and E. Dagotto, Phys. Rev. Lett. **59**, 617 (1987).
- [110] J.B. Kogut, E. Dagotto, and A. Kocić, Phys. Rev. Lett. **61**, 2416 (1988).
- [111] J.B. Kogut, E. Dagotto, and A. Kocić, Nucl. Phys. **B317**, 253 (1989).
- [112] A. Kocić, J.B. Kogut, M-P. Lombardo, and K.C. Wang, Nucl. Phys. **B397**, 451 (1993).
- [113] V. Azcoiti, G. Di Carlo, A. Galante, A.F. Grillo, and V. Laliena, Phys. Lett. **B416**, 409 (1998).
- [114] M. Göckeler, R. Horsley, V. Linke, P.E.L. Rakow, G. Schierholz, and H. Stüben, Nucl. Phys. **B487**, 313 (1997).
- [115] A. Kocić, J.B. Kogut, and K.C. Wang, Nucl. Phys. **B398**, 405 (1993).
- [116] S.J. Hands, A. Kocić, J.B. Kogut, R.L. Renken, D.K. Sinclair, and K.C. Wang, Nucl. Phys. **B413**, 503 (1994).
- [117] E. Dagotto, A. Kocić, and J.B. Kogut, Phys. Lett. **B232**, 235 (1989).
- [118] J.B. Kogut, E. Dagotto, and A. Kocić, Nucl. Phys. **B317**, 271 (1989).
- [119] V. Azcoiti, G. Di Carlo, and A.F. Grillo, Int. J. Mod. Phys. **A8**, 4235 (1993).
- [120] V. Azcoiti, G. Di Carlo, A. Galante, A.F. Grillo, V. Laliena, and C.E. Piedrafita, Phys. Lett. **B353**, 279 (1995).
- [121] M. Göckeler, R. Horsley, E. Laermann, P. Rakow, G. Schierholz, R. Sommer, and U.-J. Wiese, Phys. Lett. **B251**, 567 (1990).
- [122] M. Göckeler, R. Horsley, P.E.L. Rakow, G. Schierholz, and R. Sommer, Nucl. Phys. **B371**, 713 (1992).
- [123] M. Göckeler, R. Horsley, V. Linke, P.E.L. Rakow, G. Schierholz, and H. Stüben, Phys. Rev. Lett. **80**, 4119 (1998).

- [124] A. Kocić, J.B. Kogut, and S.J. Hands, Phys. Lett. **B289**, 400 (1992).
- [125] M. Göckeler, R. Horsley, P.E.L. Rakow, and G. Schierholz, Phys. Rev. **D53**, 1508 (1996).
- [126] S. Hands and J.B. Kogut, Nucl. Phys. **B462**, 291 (1996).
- [127] S. Kim, A. Kocić, and J.B. Kogut, Nucl. Phys. **B429**, 407 (1994).
- [128] V. Azcoiti, G. Di Carlo, A. Galante, A.F. Grillo, V. Laliena, and C.E. Piedrafita, Phys. Lett. **B379**, 179 (1996).
- [129] P.E.L. Rakow, Nucl. Phys. **B356**, 27 (1991).
- [130] V.P. Gusynin, Mod. Phys. Lett. **A5**, 133 (1990).
- [131] K-I. Kondo, Nucl. Phys. **B351**, 259 (1991).
- [132] T. Appelquist, K. Lane, and U. Mahanta, Phys. Rev. Lett. **61**, 1553 (1988).
- [133] B. Holdom, Phys. Rev. Lett. **62**, 997 (1989).
- [134] K-I. Aoki, In *Proceedings of International Workshop on Perspectives of Strong Coupling Gauge Theories, Nagoya, 1996*, K. Yamawaki, editor, page 479, Singapore, 1996. World Scientific.
- [135] D.C. Curtis and M.R. Pennington, Phys. Rev. **D42**, 4165 (1990).
- [136] D.C. Curtis and M.R. Pennington, Phys. Rev. **D44**, 536 (1991).
- [137] D.C. Curtis and M.R. Pennington, Phys. Rev. **D46**, 2663 (1992).
- [138] C.J. Burden and C.D. Roberts, Phys. Rev. **D47**, 5581 (1993).
- [139] A. Bashir and M.R. Pennington, Phys. Rev. **D50**, 7679 (1994).
- [140] A. Bashir, A. Kizilersü, and M.R. Pennington, Phys. Rev. **D57**, 1242 (1998).
- [141] V.P. Gusynin, V.A. Kushnir, and V.A. Miransky, Phys. Rev. **D39**, 2355 (1989).
- [142] W.A. Bardeen, C.N. Leung, and S.T. Love, Nucl. Phys. **B323**, 493 (1989).
- [143] There are quite few attempts to solve Bethe-Salpeter equations straightforwardly in Minkowski space, for the most recent one see: K. Kusaka, K. Simpson, and A.G. Williams, Phys. Rev. **D56**, 5071 (1997).
- [144] A. Erdélyi, W. Magnus, F. Oberhettinger, and F.G. Tricomi, *Higher transcendental functions, volume 2.*, McGraw-Hill, New York, 1953.

- [145] E.S. Fradkin, Sov. Phys. JETP **28**, 750 (1955).
- [146] L.D. Landau, A. Abrikosov, and L. Halatnikov, Suppl. Nuovo Cimento **1**, 80 (1956).
- [147] L.D. Landau, A. Abrikosov, and L. Halatnikov, Dokl. Akad. Nauk. **95**, 497 (1954).
- [148] L.D. Landau, A. Abrikosov, and L. Halatnikov, Dokl. Akad. Nauk. **95**, 773 (1954).
- [149] L.D. Landau, A. Abrikosov, and L. Halatnikov, Dokl. Akad. Nauk. **95**, 1177 (1954).
- [150] R. Jost and J.M. Luttinger, Helv. Phys. Acta **23**, 201 (1950).
- [151] J.L. Rosner, Phys. Rev. Lett. **17**, 1190 (1966).
- [152] J.L. Rosner, Ann. Phys. (N.Y.) **44**, 11 (1967).
- [153] M. Baker and K. Johnson, Phys. Rev. **183**, 1292 (1969).
- [154] S.L. Adler, Phys. Rev. **D5**, 3021 (1972).
- [155] K. Johnson and M. Baker, Phys. Rev. **D8**, 1110 (1973).
- [156] A. Kocić, E. Dagotto, and J.B. Kogut, Phys. Lett. **B213**, 56 (1988).
- [157] E.V. Gorbar, Ukr. Fiz. Zh. **35**, 982 (1990).
- [158] V.P. Gusynin, Ukr. Phys. J. **36**, 1819 (1991).
- [159] E.V. Gorbar and E. Sausedo, Ukr. Phys. J. **36**, 1025 (1991).
- [160] S. Coleman, *Aspects of symmetry*, Cambridge University Press, Cambridge, 1985.
- [161] M. Harada, Y. Kikukawa, T. Kugo, and H. Nakano, Prog. Theor. Phys. **92**, 1161 (1994).
- [162] K-I. Kondo, S. Shuto, and K. Yamawaki, Mod. Phys. Lett. **A6**, 3385 (1991).
- [163] A.P. Prudnikov, Yu.A. Brychkov, and O.I. Marichev, *Integrals and series, volume 2: special functions*, Gordon and Breach Science Publishers, New York, 1986.
- [164] P. Jain and H.J. Munczek, Phys. Rev. **D48**, 5403 (1993).
- [165] P. Maris and Q. Wang, Phys. Rev. **D53**, 4650 (1996).
- [166] A.I. Akhiezer and V.A. Berestetskii, *Quantum Electrodynamics*, John Wiley & Sons, New York, 1965.

# Samenvatting

In dit proefschrift wordt het *Gauged Nambu–Jona-Lasinio* (GNJL) model behandeld. Het GNJL model is een quantumvelden-theoretisch model voor dynamische chirale symmetriebreking. De begrippen *chirale symmetrie* en *chirale symmetriebreking* worden gebruikt in de hoge energie fysica. Chirale symmetriebreking verschafft een mechanisme om massa's van elementaire deeltjes (zoals bijv. het elektron, quarks, neutrino's (?)) te genereren.

In de jaren dertig en veertig bleek dat voor het modelleren van het gedrag van een elementair deeltje, zoals het elektron, zowel een quantummechanische beschrijving als een relativistische beschrijving nodig was. Dit heeft aanleiding gegeven tot de quantumvelden-theorie. In de jaren zeventig zijn de quantum-velden-theoretische modellen van de electromagnetische, de zwakke en de sterke wisselwerking verenigd in het Standaard Model. Het Standaard Model beschrijft de interacties tussen de elementaire deeltjes (elementair voor zover we dat experimenteel kunnen testen) in termen van zogenaamde ijktheorieën. Deze ijktheorieën hebben een bijzondere eigenschap die *renormaliseerbaarheid* wordt genoemd en die hen toepasbaar maakt over een heel groot energiegebied.

Eén van de vraagstukken in de natuurkunde is de oorsprong van de massa's van de elementaire deeltjes en hun verscheidenheid. Deze massa's volgen niet uit het Standaard Model. Hoewel hierover veel ideeën zijn, bestaat er nog geen succesvol model waarmee de massa's berekend kunnen worden. Het enige dat we nu kunnen is de massa's van de elementaire deeltjes meten met behulp van deeltjesversnellers en de gemeten waarden gebruiken als uitgangspunt in specifieke modellen. Om massa's aan elementaire deeltjes toe te kennen gebruiken we in het Standaard Model het zogenaamde Higgs mechanisme. Dit Higgs mechanisme voorspelt tevens het bestaan van een Higgs boson, een deeltje dat nog niet is waargenomen.

De wiskundige formulering van quantumvelden-theorieën is erg ingewikkeld, en niet compleet. De interessantste en fysisch meest relevante modellen leiden tot een oneindig groot systeem van gekoppelde bewegingsvergelijkingen. Deze worden ook wel *Schwinger–Dyson* vergelijkingen genoemd. Dergelijke vergelijkingen zijn praktisch onoplosbaar en dus zijn we gedwongen benaderingen te ontwikkelen waarmee we iets concreets kunnen uitrekenen.

Het Standaard Model is erg succesvol. Dat hebben we te danken aan het feit dat de koppelingsconstanten (die de sterkte van de fundamentele natuurkrachten weergeven) in de meeste gevallen vrij klein zijn. Daardoor kunnen we gebruik maken van een expansietechniek die storingstheorie heet.

Een direct gevolg van renormalisatie is dat koppelingsconstanten energie-afhankelijk zijn. Zo hangt de sterkte van een bepaalde interactie tussen deeltjes af van de afstand tussen die deeltjes. Meestal is het zo dat een interactie vrij zwak is voor lange afstanden en sterker wordt naarmate de afstand tussen de deeltjes kleiner wordt (het omgekeerde is ook mogelijk). Een aantal fysische verschijnselen is het gevolg van een sterke wisselwerking tussen deeltjes, en kan dus niet, i.v.m. grote koppelingsconstanten, met storingstheorie beschreven worden. Voorbeelden hiervan zijn massageneratie en de formatie van gebonden toestanden zoals hadronen. Deze hadronen zijn gebonden toestanden van twee of drie quarks. De *sterke wisselwerking* tussen quarks wordt beschreven door QCD (quantumchromodynamica). Hoewel we denken dat QCD de juiste theorie is voor de dynamica van quarks is het erg moeilijk om uit QCD de hadronen te herleiden.

Zulke niet-storingsachtige fenomenen gaan vaak samen met het optreden van een faseovergang in het model als functie van de koppelingsconstante. Als de koppelingsconstante boven een bepaalde critische waarde komt, ontstaan gebonden toestanden van fermionen en wordt een massa gegenereerd (*dit is dynamische chirale symmetriebreking*). Dergelijke chirale faseovergangen hebben veel overeenkomsten met faseovergangen in modellen voor bijvoorbeeld ferromagnetisme in de statistische mechanica.

Wat het GNJL model interessant maakt is het feit dat een combinatie van volgend sterke en attractieve *vier-fermion* interacties en een zogenaamde *Abelse* ijkinteractie<sup>1</sup> zo'n chirale faseovergang veroorzaakt. De faseovergang hangt samen met de formatie van gebonden toestanden en massageneratie. Het blijkt dat de gebonden toestanden in het GNJL model veel compacter zijn en sterker gebonden dan in QCD. Dit suggereert dat de gebonden toestanden relevant zijn voor de beschrijving van de dynamica van de fermionen over een heel groot energiegebied. Technisch gesproken betekent dit dat de vier-fermion interactie renormaliseerbaar is; de dracht van de vier-fermion interacties is veel langer dan op grond van storingstheorie berekend kan worden.

Het GNJL model zegt daarom veel over de mogelijke rol die vier-fermion interacties kunnen spelen voor het modelleren van massa's van elementaire deeltjes.

Hieronder volgt een korte samenvatting per hoofdstuk.

**Hoofdstuk 1.** Hierin introduceren we het pad-integraal formalisme en de daaraan gerelateerde Schwinger–Dyson vergelijking. De renormalisatiegroep-methode wordt uitvoerig behandeld en de connectie tussen faseovergangen in statische mechanische modellen en de renormalisatie van quantumvelden theorieën wordt gemaakt. Aan

---

<sup>1</sup>Dit in tegenstelling tot QCD dat gebaseerd is op een niet-Abelse ijktheorie.

het eind introduceren we het Goldstone mechanisme en de Lagrangeaan van het GNJL model.

**Hoofdstuk 2.** Dit hoofdstuk is een noodzakelijk kwaad en nogal technisch van aard. De Schwinger–Dyson vergelijkingen voor een aantal specifieke Green functies (correlaties functies) worden afgeleid. Ook worden de zogenoemde Ward–Takahashi identiteiten behandeld. Dit zijn vergelijkingen die de symmetrieën van het model representeren en uitermate belangrijk zijn in het bepalen van een geloofwaardige benaderingsmethode. De Ward–Takahashi identiteiten zijn het centrale uitgangspunt voor het formuleren van niet-storingsachtige benaderingen.

**Hoofdstuk 3.** In hoofdstuk 3 worden een aantal specifieke niet-storingsachtige benaderingen geïntroduceerd en onder de loep genomen: de “ladder” benadering, de “quenched” benadering en de “mean-field” (Hartree–Fock) benadering voor de Schwinger–Dyson vergelijking (de *gap-vergelijking*) voor de massa van het fermion in het GNJL model. De basiseigenschappen van de chirale faseovergang die de gap-vergelijking beschrijft worden behandeld. De resultaten van deze specifieke benaderingen worden vergeleken met andere niet-storingsachtige technieken zoals numerieke roostersimulaties en niet-storingsachtige renormalisatiegroep technieken. Hoewel dit hoofdstuk geen nieuwe resultaten beschrijft, geeft het een overzicht van de literatuur en vormt het een raamwerk voor het begrijpen van hoofdstuk 4 en 5.

**Hoofdstuk 4.** Dit hoofdstuk is gewijd aan het berekenen van de Yukawa vertex en de scalaire instabiele gebonden toestanden (resonanties) in de quenched ladder benadering.

We ontwikkelen een methode waarmee we analytische uitdrukkingen kunnen vinden voor de Yukawa-vertex en de scalaire propagator die deze resonantie represeneert. De scalaire propagator is te beschouwen als een soort Higgs deeltje. De Yukawa vertex beschrijft de interactie tussen fermionen en gebonden toestanden en is een functie van de impulsen van de ingaande fermionen en de uitgaande gebonden toestand.

De resultaten worden uitvoerig vergeleken met resultaten van andere auteurs. Het nieuwe aan onze berekeningen is dat het impuls gedrag van de Yukawa-vertex wordt uitgebreid en dat het fasediagram uitvoeriger wordt behandeld dan in eerdere studies. Een van de conclusies die uit hoofdstuk 4 getrokken kan worden is het feit dat de Hartree–Fock benadering voor vier-fermion interacties in het GNJL model in het algemeen inconsistent is.

**Hoofdstuk 5.** In dit hoofdstuk wordt de *continuum limiet* behandeld. Dit komt er kortweg op neer dat we onderzoeken of het GNJL model een niet-triviale renormaliseerbare theorie is. De vier-fermion interacties worden nu benaderd in een  $1/N$

expansie<sup>2</sup> in plaats van de Hartree–Fock benadering.

Gekeken wordt naar de vacuumpolarisatie. Dat is een functie die de effectieve koppelingscontante oftewel de effectieve lading van de fermionen beschrijft. Uiteindelijk bepaalt het gedrag van de vacuumpolarisatie of het GNJL model een *niet-triviaal* renormaliseerbaar model is. De vacuumpolarisatie is een functie van zowel de Yukawa-vertex als de scalaire propagator waarvoor we in hoofdstuk 4 expliciete uitdrukkingen hebben afgeleid.

**Conclusie.** Het doel van dit proefschrift was om het sterke koppelingsgedrag en de chirale faseovergang in het GNJL model beter te begrijpen en de conclusie van dit proefschrift kan als volgt worden samengevat. We hebben aangetoond binnen het kader van een aantal niet-storingsachtige benaderingen (nl. de ladder benadering en de  $1/N$  expansie) dat het GNJL model een niet-triviale renormaliseerbare theorie is, in de buurt van de chirale faseovergang, mits het aantal typen fermionen (aangeduid met  $N$ ) groter is dan een critische waarde ( $N_c$ ).

Deze critische waarde is nogal groot ( $N_c \approx 50$ ), en is veel groter dan het aantal typen fermionen dat tot nu toe bekend is. Daarom is er wat dat betreft nog geen directe toepassing voor het model. Toch is het resultaat belangrijk omdat de enige tot nu bekende niet-triviale renormaliseerbare theorieën gebaseerd zijn op *niet-Abelse* ijktheorieën terwijl het door ons beschouwde GNJL model is gebaseerd op een *Abelse* ijktheorie.

---

<sup>2</sup>Een andere niet-storingsachtige techniek waar  $N$  een getal is dat het aantal verschillende typen fermionen aangeeft.

# Acknowledgements

This thesis would never have seen the light of day if it wasn't for the help of Valery Gusynin who has been my tower of strength. For this I cannot thank him enough. The countless e-mail exchanges containing ideas, computations, and discussions have formed the foundation of this work. With great pleasure I recall his visit to our institute and my visit to Kiev. The visit to Kiev was very important and it has given me the necessary courage and perspective. I thank him, his family, and his colleagues at the Bogolyubov institute for their hospitality.

Marinus Winnink has given me hope in anxious days. I thank him for his intensive and humorous guidance and for acting as supervisor. The, on beforehand, not so obvious combination of high energy physics and mathematical physics turned out to be very interesting and fruitful for both of us.

Also I would like thank Aernout van Enter for the interesting discussions on the theory of phase transitions and for his useful suggestions concerning the literature.

I thank Tony Dorlas, Volodya Miransky, and Mike Pennington for their willingness to form the reading committee.

Special thanks to Ayse Kizilersü and Mike Pennington for the successful e-mail collaboration in 1994–1995.

Anthony Hams I thank for the numerous discussions we had and I wish him good luck and success with his PhD research.

Thanks to Anne and Titus for helping with the ceremonial fuss.

Thanks also to my colleagues, secretaries, and “voluntary” system managers who, all in their own way, have contributed to the making of this thesis.

Last but not least I thank Karin, my family, and friends for their unconditional patience, support, and encouragements.